GLUTATHIONE-DECORATED DENDRONS AS POTENTIAL DRUG CARRIER SYSTEMS IN MULTIPLE SCLEROSIS

DHAFIR Q. MASHETA

A thesis submitted in fulfilment of the requirements of the University of Brighton for the degree of Doctor of Philosophy

2017

School of Pharmacy and Biomolecular Sciences

University of Brighton

Abstract

Multiple sclerosis (MS) is a chronic progressive demyelinating disorder of the central nervous system. It is an autoimmune neurodegenerative disease associated with inflammation in the brain white matter mediated by autoreactive T-cells. MS is not curable and the treatment is only aimed at reducing the frequency, limiting the lasting effect of relapses, relief of symptoms, preventing disability arising from disease progression and promoting nerve repair. Glucocorticoid, typically methylprednisolone (MP) is given to reduce the duration of MS relapses. However, due to the presence of the blood-brain barrier (BBB) which impedes the effective delivery of MP to the brain, high doses of MP are given to the patients to reach the minimum therapeutic concentration. Consequently, such elevated doses of MP results in an increase in the adverse effects of the drug. To overcome MP limited permeability, it must be delivered using specialised strategies to avoid high doses administration. This study aims to improve MP cell membrane penetration employing dendrons as drug carriers to achieve higher loading capacities and utilising glutathione molecule as a ligand to be recognised by glutathione receptors in the brain.

The aim was achieved by design and characterisation of dendron-drug conjugates, assessment of their cytotoxicity, validation of an *in vitro* b.End3 cells brain model, penetration studies through this model and biochemical investigation of the anti-inflammatory activity of the final molecule.

The successful synthesis of the dendrimers, dendrimer-MP conjugates and attachment with glutathione were achieved using automated solid phase peptide synthesis and characterised by high performance liquid chromatograph, mass spectrometry, nuclear magnetic resonance and Fourier transform infra-red spectroscopy.

The cytotoxicity of the drug loaded and unloaded was assessed using lactate dehydrogenase, MTT and calcein/ethidium cytotoxicity assays. Under the conditions used, the assembled drug conjugates' toxicity levels were within the acceptable range.

Transwell inserts were used to support mice immortalised brain endothelial cells, b.End3, to form an *in vitro* model of the BBB model. The model was validated by using transepithelial electrical resistance measurements, morphological examination, and permeability to paracellular marker (horseradish peroxidase). The data collected revealed that the b.End3 cell line is able to express several important barrier features of the *in vivo* BBB and can be used as

in vitro BBB model for penetration studies. The cells exerted their maximum barrier functions at Day 7 of culturing.

Fluorescent staining images confirmed the uptake of the synthesised molecules by b.End3 cells. Quantitative measurements based on high performance liquid chromatography of penetration through the b.End3 cultured cells-barrier indicated improvement in the permeability of MP conjugated to glutathione by almost 3.5 fold compared to free MP reaching 16.8% and 40.9% after 1 and 3 hours of sample introduction, respectively.

Biochemical investigations revealed that MP in its attached form retained its anti-inflammatory activity based on the reduction in lactate dehydrogenase and inflammatory cytokines release levels from C6 glial cells treated with tumour necrotic factor-α and showed greater anti-inflammatory activity compared to unconjugated MP.

It can be concluded that the ability of MP to cross an *in vitro* BBB model can be improved by using glutathione-dendronised carrier system and could provide a suitable base for other poorly penetrating medications intended for the treatment of other neurodegenerative diseases.

Contents

List of tables

List of figures

Acknowledgments

I would like to offer a special thanks to the Ministry of Higher Education in Iraq represented by the Iraqi Cultural Attaché in the UK for their grant. Their financial support has made finishing my PhD possible.

I would like to express my deepest appreciation to my supervisors, Professor Matteo Santin, Dr. Gary Phillips and Dr. Keng Ng. Without their guidance, patience and persistent help, this work would not have been accomplished.

I wish to express my sincere gratitude to Dr. Steve Meikle for providing valuable knowledge and resources to perform my laboratory work.

I should acknowledge Chris Morris and Maurizio Valeri for guiding me during tissue culture experiments.

I owe a great many thanks to Dr. Mark Best, Dr. Valeria Perugini and Dr. Guy Standen for their help and suggestions.

I would like to thank the Doctoral College staff, the Financial Department staff and Chemistry Laboratory staff for providing the required assistant to finish my work.

Finally, I sincerely want to express my love to my family especially my wife, **Shafaq**.

Authors declaration

Declaration

I declare that the research contained in this thesis, unless otherwise formally indicated within the text, is the original work of the author. The thesis has not been previously submitted to this or any other university for a degree, and does not incorporate any material already submitted for a degree.

Signed

Date

Abbreviations and definitions

3,3',5,5'-tetramethylbenzidine ……..	TMB
1-(4,5-Dimethylthiazol-2-yl)-3,5-diphenylformazan, Thiazolyl blue tetrazolium 98% ……..	MTT
Activator protein-1 …….	AP-1
Active efflux transport ……	AET
Adherens junctions …….	AJs
Adsorptive-mediated transcytosis ……	AMT
Blood-brain barrier …….	BBB
Bovine serum albumin ……	BSA
Cell-mediated transcytosis ……..	CMT
Cell-penetrating peptides …….	CPPs
Central nervous system ……..	CNS
Cerebrospinal fluid ……..	CSF
Convection-enhanced diffusion ……..	CED
Cytokine-induced neutrophil chemoattractant-1 ……..	CINC-1
Dalton …….	Da
Dimethylsulfoxide ……..	DMSO
Drug delivery system ……..	DDS
Dulbecco's Modified Eagle's Medium …….	DMEM
Enzyme-linked immunosorbent assay……..	ELISA
Fetal bovine serum ……..	FBS
Fluoren-9 ylmethyloxycarbonyl ……..	Fmoc
Fourier transform infra-red spectroscopy ……	FTIR
Glucocorticoid receptors …….	GR
Glutathione …….	GSH
Glutathione-phenylalanine generation-zero lysine ……..	GSH-F-Gen0K
Glutathione-phenylalanine generation-zero lysine-methylprednisolone	GSH-F-Gen0K-MP
Half maximal inhibitory concentration ……	IC_{50}
High performance liquid chromatography	HPLC
Horseradish peroxidase	HRP
Human insulin receptor …….	HIR
Human leukocyte antigen ……	HLA
Human serum albumin nanoparticles …….	HAS-NPs
Iduronate 2-sulfatase ……..	IDS

Immunoglobulin G ……	IgG
Interferon-gamma ……..	IFN-γ
Intracerebroventricular ……	ICV
Junctional adhesion molecules …….	JAMs
Lactate dehydrogenase ……	LDH
Low density lipoprotein ……...	LDL
Magnetic resonance imaging ……	MRI
Mass-to-charge ratio ……	m/z
Maximum wavelength of absorbance ……...	λ_{max}
Median lethal dose ……..	LD_{50}
Methylprednisolone …….	MP
Mice immortalised brain endothelial cells ……	b.End3
Molecular weight …….	MW
Multiple sclerosis …….	MS
N,N-Diisopropylethylamine ……	DIPEA
N,N,N',N'-Tetramethyl-O- (1H-benzotriazol-1- yl)uronium hexafluorophosphate ……...	HBTU
N,N-Dimethylformamide ……	DMF
Nuclear factor-κB …….....	NF-κB
P-glycoprotein …….	P-gp
Phenylalanine generation-one lysine dendron ……..	F-Gen1K
Phenylalanine generation-one lysine-methylprednisolone ……	F-Gen1K-MP
Phenylalanine generation-zero lysine dendron …….	F-Gen0K
Phenylalanine generation-zero lysine-methylprednisolone …….....	F-Gen0K-MP
Phosphate buffered saline ……...	PBS
Poly ethylene glycol …….	PEG
Polyamidoamine ……	PAMAM
Polypropyleneimine …….	PPI
Receptor-mediated transcytosis ……..	RMT
Resistance-associated protein ……..	MRP
Rotation per minute ……	rpm
Solid-phase peptide synthesis ……...	SPPS
Standard deviation ……...	SD
Tert-butoxycarbonyl ……	Boc
Tight junctions ……	TJs
Transepithelial electrical resistance ……..	TEER

Transferrin receptor ……	TfR
Trifluoroacetic acid ……..	TFA
Trisopropylsilane ……..	TIPS
Tumour necrosis factor-α ……	TNF-α
Area under curve ……..	AUC
Zonula occludens ……	ZOs

Chapter 1. Introduction and literature review

1.1 Multiple sclerosis

Multiple sclerosis (MS) is a chronic progressive demyelinating disorder of the central nervous system (CNS). It is an autoimmune disease mediated by autoreactive T-cells and associated with inflammation in the brain white matter (Hafler, 2004). The disorder is triggered by environmental factors in individuals with high-risk genetic profiles (Sawcer *et al.*, 2011). Together, these factors trigger a series of events, involving the engagement of the autoimmune system, acute inflammatory injury of myelin and axons, followed by recovery of nerve function and structural repair of damaged neurons and neurodegeneration in final stages of the disease (Frohman *et al.*, 2006).

Common symptoms of the disease include spasticity, fatigue, ataxia, paresthesia, diplopia, bowel or bladder dysfunction, numbness or weakness of the limbs, mental changes and loss of vision. MS is not curable and the treatment is only aimed at reducing the frequency and limiting the lasting effect of relapses, relief of symptoms, preventing disability arising from disease progression and promoting nerve repair (Thrower, 2009). The therapy may include immunomodulating drugs to reduce the frequency of relapses, glucocorticoids to treat acute exacerbations, and the antiviral drug, amantadine to treat fatigue. Other medications are used for specific MS-related symptoms (Benjamin *et al.*, 2011).

1.1.1 Historical perspective

MS was first described in 1868 by Jean Martin Charcot, a French neurologist at the Salpetrière Hospital in Paris. He noticed the accumulation of inflammatory cells within the brain and spinal cord white matter of patients with intermittent symptoms of neurologic dysfunction (Charcot, 1877). This observation led to the term *sclérose en plaques disseminées*, or multiple sclerosis.

In 1948, Elvin Kabat observed an increase in oligoclonal immunoglobulin in the cerebrospinal fluid of patients with MS. This observation provided further proof of the disease's inflammatory nature (Kabat *et al.*, 1950). In the last decades, several large population-based MS twin studies demonstrated a strong genetic basis to this disease (Kinnunen *et al.*, 1987; Mumford, 1992; Utz *et al.*, 1993). Lastly, the theory that MS is secondary to an autoimmune response to self-antigens in a genetically vulnerable host was generally accepted on the basis of Thomas Rivers study at the Rockefeller Institute in 1933 (Rivers *et al.*, 1933).

1.1.2 Epidemiology

The prevalence of MS in the UK is approximately 100 *per* 100,000 (NHS, 2017). Like other autoimmune diseases, it is more predominant in females being almost twice as common in

women, and it is more common in white people compared to Asian or black people (Frohman *et al.*, 2006). The disease peak age of onset is around thirty years and its exact cause remains unknown, but certain risk factors have now been identified (Ramagopalan *et al.*, 2010). These risk factors include genetics and environmental factors.

1.1.2.1 Genetics

The genetic association of MS lies within the human leukocyte antigen (HLA) gene locus on chromosome 6 (Compston *et al.*, 2008). Certain HLA types, particularly HLA DR15 and DQ6, are thought to play an important role in the pathogenesis of the disease (Compston *et al.*, 2008). Antigen recognition by T-cells may determine whether or not abnormal responses are made towards myelin proteins. Genome-wide studies revealed that other genes, including interleukin-7 receptor may also be important (Sawcer *et al.*, 2011).

Although MS is truly polygenic and does not follow any obvious Mendelian pattern of inheritance, there are clusters within some families and those with 2 or more first-degree relatives affected are 40 times more likely to develop the disease (Sawcer *et al.*, 2011). MS is more common in certain ethnic groups and the female preponderance probably relates to female-specific physiology as no specific MS associated genes have been identified on the X chromosome (Compston *et al.*, 2008).

1.1.2.2 Environmental risk factors

Certain environmental risk factors associated with the development of MS are indicated by large-scale migration and epidemiological studies (Ascherio *et al.*, 2007). These factors are believed to affect the immune system and include prior infections with Epstein-Barr virus, measles, mumps and rubella (Martyn *et al.*, 1993), smoking, sunlight exposure deficiency and vitamin D deficiency. Interestingly, a study concerned with investigating the disease among imigrants have shown that disease risk is acquired by the age of 15 and does not change with subsequent relocation (Dean *et al.*, 1971).

1.1.3 Pathogenesis

The hallmark of demyelinating disease is the formation of the sclerotic plaque, which represents the end-stage of a process involving inflammation, demyelination and remyelination, oligodendrocyte depletion and astrocytosis and neuronal and axon degeneration (Compston *et al.*, 2008). Despite no shortage of opinion, the order and relation of these separate components remain unsolved. The maturation of the individual lesions in the brain into plaques involves several stages:

- Immune engagement.

- Acute inflammatory injury of axons and microglia.
- Recovery of function and structural repair.
- Post-inflammatory gliosis and neurodegeneration.

MS is caused by a T-cell-driven autoimmune stimuli against components of the myelin sheath of the nerve cells (Hafler, 2004). Myelin is synthesised by mature oligodendrocytes, each of which contacts short segments ranging from 20-40 juxtaposed axons in white-matter tracts of the CNS (McDonald *et al.*, 2001; Polman *et al.*, 2011).

The main target of immune attacks in MS is the oligodendrocyte population (Compston *et al.*, 2008). Oligodendrocytes are key cells for the synthesis and turnover of the myelin sheath of up to 40 neighbouring neuronal axons in the CNS. Condensed myelin membranes twist around nerve cell axons to provide functional axonal conduction of electric stimuli (Figure 1.1). Voltage dependant sodium channels cluster at the unmyelinated nodes of Ranvier, between myelin segments, from where the electrical pulses are propagated and spread passively down the myelinated nerve axons to trigger another action potential at the next node.

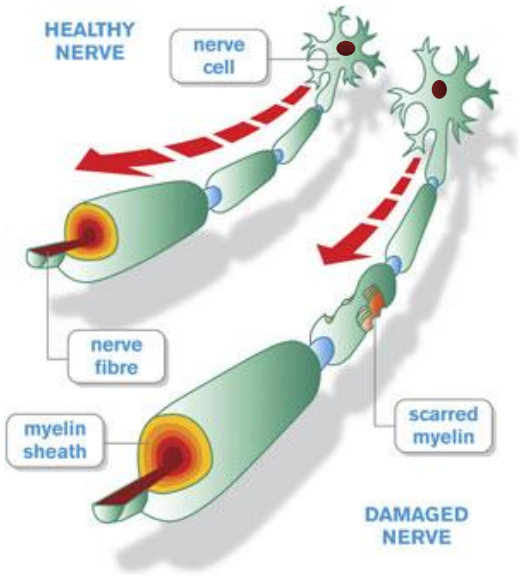

Figure 1.1 Schematic representation of nerve cell and myelin sheath protecting the axon and damaged myelin. Picture adopted from http://www.traceyourpath.com.

In genetically susceptible individuals, CD4 T-cells become primed in the peripheral blood through a process of immune dysregulation and mistaken antigen identity (Compston *et al.*, 2008). Activated T-cells will cross the blood-brain barrier (BBB), where they recognise components of the myelin sheath (Figure 1.1). Subsequently, cytokines, particularly interferon-

gamma (IFN-γ) and tumour necrosis factor-α (TNF-α) will be released by immune cells, which, in turn, activate macrophages and CD20 B-cells (Compston *et al.*, 2008). Local inflammation ensues, resulting in destruction of oligodendrocytes with demyelination of axons (Frohman *et al.*, 2006). Myelin sheath disruption leads to subsequent reduced conduction velocities of the nerve fibres. In some cases this results in the focal neurological symptoms, known as 'relapses', experienced by patients (Lublin *et al.*, 2014). Although local inflammation eventually resolves and remyelination does occur, the affected nerve fibres do not always escape damage, resulting in axonal loss observed as brain atrophy. Inflammatory episodes can be frequent in early disease, but often subside and patients enter secondary progressive disease, in which gradual axonal loss is the main cause of increased disability (Hafler, 2004).

1.1.4 Clinical features and diagnosis of MS

MS lesions in the brain and spinal cord impair and affect almost every normal function of the CNS. Clinical features differ from mild case to severe; the episodes can be relapsing-remitting or progressive, and the symptom severity and relapses increase over time. In most patients, clinical manifestations indicate the participation of motor, sensory, visual and autonomic systems but many other signs and symptoms may occur. The most frequent clinical features are:

1. *Fatigue:* It is the number one problem and most frequent symptom in two thirds of MS patients (Noseworthy *et al.*, 2000; Reder *et al.*, 1983). In MS patients, the normal motor fatigue after exercise and muscular activity is magnified and often develops quickly even after only minimal activity. It is different from weakness and might not be correlated with strength of individual muscles (Schwid *et al.*, 1999).

2. *Cognitive function:* Although language skills, higher cortical functions, and intellectual function usually appear normal in MS patients to casual observers, careful clinical observation of MS patients and sensitive neuro-psychological tests reveal slight to moderate cognitive slowing, processing of information, difficulties in finding words, reduced recent memory and decrease in effortful measures of attention in 50% of patients (Beatty, 1999).

3. *Depression:* The incidence of depression is 2-3 times higher in MS patients and their families. Severe, acute attacks of MS are associated with more depression compared to primary progression. This depression can be attributed to plaque formation and hypometabolism in different brain areas (Feinstein *et al.*, 2004).

4. *Brainstem abnormalities:* Lesions and scars in the brainstem caused by MS disrupt internuclear connections, autonomic, motor and sensory long tracts signalling. The most frequent target

for brainstem scars is the third cranial nerve (oculomotor nerve). Smell sensation is reduced in 40% of MS patients and taste is decreased in 20% (Dahlslett *et al.*, 2012).

5. *Cerebellar dysfunction and tremor:* About 50% of MS patients suffer from damage in the cerebellum or its pathways. Severe cerebellar clinical signs interact with poor pulmonary function. However, parkinsonian symptoms and dystonia are rarely caused by a MS plaque (Waubant *et al.*, 2003).

6. *Weakness and spasticity:* Patients suffer from limb weakness especially in the legs causing foot-drop, poor stair climbing or tripping. The spasticity developed in MS patients worsens with a full bowel or bladder, exposure to cold and pain. Severe spasticity can cause painful tonic spasms which are provoked by exertion or hyperventilation (Maimone *et al.*, 1991).

7. *Bladder and sexual dysfunction:* Bladder dysfunction is common and distinctly reduces the quality of life of MS patients. It is the initial clinical symptom in 5% of patients and later on develops in 90% of the patients. About two thirds of patients suffer from bladder hyperreflexia with frequency and urgency which is complicated by sphincter dyssynergia in more than half of the patients (Andrews *et al.*, 1997; Schoenberg, 1983).

8. *Sensory symptoms:* Sensory symptoms such as numbness and sensory loss are common in MS. Sensory loss in MS patients ranges from decreased olfaction to loss of pain perception in small areas or over the entire body. Deficient perception of vibration in the feet with spared position sense, is present in most MS patients which sometimes can be improved by drug therapy (Smith *et al.*, 2001).

9. *Lhermitte sign:* In 1924, Lhermitte described an electric painful current following flexion of the neck in MS. About half of MS patients have the Lhermitte sign, and 95% of them have cervical cord lesions. This rapid, brief "electric shock" or "vibration" runs from the neck down the spine. The severity of the pain is directly related to the magnitude and rapidity of neck flexion (Page *et al.*, 1982).

10. *Optic neuritis:* Approximately 2/3 of MS patients suffer from optic neuritis, especially in younger patients. Thirty-one percent of army recruits with MS suffer from optic problems. Optic neuritis typically starts with subacute loss of vision in one eye. The central scotoma is manifested as dark patch or a blurring with distortion in contrast sensitivity and colour perception.

Approximately 80% of patients present with relapsing-remitting disease. Typically, the disease passes through phases of relapse with complete recovery, relapse with persistent deficits, and secondary progression. In about 25% of MS patients, the disease never affects daily living activities (Lublin *et al.*, 2014). However, about 10% of all patients with MS are rendered

wheelchair bound and unable to work 10 years after the disease onset (Wakerley *et al.*, 2008). Episodes happen at random intervals, but initially average about one *per* year, decreasing thereafter steadily. The onset of MS is usually in the third or fourth decade (Ramagopalan *et al.*, 2010).

MS is traditionally described as clinical symptoms or signs of two CNS lesions separated in time and space that are not caused by other CNS disease. Due to the absence of a specific immune-based assay, the diagnosis of MS continues to be predicated on the clinical history and careful neurological examination of the patients; that is, finding multiple lesions and scars in time and space in the CNS. Magnetic resonance imaging (MRI) remains the most important diagnostic tool for allowing the early and more precise diagnosis of the disease. Revised diagnostic criteria classify individuals in the categories of MS into either not MS or possible MS based on evidence from MRI (McDonald *et al.*, 2001).

Cerebrospinal fluid (CSF) examination allows the identification of oligoclonal immunoglobulin G (IgG) protein bands which are present in almost all MS patients (98%), but can be absent in early stage of the disease. Also, approximately 80-90% of patients with MS have delayed visual evoked potentials (mainly optic neuritis). Finally, although there is no specific blood test for MS, the absence of other autoimmune markers (such as anti-neutrophil cytoplasmic antibodies, anti-nuclear antibodies, anti-double-stranded DNA antibodies, anti-phospholipid antibodies and extractable nuclear antigen) can be helpful.

Criteria that determine the diagnosis of MS have been revised several times in the last two decades (2001, 2005, and 2010) (Polman *et al.*, 2011). Criteria now enable diagnosis of MS when new MRI lesions define separation in time and space i.e., a new MRI lesion more than 30 days or enhancement more than 3 months after the initial episode (McDonald *et al.*, 2001). These criteria are helpful in diagnosing MS in patients after clinically excluding other demyelinating disease.

Primary problems of MS are from CNS inflammation and damage of the neurons. Secondary symptoms develop from muscle deconditioning, social disruption and drug adverse effects (Frohman *et al.*, 2006). Many symptoms of MS can be treated to improve the patient's lifestyle. Educating patients about the consequences of demyelination of the nerve fibres is an important first step. The second intervention is advising them to avoid drugs that cause weakness, fatigue, or confusion, or having a lifestyle that increases disease activity (such as drinking alcohol and smoking). Furthermore, encouraging the patients to do more mild

exercises such as cycling which can be correlated with less fatigue and fewer MS symptoms (Huisinga *et al.*, 2011).

1.1.5 Treatment of MS

The goals in MS treatment are:

1. *Reduction of relapse rate:* Since incomplete recovery from MS attacks can cause permanent disability, the accumulation of disability in MS patients during the relapsing-remitting stage of the disease can be directly correlated to the frequency of these relapses. Several drugs that can be used to reduce the relapse rate in MS are listed in Table 1.1.

Table 1.1 Disease modifying treatments for MS. (Benjamin *et al.*, 2011)

Drug	Mode of action
Interferon-ß-1a (Avonex®, Rebif®)	Immunoregulatory including antagonism of gamma interferon, reduction of cytokine release and augmentation of suppressor T-cell function
Interferon-ß-1b (Betaferon®)	Immunoregulatory including antagonism of gamma interferon, reduction of cytokine release and augmentation of suppressor T-cell function
Natalizumab (Tysabri®)	Recombinant humanised monoclonal antibody to alpha-4 integrins, inhibiting leucocyte migration from blood to CNS
Fingolimod (Gilenya®)	Sphingosine 1-phosphate receptor modulator
Mitoxantrone (Onkotrone®)	Anthracenedione derivative that inhibits DNA and RNA synthesis by intercalation of DNA base pairs. Prevents DNA repair by inhibiting topoisomerase II
Glatiramer acetate (Copaxone®)	Modifying immune processes that are responsible for the pathogenesis of MS

2. *Prevention of disability caused by relapse attacks:* Corticosteroids reduce the duration of relapses and hence their short-term morbidity. Corticosteroids enter the cell nucleus and inhibit transcription of pro-inflammatory factors, such as interleukin-1, interleukin-2, TNF-α and pro-inflammatory mediators, including elastase, collagenase, and plasminogen activator. These anti-inflammatory drugs have long been used for the treatment of acute MS relapses (Milligan *et al.*, 1987; Thrower, 2009).

In the case of preventing disability caused by progression of the disease as a result of nerve damage, the immuno-modulatory treatment is of little benefit once myelin degeneration has

reached a critical threshold and clinical progression of the disease is established. In the early stage of MS, there is an opportunity to supress or reduce those components of the inflammatory process which cause initiation of the cascade events that lead to disease progression. Thus, the aim of immunotherapies is not only the reduction of acute relapse frequency, but also the prevention of transition to the secondary permanent progressive phase of the disease (Rodriguez, 2003).

3. *Symptomatic treatment of neurological deficits:* In many situations, the priority is to mask individual symptoms caused by neurological deficits in order to improve the quality of everyday life of the patients. The most amenable symptoms of MS and the desired treatment are shown in Table 1.2.

Table 1.2 Therapy directed at the symptoms of MS (Benjamin *et al.*, 2011).

Symptom	Drug	Common side-effects
Acute relapses	Methylprednisolone	Fluid and electrolyte disturbances, Cushing syndrome
Spasticity	Baclofen	Weakness, fatigue, headache, insomnia, confusion, ataxia, frequency, urgency, dysuria, constipation
	Diazepam	Drowsiness, ataxia, dependency
	Dantrolene	Muscle weakness, drowsiness, hypertension, drooling, enuresis, diarrhoea, nausea
Paroxysmal symptoms of MS	Carbamazepine	Fatigue, weakness, ataxia
Fatigue	Amantadine	Nervousness, depression, nightmares, hallucinations, insomnia, dizziness, headache, blurred vision, orthostatic hypotension, peripheral oedema, dry mouth, gastrointestinal side effects
Intention tremor	Clonzepam	Drowsiness, ataxia, dependency
	Propranolol	Nausea, diarrhoea, bronchospasm, dyspnoea, cold extremities, bradycardia, hypotension
	Carbamazepine	See above
Urinary urgency	Oxybutynin	Dry mouth, constipation, nausea, vomiting, dyspepsia, blurred vision, dry eyes, tachycardia, facial flushing

	Propantheline	Dry mouth, constipation, nausea, vomiting, dyspepsia, blurred vision, dry eyes, tachycardia
	Amitriptyline or imipramine	Dry mouth, constipation, nausea, vomiting, dyspepsia, blurred vision, dry eyes, tachycardia
Erectile dysfunction	Sildenafil	Rash, diarrhoea, urinary tract infections, abnormal vision

4. *Treating established progression:* Remyelination of the nerve fibres might have little or no effect to offer for axons degenerated early as a direct result of the inflammatory process activation. Conversely, early remyelination treatment might be neuro-protective and its timing is important if the naked affected axon is resistant to the inflammatory milieu, but has reduced survival properties (Wolswijk, 1998). The repair of damaged nerves in MS involves several different processes concerning the two essential steps of the evolution of the disease which are the loss of myelin sheaths and the loss of axons. A realistic aim of remyelination treatment is to promote myelin regeneration and prevent further axon loss. These two objectives are closely related to each other since promoting remyelination is probably a highly effective method of preventing axon loss (Rodriguez, 2003). Myelin repair can be promoted by two different approaches. The first approach is the transplantation of neural cells with a repair enhancing and myelinogenic capacity (Baron-Van Evercooren *et al.*, 2004). The second approach is to promote or reactivate the endogenous process of nerve cell remyelination (Baron-Van Evercooren *et al.*, 2004).

An important hurdle to the effective treatment of neurodegenerative diseases including MS is the presence of the neuroprotective BBB, which prevents delivery of potentially active therapeutic compounds essential for the treatment of neurodegenerative diseases.

1.2 The BBB

First described by Paul Ehrlich (1885), the BBB is formed by the endothelial cells lining the cerebral microvessels. It is highly physiologically regulated and it is an efficient barrier that provides a sanctuary to the brain. It is designed to protect and regulate brain homeostasis and to permit selective transport of nutrients and other hydrophobic molecules that are essential for brain function. It forms a continuous, almost impermeable, cellular barrier that dramatically limits and regulates the traffic of xenobiotics, nutrients, immune surveillance cells (macrophages) and endogenous compounds into the brain parenchyma.

While this protective function of the BBB is essential for normal physiological function inside the brain microenvironment, it represents the main obstacle for the entry of drugs molecules into the CNS (Reese *et al.*, 1967). The endothelial cells forming the BBB differ from vascular endothelial cells in other regions of the body by their unique ability to form tight intercellular junctions, the absence of fenestrations between adjacent cells and minimal pinocytotic activity (Brightman *et al.*, 1969) thus limiting, to a great extent, drug penetration into the brain parenchyma. In addition, the BBB expresses various efflux transporters, which actively and continuously pump compounds out of the endothelial cells back into the blood stream (de Lange, 2004).

The most crucial factor that limits the synthesis and development of new drugs for CNS diseases is therefore, the presence of the BBB. The BBB limits to a great extent the brain penetration of most CNS drug candidates (Pardridge, 2005a). As the number of individuals suffering from CNS condition will grow with an aging population (the number of people older than 65 years will increase by almost 50% world-wide by 2020), it will become particularly problematic that only a few drugs are able to cross the BBB (Pardridge, 2005a). Solving the BBB drug delivery problem requires novel approaches to this area of pharmaceutics. The old brain-drug delivery methods such as attempting to make water-soluble small drug molecules more lipophilic *via* medicinal chemistry modifications or through cranial microscopy for trans-cranial brain drug delivery, must give way to new approaches (Gabathuler, 2010). The new technology is based on employing endogenous BBB transporters, and aims to reformulate drug structures so that these drug molecules can cross the BBB *via* utilising these endogenous transport systems (Abbott *et al.*, 1996).

However, unless more research and studies are performed to improve drug delivery to the brain through the BBB, the future of CNS drugs will be limited only to small lipid-soluble molecules with molecular weight (MW) not exceeding 400 Da that can cross the BBB *via* lipid-mediated free diffusion. Such drugs can treat limited CNS conditions, such as schizophrenia, depression, insomnia and epilepsy (Ghose *et al.*, 1999).

1.2.1 Physiology of the BBB

For optimal activity, the CNS requires a perfectly regulated and balanced environment and homeostasis with specialised characteristics far different from those in other organs of the organism. The main factor maintaining and preserving the homeostasis of the CNS is the proper function and integrity of the BBB. The essential function of the BBB as a protective

barrier for the brain parenchyma is only one aspect of its many tasks, which includes metabolic features, physical functions and transport (Bernacki *et al.*, 2008).

1.2.2 BBB structure

The BBB has to be a very stable, well organised structure to maintain and protect CNS homeostasis. However, for fast adaptation to changing conditions inside the body, the BBB also requires extreme flexibility (Chaudhuri, 2000). This special characteristic depends on many structural and functional properties of BBB components.

1.2.2.1 Endothelial cells

Brain endothelial cells differ from the endothelial cells of the peripheral circulation by the presence of tight junctions (TJs) and other tightening proteins (Figure 1.2). The high number of cytosolic mitochondria inside these cells suggests their high energy metabolism. Brain endothelial cells lack fenestrations in their plasma membranes (Abbott, 2005; Ballabh *et al.*, 2004) and their permeability is highly selective for molecules with suitable mass (MW less than 400 Da) and lipophilicity (Chaudhuri, 2000).

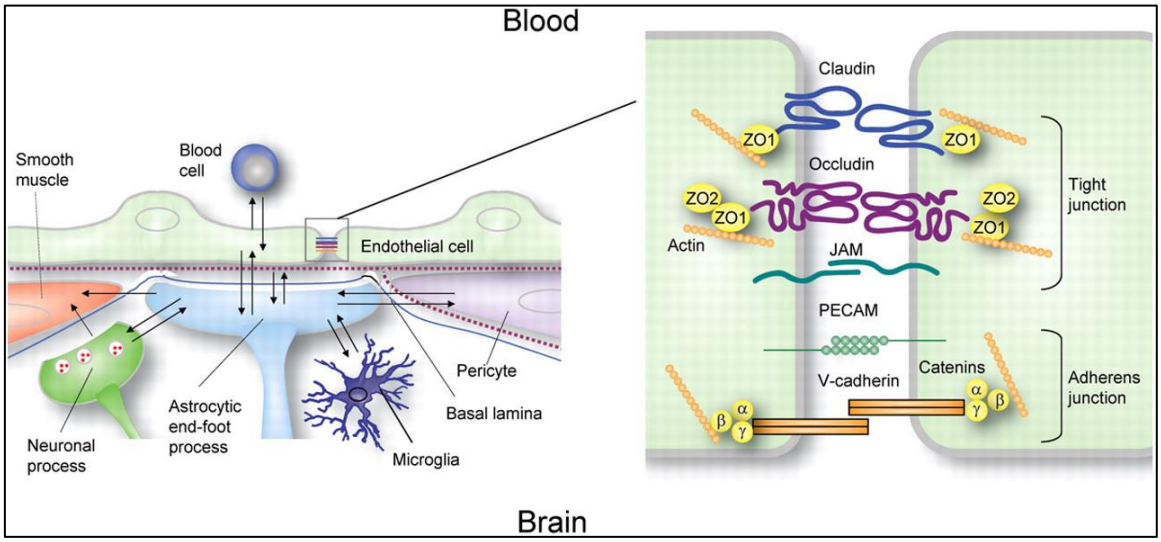

Figure 1.2 Neurovascular unit and molecular components of the physical BBB (Picture adapted from www.neurology.org).

Several identifying markers are specific for brain endothelial cells such as glucose transporter-1 (GLUT-1), von Willebrand factor (vWF), γ-glutamyl-transpeptidase, endothelial barrier antigen and OX-47 antigen (Ballabh *et al.*, 2004). The luminal surface of the BBB endothelial cells is covered by a negatively charged mesh or network of glycoproteins, proteoglycans, and glycolipids (van den Berg *et al.*, 2006). In addition, BBB endothelial cells are also unique from other endothelial cells outside the CNS due to the presence of two N-glycosylated

phosphoproteins; P-glycoprotein (P-gp) and multidrug resistance-associated protein. Finally, the most important feature of BBB endothelial cells which enables them to act as a barrier is their TJs (Balkovetz *et al.*, 1989).

1.2.2.2 Astrocytes

Like other glial cells, astrocytes, originate from the ectoderm of the neural tube (Abbott *et al.*, 2006). There are two main types of astrocyte cells that can be recognised in the brain, protoplasmic cells which are present in the grey matter, and fibrillary cells which exist in the white matter. Protoplasmic astrocytes are characterised by having large nuclei and multiple thick cytoplasmic appendices. The endings of these appendices form a cap-like structure known as end-feet (lat.: *pes sugens*) that tightly attach to neurons on one pole and blood vessels on the other to form a highly specific relay station between neurons and blood (Figure 1.2) (Reichenbach *et al.*, 2004).

Due to their unique localisation between blood and neurons and specific characteristics, astrocytic end feet are correlated with the expression and action of agrin-heparin proteoglycan. This protein is synthesised by the basal lamina in the extracellular matrix sheet (Verkman, 2002) and is important for maintaining the BBB integrity and functions (Wolburg, 2006). Moreover, astrocytes play an essential role in discharge of waste substrates from the brain, nerve cells metabolism and nutrition. In addition, these cells have the abilities of transcytosis of special molecules and active ion transport through them (Reichenbach *et al.*, 2004).

1.2.2.3 Pericytes

Pericytes are small capillary wall-associated cells that derive from the mesoderm. They are separated from endothelial cells by the basal lamina, but gap junctions provide contact points with endothelial cells (Cuevas *et al.*, 1984). There are two types of pericytes based on their location in the brain tissue which are either located at capillary straight parts or positioned at capillary connections. Anatomically, they are equipped with claw-like appendices twisting around the capillary (Peppiatt *et al.*, 2006). In the brain, pericytes are responsible for the mediation of inflammation processes, regulation of endothelial cell activity and manage capillary like structure formation and capillary diameter (Bandopadhyay *et al.*, 2001; Nag, 2003; Peppiatt *et al.*, 2006; Ramsauer *et al.*, 2002). Therefore, pericytes play an important role in the maintenance of the integrity of the BBB and brain homeostasis.

1.2.2.4 Tight junctions

TJs are junctional complexes positioned between the endothelial cells of brain microvessels (Figure 1.2). They are the most important factors responsible for BBB impermeability to drugs

(Bernacki *et al.*, 2008). TJs exist between endothelial cells and surround the cells like a continuous belt. Morphologically, they are represented by closely joined fragments of adjacent endothelial cells known as the zonula occludens (ZOs). At these joining locations, cell membranes are completely fused and form a five-layers barrier (Ballabh *et al.*, 2004). As the number of fusion spots between TJs differs, the extent of tightness in different regions is also diverse (Ballabh *et al.*, 2004).

Functionally, TJs work in several ways. They constitute a distinctive border for lipid and protein diffusion through the endothelial membranes and grant to the endothelial cells polarity, which is demonstrated by a non-even distribution of a number of membrane transporters between the abluminal and luminal membranes. Due to complete fusion of adjacent TJs, they also close the paracellular pathway to force transport of substances through the cytosol and membranes (Grieb *et al.*, 1985). An additional function of the TJs positioned between brain endothelial cells is that they divide the membranes of these cells into two compartments: a brain-facing membrane and a blood-facing membrane. This unique division is also affected by the proteins present in each part of the endothelial cell membrane, and the distinct and fundamental interactions of these protein membranes with each other regulate if and how quickly different molecules traverse the BBB (Hawkins *et al.*, 2006). TJs are characterised by their high electrical resistance and their integrity depends on an adequate extracellular Ca^{2+} ion level. A drop of electrical resistance caused by Ca^{2+} ion depletion results in TJs destabilisation. Moreover, an increase in intracellular cATP levels causes the formation of fusion spots and tightens TJs (Wolburg *et al.*, 2002).

Several TJs plasma membrane proteins have been identified, such as occludin, claudin and adherens junction molecules. In addition, cingulin and several ZO such as ZO-1, ZO-2, ZO-3 have been recognised as membrane cytoplasmic proteins that link trans-membrane proteins with actin, which is a primary cytoskeletal protein essential for the functional and structural integrity of the brain endothelium (Balkovetz *et al.*, 1989).

1.2.2.4.1 Claudins

To date, 24 members of claudin-proteins family have been identified in mice and humans (Oller-Salvia *et al.*, 2016). Claudins are approximately 22 kDa phosphoproteins which consist of four essential transmembrane domains and appear to be the fundamental building molecule of the TJs. The claudin from one endothelial cell tightly connects with an analogous claudin protein from an adjacent endothelial cell to create the primary closure spot of the TJ, and the carboxylic end of each protein links it to cytoplasmic ZO-1, ZO-2, or ZO-3. In brain tissue,

claudin 1-3, 5 and 12 have been recognised (Abbott *et al.*, 2006) along with occludin, claudin 1-3 and 5 are present in the endothelium. It has been shown that claudin-5 is expressed particularly in brain capillary endothelial cells (Sirotkin *et al.*, 1997).

1.2.2.4.2 Occludin

Like claudin, occludin is a membrane phosphoprotein, but with a larger MW (60 kDa) (Honda *et al.*, 2006). It also consists of four essential transmembrane domains (Balda *et al.*, 2000). The TJ paracellular component is formed by the two extracellular loops of both claudin and occludin proteins, and the cytoplasmic domain is tightly connected to ZO proteins (Figure 1.2). Occludin expression has been identified in humans and mice, but not human new-borns or foetuses. Recent experiments have shown that occludin expression is the highest among those of all TJ proteins (Vorbordt *et al.*, 2004). Studies revealed numerous signals for occludin localised either to membranes of neighbouring endothelial cells or to the extracellular spaces between these cells (Vorbordt *et al.*, 2004). Besides its regulatory function, occludin influence paracellular transport (Hirase *et al.*, 1997).

Together, occludins and claudins proteins form heteropolymers and transcellular tracts containing channels for the selective transport of charged and hydrophilic molecules. Moreover, occludin might be involved in preserving the electrical resistance of the BBB and aqueous pore formation (Matter *et al.*, 2003). These essential facts, together with the structural relationships existing between occludin and claudin, suggest the contribution of these membrane proteins to the selectivity of TJ-associated diffusion (Tsukita *et al.*, 2001) and their presence appears to be fundamental for the adequate function and integrity of TJs and the BBB (Petty *et al.*, 2002).

1.2.2.4.3 Junctional adhesion molecules

Junctional adhesion molecules (JAMs) are the third building material of membrane proteins found in TJ construction (Bernacki *et al.*, 2008). They are immunoglobulins in nature with molecular masses around 40 kDa. They have a single transmembrane domain which is connected with an extracellular fragment consisting of two immunoglobulin-like loops (Petty *et al.*, 2002). Three members of this family which are JAM-1, JAM-2, and JAM-3 have been identified in the rodent brain. Also, JAM-1 and JAM-3 are localised to brain endothelial vessels, and JAM-1 was found in the human cerebral cortex (Vorbordt *et al.*, 2004). Immuno-cytochemical analysis revealed that JAM-1 is positioned unevenly in inter-endothelial junctions, where it was found either alone or forming small clusters. JAMs have been

suggested to play an essential role in cellular adhesion and monocyte migration through the BBB (Palmeri *et al.*, 2000).

1.2.2.4.4 Cytoplasmic proteins

Cytoplasmic proteins found in TJ structure include ZO proteins (ZO-1, ZO-2, and ZO-3), cingulin, and 7H6 (Bernacki *et al.*, 2008). The ZO proteins are membrane-associated guanyl kinase-like proteins which are composed of three domains of the PDZ type (PDZ1, PDZ2, and PDZ3), plus one SH3 domain, and one guanyl kinase-like domain (GUK). These domains have a primary role in protein arrangement, and consequently in plasma membrane integrity of the endothelial cells (Itoh *et al.*, 1999).

Studies indicated that the PDZ1 domain of ZO proteins binds directly to the carboxylic end of claudin, while GUK domain in ZO-1 interacts with occludin (Mitic *et al.*, 2000). Moreover, JAM proteins bind directly to ZO-1 and other PDZ-containing proteins (Ebnet *et al.*, 2000). In addition, immune-cytochemical studies indicated a close structural relationship between immune-labeled occluding and ZO-1(Itoh *et al.*, 1999).

The TJ-associated protein, 7H6, which is a phosphoprotein with 155 kDa molecular mass and is responsible for TJ impermeability to large molecules and ions (Satoh *et al.*, 1996). Unlike ZO-1, 7H6 may detach from the TJ when ATP levels decrease; this disconnection results in increased paracellular permeability. Thus, it maintains a close relationship with the functional state of the junction (Mitic *et al.*, 1998).

Cingulin, a phosphoprotein with a MW between 140-160 kDa, is localised at the cytoplasmic part of TJs (Cordenonsi *et al.*, 1999). The binding of cingulin to ZO proteins and myosin suggests its role as a scaffold between the cytoskeleton and transmembrane proteins. Other TJ cytoplasmic proteins perform signalling, adaptor, and regulatory tasks such as partitioning defective proteins, Ca^{2+}-dependent serine protein kinase, and G-protein signalling (Abbott *et al.*, 2006).

The available evidence suggests that TJ proteins not only preserve the integrity of the junction but also provide physical structural support for the brain endothelium due to the multiple connections and interactions between them (Bernacki *et al.*, 2008). Disturbances in this order influence not only the cell structure, but also the TJ integrity, consequently leading to alteration in BBB functions and CNS homeostasis.

1.2.2.5 Adherens junctions

A second example of tightening structures between endothelial cells are the adherens junctions (AJs), which are transmembrane proteins represented by the large family of cadherins. In the presence of Ca^{2+}, cadherin proteins interact with each other to form a tightening and supporting structure (Takeichi, 1995). In AJs, catenins play a similar role to that of ZOs in TJs by attaching the actin cytoskeleton to cadherins. Studies have revealed that both cadherin and catenins proteins are present in the human cortex (Vorbordt *et al.*, 2004).

1.2.3 Transport routes across the BBB

Blood and CSF circulation are most important pathways to enter brain parenchyma. In the human brain, there are more than 100 billion capillaries in total, providing approximately 650 km combined length of brain capillary endothelium of and approximately 20 m^2 total surface area (Pardridge, 2003).

The unique biological and anatomical features of the BBB such as the few pinocytotic vesicles and the absence of fenestrations in endothelial cell membranes, the presence of various transporters especially P-gp, the presence of sophisticated complex of trans-membrane proteins of TJs and the lack of lymphatic drainage all result in the low and selective penetration of molecules through the BBB.

There are several transport pathways for molecules to cross the BBB (Figure 1.3), which include:

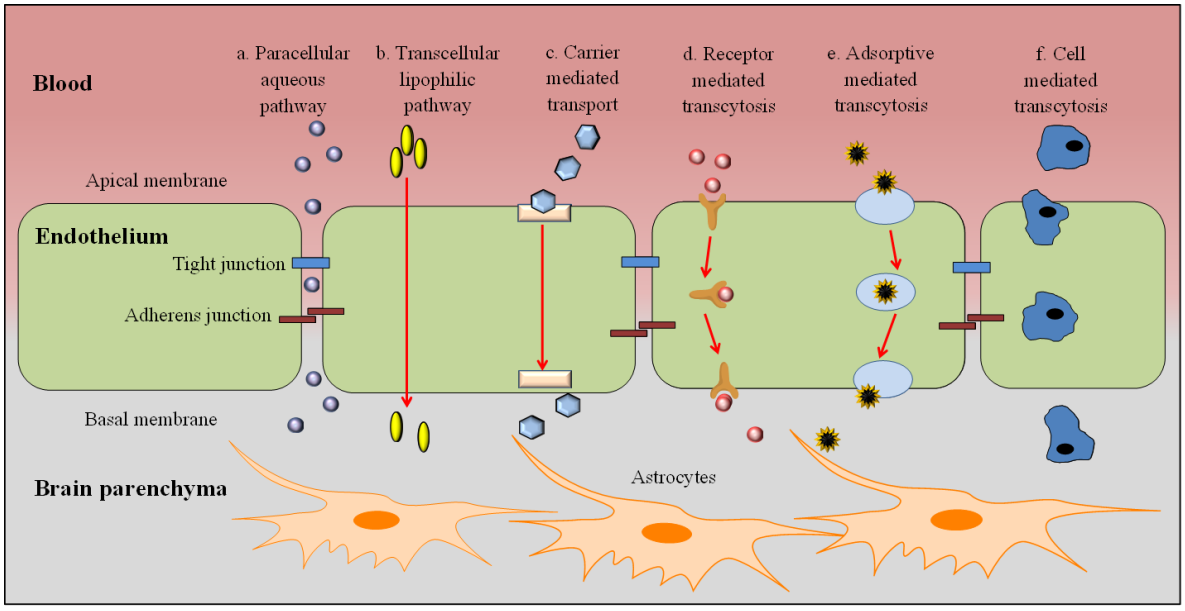

Figure 1.3 Access pathways across the BBB endothelial cells.

• *Paracellular aqueous pathway*: Small water-soluble molecules can simply diffuse through the TJs but not to any great extent. (Figure 1.3.a) In the past two decades, there has been a notable emerging knowledge and understanding of molecules involved in TJ structures, and parallel discovery of TJ modulators which can be used for temporary opening of the BBB, ranging from biological (such as viruses) and chemical substances (such as cyclodextrin) to physical stimuli (such as ultrasound) (Deli, 2009).

• *Transcellular lipophilic pathway:* Small lipid soluble substances like alcohol and steroid hormones penetrate through the BBB by dissolving in the lipid-rich plasma membrane. (Figure 1.3.b)

• *Carrier mediated transport:* Binding of a solute such as amino acids or glucose or nucleosides to a protein transporter on one side of the endothelium membrane initiates conformational changes (Figure 1.3.c). These structural changes in the protein can result in the transport of these solutes to the other side of the membrane. ATP may provide the energy to facilitate the process. On the other hand, TJ efflux pumps such as P-gp are responsible for extruding drugs from the brain and this mechanism is one of the major obstacles for the accumulation of a wide range of biologically active molecules in the brain parenchyma (Pardridge, 2005b).

• *Receptor-mediated transcytosis (RMT):* This process provides a means for highly selective uptake of macromolecules into the brain tissue (Figure 1.3.d). Brain endothelial cells have receptors for the uptake of many different types of ligands, including growth factors, insulin, enzymes and plasma proteins. RMT has been extensively studied for enhancing brain penetration and targeting. Well-characterised systems include the transferrin receptor (TfR), insulin receptor, lipoprotein receptors especially apolipoprotein E and glutathione (GSH) transport (Rip *et al.*, 2009).

• *Adsorptive-mediated transcytosis (AMT):* Also known as the pinocytosis route, this process is triggered by an electrostatic interaction between a positively charged substance, usually the charged moiety of a peptide, and the negatively charged plasma membrane surface (i.e. heparin sulphate proteoglycans) (Figure 1.3.e). Adsorptive-mediated transport has a lower affinity but higher transporting capacity compared to RMT (Herve *et al.*, 2008).

• *Cell-mediated transcytosis (CMT):* This transport route depends on immune cells such as monocytes or macrophage for the crossing of the intact BBB (Park, 2008). Unlike other transport pathways which normally permit only solute molecules with specific properties to be transported, CMT is unique in that it can be used for virtually any type of drug molecules or other materials as well as particulate carrier systems (Park, 2008).

1.2.4 Impact of pathological conditions on the BBB

The properties of the BBB are significantly changed when the brain tissue is developing a neurological disorder, or in inflammatory conditions or under attack by pathogens (Rip *et al.*, 2009). These changes affect the integrity and the functions of the BBB, especially the transport pathways. Studies suggest that the BBB's integrity is greatly compromised in brain disorders or neurological diseases such as stroke, Alzheimer's disease, MS, HIV, Parkinson's, ischemia and brain tumours (Abbott *et al.*, 2006; Holman *et al.*, 2011; Huber *et al.*, 2001). MS causes enhanced leukocyte inflammatory activation which result in the release of inflammatory cytokines/chemokines mediators inside the brain (Minagar *et al.*, 2003).

In addition, studying the functions of TJ signalling pathways, structural components and regulation of TJs under different conditions, implies that the permeability of the BBB is greatly influenced by the stimuli initiated by pathological and physiological conditions such as oxidative stress (such as free oxygen radicals like peroxide), inflammatory mediators (such as interleukin-1β, interferon-γ, and TNF-α), vasogenic agents (such as histamine), lipid mediators (such as prostaglandins), infective agents (viruses and virus components, bacteria and bacteria toxin, fungal pathogens and parasites), as well as physiological stimuli (such as intracellular Ca^{2+} levels) and immunological cells (such as leukocytes) (Deli, 2009; Stamatovic *et al.*, 2008). Transport systems and pathways across the BBB are also greatly affected in neurological disorders. For example, P-gp expression and efflux ability are changed during pathogenesis associated with a number of neurological disorders such as Alzheimer's disease (Persidsky *et al.*, 2006).

1.2.5 Drug delivery across the BBB

The global market of CNS pharmaceuticals is highly underdeveloped and would have to grow by more than 500% just to equal the cardiovascular drug market (Abdullahi *et al.*, 2017). However, there are more patients suffering from CNS disorders than patients with cardiovascular diseases (Pardridge, 2002b). The deficiency in CNS drug development is attributed to the fact that more than 98% of recently developed novel drugs, such as recombinant proteins, monoclonal antibodies, and non-viral gene medicines, are ineffective for brain disorders, because these novel drugs cannot penetrate the brain capillary endothelial wall of the BBB.

In the past, researchers focused on developing small molecule drugs for CNS disorders as it was widely believed that any small molecule crosses the BBB. However, it is well established now that only less than 2% of all small drug molecules can cross the BBB (Abbott, 2005). To

cross the BBB in pharmacologically sufficient amounts, a drug molecule must have a molecular mass less than 400 Da, plus it should be lipid soluble, and not be a substrate for an active efflux transporter localised at the BBB such as P-gp (Pardridge, 2005a). Most small molecular mass drugs, and all large molecule therapeutics, lack these structural and chemical properties, and this explains why it is so hard to develop new drugs for the brain. Only 5% of more than 7000 small molecule drugs in the Comprehensive Medicinal Chemistry (CMC) are pharmacologically active in the CNS, and these are effective in only limited CNS diseases (such as affective disorders, chronic pain and epilepsy) (Ghose *et al.*, 1999). There is an urgent need for developing new drug delivery strategies to improve penetration of drugs used for the treatment of various CNS diseases, including Alzheimer's disease, MS, Huntington's disease, Parkinson's disease, stroke, brain trauma, brain cancer, spinal cord injury and pathological infections of the brain, including acquired immune deficiency syndrome (AIDS) (Pardridge, 2005a).

1.2.6 Brain drug delivery strategies

As molecular transport to the CNS is impeded by the presence of the BBB, efficient drug delivery to the brain requires special strategies. These strategies can be divided into four different categories: (i) neurosurgical-based strategies, which develop invasive or transcranial brain-drug delivery; (ii) chemistry-based strategies, which use medicinal chemistry approaches to increase the lipid solubility of the drug; (iii) transient BBB disruption strategies; and (iv) system-mediated transport, which involve reformulation of the drug to access using endogenous BBB transporters.

1.2.6.1 Transcranial brain drug delivery

This category involves three main methods to overcome the BBB which are: (i) the intracerebroventricular (ICV) infusion of drug, (ii) the intracerebral (IC) implantation of drug and (iii) the convection-enhanced diffusion (CED) of drug. However, all these methods of bypassing the BBB experience some limitations. The ICV infusion method delivers drug to the ependymal surface of the brain but not deep enough into brain parenchyma. The entire CSF volume of the human body (about 140 mL) is completely turned over every four hours (Blasberg *et al.*, 1975). This bulk flow of fluid out of the CSF tracts is fast especially when compared with the slow rate of solute diffusion into the brain. As a result, drug concentration in brain parenchyma drops exponentially within millimetres of the ependymal surface (Blasberg *et al.*, 1975). Diffusion of any drug molecule decreases exponentially with the diffusion distance. Consequently, drug delivered to the brain by the IC implantation approach does not move significantly into the brain tissue from the original implantation site (Krewson

et al., 1995). The brain is the only organ without a lymphatic system and is not designed to eliminate significant fluid volumes, thus fluids entering the brain tissue from the CED device preferentially moves along white matter tracts (Voges *et al.*, 2003). Finally, all these techniques are invasive procedures that involve high risk factors such as long or permanent CNS damage.

1.2.6.2 Chemical modification of drug molecules

The classical chemistry-based method for delivering small molecules to the brain is to increase the lipid solubility of the drug with pharmaceutical chemistry manipulation. However, to date there is not a single example of a water-soluble drug being converted into a CNS active therapeutic drug by medicinal chemistry *via* increasing lipophilic nature of the drug (Chen *et al.*, 2017). Usually, increasing the lipophilic characteristics of drug involves the addition of side chains that block hydrogen bonding moieties, such as carboxyl and hydroxyl groups. However, these modifications might lead to numerous problems such as:

(i) The loss of affinity between the modified drug and its target receptor. Also, the lipidised drug might have unwanted pharmacokinetic effects which are absent in the parent drug.

(ii) The modifications of the drug might increase the MW over 400 Da, which is the critical threshold for drug penetration through the BBB (Fischer *et al.*, 1998). This MW increment will offset the benefit of the increased lipid solubility.

(iii) Increasing lipid solubility of a drug will increase its uptake by all body tissues leading to a rapid clearance of the drug from the blood stream. This reduced plasma concentration of the drug caused by enhancing its lipid solubility offsets the increased BBB penetration resulting in only a small increase in brain drug uptake (Pardridge, 2003).

1.2.6.3 BBB disruption

One of the approaches for delivering drug to the brain is by temporarily disrupting the BBB endothelium permeability especially the TJs. In the past two decades, there has been a gradual understanding of the molecular interactions involved in TJs, and corresponding discovery of modulators which can be applied for transient and short opening of the BBB, ranging from chemical and biological substances to physical stimuli such as high-frequency focused ultrasound and electromagnetic fields (Deli, 2009; Hynynen, 2008; Stam, 2010).

The rationale for modulating TJs opening to enhance the drug delivery to the brain by the paracellular pathway are: (i) many brain diseases and stimuli are already associated with TJ opening or increased BBB leakage phenomena; (ii) the delivery of small water soluble molecules into the brain will be increased by enhanced paracellular transport; (iii) TJ opening by different modulators may also improve the BBB passage of macromolecules and drug

delivery systems (DDS) including nanoparticles, liposomes, dendrimers conjugates, micelles, and their distribution in the brain; (iv) utilising physical stimuli such as electromagnetic fields and ultrasound will temporarily cause local BBB disruption, thus, concentrated drug can be delivered locally. The TJs of the BBB can be transiently disrupted by a number of ways such as biological, chemical and physical stimuli.

a) Enhanced permeability by biological stimuli

Several biological modulators with the ability to temporarily open TJ to improve the transport of drug molecules to the brain have been reported and studied using *in vitro* cell models (Karyekar *et al.*, 2003). A 45 kDa biological molecule ZO toxin, which is an active TJ modulator at the BBB, can promote a reversible, concentration dependent TJ transient opening based on transepithelial electrical resistance (TEER) measurements, which consequently increases the paracellular transport of permeability indicators such as sucrose and inulin without noticeable short-term toxicity in cultured bovine brain capillary endothelial cells. Moreover, it also permits an improved transport of the therapeutic agents, paclitaxel and doxorubicin which are substrates of the P-gp pump and normally have very limited transportation across the BBB (Karyekar *et al.*, 2003).

Vasoactive compounds and inflammatory stimuli such as bradykinin, histamine and vascular endothelial growth factor are another group of biological compounds which can trigger TJs opening. They are mediators or products of the inflammatory response and can enhance BBB permeability (Abbott, 2000; Kumar *et al.*, 2009). In gliomas and other brain tumours, endothelial permeability in tumour tissue is more sensitive to the effects of these biological modulators than the normal brain endothelial cells (Vajkoczy *et al.*, 2004). Therefore, these stimuli, when used in combination with gene or anticancer drugs and imaging materials, can probably promote the delivery of these macromolecules to the brain tumour for tumour diagnosis purposes, chemotherapeutic treatment tumour or gene therapy. This hypothesis is supported by the experimental data obtained on a rat glioma *in vitro* model which revealed that intracarotid histamine infusion selectively increased permeability of Evans blue-albumin stain and improved the transport of α-aminoisobutyric acid in brain tumour tissues without affecting BBB permeability in the normal brain tissues (Inamura *et al.*, 1994; Nomura *et al.*, 1994).

A synthetic peptide analogue of bradykinin protein, cereport [Arg-Pro-Hyp-Gly-Thi-Ser-Pro-Tyr (CH_2NH) Arg] has been thoroughly studied for improving drug transport through the

paracellular pathway of the BBB (Borlongan *et al.*, 2003; Emerich *et al.*, 2000; Emerich *et al.*, 1999; Emerich *et al.*, 1998). Cereport increases drug permeability of the BBB by temporarily disrupting the TJ (Sanovich *et al.*, 1995). It shows distinct dose, time and size dependent activity on human brain capillary endothelial cells and its action can be adjusted through changes in cGMP and cAMP second messenger systems (Mackic *et al.*, 1999). Studies have shown enhanced BBB transport of a number of drug molecules including loperamide, carboplatin and acyclovir by conjugation with cereport protein in different types of diseased animal (Bidanset *et al.*, 2001; Emerich *et al.*, 1999; Emerich *et al.*, 1998).

Finally, viruses are biological factors which can stimulate and temporarily open the TJs through upregulation of chemokines protein as a precursor for infiltration of inflammatory cells into the CNS (Kuang *et al.*, 2009). Histochemical analysis of CNS tissue from HIV infected patients showed substantial TJ disruption in patients who died with HIV encephalitis, which was shown by fragmentation or absence of immune-reactivity for TJ proteins especially occludin and ZO-1 (Dallasta *et al.*, 1999).

b) Enhanced uptake by chemical stimuli

There are several examples of chemical stimuli which can be used to modulate the TJ functions to increase the permeability of the BBB for drug transport (Deli, 2009). One of these examples is *via* arterial injection of hyperosmolar solutions (such as arabinose or mannitol). The shrinkage in brain endothelial cells size (caused by osmolarity differences) results in transient opening of gaps between these cells. One major limitation of this method is that it is invasive to the patients and requires considerable expertise to be performed properly (Doolittle *et al.*, 2000).

Some pharmaceutical excipients such as, oleic acid which is protein kinase C activator, showed reversible opening of the BBB to aminoisobutyric acid and Evans blue-albumin when it was given *via* arterial infusion in a rat model (Sztriha *et al.*, 1991). Another pharmaceutical excipient, lysophosphatidic acid was also reported to improve TJs permeability in cultured brain endothelial cells (Schulze *et al.*, 1997) by the activation of protein kinase C-α ducts which reduces claudin-5 expression in the TJs (Gan *et al.*, 2008). Like biological stimuli, its effect was also dose-dependent, short and reversible, and its action can be terminated by activation of protein kinase C (Schulze *et al.*, 1997). One of the most commonly used excipients in the pharmaceutical industry, sodium dodecyl sulphate, has also been shown to promote an increased transport of α-aminoisobutyric acid through the TJs at a dose of 25-100 μg/kg in

rats (Saija *et al.*, 1997). This effect can be attributed to the fact that sodium dodecyl sulphate is an anionic charged surfactant which function as a solubilisation agent and may interact with proteins or lipids in the cell membrane (Kato *et al.*, 1987).

c) Enhanced delivery by physical stimuli

The ability of energy-based physical methods, such as microwave, ultrasound and electromagnetic fields, to open the BBB has been extensively investigated (Hynynen, 2008; Stam, 2010). Ultrasound, non-invasively, induces local biological stimuli deep inside the body and removes the need for surgical intervention. Hynynen in 2008, showed that introduction of a preformed gas bubble before focused ultrasound exposure would allow transient opening of a local area of the BBB without causing delayed ischemia or acute damage to the endothelial cells (Hynynen, 2008). By combining with a diagnostic imaging device such as MRI scanner, ultrasound becomes a non-invasive approach to open targeted areas of the BBB to allow the delivery of drugs and other therapeutic molecules across the BBB (Hynynen, 2008).

Microwave energy has also been investigated for promoting drug passage across the BBB (Moriyama *et al.*, 1991). It is reported that after exposure to low level microwave energy, Chinese hamsters exhibited reversible increased permeability of the BBB to the brain penetration marker, horseradish peroxidase (Albert *et al.*, 1981). In another study, microwave irradiation facilitated central effects of domperidone drug by changing the permeability of the BBB and enhancing the entry of the drug into the CNS (Quock *et al.*, 1987). There are examples of utilizing electromagnetic field pulses to promote the permeability of the BBB. Qiu *et al.* in 2010 showed that electromagnetic field pulses increased BBB permeability to drug molecules *via* translocation of ZO-1 protein and regulation of protein kinase C signalling (Qiu *et al.*, 2010).

The problem with BBB disruption by these various stimuli is that in many cases the BBB integrity is seriously compromised resulting in loss of its proactive function. Consequently, this strategy of brain drug delivery allows for the leakage of different plasma proteins into the brain. Albumin is toxic to astrocytes (Nadal *et al.*, 1995), and astrocytosis is induced when the brain comes in contact with blood. Moreover, BBB disruption leads to vascular pathology (Lossinsky *et al.*, 1995) and to permanent neuro-pathologic changes in the brain (Salahuddin *et al.*, 1988).

1.2.6.4 Transport system-mediated drug delivery across the BBB

One of the best approachs for solving the poor penetration problem is to engineer drugs that cross the BBB utilising one of the many endogenous transporters expressed within the brain capillary endothelial cells. This can be done for small molecule as well as large molecule therapeutics (Pardridge, 2005a).

The conjugation of drug molecules with substrates of endogenous transport systems present in the BBB had been utilised to access the brain. As discussed previously, transporter proteins, specific receptors or adsorptive endocytosis can be used to improve drug delivery to the brain. The characteristic features of these transporting systems are (Gaillard, Visser*, et al.*, 2012):

1. The drug molecule is chemically modified, for example, conjugated to a hosting molecule such as a polymer or a ligand, thereby masking its intrinsic properties.
2. The drug molecule is encapsulated in a surface modified DDS such as dendrons, liposomes and nanoparticles.
3. The DDS should be non-immunogenic (unless it is designed to target monocytes or macrophages) and capable of interacting with receptors positioned at the BBB to facilitate the uptake of the drug by the BBB.
4. The DDS must be highly specific for the targeted receptor, thereby increasing transport efficiency and minimising potential side-effects of the drug.
5. All DDSs must have controlled molecular mass, thereby their properties will be uniform and consistent and their biological fate can be controlled.

Thus the ideal properties of hosting a system for drug delivery across the BBB are (Georgieva *et al.*, 2014): non-toxic, biocompatible, biodegradable, non-immunogenic, prolonged blood circulation time, stable in blood stream (no aggregation and dissociation), contain BBB-targeted moiety (such as a ligand), preserve parent drug stability with tenable drug release profiles and finally adaptable to carry small drug molecules as well as moderately large molecules such as peptides, proteins and nucleic acids.

1.2.6.4.1 Endogenous BBB transporters

The brain microvascular endothelial cells are the basic anatomical unit of the BBB. There are more than 100 billion blood capillaries in the human brain and virtually each neuron has its own blood vessel (Pardridge, 2002a). The length of capillaries in the human brain is ~400 miles and the surface area of the BBB in the human brain is ~20 m^2 (Pardridge, 2003).

Movement of substrate across the BBB is a process of penetration through two membranes in series, which are the luminal and abluminal membranes of the capillary endothelial cells. Endothelial cytoplasm separates these two adjacent membranes by only 200 nm. The endogenous transporters of the BBB are expressed on both the luminal side and abluminal membrane of the brain capillary endothelial cell. Endogenous BBB transporters utilise local pathways such as RMT, CMT and active efflux transport to deliver molecules to the brain. While certain endogenous large molecules are transported by the RMT systems across the BBB of small molecules are transported between two sides of the BBB by the CMT and active efflux transport systems (Kusuhara *et al.*, 2001; Tamai *et al.*, 2000). Although the CMT systems are usually responsible for blood to brain influx of solutes, this transport systems can also promote brain to blood efflux. The active efflux transporter (AET) systems usually mediate the brain to blood efflux transport of substrates. Also, some AET systems such as organic anion-transporting polypeptide and organic anion transporter can function as CMT systems.

1.2.6.4.1.1 Carrier-mediated transport

The GLUT1 glucose transporters are responsible for transporting glucose, deoxyglucose and other hexoses *via* the BBB to provide the brain with energy. Large neutral amino acid transporter 1 (LAT1) transports both large and small neutral amino acids, as well as certain amino acid based drugs such as methyl-dopa, L-dopa, and gabapentin (Pardridge, 2007). Levodopa which is a lipid-insoluble precursor of dopamine has been used for the treatment of Parkinson's disease because it contains the α-amino and carboxyl peripheral groups that allow it to compete for transport across the BBB by the large neutral-amino acid carrier (Wade *et al.*, 1975). However, basic amino acids, such as lysine or arginine are transported by the cationic amino acid transporters. The monocarboxylic acid transporter transports metabolism intermediates such as pyruvate, lactate, ketone bodies and certain monocarboxylic acid drugs such as probenecid. The nucleoside transporter is responsible for other protein metabolites such as nucleosides, purine and certain pyrimidine nucleosides like uridine. However, only the purine bases metabolites, but not the pyrimidine bases, can be transported across the BBB by CMT systems (Chen *et al.*, 2012).

The diversity of CMT systems opens many windows for modifying the molecular structure of drugs that normally do not cross the BBB *via* medicinal chemistry by mimicking the chemical structure of endogenous substrates of CMT systems. Like most biological transporter systems, the BBB-CMT systems are saturable at high substrate concentrations. However, these transporters are not effectively saturated by the modified-structure drugs *in vivo*. This is

attributed to the fact that the K_m of the BBB CMT systems is more than ten-fold above the existing plasma concentration of these drugs. The main drawback in this case would be in maintaining activity of the drug for its corresponding receptor in the brain beyond the BBB. Alternatively, certain medicinal chemistry approaches can be used to make the modified drug molecule substrate to certain enzymes in the brain that convert these modified drugs back to the parent drug after crossing the BBB (Georgieva *et al.*, 2014).

1.2.6.4.1.2 Active efflux transport

The most important AET system at the BBB is the P-gp pump, which is a product of the ATP binding cascade (ABC) transporter B1 gene. However, there are many other members of the ABC gene family that act as energy driven active efflux pumps at the BBB, including members of the ABCC and the ABCG2 gene family (Pardridge, 2005a). Moreover, AET of drug from brain to blood is a process performed by two efflux transporters in series, which are an energy dependent transporter and an energy-independent transporter (Pardridge, 2005a). The energy dependent transporter from the ABC gene family can be found at the luminal membrane side, whereas the energy-independent transporter can be expressed at the abluminal membrane side of the brain capillary endothelial cell.

P-gp is the main transport system responsible for extruding many molecules from the brain to the blood circulation including many drug molecules. Even if certain drug molecules manage to cross the BBB to the brain, they will not reach the minimum therapeutic effective concentration inside the brain due to the rapid and efficient removal of these drugs by the P-gp pump. Therefore, inhibition of P-gp activity may result in an improved drug delivery of certain drugs that are substrates of these active efflux transporters into the brain. This strategy of improving drug accumulation in the brain is based on co-administration of the drug with a pharmacological modulator which inhibits efflux pump systems in BBB. The principle of applying Pluronic® block (or poloxamers) copolymers to shut-off the action of P-gp efflux pump was implied by an early study conducted by Miller *et al.* (Miller *et al.*, 1997). The study examined cellular accumulation of radioactive rhodamine-123 which is a selective P-gp pump substrate in brain microvessel endothelial cell monolayers. The study indicated increase in the concentration of rhodamine-123 inside the brain tissue when co-administrated with Pluronic® P85. Later studies have confirmed that Pluronic® P85, may be used not only as an effective P-gp pump inhibitor, but also as a drug delivery carrier (Kabanov *et al.*, 2003).

However, the P-gp inhibition approach is appropriate to improve the delivery of therapeutic agents intended for the treatment of acute diseases such as brain tumours when the goal of the

delivery is to maximise the drug concentration inside the brain for a relatively short duration. The chronic administration of P-gp inhibitors may obstruct the physiological homeostatic regulation provided by P-gp pump (Begley, 2004). Moreover, extended blockade of P-gp functions in the BBB by P-gp inhibitors can lead to a considerable increase of brain concentrations of various xenobiotics including many drugs (Pardridge, 2005a). Thus, the shut off of P-gp pump function as efflux transporters in the BBB causes dramatic cytotoxicity inside the brain. Consequently, doses of these drugs that are normally well tolerated might become eventually neurotoxic (Schinkel *et al.*, 2003). Finally, losing the protective function of P-gp pump in various cells and tissues by the prolonged application of P-gp inhibitors, especially if they are poorly selective, comes with high risk of systemic cytotoxicity due to the reduction of drug elimination (Löscher *et al.*, 2005). Thus, the enhancing of drug transport into the brain by using P-gp inhibitors strategy must be applied with extreme caution and restricted to transient application.

1.2.6.4.1.3 Drug transport across the BBB via AMT

AMT has recently gained notable importance as a candidate pathway for drug delivery through the BBB due to growing evidence exhibiting the success of this transport pathway for delivering drug molecules into the brain using cell-penetrating peptides (CPPs) and cationic proteins as drug carriers (Herve *et al.*, 2008). CPPs are positively charged peptides in nature with amphipathic characteristics and are capable of entering living cells rapidly without producing cell membrane lysis or other cytotoxic effects. These CPPs utilise AMT endogenous transport pathway to enter the brain. They are a group of short poly-peptides of less than 30 amino acids that are capable of penetrating cell membranes and delivering their load into cells (Zorko *et al.*, 2005). While each CPP differs in number of amino acids and sequence, they share a few common properties which include their net positive charge, amphiphilic nature, ability to interact with lipophilic biological membranes and to adopt a distinctive secondary structure upon conjugation with lipid materials (Rousselle *et al.*, 2000). These peptides have been successfully used as host carriers for delivering drug molecules that are P-gp pump substrates by effectively by-passing P-gp pump in the BBB. For instance, they have increased the transfer of doxorubicin, an anticancer drug, into the rat brain parenchyma up to 30-fold (Rousselle *et al.*, 2000).

CPPs can facilitate the intracellular penetration of polar biomolecules *in vitro* and *in vivo* (Deshayes *et al.*, 2005) and they were shown to promote the transport of morphine-6-glucuronide to the brain tissue in a clinical trial (de Boer *et al.*, 2007). Another notable success

to increase brain uptake of poorly brain penetrating drug molecules by AMT is the use of vectors such as SynB3 peptides (Adenot *et al.*, 2007). These peptides are derived from a natural mammalian antimicrobial peptide and have high affinity for negatively charged membranes.

While CPPs carriers are mainly suitable for the delivery of small loads such as oligonucleotides and peptides, a previous study (Schwarze *et al.*, 1999) has synthesised a full-length fusion proteins that contained an eleven amino acid protein transduction domain from the HIV-1 which is a trans-activating transcriptor protein with 101 amino acids that contains 5 domains. Transduction process of the evaluated proteins was non-cell-specific and was seen to happen even across the BBB implying the ability to cross this barrier. Further proof of this mode of peptide-based delivery was introduced by further study (Cao *et al.*, 2002) which fused Bcl-xL (anti-apoptotic protein) to trans-activating transcriptor protein and injected the conjugated compound intraperitoneally into mice that were affected by stroke resulting in inhibition of neural apoptosis.

1.2.6.4.1.4 Cell-mediated drug transport across the BBB

Cell-mediated drug transport employs specific immune cells to deliver molecules to the brain. These cells engulf nano- or micro-sized carriers loaded with desired drug molecules and traffic them through the BBB to deliver their load to the target sites inside the brain. The advantages of cell-mediated shipping of drugs through the BBB are based on the following:

1) In brain disorders such as MS, Alzheimer's disease, brain tumours, Parkinson's disease, stroke, and HIV-1 associated dementia, the accompanied inflammatory response causes extensive recruitment and shipping of leukocytes (neutrophils and monocytes) in the brain tissue. Also, the process of chemotaxis causes other inflammatory cells such as phagocytes and T-cells to migrate towards the site of inflammation (Chen *et al.*, 2012).

2) Monocytes, macrophages, and neutrophils are phagocytic cells and have a trend to endocytose small sized particles, liposomes and subsequently exocytose them to release their drug loads into the external media (Daleke *et al.*, 1990; Panyam *et al.*, 2003; Rogers *et al.*, 2005).

3) The drug can be conjugated or loaded into nano- or micro-carriers in high payloads, to be then taken up by these cells (Chen *et al.*, 2012).

4) Application of a magnetic field following CMT combination with magnetic particles can further enhance the brain delivery for the clinical diagnosis of inflammation sites and tracking of nanomaterials (Chen *et al.*, 2012).

5) Blocking certain pathways that viruses and other pathogens may take for entering of the brain by competing with them on these pathways (Chen *et al.*, 2012).

1.2.6.4.1.5 Receptor-mediated transport across the BBB

Certain large peptide proteins in the blood stream such as insulin, insulin like growth factor and transferrin undergo RMT across the BBB *via* their endogenous peptide receptors (Pardridge, 1997). These transporter systems are highly specific and they uptake their substrates presented on the luminal side of the brain endothelial cells and deliver them inside the brain with the receptor recycled back to the luminal membrane surface (Chen *et al.*, 2004).

Although a number of receptors expressed in the brain endothelial cells have been discovered, sufficient knowledge of their distribution and differential expression at BBB in the diseased brain is currently lacking. This represents an issue that requires urgent attention as it has a huge impact on the effectiveness of the targeting approaches of many new DDSs, including the molecular Trojan horse approach.

The most commonly known receptors involved in RMT are the transferrin receptor (TfR), insulin receptor (NSR), lipoprotein receptors and diphtheria toxin receptor (DTR). TfR promotes the transcytosis of transferrin-bound iron through the brain capillary endothelial cell in humans and it is the most well identified endothelial cell receptor (Pardridge, 1997).

A study (Ulbrich *et al.*, 2009) has indicated a huge increase of loperamide passage across the BBB into the brain tissue using human serum albumin nanoparticles (HAS-NPs) coupled to transferrin as a carrier system to target TfR. The loperamide loaded onto these transferrin coupled HAS-NPs achieved powerful anti-nociceptive effects compared to free loperamide, implying that transferrin coupled to HAS-NPs is able to transport loperamide across the BBB which it normally is unable to cross (Ulbrich *et al.*, 2011). Targeting NSR can also improve drug penetration to the brain. However, targeting these receptors might disrupt insulin metabolism and utilisation in the brain; therefore, it must be used with caution. A study (Boado *et al.*, 2007) has indicated that the brain delivery of iduronate 2-sulfatase (which is a large molecule drug that does not cross the BBB) was improved after attaching to IgG domain suggesting the potential of using this domain for delivering drug molecules and genes through the BBB in human.

To ensure efficient drug delivery to the brain, specialised techniques must be applied to deliver poorly penetrating drugs rather than depending on simple drug diffusion to the targeted tissue.

One of the promising techniques is to conjugate limited penetration therapies with specific carrier systems capable of ferrying these drugs to the other site of desired biological barrier. Among these carriers, dendrimers have attracted attention as possible drug carriers because of their unique properties and characteristics (Yates *et al.*, 2004).

1.3 Dendrimers and dendrons

Dendrimers are highly branched three-dimensional macromolecules with highly controlled chemical structures, uniform MWs, a large number of controllable peripheral functional moieties and a tendency to adopt a sphere shape once a certain molecular mass is reached (Liu *et al.*, 1999). Tomalia proposed the term dendrimer (originated from the Greek "Dendron" which means tree, and "meros" which means part) (Tomalia *et al.*, 1985) to describe these molecules due to their characteristic structural features.

The architecture of a typical dendrimer consists of three different regions: (a) a core or focal moiety, (b) repeating building units with several interior layers called "generations" (Gen) and (c) multiple peripheral functional groups on the outer layer of repeat units (Caminade *et al.*, 2005). Removing the dendrimer core will result in formation of identical fragment units called dendrons (Aulenta *et al.*, 2003). The number of branching sprouts in these dendrons will determine its generations (e.g. Gen0, Gen1, and Gen3) and final MW (Figure 1.4). The number of peripheral groups will increase as the generation of the dendron increases (Menjoge, Kannan R.*, et al.*, 2010).

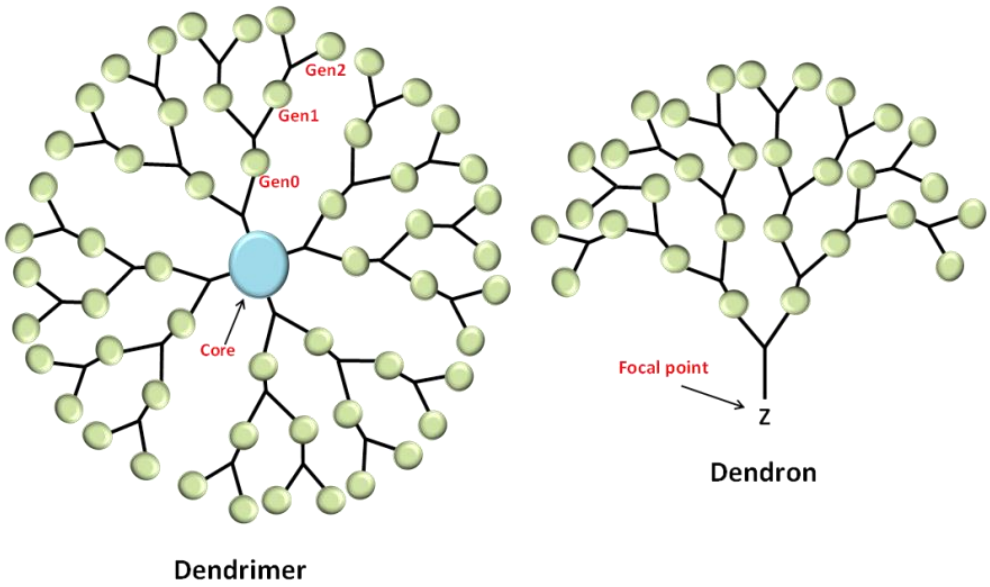

Figure 1.4 Basic structures of dendrimers and dendrons. The size of the dendrimer molecule is based on the number of repeating layers added and each layer is represented by a generation (Gen). These generations will determine the number of peripheral functional groups (Gen0=2, Gen1=4, Gen2=8, Gen3=16)

1.3.1 Types of dendrimer

Based on their structural shape, end functional groups and internal cavities, dendrimer can be classified into the following types (Tariq *et al.*, 2015):

- *Polyamidoamine (PAMAM) dendrimers*: These spheroidal shape dendrimers are highly soluble and reactive due to the presence of a high number of functional peripheral groups and empty internal spaces (Roseita *et al.*, 2001; Schiavon *et al.*, 2004; Tomalia *et al.*, 1990).
- *Polypropyleneimine (PPI) dendrimers*: These diaminobutane based core dendrimers have primary amines as peripheral groups and tertiary propylene amines as centre groups. These are commercially available up to Gen5 and are widely used in biology in application such as drug delivery and disease diagnosis (Brana *et al.*, 2002).
- *Chiral dendrimers*: These dendrimers are built by attaching structurally different but chemically alike branches to a chiral focal point (Hawaker *et al.*, 1993).
- *Multilingual dendrimers:* These are the dendrimers which hold multiple copies of a particular functional group on their peripheral surface (Pushkar *et al.*, 2006).
- *Tecto dendrimers*: These dendrimers are made up of core dendrimers that are surrounded by other types of dendrimers. Tecto dendrimers are used to perform specific diagnostic and cargo delivery functions (Pushkar *et al.*, 2006).
- *Hybrid dendrimers*: These dendrimers have a combined characteristic of both dendritic and linear polymer (Pushkar *et al.*, 2006).
- *Amphiphilic dendrimers*: These dendrimers are characterised by having both electron donating and electron withdrawing groups on their outer surfaces.
- *Peptide dendrimers*: Amino acids are the building or branching units of these dendrimers. These are widely used in medicine used for the diagnostic purposes and drug and vaccine delivery (Yasukawa *et al.*, 2004).
- *Frechet-type dendrimers*: They are characterised by a polybenzyl ether hyper branched skeleton. Their peripheral carboxylic acid groups can provide sites for further functionalisation and enhance their solubility (Yasukawa *et al.*, 2004).
- *Polyamidoamine organosilicon (PAMAMOS) dendrimers*: These silicon containing commercial dendrimers are inverted micelles which contains hydrophobic organosilicon groups in the exterior outside and hydrophilic nucleophilic PAMAM groups in the interior side (Yasukawa *et al.*, 2004).

- *Multiple antigen peptide dendrimers*: These are dendron-like molecular conjugates based upon a polylysine frame. Lysine with its alkyl amino side-chain acts as an excellent monomer for the multiple branching points (Tripathy *et al.*, 2013).

1.3.2 Physicochemical properties of dendrimers

The chemical and physical properties of dendritic molecules are highly affected by the nature of their functional peripheral groups (Zimmerman *et al.*, 2003). Thus, for example, the solubility, stability, aggregation, viscosity and chemical reactivity of each dendrimer can be altered by modifying its peripheral groups. Moreover, its conformational flexibility as well as its spatial and surface chemical structure is influenced in the same manner. The effect of the peripheral functional groups on the properties of dendrimers increases with higher generations since the number of end groups of an ideally synthesised dendrimer increases exponentially with the addition of further generations.

Dendrimers and dendrons have unique characteristic features which are in sharp contrast to those of traditional polymers such as (Svenson *et al.*, 2005):

a. A dendrimer can be synthesised as a monodisperse single compound with a uniform MW, unlike most polymers whose synthesis affords a wide range of molecular species differing in MW.
b. Dendrimers have a predictable three-dimensional architecture, especially with increasing generations.
c. As the generation number of dendrimers increases, their molecular size increases accordingly.
d. The layer after layer synthesis of dendrimers allows for site-selective functionalisation.
e. As the MW increases, the properties of dendrimers (e.g., solubility, chemical reactivity, viscosity) will depend on the nature of their peripheral groups.

1.3.3 Pharmaceutical applications of dendrimers

There is an exponential increase in the use of dendrimers in pharmaceutical and medical chemistry. A variety of applications have been explored and adopted to use dendrimers and dendrons as gene carriers and medical imaging agents for diagnostic purposes, in addition to their applications in DDSs (Abbasi *et al.*, 2014; Gagliardi, 2017; Madaan *et al.*, 2014; Noriega *et al.*, 2014). Finally, some dendrimers can act as potential therapeutic agents for specific diseases (Issa *et al.*, 2015; Meikle *et al.*, 2013; Svenson *et al.*, 2005).

1.3.3.1 Gene delivery

The first report of using PAMAM dendrimers for transfection was published in 1993. PAMAM dendrimers was conjugated with DNA into different types of cultured mammalian cells. The gene delivery efficiency was a function of both the size of the dendrimers and the dendrimer to DNA ratio (Haensler *et al.*, 1993). Recently, various polycationic materials like poly(L-lysine), polyethyleneimine and positively charged liposomes have been used as non-viral gene carriers (Gupta *et al.*, 2014). Some dendrimers with peripheral amino groups are also currently undergoing investigations as non-viral gene carriers due to their structural regularity and multivalent properties. Commercially available PAMAM and PPI dendrimers are the most representative dendrimers for use as non-viral gene hosts due to their high affinity to negatively charged nucleic acids and relatively low cytotoxicity (Abbasi *et al.*, 2014). These polycationic dendrimers form conjugates with DNA through electrostatic bonds between the protonated primary amino groups on the dendrimer surface and the negatively-charged phosphate moieties of nucleic acids. Moreover, PAMAM and PPI dendrimers with tertiary amine groups have a high buffering capacity and thus, act as a weak base to retard degradation caused by acidification within the endosome-lysosome (Dennig *et al.*, 2002; Madaan *et al.*, 2014).

Besides PAMAM and PPI dendrimers, poly(L-lysine) dendrimer are often used for gene delivery. Poly(L-lysine) dendrimers with 64 and 128 peripheral amino groups expressed efficient gene transfection properties in different cultivated cell lines (Ohsaki *et al.*, 2002). Finally, polyphenylene dendrimers with up to 16 lysine repeat units or short peptide sequences with up to 5 lysine or glutamic acid monomers have been successfully synthesised to study nucleic acids complexation and condensation as well as for their use as building monomers for innovative supramolecular architectures (Herrmann *et al.*, 2003).

1.3.3.2 Diagnostic applications of dendrimers

Dendrimers are extremely appropriate and used as image contrast media and as molecular probes because of their unique characteristics and distinct morphology (Patel, 2013). For instance, the immobilisation of sensor units such as avidin (Yoon *et al.*, 2000) and sulfur dioxide (Albrecht *et al.*, 2000) on the surface of dendrimers is a very efficient way to produce an integrated molecular probe. A previous study (Stears *et al.*, 2000) has reported a highly sensitive sulfur dioxide sensor that consists of a dendrimer having arylplatinum complexes as surface functional moieties. Several nucleobase-based dendrimers and DNA-based dendrimers have been introduced for amplifying purposes of hybridisation signals. A fluorescent oligonucleotide dendrimeric signal-amplification system was introduced to microarray

technology for enhancing signal detection on DNA microarrays. A highly fluorescent dendritic molecule with an optically active binaphthyl derivative at the focal point of the phenyleneethylene-based dendrimer has been utilised as a signal amplification method for the detection of chiral amino alcohols (Gong *et al.*, 2001). A number of research groups have studied the use of dendrimers as a new class of high MW MRI imaging agents (Kobayashi, 2003; Kobayashi *et al.*, 2001).

Hydrophilic-iodinated dendritic nanoparticles, consisting of four generation dendrimers conjugated to triiodobenzene derivatives, have been explored as contrast agents for computed tomography imaging (Yordanov *et al.*, 2002). The high iodine content of these materials yields higher spatial resolutions compared to iodinated small molecules. Another type of dendritic iodinated imaging agent has a polyethyleneglycol (PEG) focal-core with two dendritic poly(L-lysine) dendrons and triiodobenzene derivatives at both PEG termini. An array of 6 dendritic contrast imaging agents was synthesised originally, using different PEG cores with t-Boc lysine-generated dendrimer (to act as amplifiers) containing 16 to 64 peripheral amine groups for conjugation with reactive triiodo moieties (Fu *et al.*, 2006).

1.3.3.3 Therapeutic applications of dendrimers

The multi-valence surface of a dendrimer can be very beneficial for immobilising a large number of functional materials. Numerous sugar-modified dendrimers have been synthesised to explore the cluster effect of sugar groups on various biological functions. For example, mannose modified poly(L-lysine) dendrimers were examined for their inhibitory action with respect to the type 1 adhesion of fimbriated *E. coli* to red blood cells (Nagahori *et al.*, 2002).

Specific types of polyanionic dendrimer may reduce the cellular internalisation of viruses through competition with the negatively-charged cell surface. For example, PAMAM dendrimers with naphthyl sulfonate residues at the surface have been noticed to have antiviral activity (Myriam *et al.*, 2000). Moreover, poly(L-lysine) dendrimers with sulfonate surface groups were found to be useful as viral inhibitors for the herpes simplex virus *in vitro* (Bourne *et al.*, 2000). Dendrimers also seem to provide promising candidates to be used in boron neutron capture therapy and (Shukla *et al.*, 2003) photodynamic therapy (Dichtel *et al.*, 2004). Finally, osteoconductive phosphoserine-modified poly(L-lysine) dendrons were used in tissue regeneration (Meikle *et al.*, 2013) and poly(L-lysine) dendrons have been applied as modulators of quorum sensing in *Pseudomonas aeruginosa* and might represent a novel therapeutic strategy for the treatment of antibiotic-resistant *P. aeruginosa* infections (Issa *et al.*, 2015).

1.3.3.4 Dendrimers for drug delivery

The discovery and development of a novel drug is generally a very long and expensive process which may take up to 15 years and cost up to 500 million pounds (Bolten *et al.*, 2002). Despite the fact that various potential new drugs have been developed, many fail to provide the desired therapeutic effects in the clinical trials due to undesired side effects (Ghose *et al.*, 1999). Controlled drug release and site-specific drug delivery may significantly enhance the therapeutic effect of drugs by lowering undesired localisation, allowing for easier optimisation of the drug concentration (Esfand *et al.*, 2001).

A pioneering work reported the creation of a dendritic box (Jansen *et al.*, 1994), which has protected amino acid groups on the 64 amine terminal of PPI dendrimers. This dendrimer could simultaneously trap up to four large guest molecules (rose Bengal stain) and 8-10 small guest molecules (para-nitrobenzoic acid). Upon deprotection of the terminal moieties, the surface outer shell opened and the loaded molecules were allowed to leak from the dendrimer. Cross-linking, acid-base interactions, and hydrogen bonding have been utilised for the formation of dendrimer-guest conjugates (Boas *et al.*, 2002). These general host-guest chemistry binding strategies are promising for the development of drug delivery hosts due to the ability to bind several different chemical moieties simultaneously.

The use of dendronised polymers in numerous biomedical applications such as in drug and gene delivery and in imaging has increased due to the adaptability of dendrimer chemistry, allowing the synthesis of a broad range of molecules with different functionality (Abbasi *et al.*, 2014; Gagliardi, 2017; Gupta *et al.*, 2014). One of the interesting features of dendrimers is their unique density distribution, e.g., the relatively flexible inner space around the focal point and the densely packed peripheral functional moieties. This special architecture has the potential to be used as a host molecule for encapsulating small molecules into the flexible inner space (Patri *et al.*, 2012). Alternatively, the highly functional peripheral groups of dendrimers can be used for multiple conjugating interactions especially in drug delivery (Gupta *et al.*, 2014; Longmire *et al.*, 2011; Svenson *et al.*, 2005).

It has been demonstrated that dendronised polymers can be used in pharmaceutical and skin care products (Sahoo *et al.*, 2007). Functionalisation of PAMAM dendrimer with antiperspirant deodorant constituents has been documented to successfully increase their efficacy on skin (Menjoge, Kannan*, et al.*, 2010). Moreover, dendrimer-based products have been utilised for different cancer therapy such as for glioblastoma, prostate cancer, and bone metastases (Lee *et al.*, 2012).

In addition to the above basic host-guest chemistry strategies, numerous therapeutic agents have been explored as guest molecules for drug delivery. Ibuprofen, which is an anti-inflammatory drug, was evaluated by conjugation and encapsulation into third and fourth generation PAMAM dendrimers (Tanis *et al.*, 2009). In this study, up to 78 ibuprofen molecules were found to be conjugated to the PAMAM dendrimers by electrostatic bonding between the carboxyl group of the drug and the amine groups of the PAMAM dendrimer. The conjugated ibuprofen was found to enter epithelial cells *in vitro* much more rapidly compared to the free ibuprofen, implying that dendrimers may be able to efficiently ship complexed drugs inside of cells (Kolhe *et al.*, 2003). In another study, the anticancer drug, doxorubicin, was covalently bound to the periphery of a polyester-based, second generation dendrimer via an acid labile hydrazone linkage. The cytotoxicity of doxorubicin was significantly lowered, and the drug was successfully taken up by several cancer cell lines (Padilla *et al.*, 2002). Recent research has shown significant improvement in the bioavailability of pilocarpine in the eye by using surface-modified dendrimers (Srinivas *et al.*, 2014).

For target specific drug delivery, several targeting groups have been successfully introduced onto the outer surface of dendrimers. For example, folate was combined with a PAMAM dendrimer for the targeting delivery of methotrexate (anticancer drug) into cancer cells (Quintana *et al.*, 2002). Poly(L-glutamic acid) chains with a folate moiety were introduced to the periphery of second or third generation PAMAM dendrimers to create a novel biodegradable polymers (Tansey *et al.*, 2004). The controlled release of adriamycin and methotrexate (anticancer drugs) were achieved after encapsulating into PEG-modified dendrimers (Xu *et al.*, 2014). The highly functional Gen3 PAMAM dendrimer-paclitaxel conjugates demonstrated good stability under physiological conditions and 12-fold greater permeability across Caco-2 cell cells monolayers *in vitro* than paclitaxel alone (Madaan *et al.*, 2014).

MS acute relapses are treated by anti-inflammatory drugs, glucocorticoids. Methylprednisolone (MP) is the drug of choice in such treatment. However, MP poor penetration through the BBB urges the use of high doses of the drug reaching 10-20 fold the stated daily dose (Gaillard, Appeldoorn*, et al.*, 2012).

1.4 Methylprednisolone

Methylprednisolone (MP) (Figure 1.5) belongs to the glucocorticoid family which is a class of steroid hormones that bind to the glucocorticoid receptor (GR), which is present in almost every vertebrate animal cell (Pelt, 2011). The name glucocorticoid (glucose + cortex + steroid)

originates from its role in the adjustment of glucose metabolism, its synthesis in the adrenal gland cortex and its steroidal structure. Glucocorticoids are very effective anti-inflammatory drugs in the treatment of many acute and chronic inflammatory conditions and immune diseases such as rheumatoid arthritis, asthma, inflammatory bowel disease and MS (Mohamadi *et al.*, 2017). Cortisol (or hydrocortisone) is the most important endogenous human glucocorticoid. It regulates or supports many important metabolic, cardiovascular, homeostatic and immunologic functions (Mohamadi *et al.*, 2017). Various synthetic glucocorticoids are available which are used either as replacement therapy in cortisol deficiency or to suppress the immune system in specific clinical cases. The most powerful synthetic glucocorticoids include betamethasone, dexamethasone and MP. Glucocorticoid effects may be broadly classified into two major categories which are immunological effects (or the anti-inflammatory action) and metabolic effects. In addition, glucocorticoids play important roles in foetal development and body fluid homeostasis (Liu *et al.*, 2013).

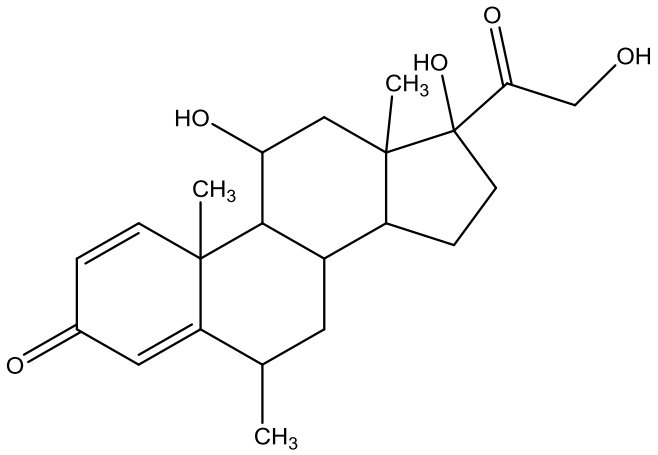

Figure 1.5 Chemical structure of MP. The chemical formula is $C_{22}H_{30}O_5$ and the MW is 374.48 Da.

1.4.1 Inflammation suppression by MP

Chronic inflammatory conditions involve the accumulation and activation of many immune and inflammatory cells which release several inflammatory mediators that initiate a cascade resulting in activation of structural cells at the site of inflammation. Each inflammatory response will have a different pattern of inflammation depending on the type of mediators and cells that are involved in the process (Barnes, 1998, 2004). However, all inflammatory cascades are characterised by elevated expression of multiple inflammatory mediators, some of which are common to all inflammatory cases, whereas others are more unique to a specific response. The elevated expression of most of these inflammatory mediators is regulated at the level of gene transcription through the activation of pro-inflammatory transcription factors, such as nuclear factor-κB (NF-κB) and activator protein-1 (AP-1) (Barnes, 2006b). These pro-

inflammatory transcription factors are activated in almost all inflammatory responses and play a critical role in perpetuating and amplifying the inflammatory process. For example, NF-κB is activated in chronic obstructive pulmonary disease patients and the respiratory airways of asthmatic patients (Di Stefano *et al.*, 2002; Hart *et al.*, 1998), in the joints of patients suffering rheumatoid arthritis (Muller *et al.*, 2002) and also activated the blood vessels of patients with atherosclerosis (Monaco *et al.*, 2004).

Regardless of the cause inflammation, glucocorticoids can act as potent anti-inflammatory agents (Barnes, 2006b). These drugs not only suppress immune responses, but also inhibit the two main products of inflammatory conditions, prostaglandins and leukotrienes (Rhen *et al.*, 2005). Glucocorticoids impose their potent anti-inflammatory affects through the activation and suppression of many pro-inflammatory and anti-inflammatory genes, as well as having post-transcriptional effects (Barnes *et al.*, 2009).

1.4.1.1 Gene activation

After diffusing across the cell membrane, glucocorticoids bind to glucocorticoid receptors (GR) in the cytoplasm (Rhen *et al.*, 2005). This binding will activate and release GR from chaperone proteins and GR will be rapidly mobilised to the nucleus where they exert their molecular effects. The mechanism of nuclear translocation of GR involves both the nuclear import protein importin-α and importin-13 (Goldfarb *et al.*, 2004; Tao *et al.*, 2006). Once inside the nucleus, GR undergoes homodimerisation followed by complexation with glucocorticoid response elements resulting in switching-on (or sometimes switching-off) gene transcription. Switching-on glucocorticoid-responsive genes results from an interaction between the DNA-bound GR and transcriptional coactivator molecules such as cAMP response element-binding protein (Ito *et al.*, 2000). The main genes that are switched on by glucocorticoids are mostly genes encoding β_2-adrenergic receptors which contribute to the anti-inflammatory actions of glucocorticoids (Barnes, 2006a; Clark, 2003).

1.4.1.2 Switching-off inflammatory genes

The major effect of glucocorticoids in reducing inflammatory conditions is by switching off many activated inflammatory genes which encode for chemokines, cytokines, adhesion molecules, inflammatory enzymes and receptors (Barnes *et al.*, 2005). These inflammatory genes are usually activated at sites of inflammation by pro-inflammatory transcription mediators, such as NF-κB and activator protein-1 (Clark, 2003). After being activated by glucocorticoid, GR interact with corepressor molecules to supress NF-κB-associated coactivator activity thus reducing the inflammatory response (Barnes, 2006b; Ito *et al.*, 2000).

An additional mechanism by which glucocorticoids might reduce inflammation responses is their potent inhibitory effects on signalling pathways of mitogen-activated protein kinase by the induction of protein kinase phosphatase-1 which, in turn, can supress the expression of many inflammatory genes (Barnes, 2006a; Clark, 2003).

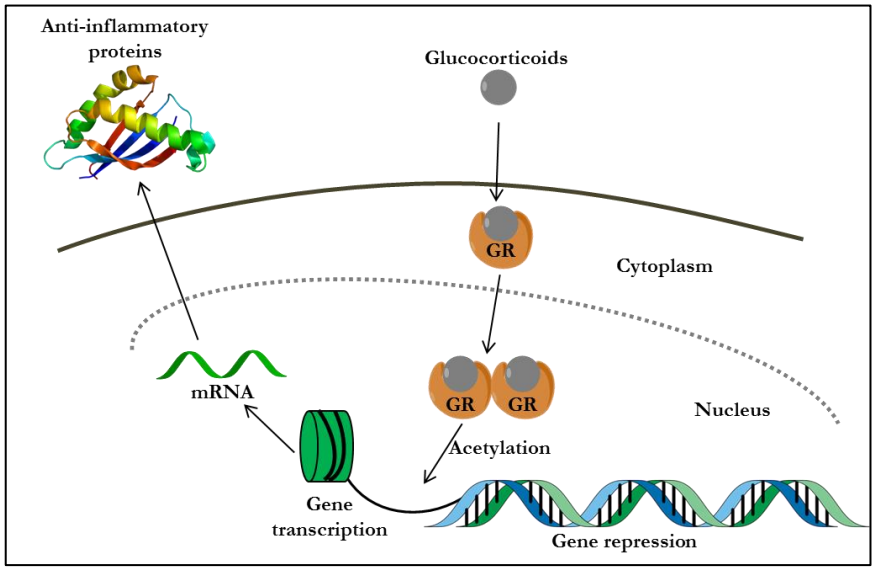

Figure 1.6 Activation of anti-inflammatory gene expression by glucocorticoids.

1.4.1.3 Post-transcriptional effects

When cells are stimulated by inflammatory factors, some pro-inflammatory genes such as TNF-α, which usually have unstable messenger RNA that is rapidly degraded by certain RNAses become stabilised, consequently enhancing the inflammatory process (Barnes, 2006b). Glucocorticoids reverse this stability, causing rapid degradation of inflammatory mRNAs and reduce inflammatory protein synthesis (Bergmann *et al.*, 2004). This action may be mediated *via* the elevated gene expression of proteins that destabilise mRNAs of inflammatory proteins (Smoak *et al.*, 2006).

1.4.2 Side-effects of MP

Despite its efficient anti-inflammatory action, MP causes many side-effects especially if it is used in relatively high doses for prolonged periods and treatment is suddenly stopped (Dostert *et al.*, 2004). The systemic adverse reactions of MP include fluid and electrolyte disturbances, peptic ulceration that may cause stomach perforation and haemorrhage, muscle weakness, development of Cushingoid state, growth suppression in children and ophthalmic problems (Smith *et al.*, 1983). Moreover MP inhibits endogenous cortisol and adrenocorticotropic hormone (ACTH) secretion by a negative feedback effect on the pituitary gland (Smith *et al.*, 1983). This hypothalamus-pituitary-adrenal axis suppression is dose-dependent and usually

only occurs when the dose of MP is higher than 10 mg per day. Usually, suppression after short courses of steroid therapy is not a problem, but prolonged suppression requires careful attention. For these reasons, MP therapy especially when used in high doses (more than 60 mg per day) for prolonged periods and must not be stopped suddenly and must be reduced slowly (Spies *et al.*, 2011).

1.4.3 MP for the treatment of MS

MS patients often exhibit a relapsing-remitting pattern (acute phase) in the early stages of the disease. These relapses are caused by recurrent leakage of auto-aggressive T-lymphocytes and monocytes through the BBB into the brain, where they promote inflammation and lead to nerve demyelination, gliosis and axonal function degeneration (Wang *et al.*, 2003). Although most patients fully recover after a relapse, it can take long durations (weeks or months) (Jongen *et al.*, 2016).

High-dose intravenous MP (500-1000 mg daily) treatment given over a period of 3-5 days is often used as the standard therapy for MS acute phases (Sellebjerg *et al.*, 2005). MP poor permeability through the BBB explains the use of such elevated doses (>10 folds the daily recommended dose). Although treatment with such high-doses of MP shortens the period of the relapses and increases the recovery chance, the exact mechanisms by which MP exert such beneficial effects are not well established. It may be related to the drug multiple biological ways of exerting its actions (Andersson *et al.*, 1998). Some of the beneficial effects of MP in the treatment of MS acute phases are thought to be mediated through the suppression of immune functions (Elovaara *et al.*, 2006).

Like other corticosteroid drugs, MP is associated with a number of adverse effects, affecting the skin, skeleton, muscles, eyes, CNS, electrolytes balance, metabolism, and the endocrine, cardiovascular, immune, and gastrointestinal systems, usually in a dose-dependent way (Schacke *et al.*, 2002). Although most serious adverse effects are related to the long-term oral administration, short-term corticosteroid-induced symptoms are frequent, especially with high-dose treatment needed to treat MS relapses (Jongen *et al.*, 2016). Although the adverse effects of short-term MP treatment of MS relapses seldom require hospitalisation or medical interventions, from a patient perspective, they may cause a disturbance to patients and affect the quality of life (Guidry *et al.*, 2009). A recent study (Jongen *et al.*, 2016) has indicated that all patients treated with high-dose intravenous MP suffered from adverse effects. The most common severe adverse effects were muscle weakness, sleep disturbance, nausea or having stomach pain and being agitated. Furthermore, in MS patients, the distress from CNS related

adverse effects, like change in mood, sleep disturbance, and behavioural change may add to the burden of MS-related CNS symptoms. Thus, minimising the adverse effects of MP in MS patients by improving its penetration through the BBB is a crucial improvement for MS patients.

1.5 Aims and objectives of the thesis

Prevention of the uptake of most pharmaceuticals into the brain due to the presence of the BBB is the main obstacle in the treatment of many neurodegenerative diseases including MS. This property arises from the TJs within the brain capillary endothelium. Nevertheless, drugs intended for CNS disorders can be reengineered for BBB transport utilising endogenous transport systems within the BBB endothelium. Poorly penetrating large molecule drugs can be incorporated with molecular "Trojan horse" delivery systems to employ RMT systems within the BBB. Among these poorly penetrating drugs across the BBB is MP which is used in MS. The penetration of MP to the brain which is hampered by the presence of BBB imposes the use of high doses of MP to treat MS relapses. Such high doses will cause numerous adverse effects in the patients and more advanced methods are needed to deliver MP to the CNS. One of the promising methods is the attachment of MP to certain peptides including dendrons which can penetrate through physiological barriers with the aim of improving MP penetration.

Four specific research questions emerge regarding the possibility of improving MP permeability across the BBB using special drug delivery approaches. The aim of the thesis will be to answer these main questions:

1) Is it possible to conjugate MP to a specially engineered dendronised carrier?

If so,

2) To what extent does such conjugation improve MP permeability across a model of the BBB?

Also

3) What are the cytotoxicity patterns of the synthesised conjugates compared to their parent compounds (free drug and dendrons)?

And

4) Does the attached MP retain its anti-inflammatory activity or will the conjugation with the carrier result in the loss of the pharmacological activity of the drug?

In answering these key research questions, this study will seek to address the following objectives:

i. Design, synthesise and characterise a glutathione-dendron based carrier system for MP.
ii. Investigate the cytotoxicity levels of the conjugated molecules using different cytotoxicity assays.

iii. Detect the potential increment in MP permeability of the BBB by an *in vitro* BBB model when the drug is conjugated to the specialised carrier system.

iv. Test the ability of the conjugated MP to retain its anti-inflammatory activity compared to unmodified free drug utilising an *in vitro* model based on target neuro glial cells.

Chapter 2. Synthesis and characterisation of dendron-MP conjugates

2.1 Introduction

Since their introduction in the 1980s, dendrimers have attracted considerable attention due to their unique structure and properties. Their distinctive properties such as multivalency, high degree of branching, well-defined molecular architecture, excellent uniform structure and highly adaptable chemical structure make them promising new scaffolds for medicinal and diagnostic chemistry (Bosman *et al.*, 1999). Dendrimers can hold many terminal functional groups that can be chemically attached to other moieties in order to adjust their surface properties for various applications. Moreover, by using the homogeneity of their three-dimensional structure, a variety of biologically active agents can be incorporated into dendrimers to form biologically active conjugates, including novel drug carriers (Madaan *et al.*, 2014). Thus, interest has increased in the design and synthesis of novel biocompatible dendrimers for application in many fields of molecular bioscience including the development of vaccines, antimicrobials, and antivirals, as well as to act as carrier hosts and permeability enhancers for drug delivery (Svenson *et al.*, 2005).

Unlike traditional polymers, dendrimers have drawn considerable attention in different biological applications owing to their high solubility (Soto-Castro *et al.*, 2012), biocompatibility (Duncan *et al.*, 2005), polyvalency (Patton *et al.*, 2006) and precise MW (Tomalia, 2005). These advantages make them an ideal carrier for drug delivery and site-targeting applications. Different categories of drugs that have been incorporated in these versatile carriers such as anticancer drugs, nonsteroidal anti-inflammatory drugs, antiulcer drugs, anti-HIV drugs, diuretics, antifungal drugs, anti-hypertensive drugs and antibiotics (Madaan *et al.*, 2014).

2.1.1 Dendrons synthesis

Dendrons are synthesised by a fully controlled stepwise reaction (Grayson *et al.*, 2001). Two main synthetic strategies are used to construct dendritic structures, which are the divergent approach and convergent approach.

The divergent method was first introduced by Newkome (Newkome *et al.*, 1985) in the 1980s. The divergent approach (Figure 2.1) to dendron synthesis is based on a stepwise layer after layer addition that starts from the focal core and builds up the molecule towards the periphery using a pair of basic chemical operations which are (i) coupling of building units and (ii) deprotection or modification of peripheral moieties of the outer surface to create new reactive functionalities. This pair of basic procedures is often referred to as the ″growth of a generation″. The first-generation dendrons are formed by simply attaching a branched unit to the focal core, whereas to make a second-generation dendron, the peripheral groups of the

first generation dendron must interact with the branched building blocks. This reaction is fully controllable, as other functional groups on the building blocks are protected. Thus, modification or deprotection of newly attached peripheral functional groups results in the next branching generation. This process is repeated until the desired number of branching generations is obtained.

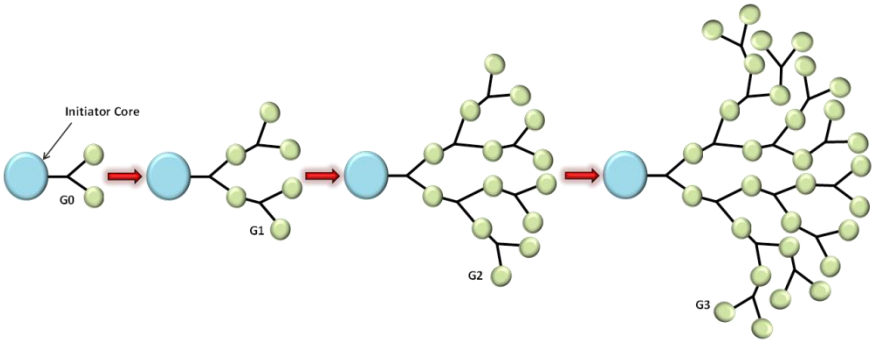

Figure 2.1 Divergent method of dendron synthesis. The dendron synthesis starts from the focal core and builds up the molecule towards the periphery using coupling and deprotection reactions.

The convergent growth strategy, an alternative method to the divergent approach for producing precisely controlled dendritic architectures, was introduced by Hawker and Fréchet (Hawker *et al.*, 1990). Unlike the divergent method, the reaction in the convergent method starts at the surface groups of a dendritic molecule and proceeds to the core or focal point (Figure 2.2). In addition to the divergent and convergent approaches, various alternative synthesis techniques have been proposed that aim to reduce the number of synthetic and purification steps and increase the final product yields, such as double-exponential dendrimer growth approach (Kawaguchi *et al.*, 1995) the double-stage convergent growth approach (Ihre, 1998; Labbe *et al.*, 1996) and orthogonal coupling (Zeng *et al.*, 1996).

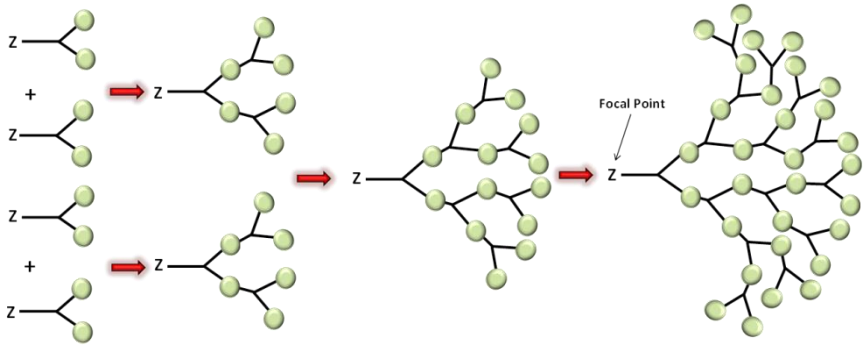

Figure 2.2 Convergent method of dendron synthesis. The synthesis begins at the surface functionalities of a dendritic molecule and proceeds to the core.

2.1.2 Solid-phase peptide synthesis

Peptide synthesis may be conducted both in liquid-phase (Takahashi *et al.*, 2012) and solid-phase (Schnolzer *et al.*, 2007). Solid-phase peptide synthesis (SPPS) has become the primary method for synthesising peptides and small proteins that are essential for research in biomedicine, biology, drug discovery and many other fields (Søren *et al.*, 2012). SPPS starts with a solid support resin which is usually a copolymer of polystyrene with 1% divinylbenzene that should be insoluble throughout the overall conditions of the synthesis. The resin will act as an anchor for the building units which form the synthesised peptide.

SPPS is defined by several factors, mainly the set of N-terminus protecting groups, side-chain protecting groups, supporting resins, linkers (handles) and coupling reagents. The principle involves the sequential coupling of N-terminus and side-chain protected amino acids to a growing peptide chain attached to a solid support (insoluble resin) in the C to N direction. Typically, the C-terminal amino acid is first anchored at the carboxy terminus to the solid support by a cleavable handle. Then, the N-terminus protecting group can be removed without affecting the side-chain protecting groups, thus the polypeptide chain is prepared for the next coupling cycle (Figure 2.3). SPPS reactions are driven to completion by the use of soluble reagents in excess, which can be removed by washing and filtration (Pires *et al.*, 2014). After achieving the desired sequence of amino acids, the peptide is released from the solid support, accompanied by the removal of the semi-permanent side-chain protecting groups (Figure 2.4).

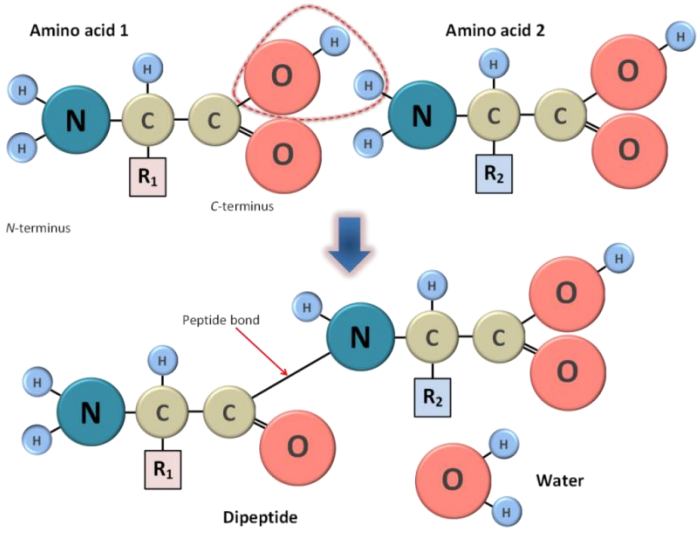

Figure 2.3 Amide linkage formation between two amino acids. R_1 is the side chain of the first amino acid and R_2 is the side chain of the second amino acid. The reaction involves covalent bond formation between the C-terminus of the first amino acid with N-terminus of the second amino acid with the formation of water molecule.

The two most widely used N^{α} -protecting groups in SPPS are 9-fluorenylmethyloxycarbonyl (Fmoc) and tert-butoxycarbonyl (Boc) (Fields *et al.*, 1990; Hudson, 1988; Merrifield, 1986; Miranda *et al.*, 1999). The Fmoc method is usually preferred over the Boc strategy for routine peptide synthesis as the latter normally requires the use of corrosive and toxic hydrofluoric acid, as well as hydrofluoric acid apparatus. The Fmoc group can be removed under mild conditions with secondary amines, typically 20% piperidine in N,N-Dimethylformamide (DMF) (Remuzgo *et al.*, 2009).

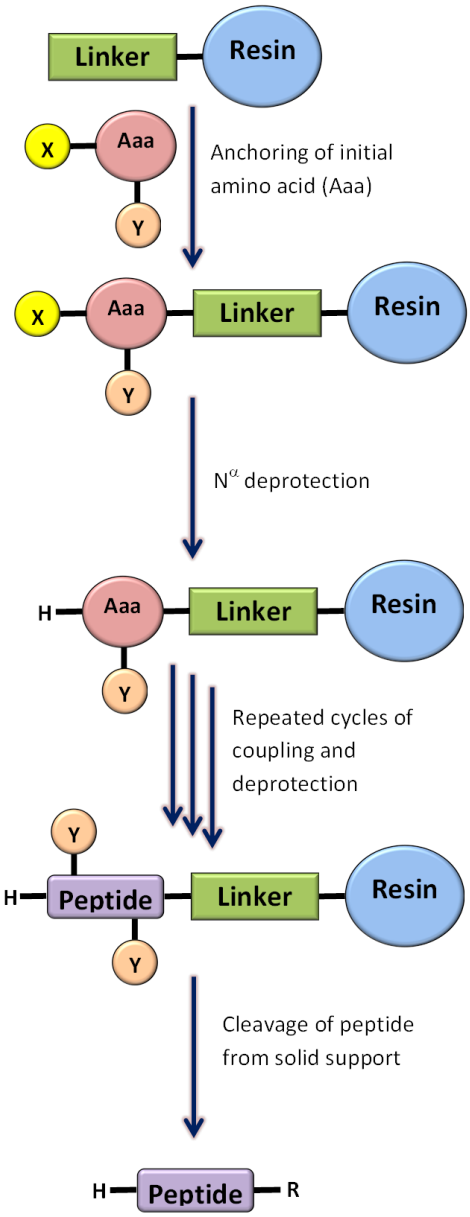

Figure 2.4 The principle of SPPS. Where X is the temporary N-terminus protecting group, Y is the semi-permanent side-chain amino acid (Aaa) protecting groups and R is the C-terminal functionality, typically OH or NH_2.

Aims of the chapter

This chapter of the study is concerned with the design of the dendronised carrier system for MP to achieve the following aims:

- Synthesise Gen0 and Gen1 dendrons using phenylalanine as the core amino acid and applying lysine amino acid as the branching unit.
- Attach MP to the peripheral amine groups of the lysine amino acid.
- Purify and characterise the synthesised compounds by different analytical techniques including high performance liquid chromatography, mass spectrometry, nuclear magnetic resonance and Fourier transform infra-red spectroscopy.

2.2 Materials

The materials used in the experimental methods and their supplied companies are detailed in Table 2.1.

Table 2.1 List of materials used in Chapter 2.

Material	Company	Catalogue number
6α-Methylprednisolone 21-hemisuccinate sodium salt	Sigma-Aldrich UK	M3781
Acetonitrile (HPLC grade)	Fisher Scientific	A/0626/17
Dichloromethane	Fisher Scientific	10110342
Diethylether (HPLC grade)	Fisher Scientific	D/2450/PB17
Fmoc-Phe-OH	Novabiochem	8520160025
Fmoc rink amide linker	Iris Biotech GmbH	145069563
Fmoc-Lys(Fmoc)-OH	Novabiochem	8520410025
Glass wool	Sigma-Aldrich UK	20411
Methanol (HPLC grade)	Fisher Scientific	M/4056/17
N, N-Dimethylformamide	AGTC Bioproducts	AGMHP1044
N,N-Diisopropylethylamine	Sigma-Aldrich UK	387649
N,N,N',N'-Tetramethyl-O-(1H-benzotriazol-1-yl)uronium hexafluorophosphate	Novabiochem	8510060025
Parafilm	Fisher Scientific	SEL-400-030P
Pasteur pipettes (long 270 mm)	Fisher Scientific	FB50255
Pasteur Pipettes (short 150 mm)	Fisher Scientific	FB50521
Piperidine (reagent plus)	Sigma-Aldrich UK	104094
Pipettor tip finn bulk pack polypropylene	Fisher Scientific	11527462

natural		
Pipettor elite single channel variable volume fully autoclavable 0.5-5mL	Fisher Scientific	11895762
Poly propylene conical base 50 mL centrifuge tubes	Sterilin	50CTB
PP-reactor with PE frit 10ml	MultiSynTech© GmbH	V100PE087
TentaGel S -NH_2 Resin (Bead size 90 μm)	Iris Biotech GmbH	S30902
Timer traceable counts up /down with alarm 60 mm × 50 mm	Fisher Scientific	12695296
Trifluoroacetic acid (TFA)	Sigma-Aldrich UK	T6508-25MC
Trisopropylsilane (TIPS)	Sigma-Aldrich UK	6485-79-6
Zeba spin desalting colmns 0.5 mL	Thermos Scientific	89883

2.3 Methods

2.3.1 Synthesis of Gen0 and Gen1 dendrons

TentaGel S-NH_2 resin (0.5 g) was weighed and placed in a reaction vessel. The reaction vessel was fitted to a microwave peptide synthesiser and a small stirring bar was added inside the vessel. [N, N-Dimethylformamide] (DMF) (5 mL) was added and the resin was allowed to swell for 15 minutes. The liquid was removed and Rink amide linker (0.4 mmol), N,N,N',N'-Tetramethyl-O-(1H-benzotriazol-1-yl)uronium hexafluorophosphate (HBTU) (0.4 mmol), N,N-Diisopropylethylamine (DIPEA) (140 μL) and DMF (3 mL) were placed in a glass vial. The vial was sonicated for 10-20 seconds to solubilise materials and added to the reaction vessel.

The microwave peptide synthesiser (Biotage Initiator, UK.) was set on coupling reaction conditions represented in Table 2.2 for attaching the linker to the solid resin. Upon completion of the reaction, the solvent was removed from the reaction vessel and the resin was washed three times with 3 mL DMF each time to remove any unreacted chemicals. Piperidine (20% $^{v}/_{v}$ in 3 mL DMF) was added to the reaction vessel and the device was set on deprotection conditions (Table 2.2). The deprotection step aimed to remove the protecting

moieties from the periphery amine groups, thus rendering them ready for coupling with the C-terminal of the next amino acid. When the first deprotection reaction was finished, the resin was washed 3-4 times with DMF. The steps of deprotection and washing were repeated 2 more times to ensure complete removal of deprotecting groups. The amine groups were then ready for the next coupling process.

Table 2.2 Coupling and deprotection reaction conditions set for dendron synthesis in microwave peptide synthesiser.

Program	Duration (Minutes)	Power (Watts)	Initial power (Watts)	Temperature (^{o}C)	Stirring rate (rpm)
Coupling	5	50	10	50	900
Deprotection	2	0	0	Off	900

The above steps were repeated to obtain the required sequence of peptide with the same exact procedures except 0.4 mmol of the desired amino acid was used instead of the linker. Thus, 0.4 mmol of Fmoc-Phe-OH and 0.4 mmol of Fmoc-Lys(Fmoc)-OH were used to achieve phenylalanine generation-zero lysine dendron (F-Gen0K) (Figure 2.5).

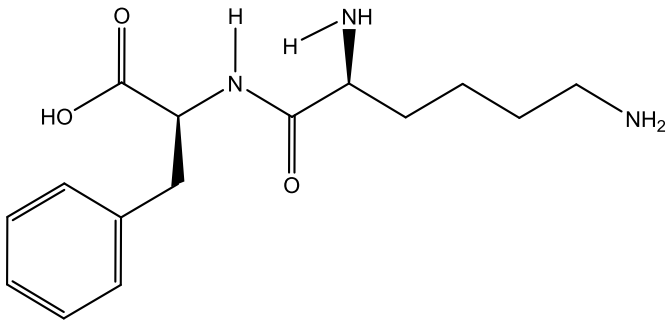

Figure 2.5 Chemical structure of F-Gen0K. The chemical formula is $C_{15}H_{23}N_3O_3$ and the MW is 293.17 Da.

To assemble phenylalanine generation-one lysine dendron (F-Gen1K) (Figure 2.6), two further coupling steps of lysine were performed consecutively. After the assembly of F-Gen0K and F-Gen1K, the resin was removed into a fritted syringe and washed with 40 mL of dichloromethane, 40 mL of methanol, and 40 mL of diethylether respectively. The remaining washing solvent was left to evaporate for 24 hours. The synthesised dendrons were weighed before being cleaved from the resin.

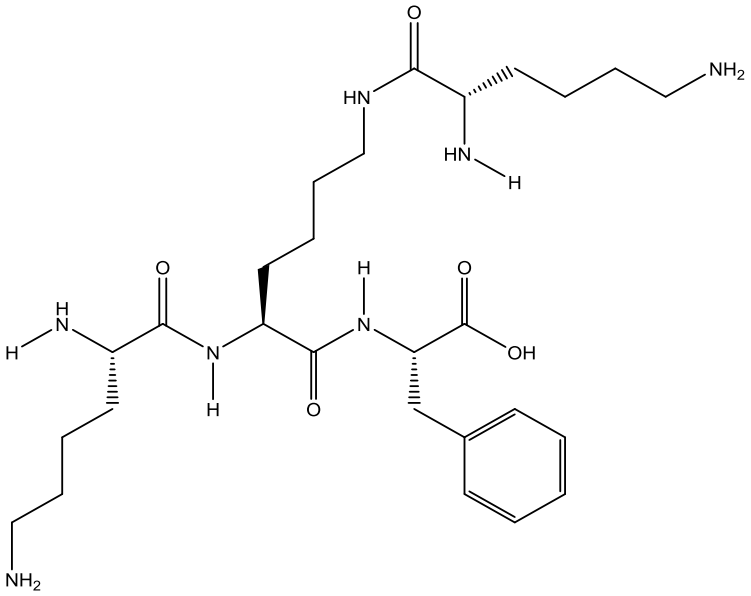

Figure 2.6 Chemical structure of F-Gen1K. The chemical formula is $C_{27}H_{47}N_7O_5$ and the MW is 549.36 Da.

2.3.2 Cleavage of dendrons from solid support

Following coupling of all Fmoc-amino acids of the peptide sequence, the peptide was cleaved from the solid support and the side-chains-protecting groups were removed. Choosing the appropriate cleavage mixture is essential for obtaining the desired peptide, free of any protecting group or structural modification. One of the most common cleavage mixtures is trifluoroacetic acid (TFA)-based supplemented with nucleophilic scavengers that prevent re-assembly or modification of the reactive sites of the peptide once deprotected.

The cleavage solution was prepared according to Table 2.3. Two milliliters of the cleavage solution was dropped carefully on 100 mg of dried resin-peptide. The cleavage reaction was incubated for 3 hours with occasional gentle shaking. The solution was passed down a Pasteur pipette filled with 1 cm of glass wool and the crude peptide was collected in a 50 ml plastic centrifuge tube containing 20 ml of chilled diethylether. The solution was then centrifuged at 3500 rpm for 5 minutes to pellet the dendron. The diethylether was then decanted carefully from the tube. Fresh diethylether (20 mL) was added and the sample was vortexed to disrupt the peptide pellet. The procedure was repeated twice and the diethylether was subsequently decanted. The dendron was then freeze-dried for 24 hours (Freeze drier. Christ Alpha2-4, UK), dissolved in methanol and filtered through a syringe filter with a pore diameter of 0.22 μm prior to characterisation.

Table 2.3 Quantities of materials used to prepare one mL of cleavage solution.

Material	Quantity	Percentage in final mixture
Deionised H_2O	25 µL	2.5% $^{v}/_{v}$
Trisopropylsilane (TIPS)	25 µL	2.5% $^{v}/_{v}$
Trifluoroacetic acid (TFA)	950 µL	95% $^{v}/_{v}$

2.3.3 Covalent binding of MP to dendrons

Methylprednisolone hemisuccinate sodium salt was covalently bound to F-Gen0K (Figure 2.7) and F-Gen1K (Figure 2.8) dendrons using the same principle of amino acid linkage via peptide linkage between the peripheral amine groups of the lysine amino acids and the carboxyl group of the drug.

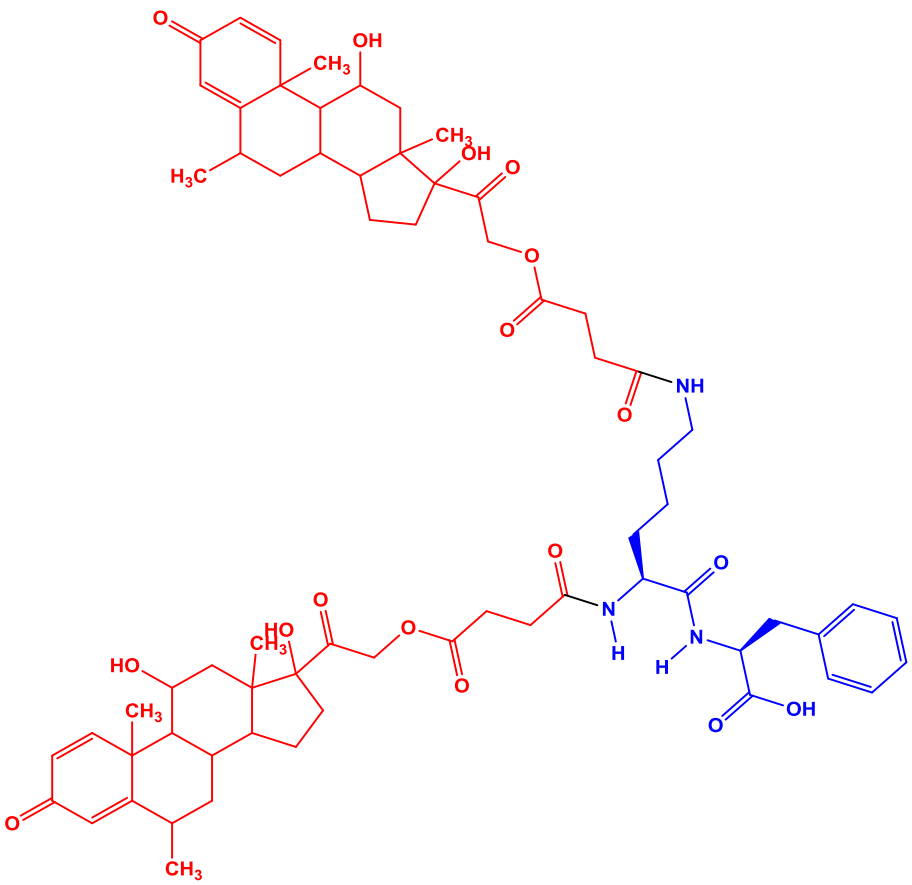

Figure 2.7 Chemical structure of F-Gen0K-MP. The Chemical Formula is $C_{67}H_{87}N_3O_{17}$, MW is 1205.60 Da. The blue structure represents the dendron and the red structures are two MP molecules loaded onto it through amide linkage.

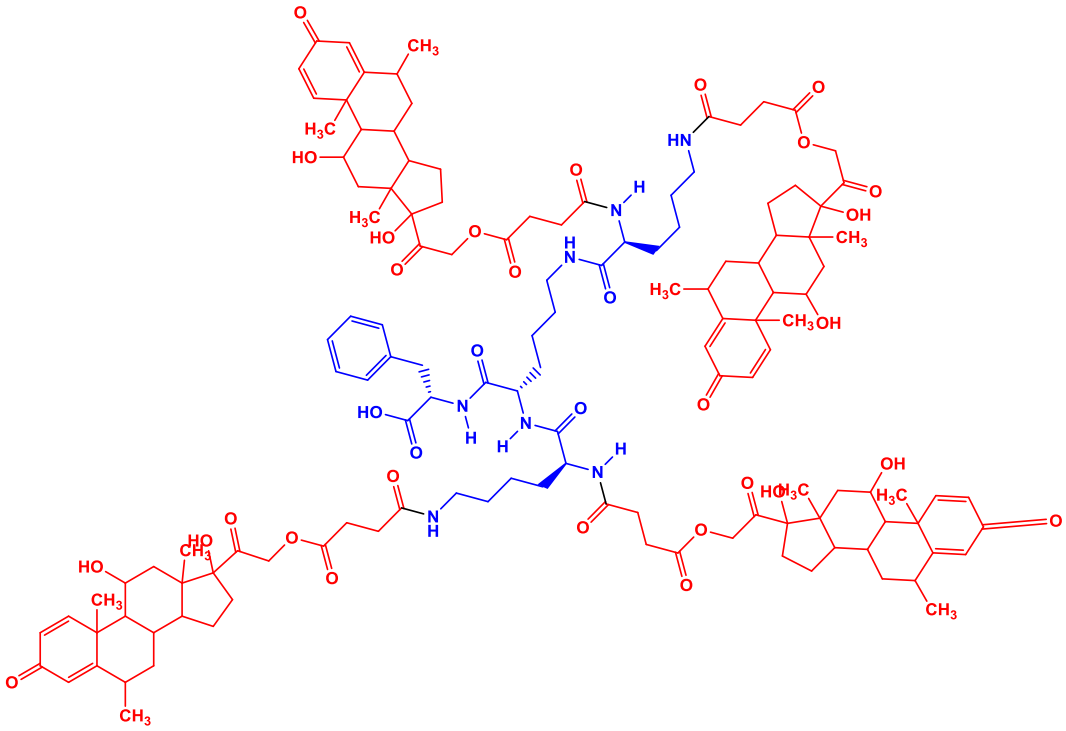

Figure 2.8 Chemical structure of F-Gen1K-MP. The Chemical Formula is $C_{131}H_{175}N_7O_{33}$, MW is 2374.22 Da. The blue structure represents the dendron and the red structures are four MP molecules loaded onto it through amide linkage.

The peripheral amine groups were deprotected using the same protocol mentioned in Section 2.4.1. However, repeating the experiment several times revealed that grafting the drug to the dendron using a manual method instead of using the peptide synthesiser microwave yielded a higher degree of attachment and a higher purity of the final product. Thus, the dendrons attached to the solid support were transferred to 10 mL plastic syringe filters for manual coupling. The attachment of drug to F-Gen0K dendrons involved two coupling steps, each using 0.4 mmol of the drug plus activating agents (HBTU and DIPEA) in 3 mL of DMF.

Drug conjugation to F-Gen1K required four coupling steps. Each coupling process was performed for 30 minutes in an incubator (Stuart® orbital incubator S150) at 40°C and shaking at a speed of 30 rpm. After each coupling step, the peptide was washed 3-4 times with DMF to remove any unreacted moieties. The final dendron-drug conjugates were then washed and cleaved from the resin using the same procedures described for dendrons. A small quantity of the freeze dried dendron-drug conjugates was dissolved in methanol to achieve a final concentration of 1 mg/mL and filtered through a 0.22 µm pore diameter syringe filter and used for characterisation. The rest of the dendron-drug conjugates were stored at 4 °C to be used later in further experiments.

2.3.4 Purification of the synthesised molecule

Samples were purified using Zeba® spin desalting columns (0.5 mL). These columns contain a high-performance size-exclusion chromatographic resin that offers desalting or buffer exchange for peptide samples. It offers ≥ 95% retention of salts and other small molecules. The columns were washed with 0.3 mL methanol and centrifuged at 1500 rpm for one minute. The washing process was repeated twice to ensure complete removal of the column preserving liquid, then 130 μL of the sample (dissolved in methanol) was added to the column and the filtered sample was collected after centrifugation for 2 minutes.

2.3.5 Characterisation of denrons and dendron-drug conjugates

There are many analytical techniques used for the identification and characterisation of the chemical composition, the morphology, the shape and the homogeneity of biomolecules including dendrons and its derivatives. In this study, high performance liquid chromatography (HPLC), mass spectrometry, NMR, and Fourier transform-infrared spectroscopy (FTIR) were used for the characterisation of the synthesised molecules.

2.3.5.1 Characterisation and purification by HPLC

High performance liquid chromatography can be used to separate mixtures of materials into their components on the basis of their molecular structure and composition. It is composed of a stationary phase (either solid or liquid supported on a solid) and a mobile phase (liquid or gas). The mobile phase runs through the stationary phase under high pressures of up to 400 atmospheres carrying the components of the mixture with it (Batrawi *et al.*, 2017). Sample components that exhibit stronger affinities with the stationary phase will have a slower movement through the column compared to components with weaker interactions (Siddiqui *et al.*, 2017). This variance in rates causes the separation of different components. As shown in Figure 2.9, basic HPLC instrumentation includes a pump, injector, column, detector and acquisition and display system. The essential part of the system is the column unit where separation of components occurs.

Samples of F-Gen0K-MP and F-Gen1K-MP were dissolved in methanol filtered through a syringe filter with a pore diameter of 0.4 μm and run through HPLC (Agilent 1260 infinity, G7117 Diode array detector and G7167 auto sampler). The conditions were set using a reversible phase C18 Fortis® column (150 mm, 4.6 mm and 5 μm pore size). The mobile phase consisted of a gradient of 0.1% $^{v}/_{v}$ TFA acid in acetonitrile and 0.1% $^{v}/_{v}$ TFA in water using 0.6 mL/minute flow rate and a run time of 20 minutes with a maximum pressure of 400 pounds *per* square inch. The maximum wavelength of absorbance (λ_{max}) for F-Gen0K-MP (274

nm) and F-Gen1K-MP (280 nm) were previously determined by spectrophotometry (Lambda 25 UV-VIS spectrophotometer/PerkinElmer). The desired peaks were collected and the process was repeated several times to retrieve as much of the purified sample as possible. The collected samples were freeze-dried for 24 hours (Freeze drier. Christ Alpha 2-4, UK) to remove any solvents.

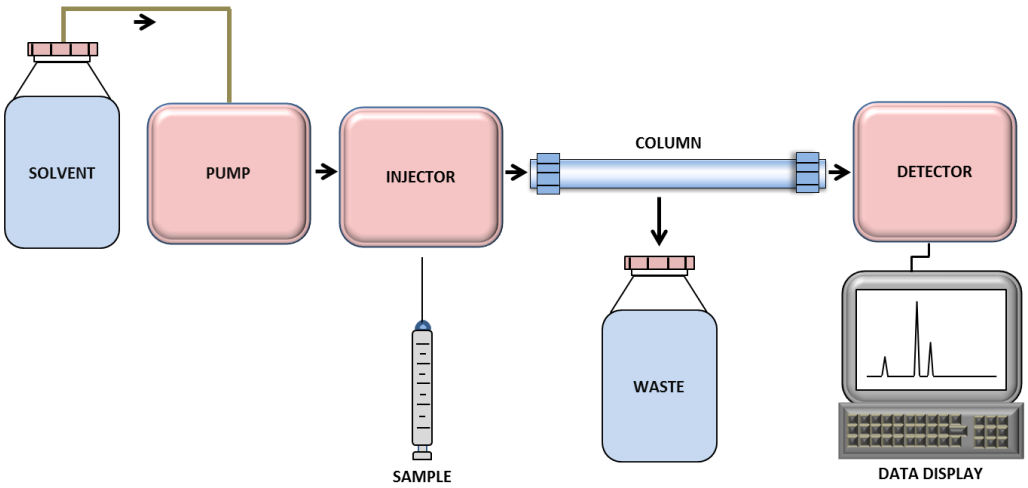

Figure 2.9 Basic principle components of HPLC. The column separates the compounds depending on their polarity. Non polar stationary phase attracts the nonpolar compounds causing polar compound to elute first then the nonpolar compound, while in a polar stationary phase the nonpolar compound elutes first.

2.3.5.2 Mass spectrometry

Mass spectrometry allows precise determination of the molecular mass of peptides as well as their sequences (Sparkman, 2000). A mass spectrometer generates multiple ions from the sample under investigation; it then separates them according to their specific mass-to-charge ratio (m/z), and then records the relative abundance of each ion type. The first step in the mass spectrometric analysis of compounds is the production of gas-phase ions of the compound by electron ionisation. This molecular ion undergoes fragmentation. Each primary product ion derived from the molecular ion, in turn, undergoes fragmentation. The ions are separated in the mass spectrometer according to their m/z ratio, and are detected in proportion to their abundance. A mass spectrum of the molecule is thereby generated. It displays the result in the form of a plot of ion abundance versus m/z (Sparkman, 2000). The ions provide information concerning the nature and the structure of their precursor molecule (Figure 2.10).

To perform the analysis, the drug (MP), the synthesised dendrons (F-Gen0K and F-Gen1K) and dendron-drug conjugates (F-Gen0K-MP and F-Gen1K-MP) were dissolved in methanol at a final concentration of 1 mg/mL. The solutions were filtered through a syringe filter with a

pore diameter of 0.22 µm. Fifty microliters of each solution was injected into the spectrophotometer (Mass spectrometry-Electrospray micoTOF, Bruker Daltonics). The results showed the available peaks at the m/z ratio and their intensity.

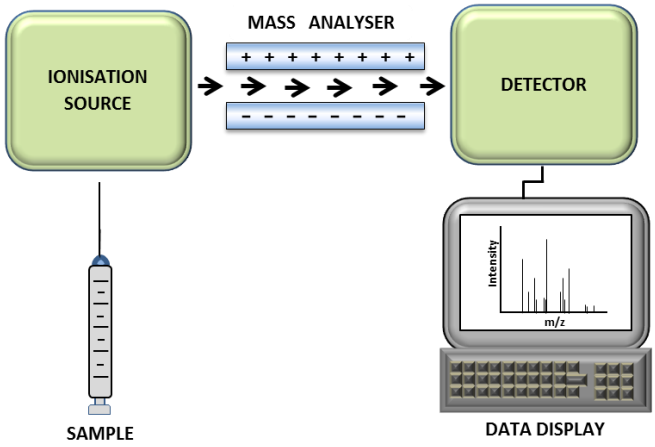

Figure 2.10 Basic steps in mass spectrometry analysis. A mass spectrometer consists of three components: an ionisation source, a mass analyser, and a detector. The output data are a mass spectrum which is a plot of the ion signal as a function of the mass-to-charge ratio and its intensity.

2.3.5.3 Fourier transform infra-red spectroscopy

FTIR spectroscopy relies on the fact that most molecules absorb light in the infra-red region of the electromagnetic spectrum. This absorption corresponds specifically to the bonds present in the molecule (Griffiths *et al.*, 2007). The frequency range is measured as wave numbers typically over the range 4000-650 cm^{-1}. While FTIR is frequently used for polymer testing and pharmaceutical analysis, the application of the technique is virtually limitless offering both qualitative and quantitative analysis of a wide range of organic and inorganic samples. The background emission spectrum of the infrared source is first recorded, followed by the emission spectrum of the IR source with the sample in place. The ratio of the sample spectrum to the background spectrum is directly related to the sample's absorption spectrum. The resultant absorption spectrum from the bond natural vibration frequencies indicates the presence of various chemical bonds and functional groups present in the sample. FTIR is particularly useful for identification of organic molecular groups and compounds due to the range of functional groups, side chains and cross-links involved, all of which will have characteristic vibrational frequencies in the IR range (Griffiths *et al.*, 2007).

FTIR spectrophotometery (FTIR, Perkin Elmer Spectrum 65) can be used for solid and liquid samples. Here, solid samples were used. The method involved initial calibration of the background and standardisation of the device. The FTIR was set on 32 scans. Five milligrams

of the material under investigation (powder form) was placed in the device to be measured and the sample scanned 32 times at wavelengths of 650 and 4000 cm^{-1}.

2.3.5.4 Nuclear magnetic resonance

NMR spectroscopy utilises the magnetic properties of specific atomic nuclei to determine the physical and chemical properties of atoms or the molecules forming different compounds. The technique relies on the NMR phenomenon to provide comprehensive information about the molecular structure, kinetics, reaction state and chemical habitat of molecules. Changes in the resonance frequency of the intramolecular magnetic field surrounding an atom in a molecule can reveal details of the electronic structure of that molecule. For most small molecules when placed in a magnetic field, NMR active nuclei such as 1-dimensional proton (^{1}H) or carbon-13 (^{13}C) absorb electromagnetic radiation at a frequency specific to that isotope (Shah *et al.*, 2006). The frequency of the resonant, the absorbed energy and the signal intensity are proportional to the strength of the applied magnetic field.

The samples were dissolved in methanol and excited *via* pulsations in a in a magnetic field. The realigned magnetic fields produced by ^{1}H or ^{13}C atoms induce a radio signal which generates the output signal as a spectrum. The NMR spectrum is a plot of the radio frequency used versus absorption. A signal in the NMR spectrum is referred to as a resonance. Different types of ^{1}H or ^{13}C atoms ideally generate different signals in NMR spectrometry based on the surrounding environment to that atom such as the attachment to a different type of atom (such as CH versus OH) or due to the number of adjacent H atoms (such as $-CH_3$ versus $-CH_2-$) or even at a different point in a chain (such as comparison of the H atom in the methylene (CH_2) groups in $CH_3CH_2CH_2OH$) (Shah *et al.*, 2006).

2.4 Results

2.4.1 Purification of dendron-MP conjugates by HPLC

F-Gen0K-MP was purified by collecting its distinctive peak which appeared after 15.8 minutes (Figure 2.11). The sample was collected from 15.5 minutes to 17.5 minutes using the automated sampler collector of the HPLC. The collected sample was rerun through HPLC gave a single peak (Figure 2.11) providing an indication of the successful separation of the desired peak.

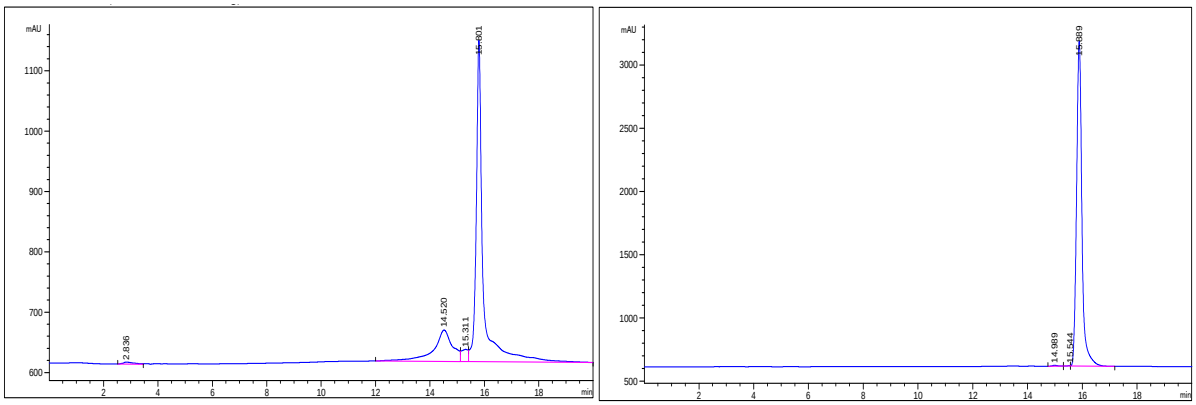

Figure 2.11 HPLC spectra of F-Gen0K-MP. HPLC spectra of crude F-Gen0K-MP (left) and its spectra after separation of the desired peak (right).

The process was repeated for F-Gen1K-MP by collecting its distinctive peak between 10.5 to 12 minutes (Figure 2.12) to collect its purified sample which gave a distinctive peak at 11.8 minute.

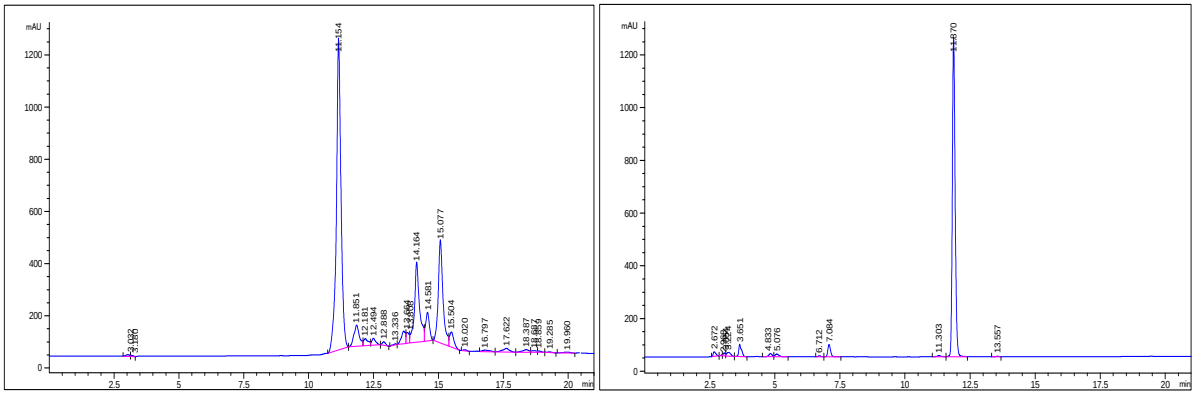

Figure 2.12 HPLC spectra of F-Gen1K-MP. HPLC spectra of crude F-Gen1K-MP (left) and its spectra after separation of the desired peak (right).

2.4.2 Mass spectrometry analysis of dendron-MP conjugates

Based on mass spectrometry spectra, both F-Gen0K and F-Gen1K were synthesised efficiently using the SPPS method. The exact MW of F-Gen0K (293 Da) and F-Gen1K (549 Da) appeared as distinctive peaks in MS peaks analysis (Figures 2.13 & 2.14).

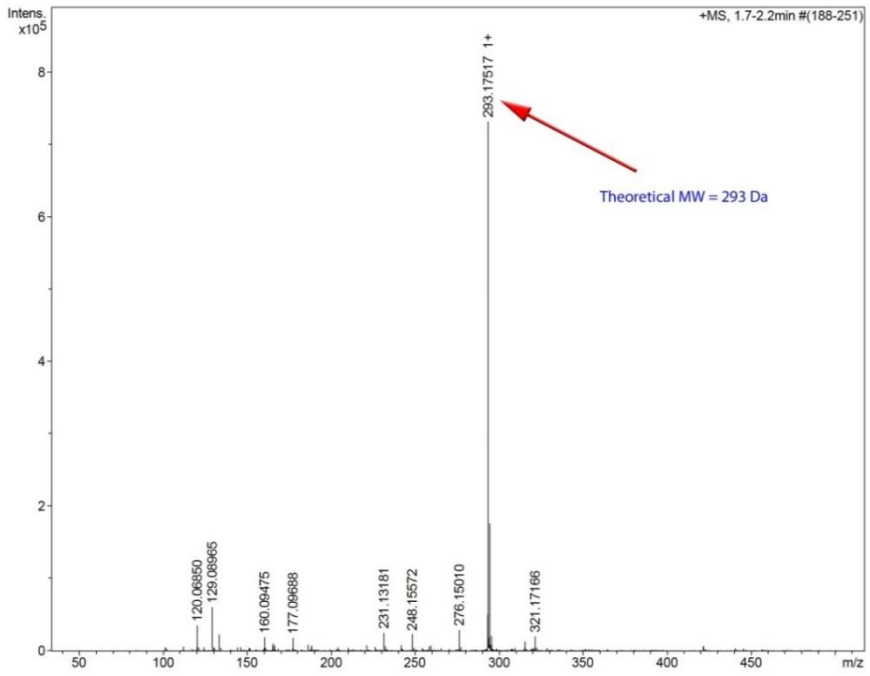

Figure 2.13 Mass spectrometry of F-Gen0K dendron. The MW of the synthesised dendron was equal to the theoretical MW which is 293 Da.

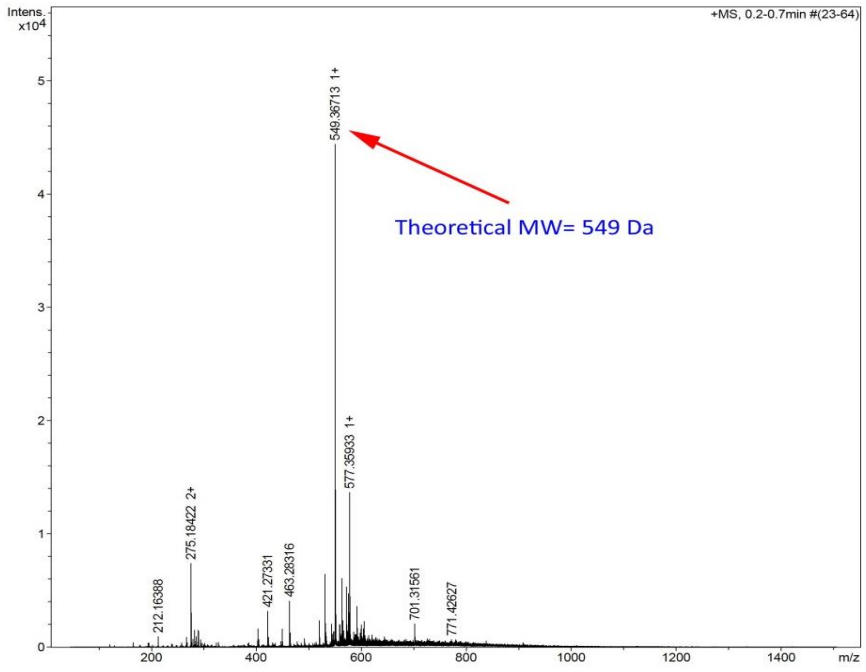

Figure 2.14 Mass spectrometry of F-Gen1K dendron. The actual and theoretical molecular weights were the same (549 Da).

The mass spectrum of F-Gen0K-MP confirmed the attachment of two drug molecules to the peripheral functional groups of the dendron (Figure 2.15).

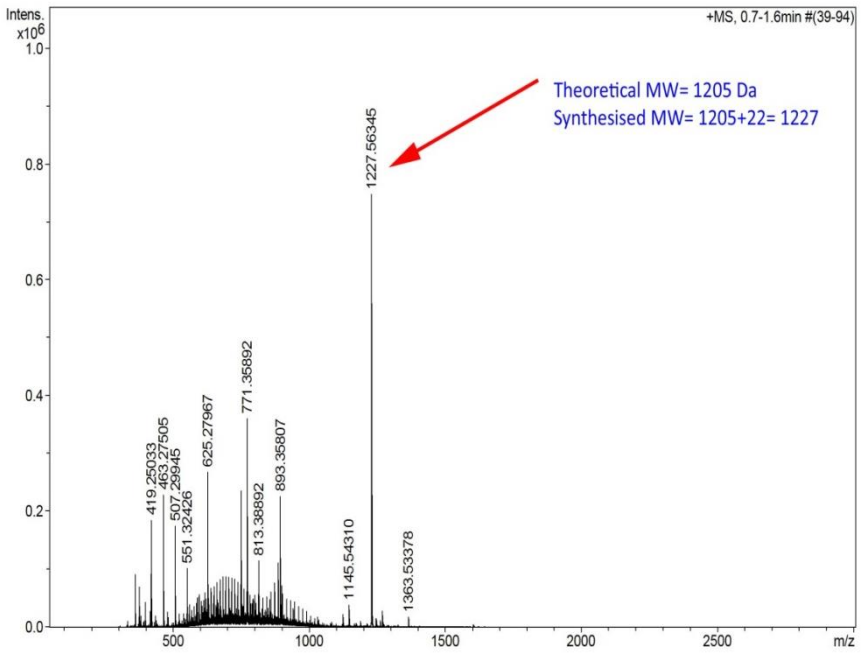

Figure 2.15 Mass spectrometry of F-Gen0K-MP conjugate. The theoretical MW of PheG0K-MP is 1205 Da, but the actual MW based on the MS spectra was 1227 Da. The difference can be attributed to the fact that the synthesised dendron contained sodium ion (sodium MW is 23 Da).

The synthesised MW of F-Gen1K-MP appeared in mass spectroscopy as 2397 Da rather than the theoretical value of 2375 Da (Figure 2.16) due to the presence of sodium ions as a result of using the sodium salt of the drug (MP).

To confirm that this increment in the MW of the synthesised molecules was caused by the presence of sodium from the drug, a mass spectrometry for the pure drug in methanol was performed (Figure 2.17). The spectra included a distinctive peak of MP with a MW equal to 496 Da as well as a second peak with sodium ion with a MW of 518 Da (MP + sodium).

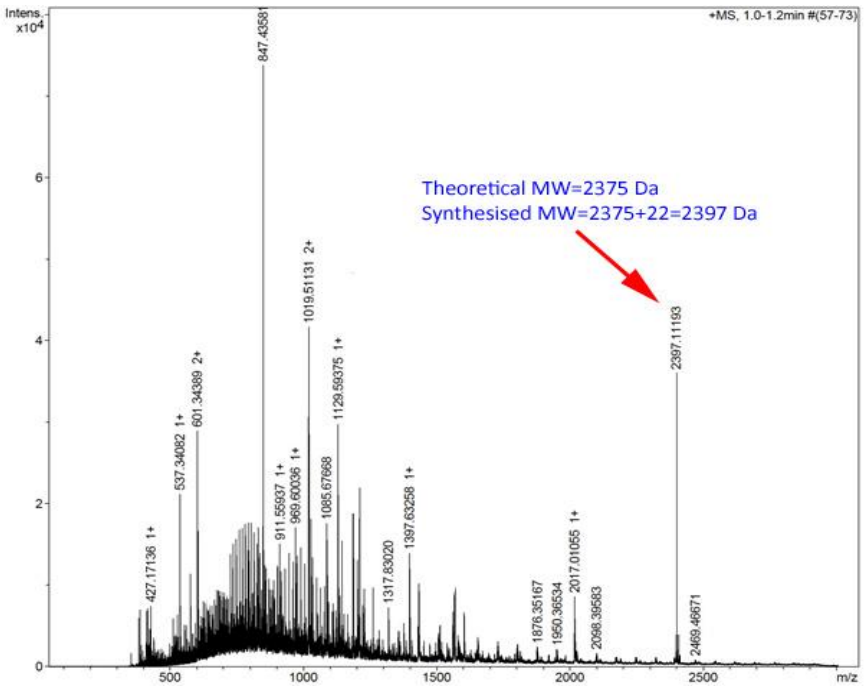

Figure 2.16 Mass spectrometry of F-Gen1K-MP conjugate. The synthesised dendron-drug conjugate peak appeared higher than the theoretical MW by 22 Da due to the presence of sodium ion. However, several other peaks appeared in the spectra suggesting ionisation of the molecule by the ioniser or fragmentation of the synthesised molecule during the cleavage as a result of the compact structure and relatively high MW of Gen0 dendron-drug conjugate.

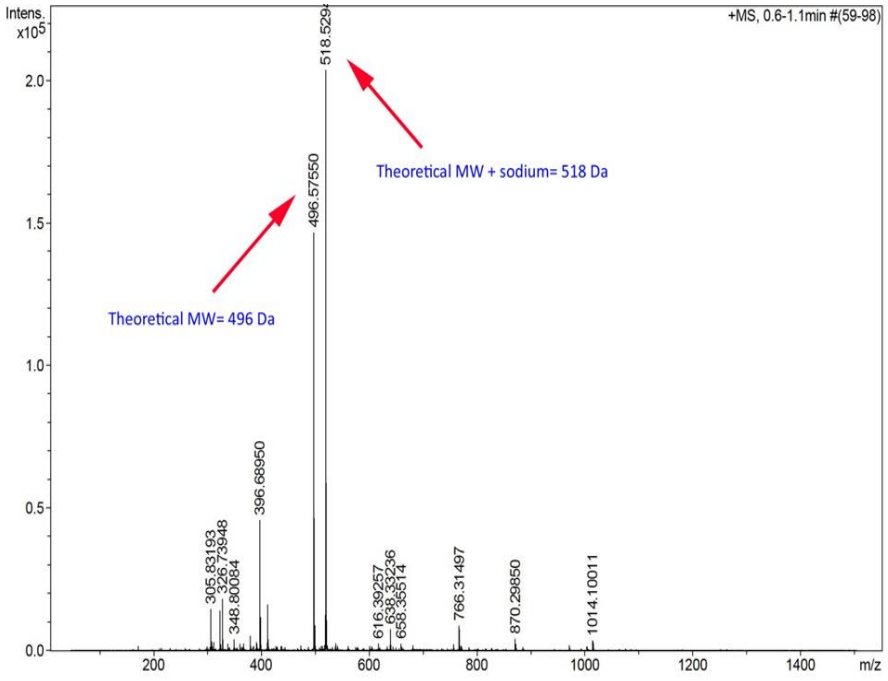

Figure 2.17 Mass spectrometry of pure MP. Both the MW of MP and that of MP plus sodium appeared in the spectra.

2.4.3 FTIR analysis of dendron-MP conjugates

The combined FTIR troughs of MP, F-Gen0K and F-Gen0K-MP are shown in Figure 2.18. Based on the chemical structure of these molecules (Figures 1.5, 2.5 & 2.7), the characteristic chemical bonds that can be detected by FTIR are the peripheral amine groups of F-Gen0K (Figure 2.5) which should disappear in F-Gen0K-MP (Figure 2.7) due to the formation of amide bonds. Moreover, the ketone-group peak of MP (Figure 1.5) should appear in the final dendron-drug conjugate, but not the free dendron.

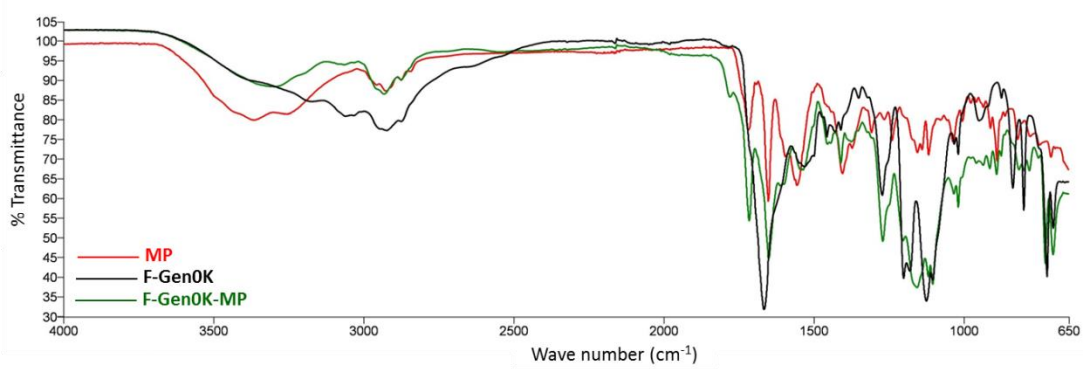

Figure 2.18 FTIR spectra of MP, F-Gen0K and F-Gen0K-MP with wave number ranging from 650 to 4000 cm^{-1}.

For clearer analysis the wavelength spectra (Figure 2.18) ranging from 650 to 4000 cm^{-1} was split into two spectra (Figures 2.19 & 2.20). The distinctive trough of the amine groups which appear at around 3100 cm^{-1} in F-Gen0K dendron disappeared in the dendron-drug spectrum (Figure 2.19). The disappearance of the NH_2 trough signifies the formation of amide bond linkages between the carboxyl groups of the drug with the peripheral amine groups of the dendron. The unique ketone-group trough of free MP appeared at around 1700 cm^{-1} in the spectra of F-Gen0K-MP (Figure 2.20) providing evidence of the successful attachment of the drug to the dendron.

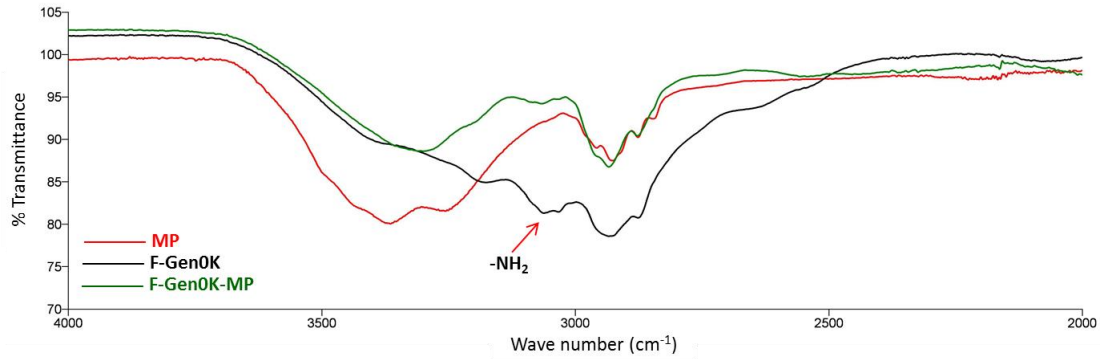

Figure 2.19 FTIR spectra of MP, F-Gen0K and F-Gen0K-MP with wave number ranging from 4000 to 2000 cm^{-1}. Absence of NH_2 group trough in F-Gen0K-MP molecule compared to F-Gen0K molecule at 3085 cm^{-1} due to amide bond formation.

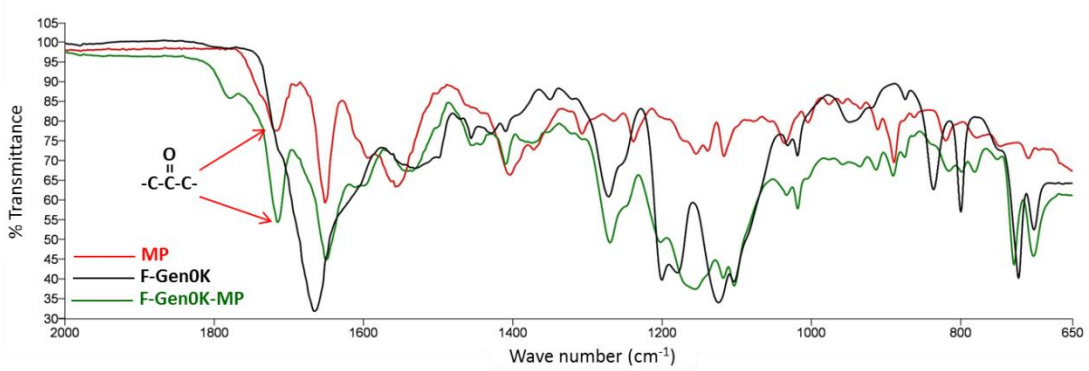

Figure 2.20 FTIR spectra of MP, F-Gen0K and F-Gen0K-MP with wave number ranging from 2000 to 650 cm^{-1}. Appearance of MP-ketone trough in the F-Gen0K-MP molecule but not in the free dendron.

Due to the similarity in the functional groups of F-Gen0K-MP to F-Gen1K-MP, the same FTIR findings were observed in F-Gen1K-MP spectrometry when compared to F-Gen1K dendron and MP (Figures 2.21-2.23).

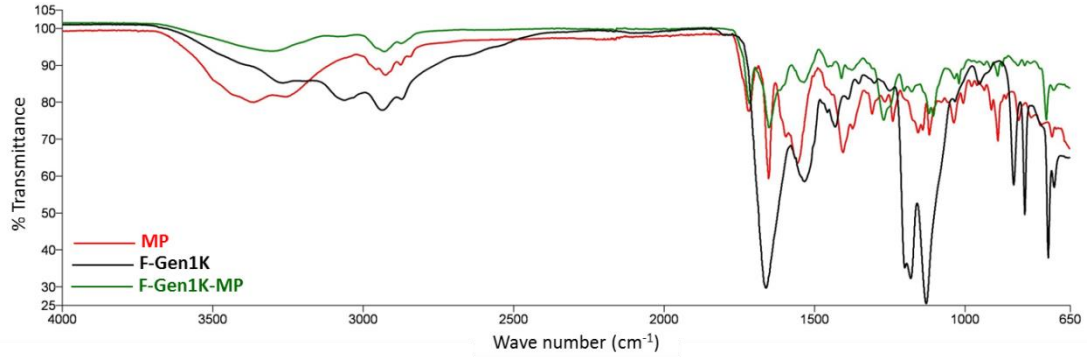

Figure 2.21 FTIR spectra of MP, F-Gen1K and F-Gen1K-MP with wave number ranging 4000 to 650 cm^{-1}. The MP-ketone trough could be detected in F-Gen0K-MP molecule but not in the free dendron.

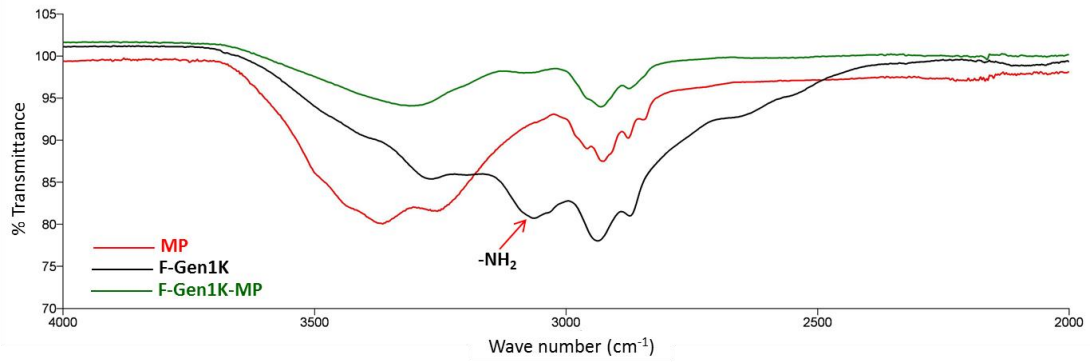

Figure 2.22 FTIR spectra of MP, F-Gen1K and F-Gen1K-MP with wave number ranging from 4000 to 2000 cm^{-1}. The NH_2 group trough appeared in F-Gen0K at 3085 cm^{-1} molecule but disappeared in F-Gen0K-MP molecule due to drug attachment to this group.

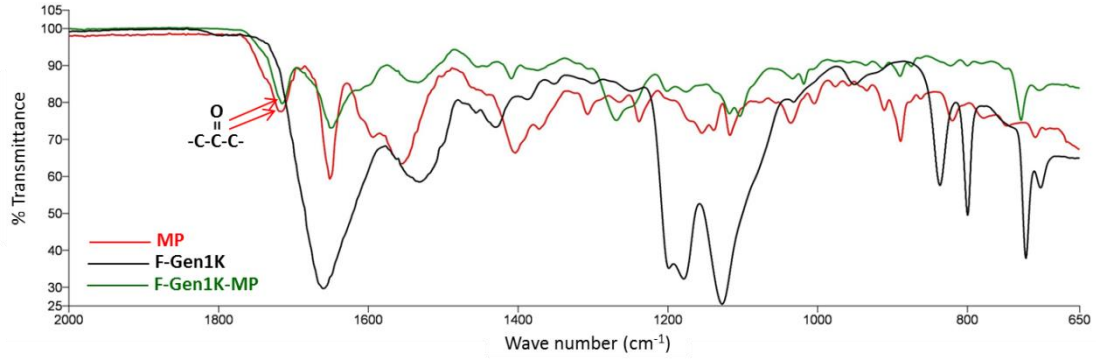

Figure 2.23 FTIR spectra of MP, F-Gen1K and F-Gen1K-MP with wave number ranging from 2000 to 650 cm^{-1}. The unique ketone-group trough of free MP appeared in the final synthesised molecule, F-Gen1K-MP.

2.4.4 NMR analysis of dendron-MP conjugates

The NMR spectra of F-Gen0K dendron, MP and F-Gen0K-MP were integrated in a single diagram for comparison (Figure 2.24). For more comprehensive comparison the radio frequency ranging from 5.5 to 8.0 ppm was enlarged (Figure 2.25). The protons of the phenyl group of phenylalanine amino acid appeared as a distinctive peak at 7.2 ppm in both the dendron and the loaded dendron. The hydrogen atoms near to the C=O group of the hexagonal ring in MP gave unique peaks which can be seen in both the free drug and its attached form. These peaks were slightly shifted towards the up-field in F-Gen0K-MP molecule when compared with the same H atoms of the free drug. The presence of the resonance signals of H atoms which are unique to MP and F-Gen0K in the NMR spectrum of the F-Gen0K-MP molecule provide suitable evidence of the successful attachment of MP to Gen0 dendron.

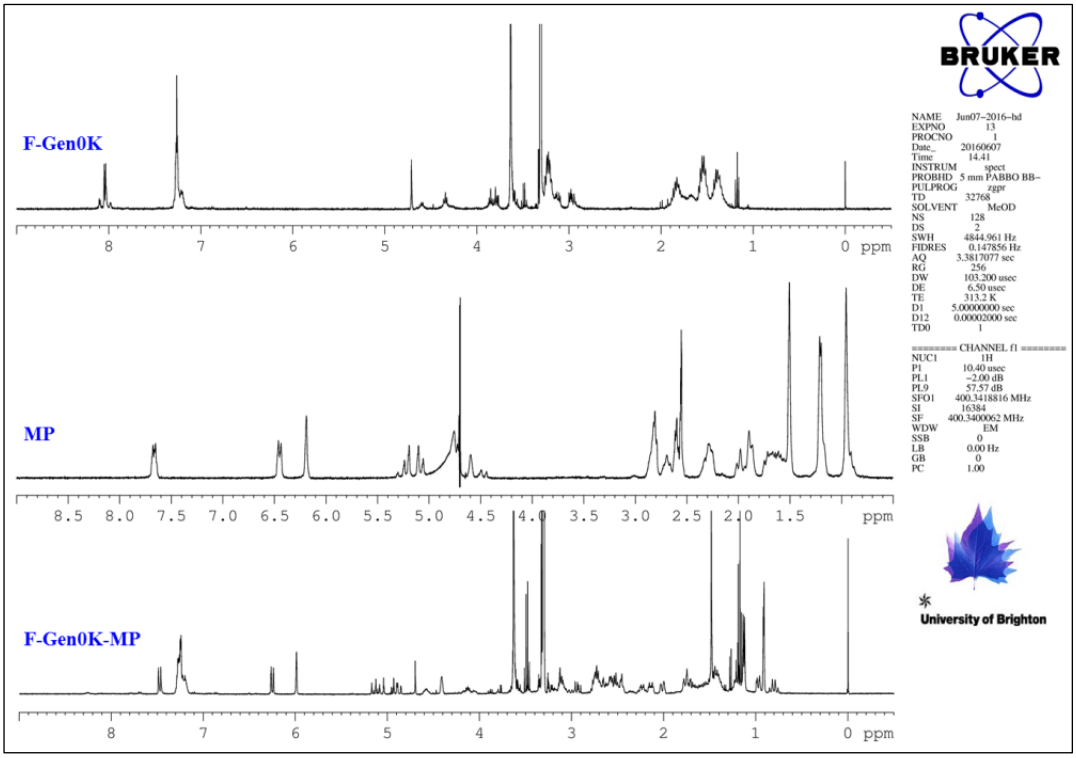

Figure 2.24 NMR peaks of free MP, F-Gen0K dendron and F-Gen0K-MP. Comparisons of the H atoms spectra of free F-Gen0K and free MP with final molecule, F-Gen0K-MP.

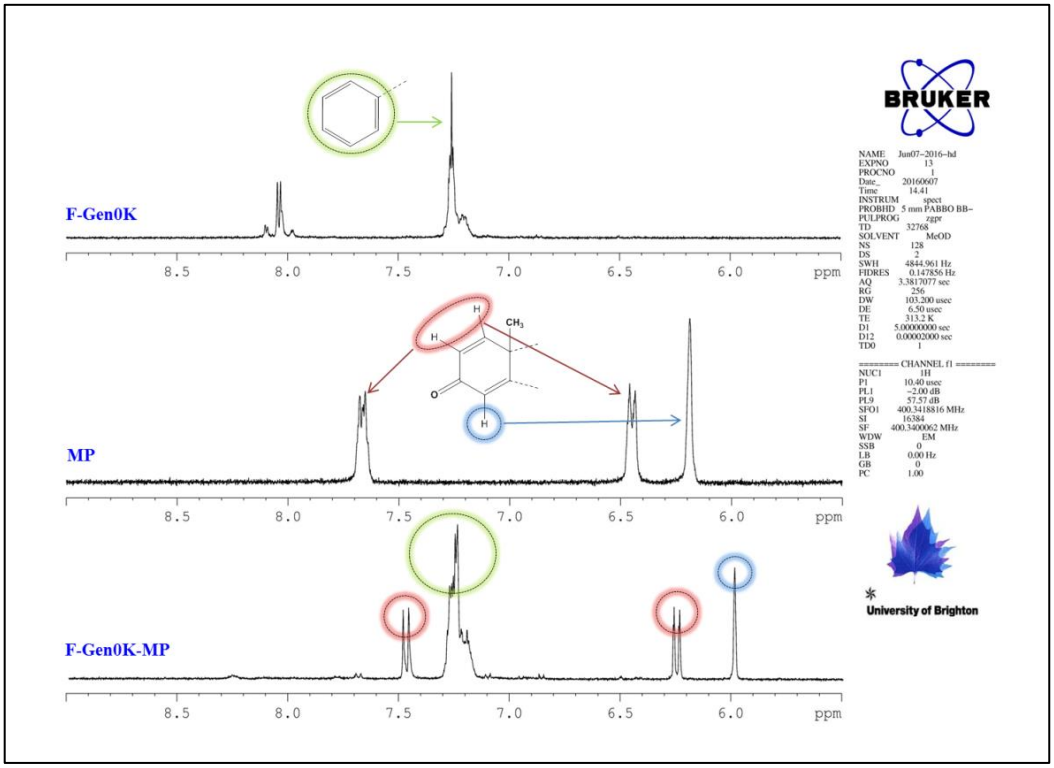

Figure 2.25 NMR peaks of free MP, F-Gen0K dendron and F-Gen0K-MP with ppm ranging from 5.5 to 9. The peaks of the protons of the phenyl group of phenylalanine amino acid in the dendron (green) and the peaks of the hydrogen atoms of the hexagonal ring in free MP (red and blue) all appeared in the synthesised F-Gen0K-MP molecule with slight shifting.

The same H atoms were compared in NMR spectrums of F-Gen1K dendron, MP and F-Gen1K-MP (Figures 2.26 & 2.27). The results showed similar patterns to F-Gen0K-MP where the tested peaks of the drug and dendron could be also found in F-Gen1K-MP spectra.

The data obtained by analysing the NMR spectra of F-Gen0K-MP and F-Gen1K-MP which showed the appearance of the H atom peaks which are unique in free MP (from the hexagonal ring) and in free dendron (from the phenyl group) in the final synthesised molecules provides strong evidence of the successful attachment of the drug to the dendrons.

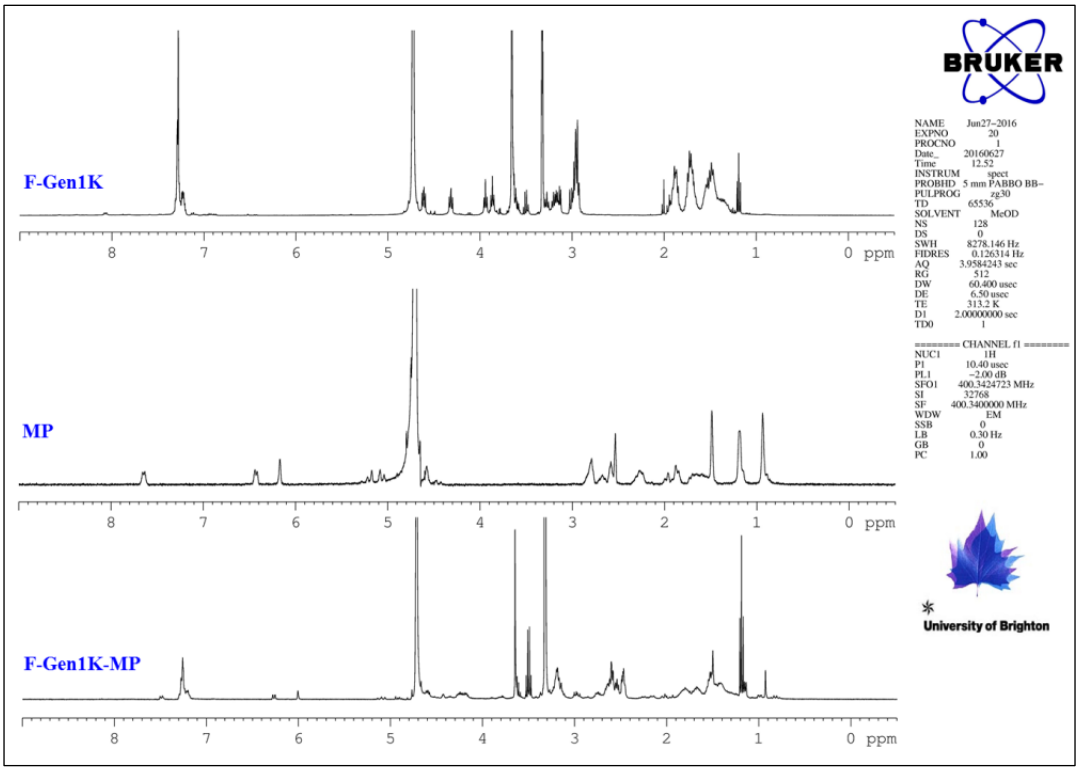

Figure 2.26 NMR peaks of free MP, F-Gen1K dendron and F-Gen1K-MP. Comparisons of the H atoms spectra of free F-Gen1K and free MP with final molecule, F-Gen1K-MP.

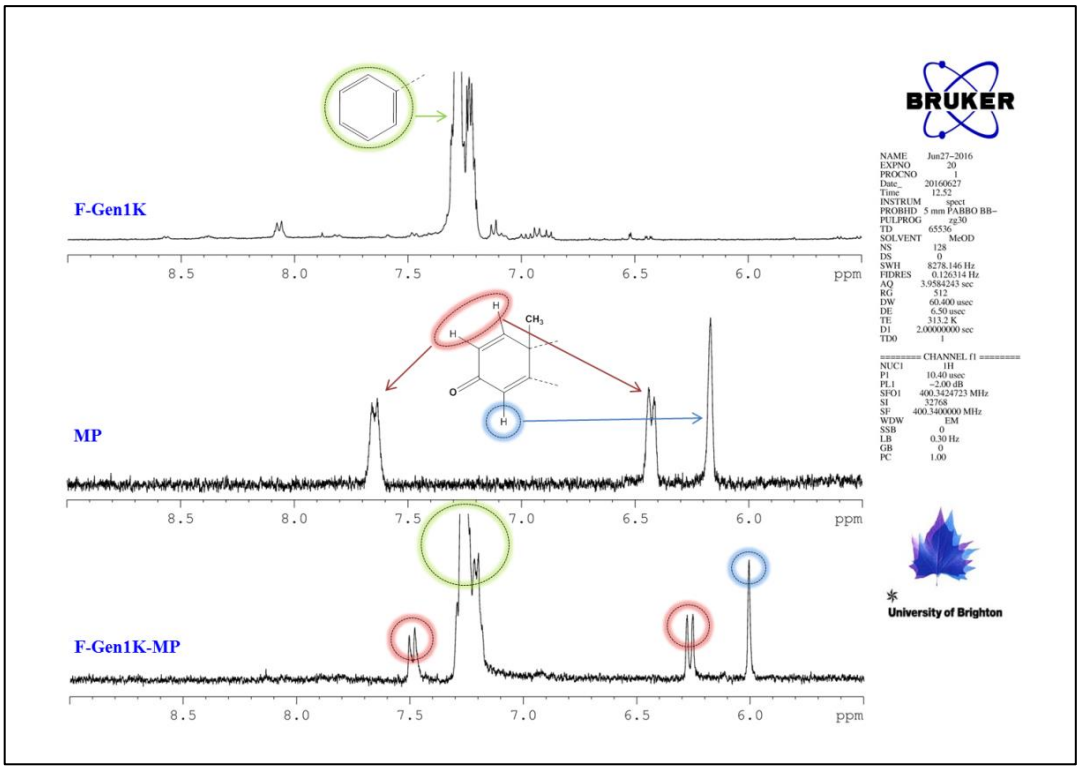

Figure 2.27 NMR peaks of free MP, F-Gen1K dendron and F-Gen1K-MP with ppm ranging from 5.5 to 9. The peaks of the protons of the phenyl group of phenylalanine amino acid in the dendron (green) and the peaks of the hydrogen atoms of the hexagonal ring in free MP (red and blue) all appeared in synthesised F-Gen1K-MP molecule with slight shifting.

2.5 Discussion

Due to its limited penetration to the brain, new approaches should be applied to improve MP permeability for the treatment of relapses in MS patients (Holtman *et al.*, 2014). Such a better permeability will result in lowering the dose of MP administrated to the patients and thereby remarkably reduce the drug's side-effects.

One of these permeability enhancement approaches is to use dendrons as drug carriers for MP. The well-defined size monodispersity, structure and controllable surface active groups of dendrimers and dendrons make them excellent candidates as drug carriers. The use of these molecules offers several advantages, including the fact that these structures are well-defined molecules what consequently, allow the development of highly-controlled DDSs and have the potential for high drug molecule payloads.

The loading capacity of dendrimers for guest molecules, especially drugs, may be potentially increased by the formation of a reversible complex with the large number of active groups on the dendrimer surface (Svenson *et al.*, 2005). Due to its multiple functional peripheral groups, one dendrimer molecule can be loaded with multiple drug molecules (four MP drug molecules were loaded on F-Gen1K dendron) and the number of drug molecules can be increased using higher generations of dendrimers. The number of peripheral amine groups available for drug attachment doubles with each increasing generation. However, it should be kept in mind that not all of the peripheral surface groups in a high generation dendron (especially Gen3 and higher) may be available for drug attachment, either due to back-folding of peripheral chains into the dendrimer or steric hindrance caused by molecule crowding (Kolhe *et al.*, 2003). This was avoided in this study by choosing low generation dendrons (Gen0 and Gen1).

There are several issues that were considered prior to F-Gen0K-MP and F-Gen1K-MP synthesis such as the method of synthesis, the type of N^{α}-protecting group (which will govern the overall synthesis strategy), the type of amino acids side-chain protection, class of solid support and linker, the choice of coupling reagents (efficient amide-bond formation) and the type of cleavage mixture.

In this study, the SPPS method was chosen to perform the assembly of required dendrons and dendron-MP conjugates. This method was first introduced in 1985 by Merrifield who synthesised a tetrapeptide under heterogeneous controlled conditions from the C to the N terminus on a polymeric insoluble solid support (Merrifield, 1985). In SPPS the peptide synthesis is performed between two phases, liquid soluble reagents and an insoluble solid

support (Merrifield, 1986). The highly refined organic chemistry in SPPS has made this method the first choice not only to assemble peptides but also small proteins (Søren *et al.*, 2012). Synthesising F-Gen0K-MP and F-Gen1K-MP on an insoluble solid support offered many advantages. For example, separation of the intermediate dendrons from unreacted soluble reagents and solvents was simply performed by filtration and washing with DMF thus saving time and labour compared to liquid-phase synthesis. Moreover, coupling and deprotection steps were amenable to automation and excess reagents was employed to help to drive reactions to completion. Finally, physical losses were minimised as the assembled dendron-MP conjugates remained attached to the solid support.

However, SPPS has some drawbacks. The analytical techniques employed for monitoring the progress of reaction in liquid phase synthesis are generally not suitable for SPPS and only limited to simple qualitative colour tests that detect the presence of residual amines such as the ninhydrin test (Chan *et al.*, 2009). The other disadvantage of SPPS is the accumulation of by-products arising from incomplete reactions, side reactions and impure reagents on the resin during synthesis, thus affecting the purity of final product. This was avoided by choosing amino acids with Fmoc protecting chains, using a peptide microwave synthesiser to assemble dendrons, and by choosing the right cleavage mixture which led to the successful synthesis of desired molecules as confirmed by mass spectrometry (Figures 2.13-2.16).

Fmoc-amino acids ensured the occurrence of the reaction only at the site of interest for the formation of the amide linkage peptide bond (Hudson, 1988). Also, Fmoc-amino acids helped to prevent secondary reactions (Pires *et al.*, 2014), like the incorporation of dipeptide derivatives instead of an amino acid derivative, thus ensuring the purity of the final molecules. Despite using the optimal cleavage mixture, the final products suffered from some fragmentation especially F-Gen1K-MP as suggested by the appearance of multiple peaks in its mass spectrometry (Figure 2.16). The synthesised molecules were purified by HPLC by collection of the desired peak and freeze drying it to obtain a pure final product that can be used in subsequent cytotoxicity experiments and penetration experiments.

Phenylalanine and lysine amino acids with Fmoc protecting groups were chosen to synthesise F-Gen0K-MP and F-Gen1K-MP rather than Boc amino acids as they were easier and safer to handle as they did not require hydrofluoric acid (HF) in the synthesis. The Boc strategy, initially developed by Merrifield (Merrifield, 1986), requires repetitive usage of TFA for removal of Boc groups, and often using HF for release of the assembled peptide from the

solid support. Thus, this method normally requires the use of corrosive and toxic HF and should be conducted in HF apparatus. However, the Fmoc group can be removed under mild conditions with secondary amines (typically 1:4 piperidine : DMF mixture). Using precise microwave rays to heat the reaction mixture to desired temperatures during the coupling and deprotection steps offered several advantages such as enabling a high degree of predictability and reproducibility of peptide synthesis, which was obvious from the consistency of results in repeated synthesis cycles. Moreover, using the peptide synthesiser for the synthesis of F-Gen0K and F-Gen1K offered other benefits such as a reduction in the time of coupling process, saving about 25 minutes *per* coupling step compared to the manual method. Also, it offered more controllable reaction conditions such as temperature, duration of reaction and stirring rate.

The set of reaction conditions listed in Table 2.2 were used based on previous studies in the Brighton Centre for Regenerative Medicine (BCRM), University of Brighton which indicated that these conditions were the optimum conditions for synthesising dendrons ranging from Gen1 to Gen3. Unlike conventional-conductive heating which transfers energy to the reaction compounds by thermal conductivity or convective currents, heating transfer by microwave (dielectric heating at 2.45 GHz) occurs by disposing the energy directly to the solvent, due to interactions of the reaction material with the alternating electric field (Søren *et al.*, 2012).

However, the synthesis of F-Gen0K-MP and F-Gen1K-MP using an automated microwave method was unsuccessful and a manual method was used to achieve the synthesis. This might be attributed to the set of reaction conditions for the peptide synthesiser which are optimum for standard peptide synthesis but might not be ideal for other molecules such as MP.

Another factor that could be the reason for the unsuccessful attachment of MP to dendrons by the peptide synthesiser is the duration of reaction. Using the automated method the coupling reaction was set on 5 minutes while in the manual method it was extended to 30 minutes, giving an indication that attaching MP to dendron by the coupling reaction required a longer time than coupling amino acids.

The cleavage of the synthesised dendron from the solid support is a crucial step in SPPS. Choosing the right cleavage mixture and the optimum conditions of reaction can play an essential role in sample minimising incomplete cleavage and fragmentation. Based on the amino acids used for the assembly of dendrons and method of synthesis, a mixture of TFA, TIPS and water was used (in 38:1:1 ratio, respectively). When the final peptide contains side

chains liable to alkylation, such as sulfhydryl, thioether, indole and phenol, the use of a mixture of different nucleophilic scavengers is recommended (King *et al.*, 1990). The process of cleavage by TFA leads to the formation of carbocations that are highly reactive intermediates. These carbocation intermediates might specifically react with electron-rich amino acids side chains, generating undesirable products (Søren *et al.*, 2012). To prevent this, good nucleophilic species such as water and TIPS are added to the cleavage reaction.

Other factors contributing to the successful synthesis of F-Gen0K-MP and F-Gen1K-MP were choosing the right type of solid support, linker, and the solvent and coupling reagents of the reaction. The solid resin is an insoluble and inert support which is attached to a linker to furnish proper acid lability to the peptidyl-resin linkage by the presence of electron-releasing groups.

The Rink amide linker was used as a support for the solid phase (Howl, 2005). Since most peptides are naturally found in the amide form and due to the fact that C-terminal of amides are generally more stable than C-terminal of acids, a resin with an $–NH_2$ group (as Rink amide) is very widely employed. The coupling of the Fmoc amino acid of the linker will occur at the amino group of the resin. Then, the resin must be washed with DMF to remove soluble impurities (Benoiton, 2005). The solvent used for both coupling and deprotection reactions in SPPS was DMF as it has a very good ability to be heated by microwaves (Gabriel *et al.*, 1998) and MP exhibited good solubility in it.

To achieve the coupling of the carboxylic acid moiety of the next amino acid or MP with the N^{α}-amino group of the growing dendron, ammonium salt (HBTU) was used (Al-Warhi *et al.*, 2012). DIPEA was used to deprotonate the acid group of the Fmoc amino acid using DMF as the solvent of reaction (Montalbetti *et al.*, 2005). DIPEA and HBTU reduced coupling time and minimised epimerisation. The final washing solvents (dichloromethane, methanol, diethyl ether) were used to remove any unreacted species, to ensure easy drying of the resin-peptide grains and to help prevent losses of resin sticking to the glass or plastic syringe.

One of the essential factors that will determine dendron properties and behaviour is the root amino acid of dendron. Here, phenylalanine was used as the root amino acid based on an unpublished study (unpublished data, University of Brighton) that indicated the enhancement of entry of phenylalanine-root dendrons through the lipid membrane of epithelial cells. Phenylalanine was included in the carrier system to increase hydrophobicity that allows better penetration across the BBB and more retention in the targeted tissue. Lysine amino acid is

used as the branching amino acid. It has two peripheral functional sites which can be used to attach two amino acids (further branching) or two desired drug molecules (higher loading).

The attachment of four drug molecules to a Gen1 dendron was less efficient than attaching two drug molecules to a Gen0 dendron which was suggested by the appearance of noisy peaks in mass spectrometry in Figure 2.16. This might be related to the steric hindrance caused by drug molecules, which prevented the coupling of further MP molecules to the free amine groups of Gen1 dendron. Furthermore, one of the drawbacks in this work was the relatively low quantity yields of the final products (30-35% of the quantity of MP used) compared to the quantities of material used for its synthesis which required repeating the synthesis to get the desired quantity. Another problematic issue that appeared in this study was its limitation on the type of salt of MP that can be attached to dendrons. Only MP salts that contain a carboxylic group in their side chains can be attached to the peripheral amine groups of the dendrons through amide linkage. The attachment of an MP salt without a carboxylic group to dendrons by SPPS was unsuccessful.

The identification and characterisation of new molecules requires more than one technique. Here, HPLC, mass spectrometry, NMR and FTIR were used. Although these tests differ from each other, integrating data from the 4 tests provided strong confirmation of synthesis success. The appearance of a single peak in HPLC run of F-Gen0K-MP (Figure 2.11) and F-Gen0K-MP (Figure 2.12) after sample purification strongly indicated the purity of these products. The theoretical MW of the synthesised dendrons and dendron-MP conjugates were computed using (ChemBioDrawUltra®, version 15.0.0.106) program and compared with the mass spectrometry peaks (Figures 2.18 & 2.23). The appearance of the theoretical MWs or its ionised fractions as distinctive peaks in mass spectrometry confirmed the synthesis of the desired molecules.

Looking for the disappearance and the appearance of molecular bond troughs in FTIR spectra of the drug, dendrons and dendron-drug conjugates (Figures 2.12-2.16) also implied the successful synthesis of F-Gen0K-MP and F-Gen1K-MP. The success of attaching MP to both Gen0 and Gen1 was also confirmed by analysing NMR spectra which revealed the presence of the unique H atoms of the drug in the final molecules (Figures 2.24-2.27) with slight shifting in the positions of these peaks caused by changing in the environment after attachment. The successful synthesis of both F-Gen0K-MP and F-Gen1K-MP conjugates will allow the study to proceed through the attachment of a ligand (glutathione) to it to achieve higher penetration

through the BBB (Chapter 4). The covalent attachment of MP molecules to the surface groups of Gen0 and Gen1 dendrons through biodegradable or hydrolysable linkages provides the opportunity for a greater control over drug release compared to electrostatic interaction of drugs to the dendrimers. Different biologically active molecules, such as antibodies (Roberts, 1990) and sugars (Reuter *et al.*, 1999) have been attached to the peripheral ends of dendrimers. A study reported the development of dendrimer conjugates with potential use as host for the delivery of anticancer agents (Abu-Rmaileh *et al.*, 2003). Zhuo synthesised a series of Gen5 PAMAM dendrimers with a cyclic core, and showed their successful conjugation with 5-fluorouracil (anticancer drug) (Zhuo *et al.*, 1999). Yang and Lopina have conjugated antibiotic (penicillin V) with Gen2.5 and Gen3 PAMAM dendrimers *via* ester and amide bonds (Yang *et al.*, 2003). The use of an amide linkage increases bond stability, whereas the ester linkage of drug to the dendrimer provided a better means of controlling drug release via hydrolysis.

The data of mass spectrometry and comparisons of NMR and FTIR peaks indicated the success in synthesising F-Gen0K-MP and F-Gen1K-MP molecules plus confirmation of its purity by HPLC experiments suggest the possibility of using dendrons as a MP carrier to deliver it to the desired site of action with high loading capacity. Nevertheless, these dendron-MP conjugates are novel molecules and their toxicity levels are not revealed yet and despite the fact that the toxicity of their parent molecules (MP and dendrons) are within the acceptable range, it might have different toxicity patterns. Thus, prior to investigating BBB penetration experiments (Chapter 6), the cytotoxicity of Gen0K-MP and F-Gen1K-MP molecules on brain endothelial cells was examined. This is the focus of Chapter 3.

2.6 Conclusion

This chapter discussed in detail the methodology of synthesis of dendrons and the procedures for attaching MP to its outer groups. It also highlighted the different protocols for confirmation of the synthesis of the dendron-drug conjugates. The following points can be concluded from the results of this chapter:

- Dendrons of different generation can be synthesised efficiently using SPPS both manually or using a peptide synthesiser.
- MP hemisuccinate sodium salt can be attached to the peripheral amine groups of dendrons by amide linkage. The manual method of drug attachment to the dendron carrier system by SPPS gave better results compared to the automated method. This might be attributed to the longer duration of reaction of the manual method (30 minutes) thus allowing more time for reaction to occur.

- SPPS cannot be used for the attachment of MP salts without carboxyl groups in their side chains to dendrons.
- Two drug molecules can be attached to a Gen0 dendron and four to a Gen1 dendron.

  MW determination by mass spectrometry provided conclusive confirmation of the successful synthesis of dendron-drug conjugates.

Chapter 3. *In vitro* cytotoxicity of dendron-MP conjugates on endothelial cells

3.1 Introduction

In vitro toxicity testing can be defined as the laboratory analysis of the toxic effects of newly developed chemical substances on mammalian cells or cultured bacteria (Gerets *et al.*, 2009). *In vitro* experimental techniques are used primarily to understand the potential risk of chemicals and/or to confirm the lack of certain toxic properties of potentially useful new chemicals such as therapeutic drugs, diagnostic agents, food additives and agricultural chemicals in its early stages of the development. It has become a powerful approach used to identify the consequences of exposure and to assign hazard (Wilhelm *et al.*, 2014). These methods are routinely used in toxicity testing, risk evaluation and safety assessment due to its unique advantages.

The use of non-animal test methods, such as *in vitro* toxicity studies, provides a valuable means to improve knowledge about hazardous effects caused by newly developed chemicals and for predicting the potential effects on humans (Gerets *et al.*, 2009). The widest use of *in vitro* methods is for highlighting mechanisms of toxicity and/or exploring the biological process involved in toxic stimuli to new molecules.

Cell lines that can be used in *in vitro* toxicity testing provide an almost unlimited supply of cells with similar genotypes and phenotypes. Their usage offers several advantages such as avoiding variation between individuals and bypassing ethical issues associated with animal and human experiments. Cell lines can be classified into two main types each with its own advantages and disadvantages which are primary cell lines and immortalised cell lines (Schaeffer, 1984).

Primary cell cultures are produced by growing cells from tissue taken directly from a healthy or diseased mammal. These primary cell cultures become a cell line once they are transferred into the next culture container by passage process (Omidi *et al.*, 2003). Passaging is the process of subdividing cell cultures to yield more cells. The advantage of primary cell cultures is that they retain many of the characteristic features of primary tissue from which they were originally taken. However, these cells can only be used over a limited time since they continue growing until the end of the natural proliferative lifespan is reached and senescence occurs.

An immortalised cell line is a population of cells taken from a multicellular organism which normally do not proliferate indefinitely but, due to a certain mutagenic effect, have eluded normal control of cellular proliferation and instead can keep dividing (Eigenmann *et al.*, 2013). The cells can therefore, be grown *in vitro* for prolonged periods. The mutations necessary to induce immortality in these cells can happen naturally or be intentionally produced by

transfection with viral genes. Nevertheless, despite their prolonged life span, immortalised cell lines are usually obtained from mice (since human cells never immortalise spontaneously and have a short lifespan) (Schaeffer, 1984).

MP was conjugated with dendrons to improve its penetration through *in vitro* BBB model. The successful synthesis of F-Gen0K-MP and F-Gen1K-MP and its purification and characterisation were confirmed. Nevertheless, these conjugates are novel molecules and their potential toxicity has not been investigated yet. Although the toxicity levels of their parent molecules (MP and dendrons) are within the acceptable range, the dendron-drug complexes might have different toxicity patterns.

The unique biocompatibility and biodegradable properties of dendrons have been demonstrated to make them successful vehicles and biomaterials (Tomalia, 2005). However, dendrimer biocompatibility is thought to be influenced by different properties of the polymers such as MW charge density and type of the cationic functionalities, structure and sequence (block, random, linear and branched) and conformational flexibility (Fischer *et al.*, 2003).

It has previously been found that the *in vitro* cytotoxicity of dendrimers is concentration-, generation- and surface charge-dependant (Yang, 2009). Furthermore the cytotoxic effects of corticosteroids including MP are dose-dependent (Wyles *et al.*, 2015).

MP, like other corticosteroids, is associated with a number of adverse effects, affecting the skin, skeleton, muscles, eyes, CNS, electrolytes balance, metabolism especially fats and the endocrine, cardiovascular, immune and gastrointestinal systems, usually in a dose-dependent manner (Schacke *et al.*, 2002). In the USA in 2004, corticosteroids were the most common specific cause for drug-related adverse effects, accounting for almost 10.3 % of all drug-related adverse effects and 141,000 hospital stays (Jongen *et al.*, 2016). Although most serious adverse effects of corticosteroids are related to their long-term oral use, short-term steroid-induced symptoms are frequent, especially with high-dose intravenous treatment needed to treat MS relapses (Troiano *et al.*, 1987). Such adverse effects of MP upset MS patients and affect their quality of life (Guidry *et al.*, 2009). Furthermore, in MS patients, the distress from CNS-related adverse effects caused by MP high doses, like mood change, behavioural change and sleep disturbance, may add to the burden of MS-related CNS symptoms (Troiano *et al.*, 1987).

Thus, prior to using these novel molecules in any further experiments, their *in vitro* cytotoxicity on brain endothelial cells must be examined. Moreover, the toxicity levels of conjugated MP (F-Gen0K-MP and F-Gen1K-MP) compared to free MP must be investigated.

This chapter will use established methods to test the *in vitro* cytotoxicity of each of the dendron-MP complexes synthesised and characterised in Chapter 2 using a brain endothelial cell line (b.End3).

Aims of the chapter

To ensure the biocompatibility of the synthesised molecules with the brain model, their cytotoxicity patterns were investigated. Thus this chapter aimed to:

- Measure the *in vitro* cytotoxicity levels of synthesised dendron-MP conjugates and compare it with free drug and free dendrons.
- Illustrate the impact of increasing concentration and duration of exposure on the toxicity levels of MP-dendron molecules (F-Gen0K-MP and F-Gen1K-MP).
- Compare the toxicity levels of equimolar concentrations of F-Gen0K-MP and F-Gen1K-MP with free MP.

These aims were achieved by using different cytotoxicity assays including lactate dehydrogenase assay (LDH), MTT cell viability assay and calcein/ethidium viability-cytotoxicity assay on endothelial cells. Moreover, the Hoechst/propidium iodide test was used to detect any apoptotic damage caused by the tested agents which is not detected by other assays.

3.2 Materials

The materials used in the experimental methods and their supplied companies are detailed in Table 3.1.

Table 3.1 List of materials used in Chapter 3.

Material	Company	Catalogue number
1-(4,5-Dimethylthiazol-2-yl)-3,5-diphenylformazan, Thiazolyl blue tetrazolium 98% (MTT)	Sigma-Aldrich UK	M2003-1G
96-well plates (Thermo Scientific Nunc® 96 Microwell™	Fisher Scientific UK	10445543
CryoTube™ Vials from Nunc®	Fisher Scientific UK	CRY-960-070B
CytoTox 96® Non-Radioactive Cytotoxicity (LDH) Assay	Promega, Southamption, UK	G1780
Dimethylsulfoxide (DMSO) Hybri-Max®	Sigma-Aldrich UK	D2650
Dulbecco's Modified Eagle's Medium (DMEM) (ATCC-30-2002) high glucose medium.	Sigma- Aldrich UK	ED2SS
Falcon™ 12-well Multiwell plate	Becton-Dickson UK	351143
Falcon™ 24-well Multiwell plate	Becton-Dickson UK	351147
Falcon™ 6-well Multiwell plate	Becton-Dickson UK	353046
Fetal Bovine Serum (FBS), heat inactivated, EU approved	PAA Laboratories Ltd., UK.	A15-104
Fisherbrand® 4 mL single use UV curvette	Fisher Scientific UK	FB55923
Fisherbrand™ conical centrifuge tubes (15 mL).	Fisher Scientific UK	11879640
Hoechst 33258 solution 1 mg/mL in water >98%	Sigma-Aldrich UK	94403
LIVE/DEAD® Viability/Cytotoxicity Kit, for mammalian cells	ThermoFisher UK	L3224
Penicillin/streptomycin(P/S)	PAA Laboratories Ltd, UK	P11-010
Phosphate buffered saline (PBS) tablets	Fisher Scientific UK	BR014G
Propidium iodide solution 1 mg/mL in water	Sigma-Aldrich UK	P4864
Syringe (2 ml, disposable) Plastipak™	Becton Dickinson UK	300185
Syringe (10 ml, disposable) Discardit™II	Becton Dickinson UK	309110
T-25 Thermo Scientific Nunc® tissue culture flask	Fisher Scientific UK	TKT-130-050P 60
T-75 Thermo Scientific Nunc® tissue culture flask	Fisher Scientific UK	TKT-130-370U
Triton X-100 lysis solution (1% solution in PBS)	MatTek Corporation	TC- TRI

Trypsin 0.05% $^{w}/_{v}$ EDTA (1X), from Invitrogen	Fisher Scientific	VX25300054
Elite micropipette 8 channel / 30-300 µL fully autoclavable	Fisher Scientific UK	11845772

3.3 Methods

3.3.1 BBB *In vitro* cell line

The cell line used to conduct cell culture studies was immortalised mouse brain endothelial cells, b.End3 purchased from ATCC® laboratories. This brain microvascular cell line was isolated from mice transformed with the Polyoma virus middle T-antigen (Williams *et al.*, 1989). The b.End3 cell line has characteristic elongated spindle shape morphology (Figure 3.1). It comprises fast growing cells and typically grew to 75-85% confluence within 2-3 days. The cells were grown in 75 cm^2 flasks in complete culture medium consisting of DMEM medium plus 10% $^{v}/_{v}$ heat-inactivated fetal bovine serum (FBS), and 100 units/mL penicillin and 100 µg/mL streptomycin.

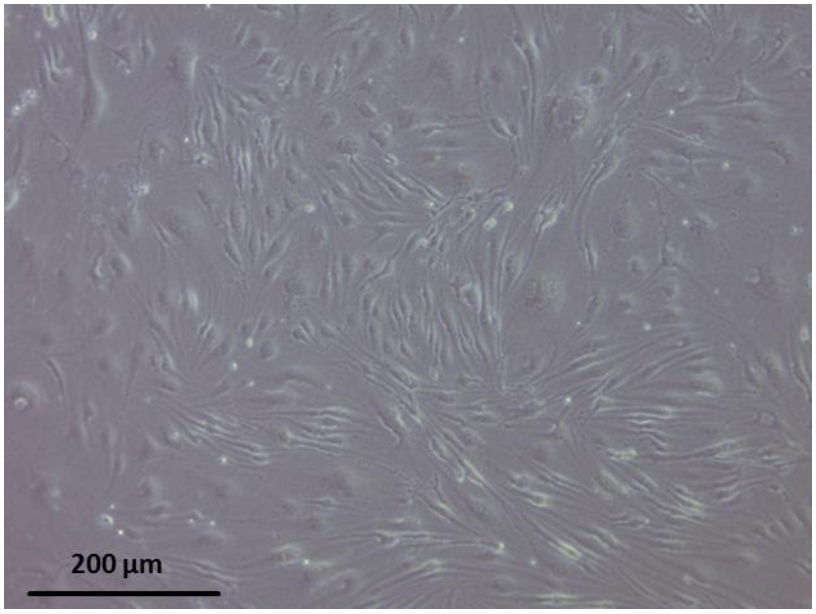

Figure 3.1 Phase-contrast light microscopy of b.End3 cells. The cells are characterised by elongated spindle shape morphology.

3.3.1.1 Freezing and storage of b.End3 cell stocks

Cells at passages between 2 to 5 with 80-90% confluence were used to obtain a stock of cells. The freezing medium was prepared by mixing 10% $^{v}/_{v}$ FBS and 10% $^{v}/_{v}$ DMSO in culture medium. The cell pellet was resuspended in this freezing solution to achieve a cell density of 1×10^{6} cells/mL then 1 mL was transferred into sterile cryovials. Cells were frozen slowly (approximately 1°C *per* minute, to -70°C) and then transferred to liquid nitrogen for long-term storage.

3.3.1.2 Thawing b.End3 cells from freezing

The vial was thawed by gentle agitation in a 37°C water bath for approximately 2 minutes. Once thawed, the vial was removed from the water bath, and sprayed with 70% $^{v}/_{v}$ ethanol. The vial contents were transferred to a centrifuge tube containing 9 mL complete culture medium and centrifuged at 125 ×g for 5 minutes (Sigma/Phillips-Harris 2K15). The supernatant was decanted and the cell pellet was resuspended in 1 mL of complete culture medium before seeding into a T-25 surface treated polystyrene flask containing 9 mL of complete culture medium.

3.3.1.3 B.End3 routine cell culture and passage

The immortalised b.End3 cells were incubated at 37°C in a humidified, 5% CO_2, 95% air atmosphere (Sanyo-MCO715). Cell stocks were maintained by routinely culturing as monolayers at a seeding density of 3×10^4 cells/cm^2 in T-75 flask, surface treated polystyrene flasks for cell culture. The medium was changed every 2-3 days after washing with phosphate buffered saline (PBS) to remove cell debris. The cells were allowed to grow to approximately 80-90% confluence prior to routine passage. Passage was carried out by trypsinisation (0.05% $^{w}/_{v}$ trypsin/EDTA (1X) for 5 minutes at 37°C, 5% CO_2 and 95% air). Cell suspensions were removed from the flask and centrifuged at 500 ×g for five minutes. Cell pellets were re-suspended in fresh medium and cells counted using a haemocytometer.

3.3.1.4 Preparation of 24-well plate for experiments

The cells were seeded in 24-wells plate at a seeding density of 3×10^4 cells/cm^2 and left to grow to 80% confluence. Prior to treatment, the cells were washed with PBS and the medium in the wells was replaced by 1 mL of fresh complete culture medium for each well. The cells were treated with the experimental agents under investigation for toxicity studies (Table 3.2) and incubated for 24 and 48 hours. After incubation, the cells were subjected to cytotoxicity assays.

Table 3.2 Concentration range of materials under investigation added to the cells. The materials were dissolved in complete culture medium in the desired concentrations and passed through a filter with a pore diameter of 0.22 μm for sterilisation.

	Material				
	MP	**F-Gen0K**	**F-Gen1K**	**F-Gen0K-MP**	**F-Gen1K-MP**
Conc. μM	25	25	25	25	25
	50	50	50	50	50
	100	100	100	100	100
	200	200	200	200	200
	300	300	300	300	300
	400	400	400	400	400
	500	500	500	500	500

3.3.2 LDH assay of dendron-MP conjugates

Different methods have been developed to study cell viability and proliferation *in vitro* (Cook *et al.*, 1989). One parameter for cell death is the integrity of the cell membrane, which can be examined by measuring the cytoplasmic enzyme activity released by damaged cells. Lactate dehydrogenase (LDH) is a soluble cytosolic enzyme present in most eukaryotic cells. It is released into culture medium upon cell death due to damage of the plasma membrane. The LDH assay provides a colorimetric method to measure LDH activity using a reaction mixture containing lactate, NAD^+, diaphorase (electron acceptor) and tetrazolium salt (Nachlas *et al.*, 1960). LDH catalyses the reduction of NAD^+ to NADH in the presence of L-lactate, while the formation of NADH can be measured in a coupled reaction in which tetrazolium salt is reduced to a red formazan product (Figure 3.2). The amount of the highly soluble formazan can be measured at 490 nm spectrophotometrically. LDH is an intracellular enzyme and can only be measured upon its release following cell lysis or membrane blebbing and as such, gives an indication of loss of cell membrane integrity (Yang, 2009).

$$NAD^+ + Lactate \xrightarrow{LDH} Pyruvate + NADH$$

$$NADH + INT \xrightarrow{Diaphorase} NAD^+ + Formazan\ (red)$$

Figure 3.2 The chemical principle of LDH assay.

The Promega CytoTox 96® Non-Radioactive Cytotoxicity Assay kit was used for quantification of LDH release as an indicator of cellular toxicity. Following treatment of 24-well plate with desired molecules to be tested (Table 3.1), 50 μL of the supernatant medium was collected in duplicates from each plate after 24 and 48 hours including samples from untreated cells (control). A 'blank' sample (medium only containing no cells) was also incubated to account for background absorbance. To determine LDH released by 100% lysis of cells, two wells were treated with 100 μL lysis-solution (1% $^{v}/_{v}$ Triton™-X100, supplied with the kit) and incubated for 45 minutes, followed by duplicate sample collection from each well. Finally, all collected samples (experimental, control, blank and complete lysis) were transferred to 96-well plates. To each well, 50 μL of LDH assay solution was added and incubated in the dark for 30 minutes. After incubation, 50 μL of stop solution (1M acetic acid, supplied with the kit) was added to each well. The absorbance of each well was measured at 490 nm using a spectrophotometer (Thermo Multiskan Ascent 354) and the average absorbance for each duplicate was calculated. Absorbance was converted to a measurement of toxicity based upon the percent of total LDH released from the cell, using Equation 4.1.

Equation 4.1 Calculation of cytotoxicity percentage from LDH release.

$$\%\ Cytotoxicity = \left(\frac{\big((S - CF) - (NC - CF)\big)}{\big((PC - CF) - (NC - CF)\big)}\right) \times 100\%$$

Where:

S is the sample absorbance

CF is the average cell free blank absorbance

NC is the average negative control, or non-treated healthy population absorbance value

PC is the average positive control, or fully lysed cell population absorbance value.

Toxicity values greater than 50% were generally considered to be indicative of a toxic response. This equates to the median lethal dose (LD_{50}), a crude measure of acute toxicity based on the dose or concentration (LC_{50}) required to kill half the members of the tested population over the given treatment time (Zbinden *et al.*, 1981).

3.3.3 MTT assay of dendron-MP conjugates

The MTT (3-[4,5-dimethylthiazol-2-yl]-2,5 diphenyl tetrazolium bromide) test has been widely used as a rapid and sensitive method for the assessment of cytotoxicity of newly developed materials. Tetrazolium salt 3-(4,5-dimethylthiazol-2-yl)-2, 5-diphenyltetrazolium bromide is a water-soluble dye which is reduced by mitochondrial succinate dehydrogenase enzyme to yield a purple formazan product (water-insoluble) (Figure 3.3), which cannot cross the plasma membrane and accumulates in the cells (Mosmann, 1983). The reduction reaction occurs in live (viable) cells, but not necrotic (non-viable) cells (Edmondson *et al.*, 1988). The cell membranes are then lysed by adding DMSO, releasing the solubilised formazan product, determined using a spectrophotometer at 540 nm. This assay requires fewer cells than other cytotoxicity assays (Edmondson *et al.*, 1988). In addition, it allows for multiple sample concentrations on a single 96-well plate that can be read at the same time using an automated spectrophotometric microplate reader.

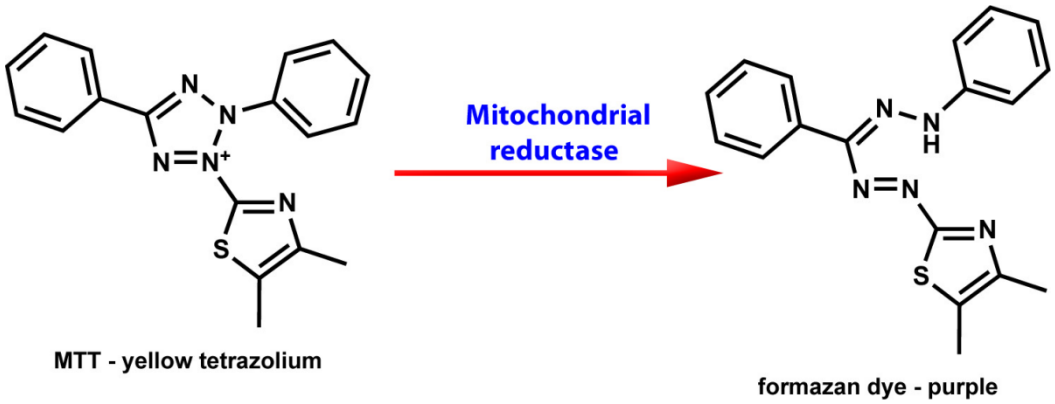

Figure 3.3 The chemical principle of MTT test. The reduction of MTT to formazan by mitochondrial reductase enzyme released by viable cells which can be read at 540 nm.

Eighty *percent* confluence cells in 24-well plates were treated with different concentration of the desired molecules (Table 3.1) and incubated for 24 and 48 hours. MTT solution was freshly prepared at a 0.2 mg/mL concentration in total culture medium without FBS in 50 mL centrifuge tube protected from light by a foil cover and incubated at 37°C. Prior to use, the solution was sterilised by filtration using a 0.22 μm pore size filter. After completion of a 24 hours incubation period, the supernatant was removed from wells and 500 μL of warm MTT solution was added to each well without disrupting the cell layer. The wells were incubated for 1 hour in a cell culture incubator. Following incubation, the MTT solution was removed from wells and 125 μL of DMSO was added to each well with gentle shaking to dissolve the formazan crystals. Two × 50 μL solutions from each well were transferred to a 96-well plate including untreated cells (negative control) and cell free blank (media only). The absorbance was measured at 540 nm. The cell viability can be calculated by Equation 3.2. The same procedures were used for cell samples incubated for 48 hours.

Equation 3.2 Percent cell viability from MTT absorption

$$\%\ Cell\ Viability = \left(\frac{S - CF}{NC - CF}\right) \times 100\%$$

Where:

S is the sample absorbance

CF is the average cell free blank absorbance

NC is the average negative control, or non-treated healthy population absorbance.

For these measurements, values less than 50% were considered to be indicative of a toxic response (through loss of cell viability). This equates to the half maximal inhibitory concentration (IC_{50}) accepted as showing a drug or toxins ability to inhibit biological function.

3.3.4 Hoechst / propidium iodide assay of dendron-MP conjugates

This test provides a rapid and convenient method for detection of cell apoptosis and necrosis based upon fluorescent detection of the treated cells. The test is based on using two specific dyes, Hoechst 33342 and propidium iodide (HPI) which are molecules that release energy in the form of light emission after being excited by absorption of high energy light from xenon- or mercury-arc lamp or with an ultraviolet laser. Hoechst 33342 (excitation/emission ~350 nm/~461 nm) is suitable for staining nuclei of viable cells due to its DNA-binding capacity. It stains the condensed chromatin in apoptotic cells more brightly than the chromatin in normal cells. Propidium iodide (excitation/emission ~535 nm/~617 nm) also binds to DNA but it is impermeable through the cell membrane and is generally excluded from viable cells, thus it can stain the DNA of dead cells only rather than viable cells (Moore *et al.*, 1998). The test is performed by observation of distinct cell morphologies associated with cell apoptosis and necrosis and counting the numbers of these distinctive morphological cells. After staining with HPI, healthy cells appear blue, cells at different apoptotic phases appear bright blue with and necrotic or damaged cells appear red (Figure 3.4).

The HPI mixture was prepared by adding 50 μL of 1mg/mL Hoechst 33342 and 50 μL of 2 μg/ml propidium iodide to 900 μL of DMEM to in a centrifuge tube. The mixture was prepared in a dark environment and protected from light by covering with aluminium foil. After reaching 80% confluence, b.End3 cells cultured in 24-well plates were treated with 100, 200, 400 μM of MP, F-Gen0K dendron, F-Gen1K dendron, F-Gen0K-MP and F-Gen1K-MP dendron-drug conjugates and left for 24 hours of incubation at 37°C, 5% CO_2 and 95% air.

After incubation, the culture medium was removed from the plates and cells were washed with PBS, treated with 100 μL HPI dye *per* well and incubated for 10 minutes. Control wells containing untreated cells were also included. An Axiovert 25 inverted fluorescent microscope (mercury lamp, 350 nm and 460 nm) was used for morphological examination and counting of cells. Cell counts were taken from three different fields for each well. The mean numbers of living, apoptotic and necrotic cells in each well were recorded according to their colour, totalled and expressed as percentages of the total cell number in the field of view. Cell counts for living, apoptotic, or necrotic cells were obtained from the same treatment in duplicate wells, were averaged and expressed as percent of total cell number.

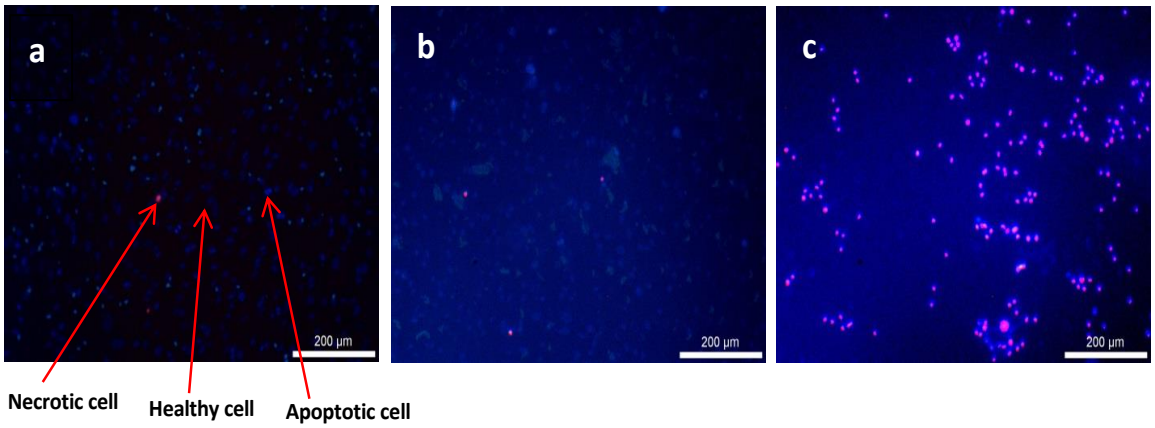

Figure 3.4 HPI fluorescent images of b.End3 cells. a. control cells (untreated), b. image of cells treated with 200 µM of F-Gen1K-MP, c. complete lysis cells after treatment with Triton X-100 lysis solution.

3.3.5 Calcein/ethidium viability-cytotoxicity assay of dendron-MP conjugates

This test gives a two-colour fluorescence staining which is based on the concurrent determination of live and dead cells with two fluorescent probes that measure distinctive parameters of cell viability-intracellular esterase activity and plasma membrane integrity. The optimal molecular dyes for this application are found to be calcein AM and ethidium homodimer-1 (Hayes, 1995).

Live cells are distinguished from dead cells by the presence of ubiquitous intracellular esterase activity, which can be determined by the enzymatic conversion of calcein AM (virtually non-fluorescent) to calcein (intensely fluorescent). The fluorescent calcein is a polyanionic dye which is well retained within live cells, producing an intense uniform green fluorescence in live cells (excitation/emission ~495 nm/~515 nm). Ethidium homodimer-1 enters cells with damaged membranes and its binding to nucleic acids with causes a 40-fold enhancement of its fluorescence activity, thereby yielding a bright red fluorescence in dead cells (excitation/emission ~495 nm/~635 nm). However, ethidium homodimer-1 is denied access to live cells with intact or undamaged plasma membranes (Papadopoulos *et al.*, 1994).

The test was performed using LIVE/DEAD® Viability/Cytotoxicity Kit for mammalian cells. The test solution was prepared by adding 1 µL of calcein AM (supplied with the kit) and 2 µL of ethidium homodimer-1 (supplied with the kit) to 1 mL of culture medium (DMEM) and mixed well. The 24-well plates were seeded with b.End3 cells and treated with 100, 200, 400 µM of MP, F-Gen0K dendron, F-Gen1K dendron, F-Gen0K-MP and F-Gen1K-MP for 24 hours using the same protocol used to prepare wells for the Hoechst/propidium iodide test (Section 3.3.4). Prior to staining, the culture medium was removed and the wells were washed three times with PBS. Following washing, 100 µL of calcein AM/ethidium homodimer-1

solution was added to each well and allowed to incubate for 30 minutes at 37°C. The staining solution was removed and the cells were washed for 3 times again with PBS to remove any traces of the dyes followed by covering the cells with DMEM. The cells were imaged using confocal laser scanning microscope system (Leica TCS SP5 / UK) using laser line visible (488 nm, 25%) and laser line visible (514 nm, 25%).

3.3.6 Statistical analysis

Any significant difference in values were reported after investigating data for normality, and carrying out a one-way ANOVA with Tukey's *post-hoc* test, using the Minitab® 17 (version 17.2.1) statistical analysis program. The mean level ($n=4$) was compared and it was considered significantly different when the P value was lower than 0.05 (two-sided confidence intervals).

3.4 Results

3.4.1 LDH assay analysis of dendron-MP conjugates

Data collected from cell samples treated with different concentrations of MP for 24 hours and 48 hours indicated a gradual increase in toxicity with increasing drug concentration (Figure 3.5). The results also indicated higher toxicity following longer periods of exposure to the drug (48 hours) compared to 24 hours exposure. However, none of the values reached the level (50%) to be considered as toxic and the highest toxicity value was approximately 12% at 400 μM concentration. Statistical analysis showed significant difference ($P<0.05$) between cells treated with low concentration of MP (25, 50 and 100 μM) when compared to high concentrations (400 and 500 μM) in both 24 and 48 incubation periods indicating an increase in cytotoxicity with increasing concentration. Comparison of each interval in 24 hours incubation with the same concentration after 48 hours exposure revealed a significant difference ($P<0.05$) in all intervals except in 100 and 500 μM concentrations. This indicates an increase in cellular toxicity in response to duration of incubation.

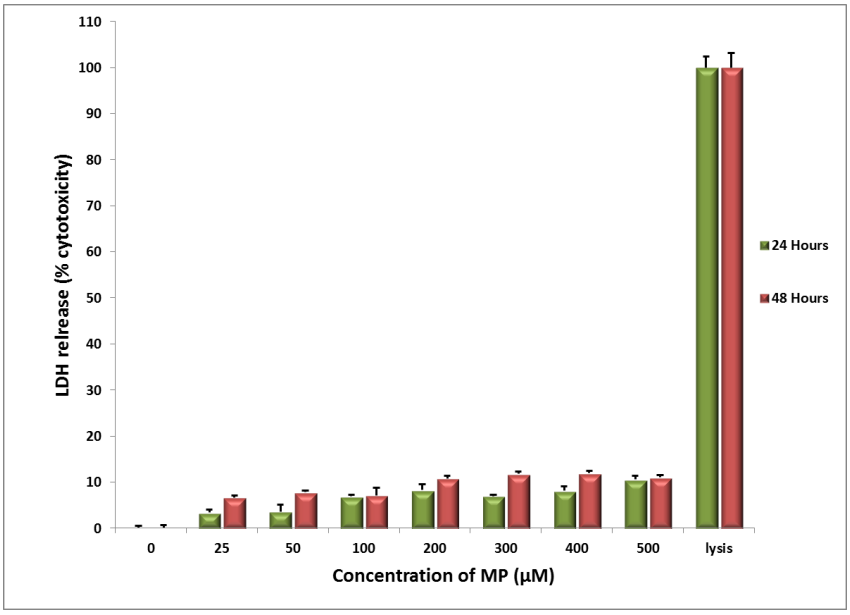

Figure 3.5 LDH release levels from b.End3 cells treated with different concentrations of MP after 24 and 48 hours incubation periods. Results are expressed as mean ± standard deviation (SD), (n=4). Higher doses (400 and 500 μM) caused significantly higher ($P<0.05$) LDH release when compared to lower doses (25 to 100 μM) in both exposure periods. Extending the duration of exposure to 48 hours caused significant difference ($P<0.05$) from the corresponding concentration after 24 hours incubation (except 100 and 500 μM).

The increase in toxicity with increasing concentration and time of exposure was also observed in F-Gen0K (Figure 3.6) and F-Gen1K dendrons (Figure 3.7). However, these levels were much below the 50% toxic level of the positive control (i.e. complete lysis) and did not reach values higher than 9% and 12% for F-Gen0K and F-Gen1K dendrons, respectively.

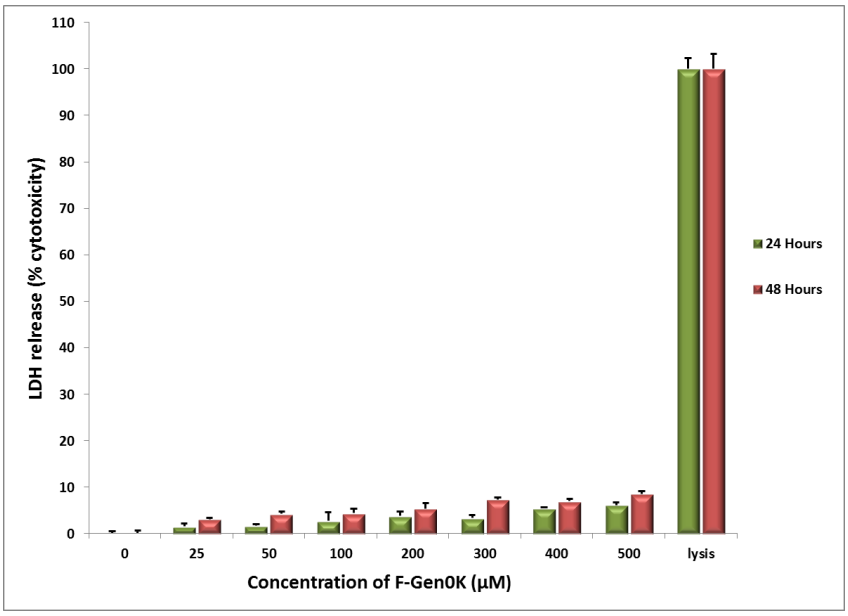

Figure 3.6 LDH release levels from cells treated with different concentration of F-Gen0K dendron after 24 and 48 hours incubation periods. Results are expressed as mean ±SD (*n*=4). The result indicated significant (P<0.05) higher cytotoxicity in high doses (400 and 500 µM) compared to lower doses (25, 50 and 100 µM) in both incubation periods. All values after 48 hours of exposure were significantly higher (P<0.05) than its corresponding concentrations after 24 hours exposure (except in 100 and 200 µM).

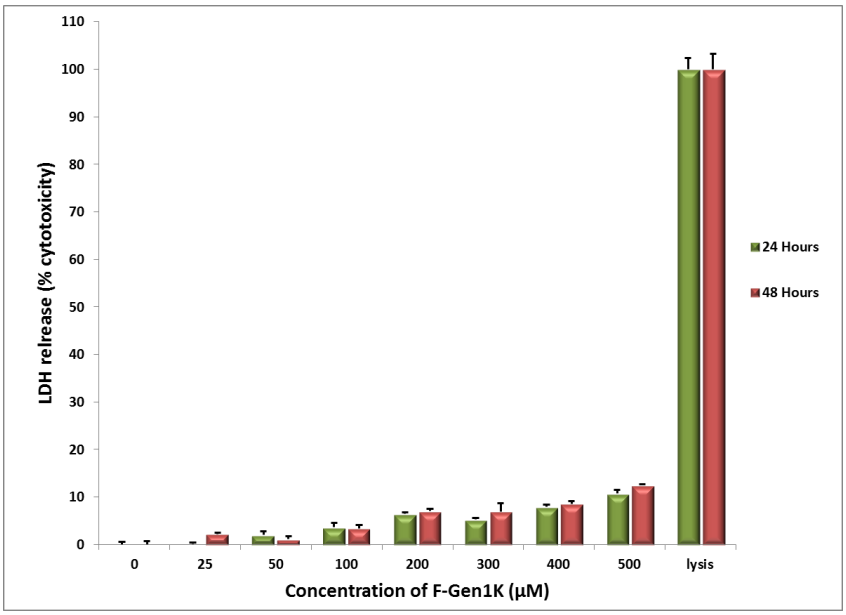

Figure 3.7 LDH release levels from cells treated with different concentration of F-Gen1K dendron after 24 and 48 hours incubation periods. Results are expressed as mean ±SD (*n*=4). Statistical interpretation of the result indicated the same trend of increasing toxicity with concentration. The LDH release levels after 48 hours were significantly different (P<0.05) from the 24 hours period at concentrations of 25, 300 and 500 µM.

Statistical analysis of LDH release levels of cells treated with F-Gen0K-MP conjugate (Figure 3.8) indicated an increase in toxicity with increasing concentration. Nevertheless, these

numbers did not reach higher than 19% which was observed from cells treated with 500 μM after 48 hours of exposure.

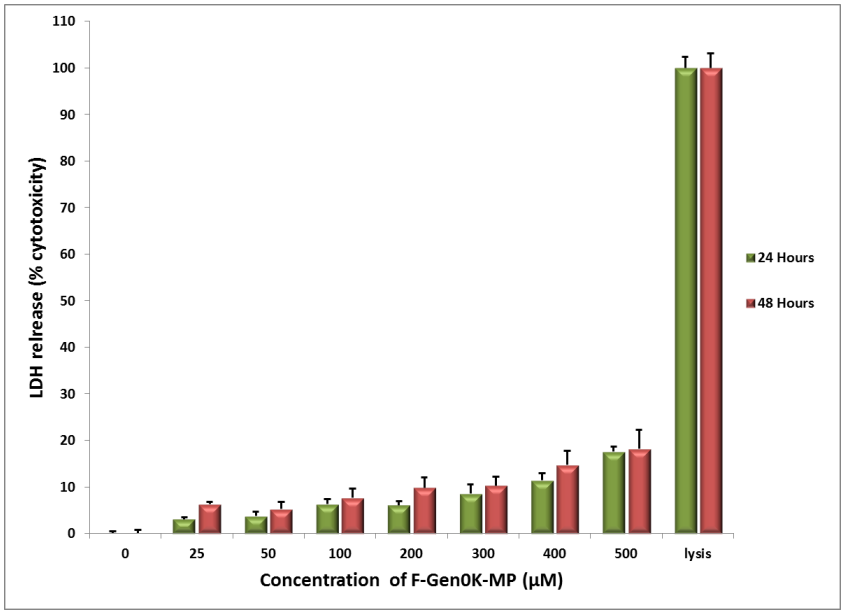

Figure 3.8 LDH release levels from cells treated with different concentrations of F-Gen0K-MP conjugate after 24 and 48 hours. Results are expressed as mean ±SD (*n*=4). Higher doses (400 and 500 μM) caused significantly higher ($P<0.05$) LDH release when compared to lower doses (25 to 200 μM). Extending the duration of exposure to 48 hours caused a significant increase ($P<0.05$) in cytotoxicity only in 25 and 400 μM doses, other doses were not significant.

The same trend of increased cytotoxicity with higher concentrations was also seen after treatment with F-Gen1K-MP (Figure 3.9). The cytotoxicity reached its maximum levels of 27% and 38% at 500 μM for 24 and 48 hours of exposure. However, all the toxicity levels of F-Gen0K-MP and F-Gen1K-MP were below the LD_{50} limit.

Each F-Gen0K-MP molecule contains two MP drug molecules since each F-Gen0K molecule has two peripheral amine groups each of which can conjugate one drug molecule. Since each F-Gen1K molecule has four peripheral amine groups, four drug molecules can be attached to it. The LDH release levels of F-Gen0K-MP and F-Gen1K-MP was compared with equimolar concentration of free MP after 24 hours (Figure 3.10) and 48 hours (Figure 3.11) incubation periods. Gen0 dendron-MP conjugate showed lower cytotoxicity figures ($P<0.05$) when compared to its equimolar concentration of the free drug after 24 hours exposure (Figure 3.10). Nevertheless, the values of F-Gen1K-MP after 24 hours and for both dendron-MP conjugates after 48 hours treatment period (Figure 3.11) did not indicate any significant difference from free MP.

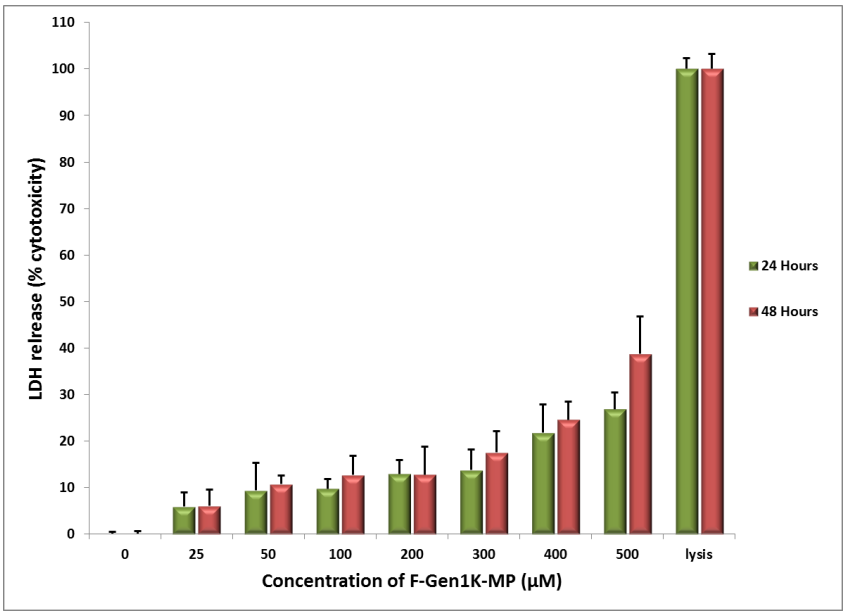

Figure 3.9 LDH release levels from cells treated with different concentration of F-Gen1K-MP conjugate after 24 and 48 hours incubation periods. Results are expressed as mean ±SD (*n*=4). The result indicated significant (P<0.05) higher cytotoxicity in high doses (400 and 500 µM) compared to lower doses (from 25 to 200 µM) in both incubation periods. Extending the duration of exposure to 48 hours caused significant increase (P<0.05) of cytotoxicity only in 500 µM dose whereas other doses were not significant.

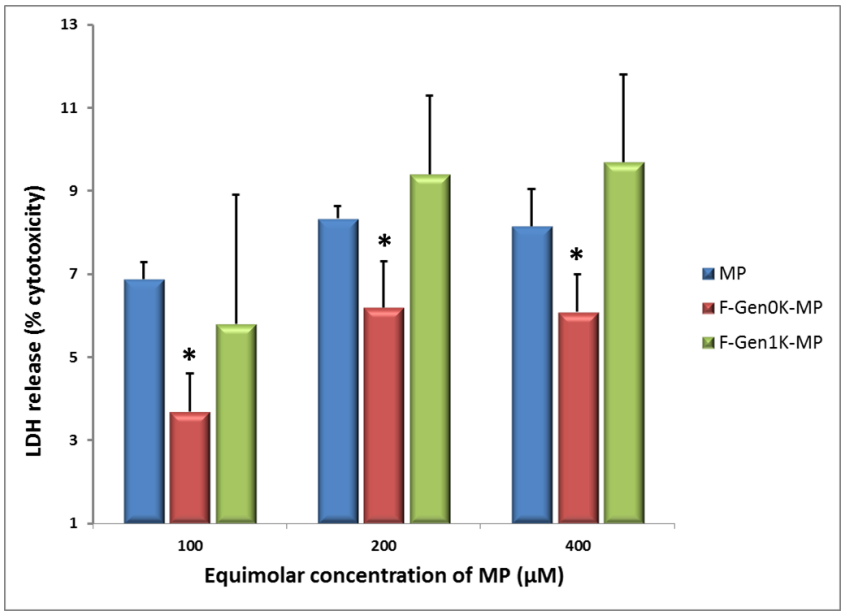

Figure 3.10 LDH release levels of equimolar concentrations of MP, F-Gen0K-MP and F-Gen1K-MP after 24 hours exposure. Results are expressed as mean ±SD (*n*=4). The (*****) indicates significant difference compared to free MP with P value equal or less than 0.5.

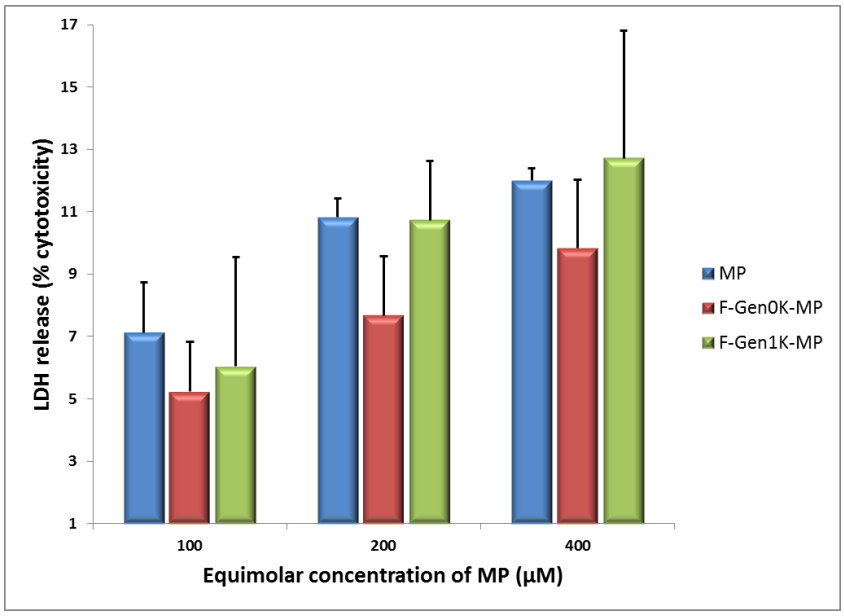

Figure 3.11 LDH release levels of equimolar concentrations of MP, F-Gen0K-MP and F-Gen1K-MP after 48 hours exposure. Results are expressed as mean ±SD (*n*=4). No significant change (P>0.05) in the release of LDH from cells treated with F-Gen0K-MP and F-Gen1K-MP compared to free MP.

3.4.2 MTT assay analysis of dendron-MP conjugates

The MTT assay results illustrated below in Figures 3.12 to 3.16 show levels of cell viability (metabolic activity), for the same b.End3 cell populations assayed for LDH, exposed for 24 and 48 hours with different concentrations of materials under investigation (Table 3.1). Unlike the LDH assay which gives an indication of cell death caused by the material under investigation, MTT results are reported as cell viability in the context of % MTT metabolised to formazan by a healthy cell population. The negative control (untreated cells) is considered as 100% viable.

All results from cells treated with the five materials under cytotoxicity analysis (MP, dendrons and dendron-drug conjugates) showed a decrease in cellular viability with increasing drug concentrations. However, the duration of exposure (24 and 48 hours) did not show significant variations (P>0.05).

For cells treated with MP, the cell viability did not drop below 90% of viable cells even at higher concentrations of MP (400 and 500 μM) (Figure 3.12). The values for F-Gen0K and F-Gen1K are shown in Figure 3.13 and Figure 3.14 respectively. For all three materials (free MP, F-Gen0K and F-Gen1K) the data indicated significant difference (P<0.05) between high concentrations (300, 400 and 500 μM) and the control group (untreated cells). However any significant difference (P>0.05) was not noticed between the durations of exposure (24 and 48 hours).

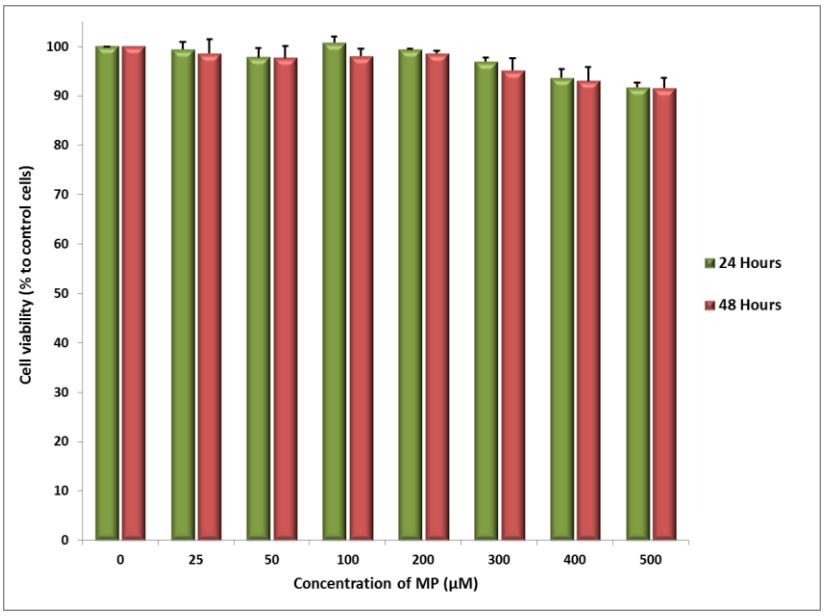

Figure 3.12 MTT cell viability results after 24 and 48 hours exposure to different concentrations of MP. Results are expressed as mean ±SD (*n*=4). Significant (P<0.05) increase in cytotoxicity are seen with elevated doses (from 300 to 500 μM) compared to the control group (untreated cells). However, a significant difference was not seen between the short (24 hours) and long (48 hours) exposure periods (P>0.05).

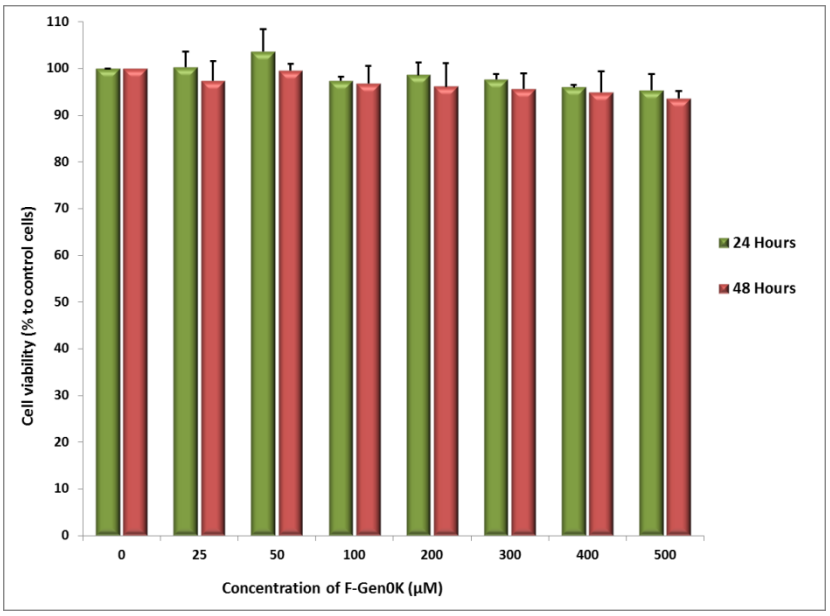

Figure 3.13 MTT cell viability results after 24 and 48 hours exposure to different concentrations of F-Gen0K dendron. Results are expressed as mean ±SD (*n*=4). The concentration effect on toxicity was only significant (P<0.05) after 48 hours of exposure at the 500 μM concentration. No significant difference in cell viability between 24 and 48 exposure periods was seen (P>0.05).

The data for Gen0 and Gen1 drug conjugates indicated a decrease in cell viability to reach 86% and 74% (Figure 3.15 and Figure 3.16 respectively) at a concentration of 500 μM at the 48 hours exposure period. It should be noted that all the MTT assay values were within the

acceptable range of cytotoxicity of biomaterials and did not drop below the 70% limit for biomaterials, even at higher concentrations.

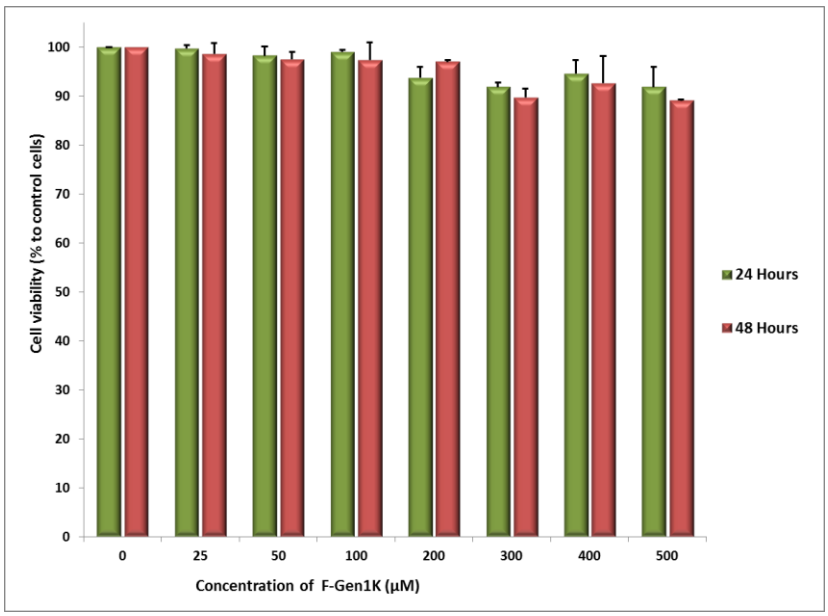

Figure 3.14 MTT cell viability results after 24 and 48 hours exposure to different concentrations of F-Gen1K dendron. Results are expressed as mean ±SD (*n*=4). Significant (P<0.05) increases in the toxicity of high concentrations (300 to 500 µm) was noticed after both durations compared to the control group. The only significant difference between the 2 duration of exposure was detected at a concentration of 100 µM.

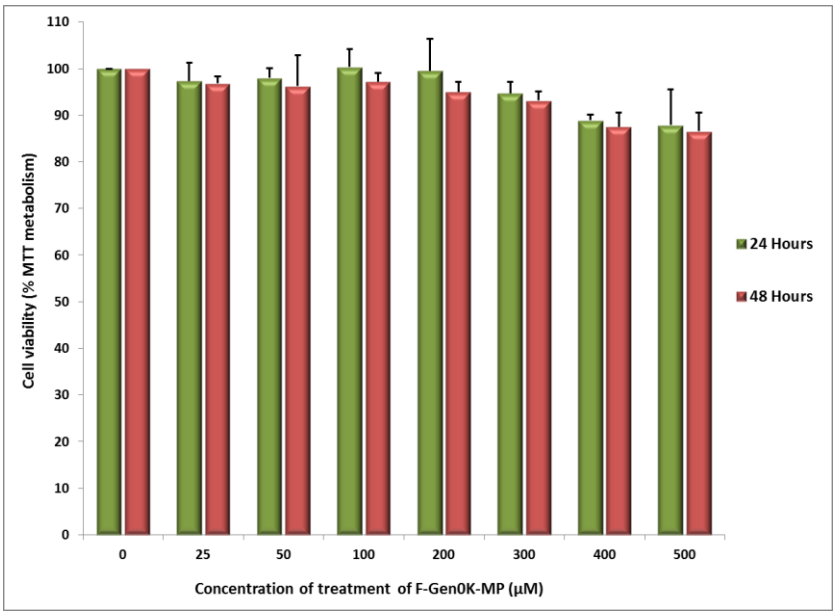

Figure 3.15 Cell viability results after 24 and 48 hours exposure to different concentrations of F-Gen0K-MP conjugate. Results are expressed as mean ±SD (*n*=4). A significant (P<0.05) increase in cytotoxicity was seen with elevated doses (from 300 to 500 µM) compared to the control group (untreated cells). However, a significant difference was not indicated between 24 and 48 hours exposure periods (P>0.05).

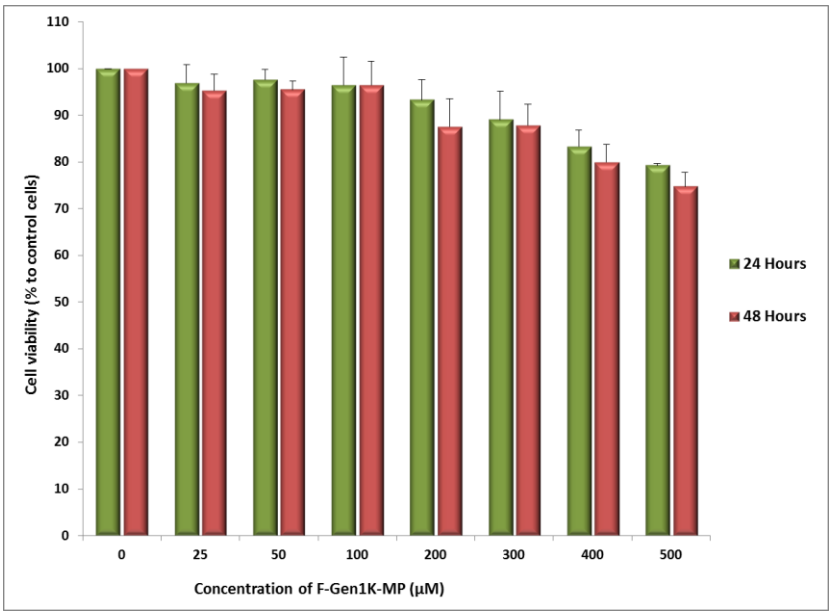

Figure 3.16 Cell viability results after 24 and 48 hours exposure to different concentrations of F-Gen1K-MP conjugate. Results are expressed as mean ±SD (*n*=4). Significant (P<0.05) increases in toxicity at high concentrations (200 to 500 µm) was noticed after both durations when compared to the control group. The only significant difference between the 2 durations of exposure was detected at 500 µM concentration.

The MTT values of F-Gen0-MP and F-Gen1-MP based on its equimolar contents of MP after 24 hours exposure are shown in Figure 3.17. The statistical analysis did not reveal any significant difference (P>0.05) in the cell viability of F-Gen0-MP and F-Gen1-MP compared to free MP. The same pattern of absence of significance difference was also observed in the cell viability values for F-Gen0-MP and F-Gen1-MP after 48 hours exposure (Figure 3.18).

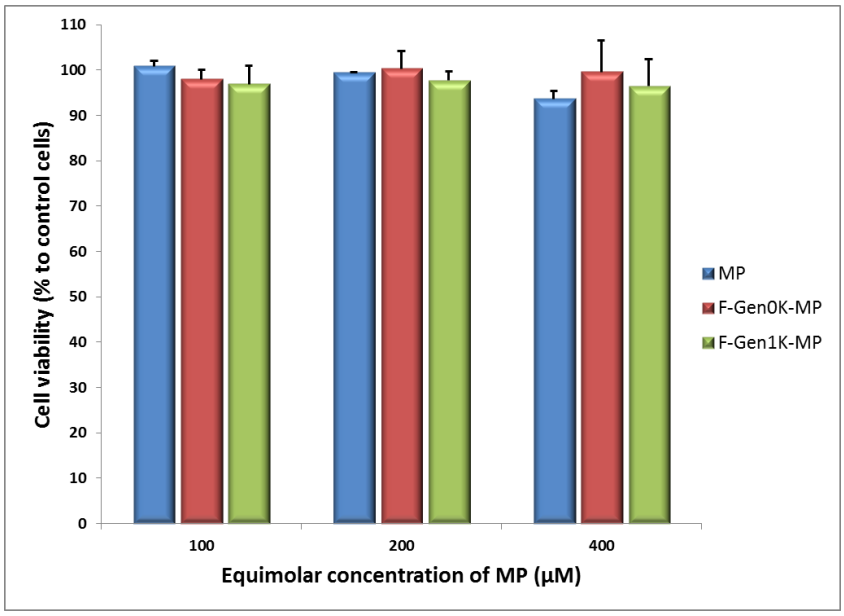

Figure 3.17 MTT cell viability results of equimolar concentrations of MP, F-Gen0K-MP and F-Gen1K-MP after 24 hours exposure. Results are expressed as mean ±SD (*n*=4). No significant change (P>0.05) was detected in cells treated with F-Gen0K-MP and F-Gen1K-MP compared to free MP.

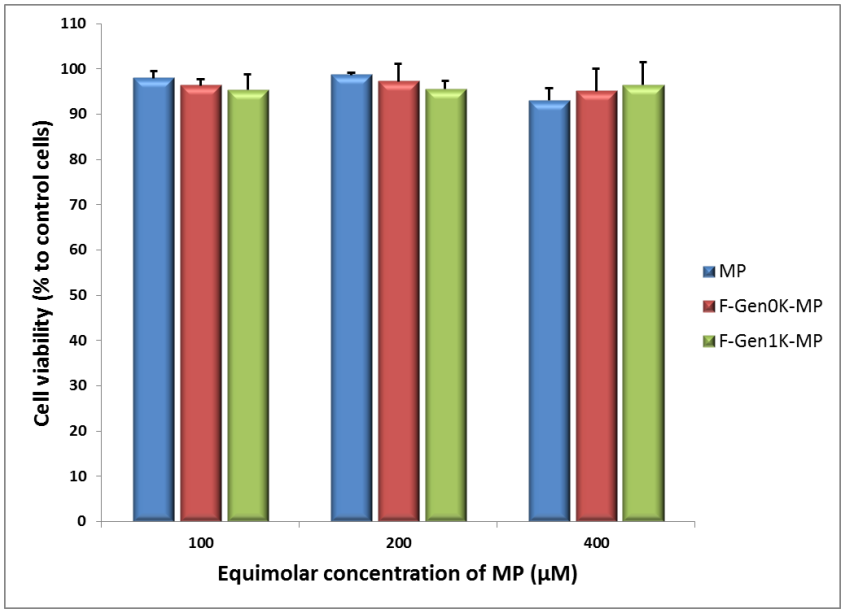

Figure 3.18 MTT cell viability results of equimolar concentrations of MP, F-Gen0K-MP and F-Gen1K-MP after 48 hours exposure. Results are expressed as mean ±SD (*n*=4). No significant change (P>0.05) was detected in cells treated with F-Gen0K-MP and F-Gen1K-MP compared to free MP.

3.4.3 HPI assay analysis of dendron-MP conjugates

Complementary to LDH and MTT assays, the HPI toxicity assay was performed to identify the percentage of viable b.End3 after 24 hours exposure to the tested material detecting not only necrotic cells but also apoptotic cell (Figure 3.19). Within the three concentrations tested (100, 200 and 400 µM) the percentages of viable cells for all molecules under investigation were within the acceptable range. Both Gen0 and Gen1 dendrons attached to

MP showed a significant difference ($P<0.05$) from the control group at 400 μM but not at lower concentrations.

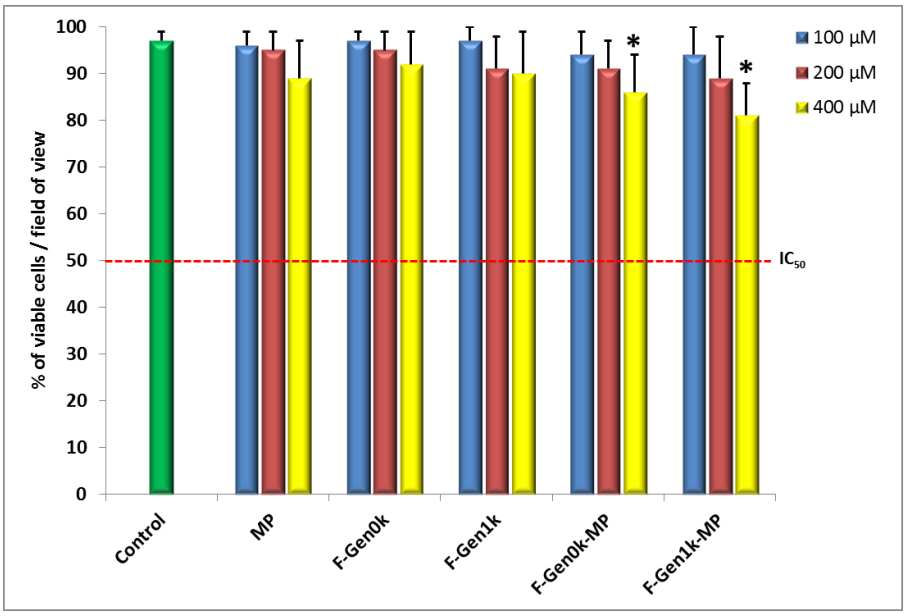

Figure 3.19 Percentage of viable b.End3 cells after treatment for 24 hours with different concentrations of MP, dendrons and dendron-MP conjugates. Results are expressed as mean ±SD (*n*=4). The green bar represents the negative control (untreated cells). The dotted line indicates the IC_{50} cytotoxicity limit. The (*) indicates significant difference from the control group with P value equal or less than 0.05.

3.4.4 Calcein/ethidium viability-cytotoxicity analysis of dendron-MP conjugates

In the confocal image of the control group cells (untreated cells), the live cells appeared with distinctive green fluorescence (Figure 3.20.a). By calculating the ratio of live cells to the total number of cells, the control group contained 98±1.4% of live cells. Whereas cells treated with lysis solution appeared with distinctive red florescent (Figure 3.20.c) with 100% dead cells. The percentage of live cells treated with 100, 200 and 400 μM of MP, F-Gen0K dendron, F-Gen1K dendron, F-Gen0K-MP and F-Gen1K-MP plus the control group are shown in Figure 3.21. The percentages of live cells were higher than LD_{50} threshold of viable cells.

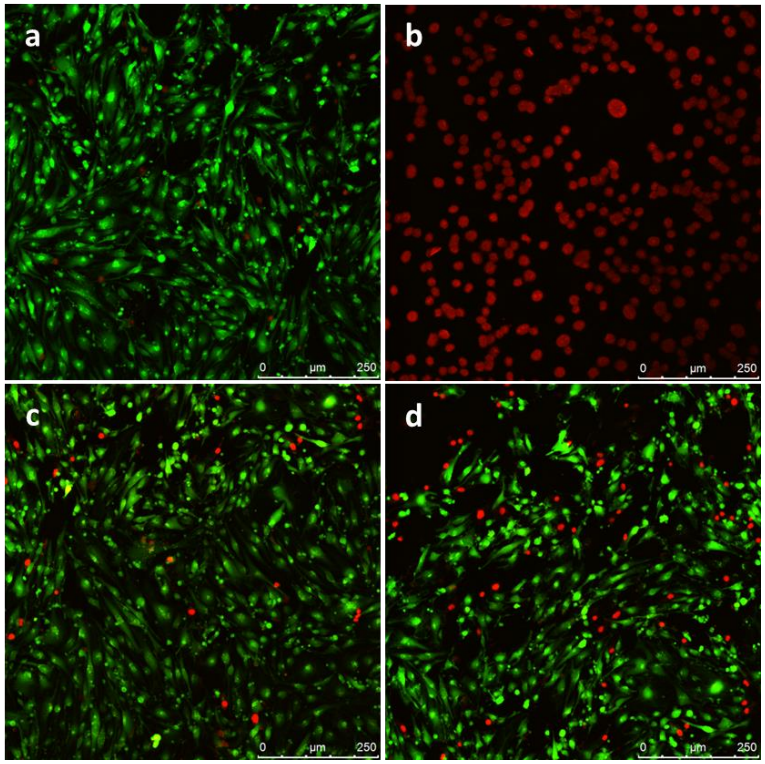

Figure 3.20 Samples of b.End3 cells fluorescent confocal images stained by calcein AM/ethidium homodimer-1. a. represents control cells (untreated cells with 98% cellular viability, b. illustrates 100% dead cells induced by Triton-x complete lysis solution, c. represents a sample of cells treated with 400 µM F-Gen0K-MP with live cells equal to 92% and d. represents a sample of cells treated with 400 µM F-Gen1K-MP with cellular viability equal to 77%.

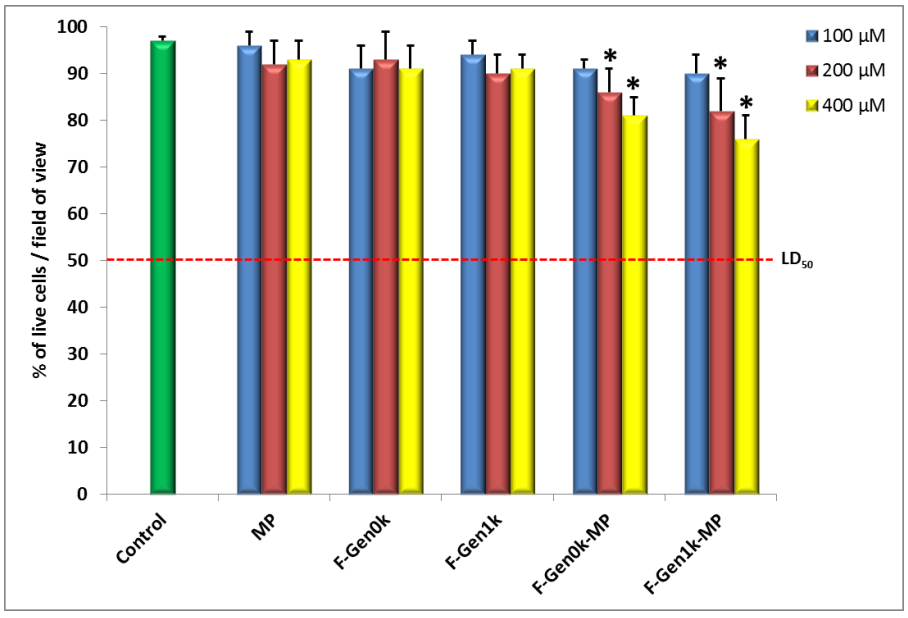

Figure 3.21 Percentage of live b.End3 cells obtained from confocal images of cells treated for 24 hours with different concentrations of MP, dendrons and dendron-MP conjugates. Results are expressed as mean ±SD (n=4). The green bar represents the negative control (untreated cells). The dotted line represents the LD_{50} threshold. The (*) indicates a significant difference from the control group with p value equal or less than 0.5.

3.5 Discussion

Due to their nano-range size, dendrimers are non-selective for a specific target tissue and might interact adversely with cell components such as plasma membranes, cell organelles (endosomes, mitochondria, nucleus) and proteins such as enzymes (Choi *et al.*, 2006; Lee *et al.*, 2008). One of the considerations of non-selective uptake of these nanoparticles is their potential to cause cytotoxicity. Thus, the use of F-Gen0K-MP and F-Gen1K-MP as efficient DDSs should fulfil at a minimum several levels of biological safety requirements inducing low toxicity and biocompatibility. (Choi *et al.*, 2010).

Most toxicity tests start by investigating the effect of doses or concentrations of the concerned molecules on the cytotoxicity *in vitro* (Choi *et al.*, 2010) using an appropriate cell type for that study. Choosing b.End3 cells for this study was based on a number of theoretical and practical considerations such as the organ system (brain endothelium) as well as the biological process being studied (penetration through the BBB) and the number of passage (Rabolli *et al.*, 2010). It is evident that understanding of the function of the BBB is a prerequisite for effective and safe drug-delivery strategies to the CNS to treat neurological disorders. In essence any *in vitro* model of the BBB should contain the brain capillary endothelial cell (Lai *et al.*, 2005). Low passage numbers have the advantage of making the reproducibility of experiments more reliable since they retain most of the physiological properties of their parent cells. These cells were easy to grow and retained their differentiating properties such as functionally expressing a variety of BBB transporters, drug-metabolising enzyme activities and mechanisms of active extrusion including P-gp (Chat *et al.*, 1998) which is the main system responsible for extruding many molecules from the brain to the blood including drug molecules.

Here, LDH, MTT, HPI tests and calcein/ethidium viability-cytotoxicity assays were used to assess the various aspects of potential toxicity levels of F-Gen0K-MP and F-Gen1K-MP molecules. Integrating the data deriving from these complementary toxicity assays gave a better and comprehensive prediction of the toxicity of these novel molecules and of the affected pathways (Choi *et al.*, 2010; Scheers *et al.*, 2001). The LDH release (Figure 3.5) and cell viability data (Figure 3.12) of free MP were investigated and used for the statistical comparison with F-Gen0K-MP and F-Gen1K-MP molecules.

The minimum effective concentration (the minimum concentration of a drug in serum required to produce a desired pharmacological effect in most patients) of MP is 75 μM (Pelt, 2011). Although, an increase in the cytotoxicity of free MP with increasing concentration and

time of exposure was noticed, the toxicity levels were within the acceptable range even at concentrations much higher than 75 μM.

F-Gen0K and F-Gen1K dendrons are positively-charged particles that can easily interact with the negatively-charged cell membrane. These interactions can lead to configurational and physiological changes in the cell membrane which in turn can cause reduction in its integrity as a barrier and cell death (Agashe *et al.*, 2006; Kolhatkar *et al.*, 2007).

Cytotoxicity data obtained from LDH and MTT assays indicated significantly ($P<0.05$) higher toxicity of F-Gen1K dendron (Figures 3.6 & 3.13) compared to F-Gen0K dendron (Figures 3.5 & 3.12). This higher toxicity could be related to the number of peripheral amine groups in Gen1 dendron (4 groups) compared to Gen0 dendron (2 groups). These results are consistent with previous reports of increasing toxicity of dendrimers with increasing concentration of free amine groups present at their periphery and generation-dependent toxicity (Chen, 2004). Not only dendrimers but also other cationic macromolecules cause destabilisation of the cell membrane leading to cell lysis (Chen, 2004). The increase in toxicity with higher doses and longer durations of exposure observed in Gen0 and Gen1dendrons are in agreement with another study which investigated the cytotoxicity of plain Gen5 PPI dendron and amino acid protected PPI dendrimers, in HepG2 and COS-7 cell lines and indicated the effect of terminal functional groups, concentration and incubation time on cytotoxicity (Agashe *et al.*, 2006).

Cell viability has been found to decrease with increases in concentration and incubation time. The cytotoxicity has been found to be concentration- as well as time-dependent (Hong *et al.*, 2006). The cytotoxicity was attributed to the presence of free primary amine groups in Gen5 PPI dendrons and the positive charge associated with them.

Although, an increase in LDH release and reduction in cellular viability with higher doses and longer exposure periods was observed in F-Gen0K-MP (Figures 3.8 & 3.15) and F-Gen1K-MP (Figures 3.9 & 3.16), these molecules can be considered nontoxic as the values did not exceed the LD_{50} threshold for the LDH assay or go below IC_{50} for the MTT assay. Moreover, statistical analysis of data obtained from LDH and MTT values revealed a significantly ($p<0.05$) higher toxicity of the F-Gen1-MP (Figure 3.8 & 3.16) molecule when compared to F-Gen0-MP (Figures 3.8 & 3.15). This relative increment in toxicity might be attributed to the higher number of MP molecules present in F-Gen1-MP (4 molecules of MP can be conjugated with F-Gen1 dendron while only 2 can be conjugated with F-Gen0 dendron).

Moreover, this higher toxicity could be explained on the fact that F-Gen1-MP is more positively charged and a larger molecule compared to F-Gen0-MP.

Perhaps, the most interesting result was generated by comparing the LDH release values of F-Gen0-MP and F-Gen1-MP based on their contents of MP with free MP after 24 hours of exposure (Figure 3.10) which revealed significantly ($P<0.05$) lower toxicity of F-Gen0K-MP but not F-Gen1K-MP compared to the same concentration of free MP due to the functionalisation of dendron with MP. Although dendrimer generation is a key factor in its cytotoxicity, it is strongly influenced by the nature of the dendrimer surface. It has been shown that functionalised dendrimers such as anionic (Chen, 2004), PEGylated (Chen, 2004), OH-terminated (Lee *et al.*, 2003), COOH-terminated (Malik *et al.*, 2000), and melamine-based dendrimers (Chen, 2004) are much less cytotoxic than NH_2-terminated dendrimers because of shielding of the internal cationic charges by surface modification. Another suggestion to explain this reduction of conjugated drug compared to free drug is that attaching MP to dendrons resulted in new molecules that could have physio-chemical properties different from its parent molecule thus causing less LDH release and lower negative effect on cellular metabolic activities. Finally, changes in the hydrophobicity of F-Gen0-MP compared to free MP might be a factor behind this variation.

However, comparison of LDH results after 48 hours exposure (Figure 3.11) and MTT results after 24 and 48 hours exposure (Figures 3.17 and 3.18) did not show any significant difference ($P>0.05$) between F-Gen0K-MP and F-Gen1K-MP values and that of free MP. This might be due to delayed toxicity caused by dendron-drug conjugate molecules or caused by increased MW of the final molecule (Xu *et al.*, 2014). In addition, cells respond rapidly but in different ways to toxic stress such as altering, for example, metabolic rates and cell growth or gene transcription controlling basic functions. Moreover, longer duration of exposure might result in amide linkage hydrolysis by lysosomal enzymes (Xu *et al.*, 2014) leading to the release of MP from dendron thus causing similar toxicity levels compared to free MP.

The LDH toxicity levels of F-Gen0-MP (Figure 3.8) and F-Gen1-MP, (Figure 3.9) were slightly higher than MTT levels (Figures 3.15 and 3.16 respectively). This might be attributed to the fact that LDH assay is based on measuring LDH release caused by cell membrane alterations while MTT assay is based on measuring the enzymatic activity of cells rather than cell integrity. Another factor of these variations in cytotoxicity levels may be due to the fact that LDH enzyme is present in the cell cytoplasm which can be easily released by cell

membrane lysis while mitochondrial reductase enzyme is located in mitochondria, an organelle more difficult to be reached by the tested molecules. Finally, the variation in LDH release levels may be a consequence of the internalisation forces caused after conjugation with the dendrons. The data of this chapter together with those obtained later from permeability tests (Chapter 6) can provide better comprehension of this issue.

An additional proof of the absence of toxicity of F-Gen0-MP and F-Gen1-MP within the tested concentration range was provided by HPI test and calcein/ethidium viability-cytotoxicity assay. Although both tests showed more cytotoxicity than the control group (Figures 3.19 & 3.20) especially at the 400 μM range, the values did not fall below the LD_{50} limit.

The results indicated that the toxicity levels of these molecules were within the accepted range and can be tested using an *in vitro* BBB model to illustrate its penetration profile (Chapter 6). However, prior to permeability studies, the functionalisation of the dendron-MP conjugate with a suitable ligand for enhanced targeting and permeability across the BBB was performed and discussed in Chapter 4.

3.6 Conclusion

The work of this chapter aimed to investigate the toxicity of the synthesised dendron-drug conjugates (F-Gen0K-MP and F-Gen1K-MP) and check if it is within the acceptable range to be used for further experiments. To achieve this aim, data from different cytotoxicity assays were analysed and integrated using b.End3 cell line as *in vitro* brain model. The following points can be concluded from the results:

- The toxicity of F-Gen0K-MP and F-Gen1K-MP were concentration and duration of exposure dependant.
- The data indicated that F-Gen0K-MP and F-Gen1K-MP conjugates toxicity levels were within the acceptable limits for the tested range of concentrations.
- F-Gen0-MP showed lower toxicity than F-Gen1-MP and free MP following short duration exposure (24 hours).
- The conjugated dendron-MP molecules can be considered safe to be used for further functionalisation and investigation.

Chapter 4. Functionalisation of dendron-MP with Glutathione

4.1 Introduction

Although MP is a powerful anti-inflammatory drug and can be used for the treatment of neurodegenerative disease, its efficacy is hindered by its limited penetration to the brain due to the presence of the BBB. To overcome this obstacle and to avoid administrating large doses of MP, it is advocated that the drug is conjugated with specialised DDS that can improve its penetration across the BBB retention into the target tissue (Georgieva *et al.*, 2014).

4.1.1 Drug delivery systems for brain delivery

DDSs are highly sophisticated systems in which a drug is attached to a carrier such as dendrimers, liposomes, micelles, polymersomes and virus-like particles (Gabathuler, 2010). These carrier systems offer great potential for improving drug loading, delivery and targeting efficiencies based on the fact that the pharmacokinetic properties of carried drugs depends on the physicochemical properties of the macromolecular carrier and can be modulated by modifying the properties of the carrier rather than those of the drug (Madaan *et al.*, 2014).

DDSs could offer several advantages compared to traditional drug delivery approaches, such as (i) prevention of premature drug degradation or interaction with its biological environment, (ii) improvement of drug delivery to the targeted or desired tissues and (iii) control over the drug-tissue distribution profile (Gabathuler, 2010). Thus, DDSs can improve the properties of free drugs by increasing their *in vivo* biodistribution and stability (Drbohlavova *et al.*, 2013), solubility and even by manipulation of pharmacokinetics to enhance their transport and, more importantly, their release at higher doses at the target site in order to be pharmacologically efficient (De Jong *et al.*, 2008).

Specialised drug carriers can be designed either through entrapment approach or direct conjugation with the drugs (Georgieva *et al.*, 2014). The delivery through biological barriers (of poorly penetrating drugs attached to such carrier systems) can be enhanced by further peripheral surface modifications such as grafting an endogenous ligand whose specific receptors are widely expressed through that barrier. This strategy for the delivery of molecules that are unable to pass the BBB involves the use of endogenous natural transport routes that are expressed on the surface of the endothelium of the BBB, such as endogenous RMT (Pardridge, 2007). Attaching a poorly-penetrating active drug molecule such as MP to a vector that accesses a specific catalysed transporter pathway creates a "Trojan horse-like" deception that tricks the BBB allowing the drug to pass through its gates (Ulbrich *et al.*, 2009). Transporting vectors, such as modified proteins, endogenous peptides and peptide-mimetic monoclonal antibodies are strategies to allow these molecules to pass through the BBB (Oller-

Salvia *et al.*, 2016). The therapeutic drug is attached to a molecular "Trojan horse" (ligand) that binds to a specific receptor on the BBB and enables receptor-mediated transport of the poorly penetrating drug across the barrier to exert the desired pharmacological action on the brain tissue (Pardridge, 2006).

During transcytosis, the binding of a ligand molecule to its specific receptors on the cell membrane triggers a series of endocytotic events. The receptors and their bound ligand cluster together and a caveolus is formed which pinches off into a vesicle, then both ligand and receptors are internalised into the endothelial cell and travel across the cytoplasm to be exocytosed at the opposite pole of the cell (Figure 4.1).

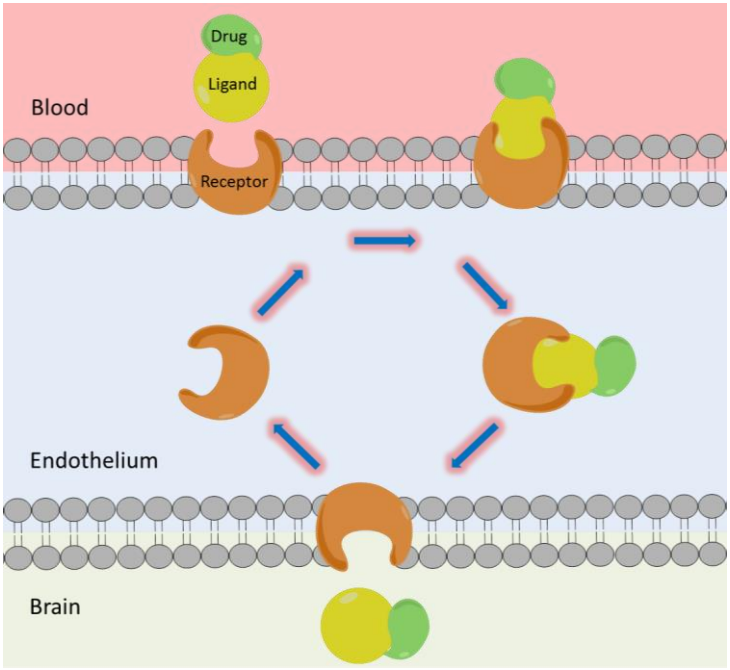

Figure 4.1 The principle of RMT. The endogenous ligand attached to the drug is recognised by corresponding receptor expressed on the endothelium surface. In general, there are three steps for RMT; (i) endocytosis at the luminal (blood) side after receptor-ligand binding; (ii) movement through the endothelia cytoplasm; and (iii) exocytosis of the drug or ligand-attached drug or cargo at the abluminal (brain) side.

Dissociation of the ligand-receptor conjugate occurs during cellular transit or during the exocytotic stage (Chen *et al.*, 2012). A number of studies have utilised RMT to improve drug penetration into the CNS *via* the BBB. Ulbrich (2009), for example, studied the possibility of using nanoparticles with covalently bound transferrin to investigate the transport of drugs across the BBB that normally cannot cross this barrier. Transferrin was coupled using the PEG cross-linker to human serum albumin nanoparticles. Transferrin-decorated nanoparticles enabled the transport of loperamide (poorly brain-penetrating drug) across the BBB and

achieved significant anti-nociceptive effects. BBB endothelial cells have different receptors for the uptake of numerous types of ligands. Some of these receptors have been targeted to deliver poorly penetrating drugs to the brain such as TfR (Visser *et al.*, 2004), lactoferrin receptor (Talukder *et al.*, 2003), apolipoprotein E receptor (Herz *et al.*, 2003), low density lipoprotein (LDL) receptor-related protein 1 and 2 receptors (Herz *et al.*, 2003), immunoglobulin G receptor (Stern *et al.*, 2002), insulin receptor (Banks, 2004), and glutathione receptor (Kannan *et al.*, 1990).

4.1.2 Glutathione and its use in DDS design

Glutathione (GSH) is a tripeptide (composed of L-glutamine, L-cysteine, and glycine) containing thiol (SH) in its structure that plays a key role in cellular biology (Figure 4.2). It has a relatively low molecular mass and can be found in living systems occurring naturally in almost all human cells (Pompella *et al.*, 2003). The cells defence mechanism against oxidative stress caused by elevated levels of reactive oxygen species is mediated by GSH. Other functions of GSH include the detoxification of the metabolites of drugs and other xenobiotic, molecules regulation of apoptosis and gene expression (Mytilineou *et al.*, 2002). It is also involved in the transmembrane transport of organic solutes into the cells (Couto *et al.*, 2013). Although GSH is the smallest reducing intracellular thiol agent within the cells, it possesses high electron-donating capacity (highly-negative redox potential) in combination with its high intracellular concentration, generating massive reducing capacity against reactive species (Giordano *et al.*, 2007). These properties underlie its powerful antioxidant activity and enzyme cofactor properties, and supports a complex thiol-exchange system, which significantly contributes to regulate cell activity (Couto *et al.*, 2013).

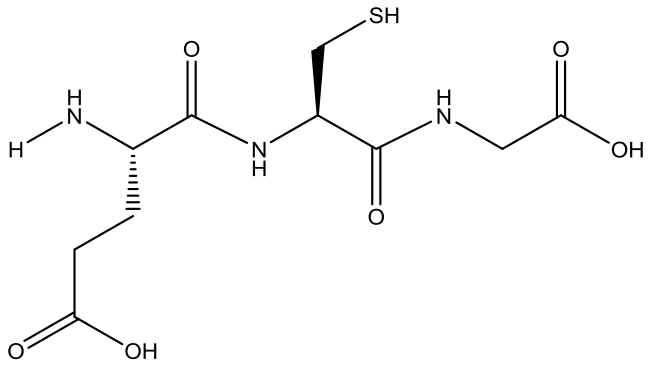

Figure 4.2 Chemical structure of GSH. The chemical formula is $C_{10}H_{17}N_3O_6S$ and the MW is 307.08 Da.

The thiol (sulfhydryl) group of GSH has a strong electron-donating nature which converts reactive oxygen species such as hydrogen and lipid peroxides to nontoxic fatty acids and/or water. After losing electrons, the molecule becomes oxidised and linked to other oxidised

molecules (dimerised) by a disulfide linkage to form glutathione disulfide or oxidised glutathione that is subsequently reduced to GSH in presence of NADPH and glutathione reductase enzyme, which are linked with hexose monophosphate shunt (Dringen *et al.*, 2000). This linkage is reversible upon re-reduction (Figure 3.3).

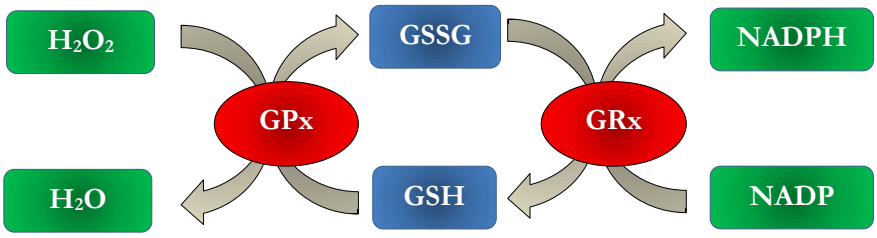

Figure 4.3 GSH oxidation-reduction cycle. Where GSH is reduced glutathione, GSSG is oxidised glutathione, GRx is glutathione reductase enzyme, GPx is glutathione peroxidase enzyme.

GSH is naturally found at high concentrations in the brain tissue and its receptor is abundantly expressed in BBB endothelial cells (Gabathuler, 2010). Therefore, using GSH as a ligand for enhancing penetration of drugs to the CNS uniquely minimises or eliminates common risks like interference with life-essential physiologic pathways or adverse immunological responses (Sies, 1999). A study (Gaillard, Appeldoorn, *et al.*, 2012) demonstrated that using liposomes decorated with GSH could safely and effectively enhance the penetration of drugs to the brain. Another study showed that the higher the amount of GSH conjugated with the brain-targeted DDSs, the more free drug penetrated to the brain tissue (Rip *et al.*, 2010). In another study, the delivery of the poorly brain-penetrating drug, doxorubicin, loaded in liposomes to the brain was highly enhanced after coating the outer surface of liposomes with GSH (Birngruber *et al.*, 2014). Based on these data, GSH was chosen as a ligand to decorate dendron-MP molecules to achieve better permeability of MP through the *in vitro* BBB model.

Aims of the chapter

Following the successful synthesis of dendrons, the next step of the project aimed to decorate the dendrons with a suitable ligand that can be recognised by the targeted *in vitro* BBB model cells and attach MP to this carrier system. Thus chapter 4 aims to:

- Design, synthesise and characterise a dendron-based DDS for MP functionalised with GSH.
- Conduct cytotoxicity studies on the GSH-dendron-MP carrier system and compare it with free MP and dendron alone.

4.2 Materials

The same materials used for dendron synthesis and cleavage listed in Table 2.1 and cytotoxicity assays listed in Table 3.1 were used in this chapter. In addition, three Fmoc amino acids listed in Table 4.1 were used for the synthesis of GSH molecule.

Table 4.1 Amino acids used for the synthesis of GSH.

Material	Company	Catalogue number
Fmoc-Cys(Trt)-OH	Novabiochem	8520080025
Fmoc-Gly-OH	Novabiochem	8520010025
Fmoc-Glu(OtBu)-OH	Novabiochem	8520090025

4.3 Methods

4.3.1 Synthesis of GSH

Since GSH molecule consists of three amino acids linked together *via* an amide linkage (Figure 4.2), SPPS was used for the synthesis of this peptide. The same procedures applied to dendron synthesis (Section 2.3.1) were used for the synthesis of GSH using L-glutamine, L-cysteine, and glycine amino acids as the building blocks. After attaching the linker to the solid support and removing its protection groups, Fmoc-Glu(OtBu)-OH was anchored on the linker by amide linkage using Biotag peptide synthesiser utilising the same reaction conditions applied in dendron synthesis (Table 2.2). Thus, 0.4 mmole of Fmoc-Glu(OtBu)-OH, 0.4 mmole HBTU, 140 μL DIPEA and 3 mL of DMF were placed in a glass vial and sonicated for a few seconds to solubilise the materials. After completion of coupling of glutamate and the linker, the mixture contents were washed several times with DMF and then a deprotection reaction was performed using 20% $^{v}/_{v}$ piperidine in DMF to remove glutamate protecting groups to introduce the next amino acid (the exact procedure is described in Section 2.3.1). Fmoc-Cys(Trt)-OH and Fmoc-Gly-OH were then introduced to the reaction with a series of deprotection and activation steps between each addition. After achieving the desired peptide sequence (Glu-Cys-Gly) which corresponds to GSH, the reaction mixture was removed from the peptide synthesiser to be washed and cleaved by the same steps used before in dendron synthesis (Section 2.3.2).

4.3.2 Synthesis of GSH-dendron conjugate

The synthesis of dendron (F-Gen0K) decorated with GSH (GSH-F-Gen0K) (Figure 4.4) was conducted using a SPPS method applying the same methodology and techniques used for dendron synthesis (Chapter 2). However, the synthesis starts from GSH and then the dendron was attached to it. Thus the first amino acid attached to the solid support and linker was glutamate that after completing the removal of the protecting groups of the linker was

followed by the covalent coupling of the cysteine and glycine. The following step in the synthesis was grafting of phenylalanine and lysine amino acids to the GSH sequence through the same deprotection and coupling reactions as described in Section 2.3.1. After washing, the resultant molecule was cleaved from the solid support using the same methodology detailed Section 2.3.2. The final product was characterised using mass spectrometry, FTIR and NMR spectroscopy. The product was purified applying the same conditions detailed in Section 2.3.4.

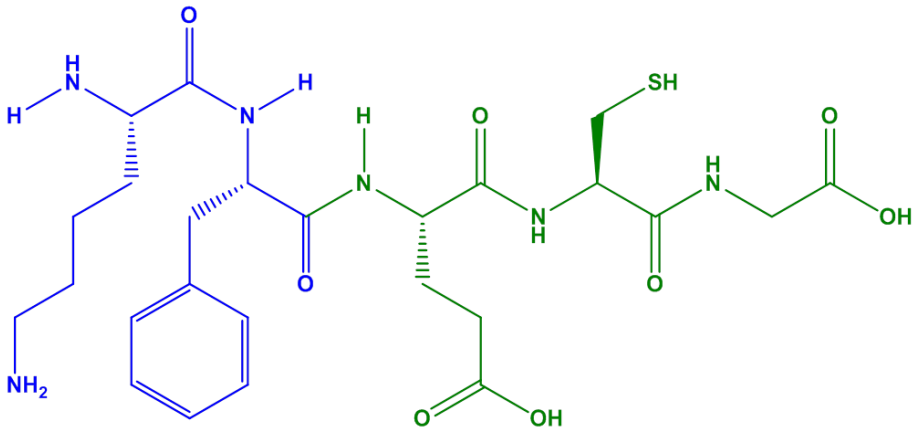

Figure 4.4 Chemical structure of GSH-F-Gen0K. The chemical formula is $C_{25}H_{38}N_6O_8S$ and the MW is 582.67 Da. The green structure represents GSH and the blue is the Generation-0 dendron linked together *via* amide linkage.

4.3.3 Synthesis of MP functionalised GSH-F-Gen0K

The same procedures and steps described in Section 2.3.3 for the covalent grafting of MP to Gen0 dendron was used to attach MP to the novel DDS molecule GSH-F-Gen0K (Figure 4.2). For each 1 mmole of GSH-F-Gen0K, 2 mmoles of MP were added since each GSH-F-Gen0K molecule contains two peripheral amine groups, each with the capability to bind one drug molecule. After cleavage from the solid support, the final product characterised using mass spectrometry, FTIR and NMR spectroscopy. The product was purified using HPLC applying the same conditions detailed in Section 2.3.5.1.

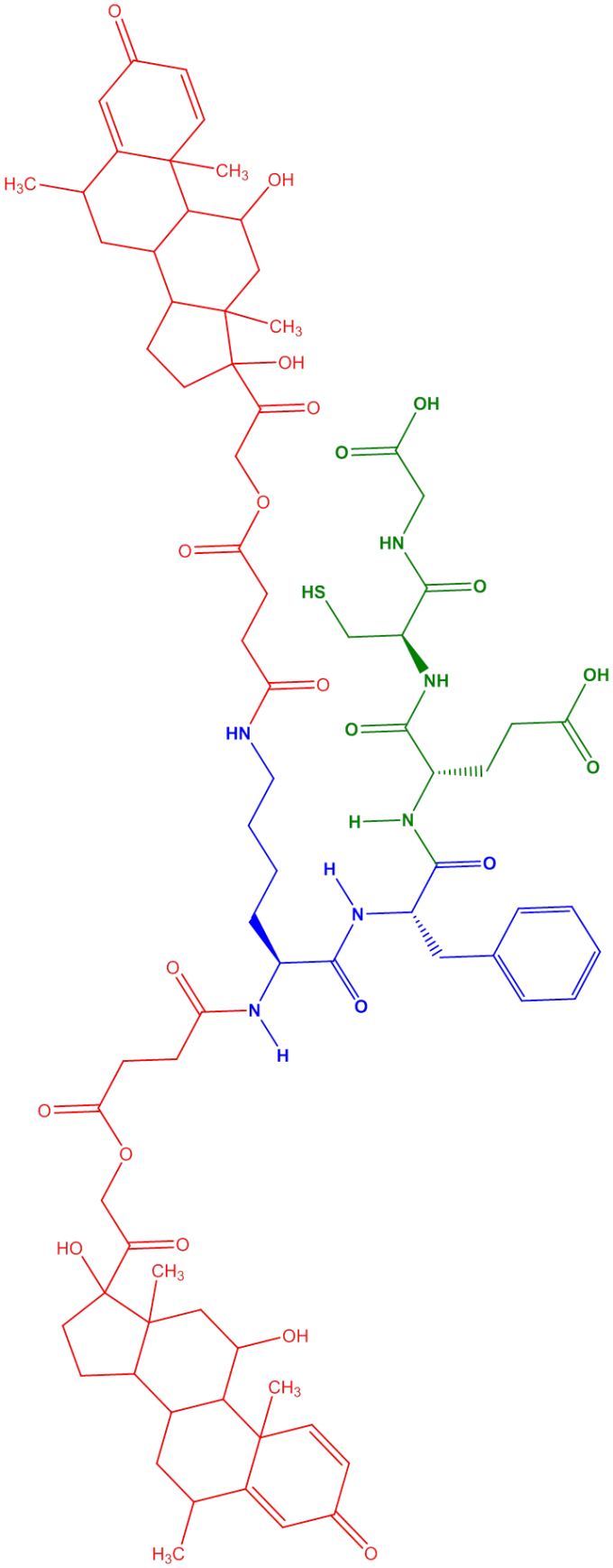

Figure 4.5 Chemical structure of GSH-F-Gen0K-MP. The chemical formula is $C_{77}H_{102}N_6O_{22}S$, and the MW is 1494.76 Da. The green structure represents GSH whereas the blue is the dendron linked together via amide linkage. The red structures are two MP moieties loaded to it.

4.3.4 Purification and characterisation of GSH-F-Gen0K-MP

In order to confirm the synthesis of the desired molecule, GSH-F-Gen0K-MP, the same laboratory techniques used for the dendron-MP characterisation and purification (Sections 2.3.4 & 2.3.5) were used including sample preparation methods, HPLC, mass spectrometry, FTIR and NMR. These tests were performed by comparing the exact MW of the synthesised GSH-F-Gen0K-MP with the theoretical MW. Moreover, the functional groups of GSH-F-Gen0K-MP were inspected by FTIR and NMR through comparing it with those of free MP and free GSH.

4.3.5 Toxicity evaluation of GSH-F-Gen0K-MP

The toxicological assessment of GSH-F-Gen0K-MP was performed on b.End3 cells using the LDH release test, MTT cell viability assay and calcein/ethidium viability-cytotoxicity assay. After preparation of 24-well plate using the same procedure described in Section 3.3.1.4, the cells were treated with different concentrations (25, 50, 100, 200, 300, 400 and 500 μM) of GSH-F-Gen0K-MP and incubated for 24 and 48 hours at 37°C, 5% CO2 and 95% air. The same protocols of cell preparations, treatment profiles, laboratory procedures and analysis of data detailed in Sections 3.3.2 to 3.3.5 were used to assess the toxicological patterns of GSH-F-Gen0K-MP.

4.3.6 Statistical analysis

Any significant difference in values were reported after investigating data for normality, and carrying out a one-way ANOVA with Tukey's *post-hoc* test, using the Minitab® 17 (version 17.2.1) statistical analysis program. The mean level ($n=4$) was compared and it was considered significantly different when the P value was lower than 0.05 (two-sided confidence intervals).

4.4 Results

4.4.1 Purification and characterisation of GSH-F-Gen0K-MP

The purity of the final product was obtained by collecting the desired fraction in HPLC. The synthesis of GSH and GSH-F-Gen0K and the loading of MP on the peripheral amine groups of GSH-F-Gen0K molecule were confirmed by conducting mass spectroscopy for MW detection and comparison of FTIR results for each molecule.

4.4.1.1 Purification and characterisation of GSH-F-Gen0K-MP by HPLC

The synthesised molecule, GSH-F-Gen0K-MP was analysed through HPLC using the same instrument and conditions detailed in Section 2.3.5.1 and detected at wave length of 272 nm (the calculation of synthesised molecules wave lengths are detailed in Chapter 6). GSH-F-Gen0K-MP appeared as distinctive peak after 16 minutes in the HPLC spectra (Figure 4.6-left) with few minor peaks. The samples were collected between 15 and 16.5 minutes to purify the product and remove the unwanted peaks. The process was repeated 5 times to retrieve as much as possible of the purified sample which was then freeze-dried for 24 hours (Christ Alpha 2-4, UK) to obtain the purified material in a powder form. To ensure its purity, the product of reaction underwent a further purification step using the same HPLC method and gave a distinctive peak at 16 minute with the absence of any contaminating peaks (Figure 4.6-right)

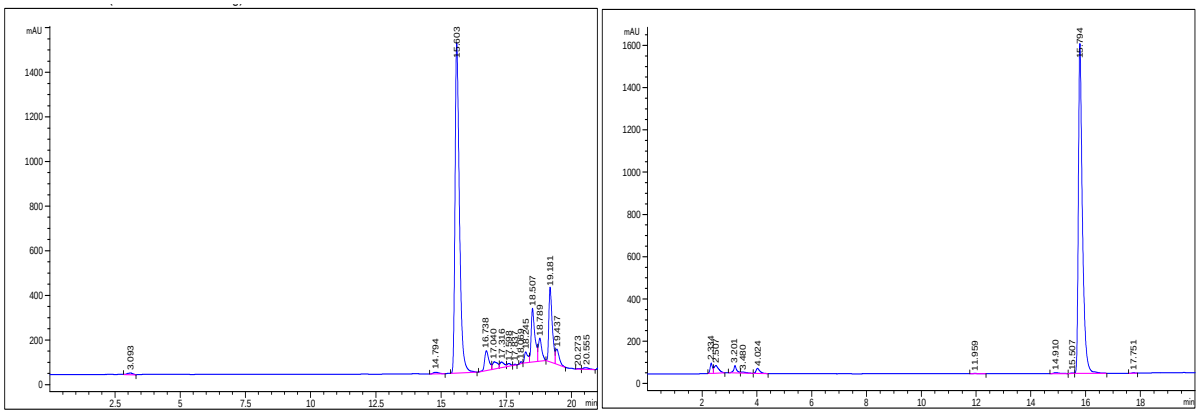

Figure 4.6 HPLC spectra of GSH-F-Gen0K-MP. HPLC spectra of crude GSH-F-Gen0K-MP (left) and its purified sample (right) which appeared in minute 16.

4.4.1.2 Characterisation of GSH-F-Gen0K-MP by mass spectroscopy

Mass spectroscopy indicated the successful synthesis of GSH (Figure 4.7) and GSH-F-Gen0K (Figure 4.8) with distinctive MW peaks of 307 and 582 Da respectively.

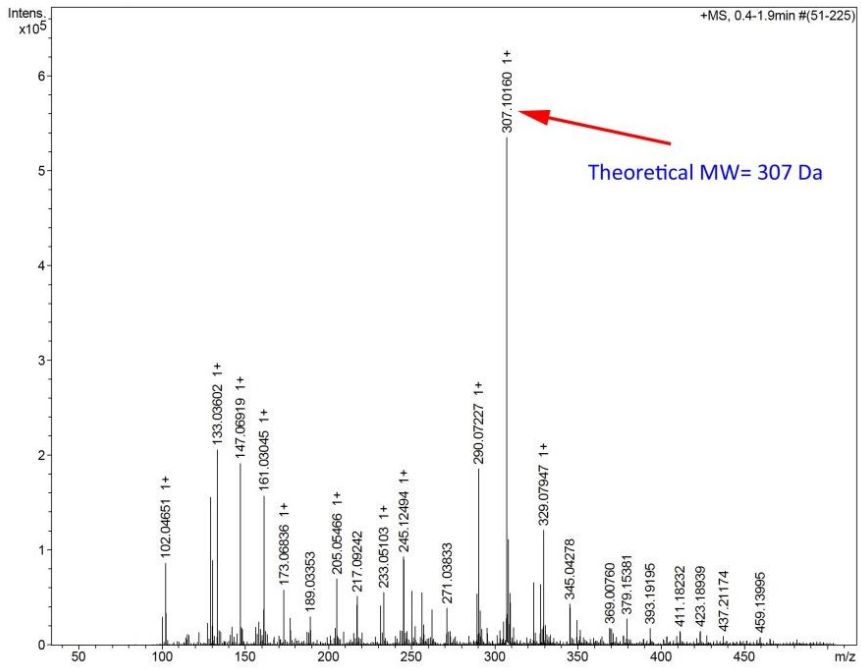

Figure 4.7 Mass spectrometry of GSH. The synthesis of GSH was confirmed by mass spectrum which showed equal numbers for both theoretical and actual MW (307 Da).

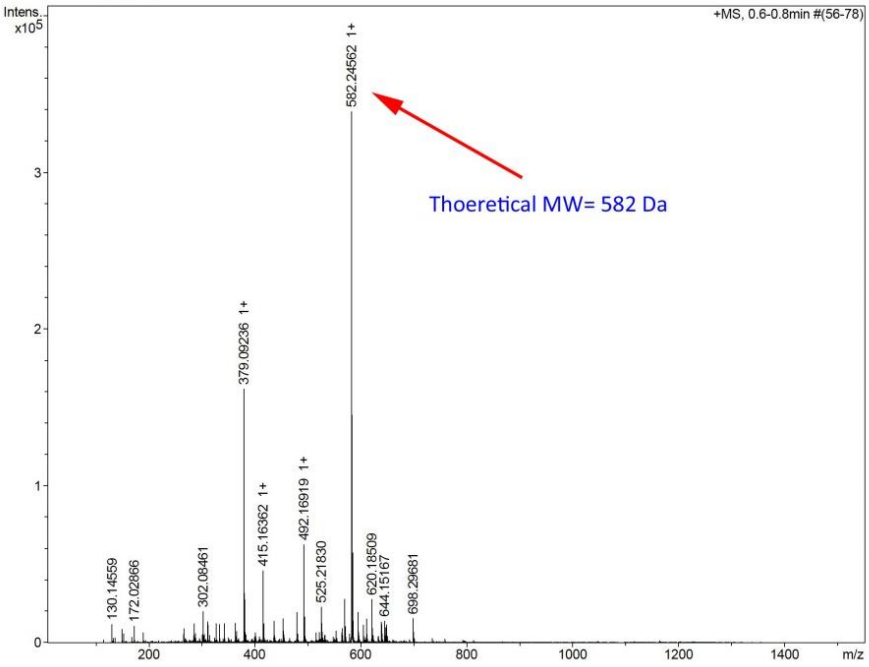

Figure 4.8 Mass spectrometry of GSH-F-Gen0K conjugate. The actual MW appeared as distinctive peak of 582 Da which is equal to the theoretical MW.

Mass spectrometry was conducted to confirm the conjugation of MP to the peripheral amine groups of GSH-F-Gen0K (Figure 4.9). Each GSH-dendron molecule can interact with two drug molecules.

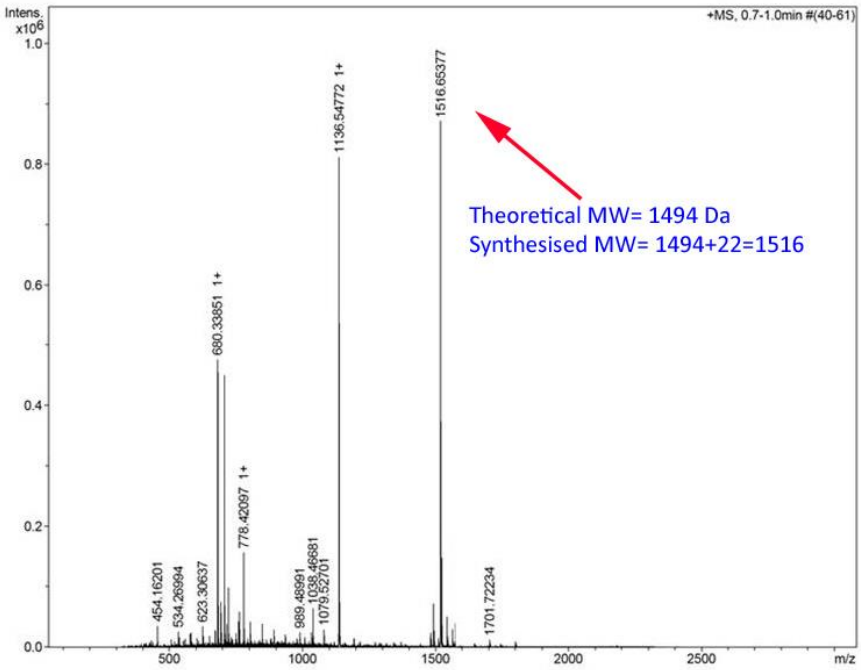

Figure 4.9 Mass spectrometry of GSH-F-G0k-MP conjugate. The actual MW that appeared in mass spectrum was 1516 which is higher than the theoretical MW by approximately 22 Da. This difference can be attributed to the presence of Na in the final molecule since sodium salt of the drug was used. Another peak (1136 Da) indicated the attachment of one drug molecule to the GSH-dendron. The drug molecule might be detached from final molecule during the cleavage of the synthesised molecule from solid support or caused by ionisation effect during mass spectrometry.

4.4.1.3 Characterisation of GSH-F-Gen0K-MP by FTIR

Another technique used to confirm the synthesis of the required ligand-dendron-drug conjugate was FTIR. The FTIR peaks of MP, GSH-F-Gen0K, and GSH-F-Gen0K-MP were combined together in a single plot (Figure 4.10) to highlight shifting and changing in group moieties of the three compounds.

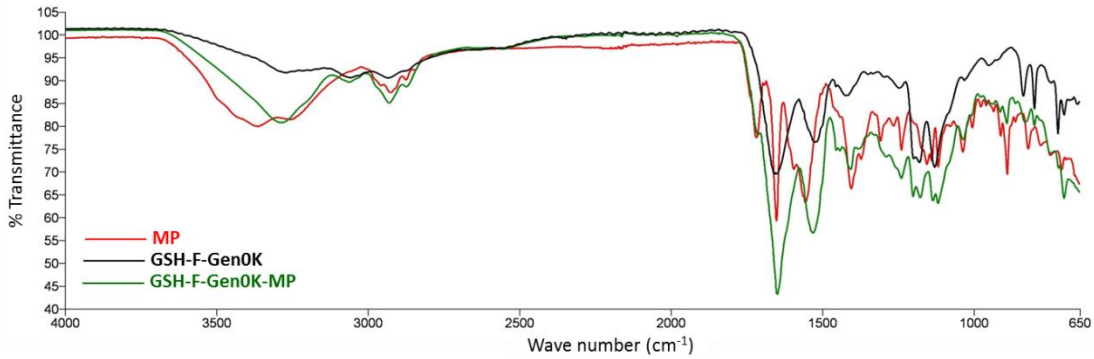

Figure 4.10 FTIR spectra of MP, GSH-F-Gen0K, and GSH-F-Gen0K-MP. The FTIR was set on 32 scans. The free MP and free GSH-dendron troughs were compared to the synthesised GSH-dendron-drug molecules to illustrate any shifting and changing in troughs. The x axis represents the wave number ranging from 4000 to 650 measured in cm^{-1} and the y axis represents the transmittance percentage.

For better comparison between troughs, the chart was split into two charts with wave numbers ranging from 4000 to 2000 cm^{-1} (Figure 4.11) and from 2000 to 650 cm^{-1} (Figure 4.12). The spectra indicated down shifting in the trough (of GSH-F-Gen0K-MP) at around 3100 cm^{-1} caused by the higher number of amide groups compared to GSH-F-Gen0K molecule (Figure 4.11). Moreover, the unique distinctive trough of the ketone group (1715 cm^{-1}) could be seen in the spectra of both free MP and GSH-F-Gen0K-MP but not GSH-F-Gen0K (Figure 4.12). These data provided evidence of the successful grafting of MP to the GHS-dendron molecule.

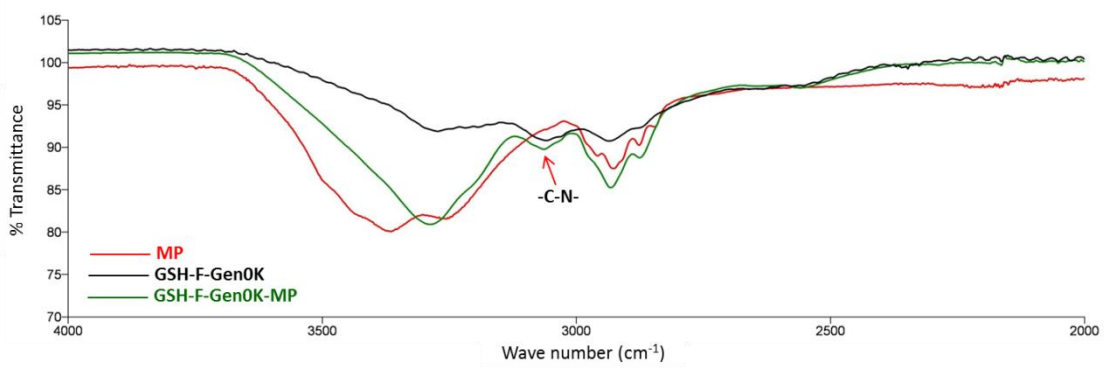

Figure 4.11 FTIR spectra of MP, GSH-F-Gen0K, and GSH-F-Gen0K-MP with wave number ranging from 4000 to 2000 cm^{-1}. The FTIR was set on 32 scans. Shifting is seen in the GSH-F-Gen0K-MP trough around 3100 cm^{-1} compared to GSH-F-Gen0K due to its higher number of amide bonds.

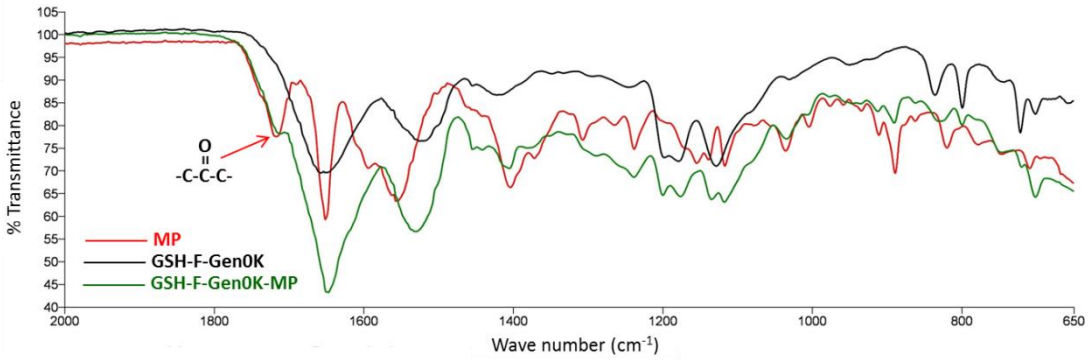

Figure 4.12 FTIR spectra of MP, GSH-F-Gen0K, and GSH-F-Gen0K-MP with wave numbers ranging from 2000 to 650 cm^{-1}. The FTIR was set on 32 scans. Appearance of an MP-ketone trough was seen in the F-Gen0K-MP molecule but not in the free GSH-dendron molecule.

4.4.1.4 Characterisation of GSH-F-Gen0K-MP by NMR

The NMR spectra of GSH-F-Gen0K, MP and GSH-F-Gen0K-MP were integrated in a single figure for comparison (Figure 4.13). For more comprehensive comparison the radio frequency (ppm) ranging from 5.5 to 8.0 was enlarged (Figure 4.14). The same functional groups used to confirm the attachment of MP to dendrons (Section 2.3.5.4) were used also used to confirm

the attachment of MP to GSH. The protons of the phenyl group of the phenylalanine amino acid appeared as a distinctive peak at 7.2 ppm in both the GSH-F-Gen0K and GSH-F-Gen0K-MP molecules spectra. The hydrogen atoms near to the C=O group of the hexagonal ring in MP gave unique peaks which can be seen in both the free drug and its attached form. These peaks were slightly shifted in the F-Gen0K-MP molecule when compared with the same H atoms of the free drug.

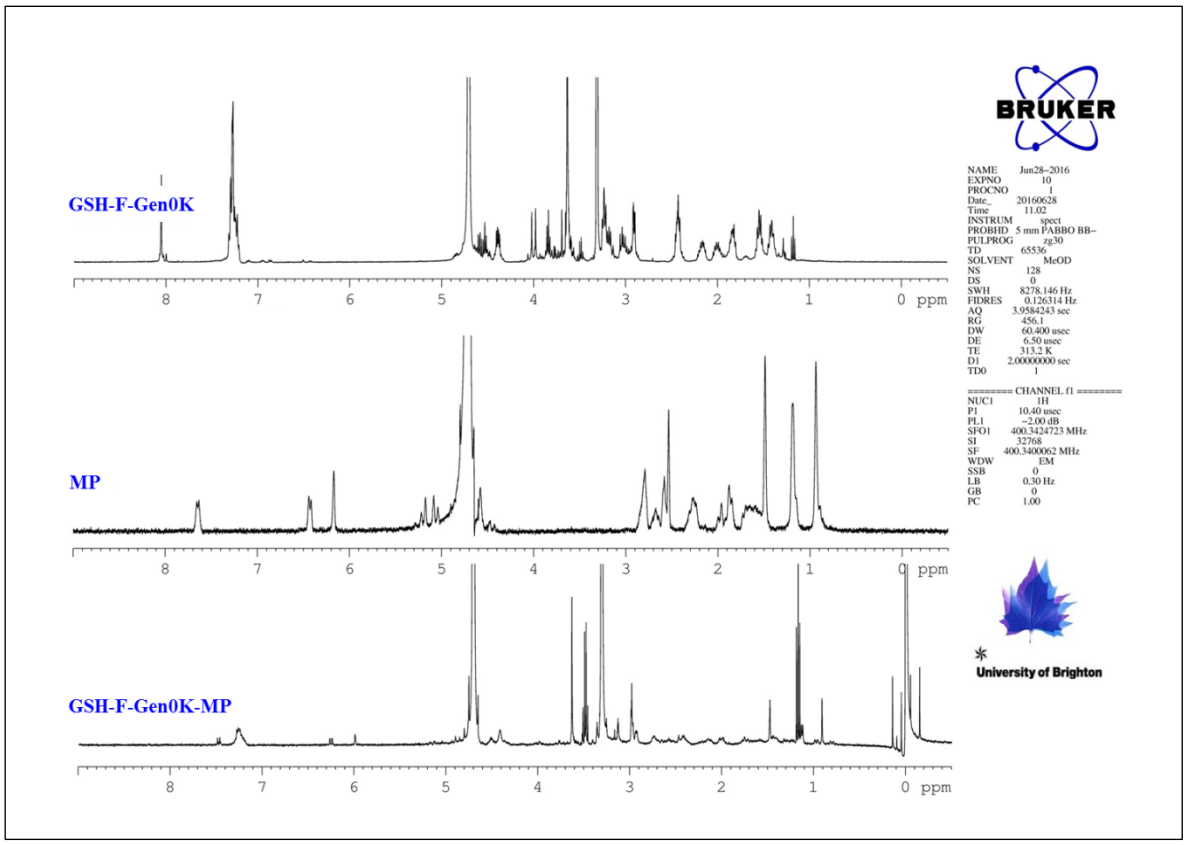

Figure 4.13 NMR peaks of free MP, GSH-F-Gen0K dendron and F-Gen0K-MP. Comparison of the H atoms spectra of free F-Gen0K and free MP with final molecule, GSH-F-Gen0K-MP.

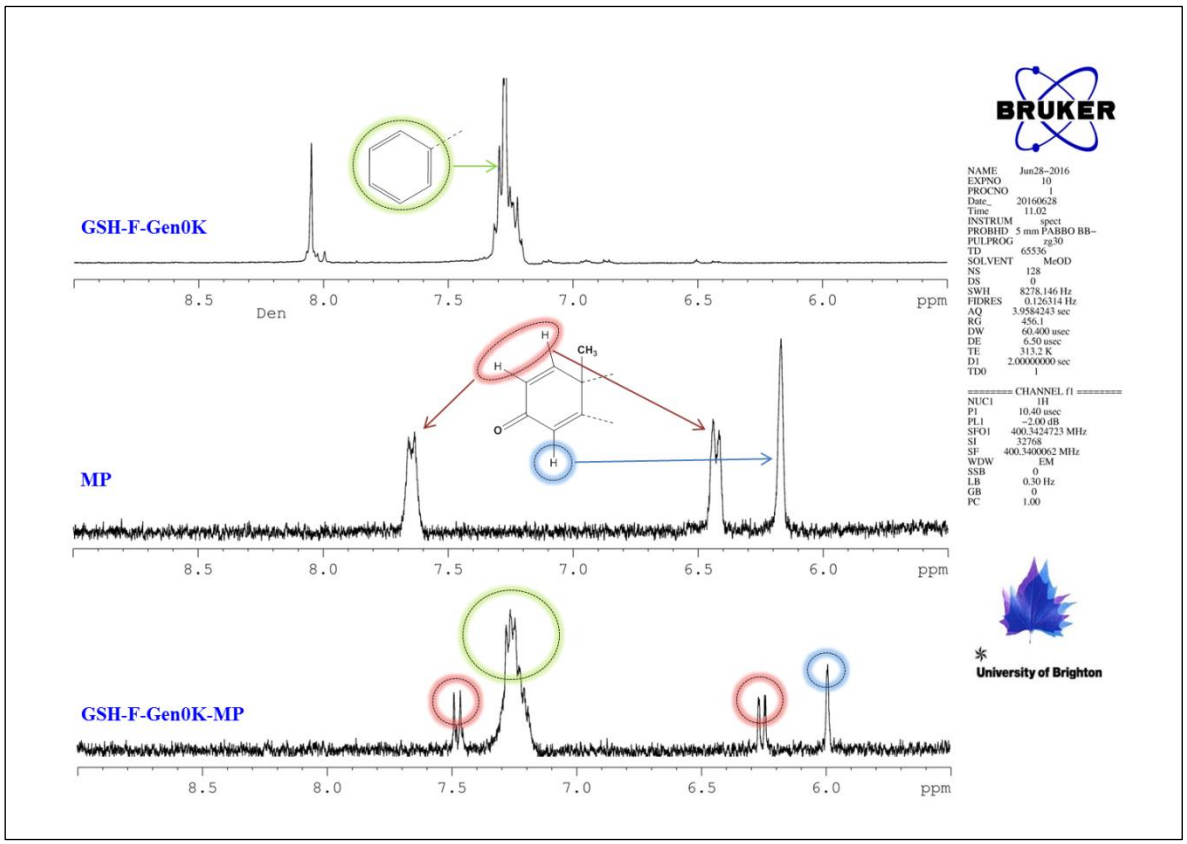

Figure 4.14 NMR peaks of free MP, GSH-F-Gen0K dendron and F-Gen0k-MP with ppm ranging from 5.5 to 9. The peaks of the protons of the phenyl group of phenylalanine amino acid in the dendron (green) and the peaks of the hydrogen atoms of the hexagonal ring in free MP (red and blue) all appeared in the synthesised GSH-F-Gen0K-MP molecule with slight shifting.

4.4.2 Toxicity evaluation of GSH-F-Gen0K-MP

LDH release, MTT cell viability tests and calcein/ethidium viability-cytotoxicity assay were performed to assess the cytotoxicity of GSH-F-Gen0K-MP molecule on b.End3 cells after 24 and 48 hours of exposure.

4.4.2.1 Toxicity evaluation of GSH-F-Gen0K-MP based on LDH release

Statistical analysis of data collected from LDH release levels indicated gradual increase in LDH release levels with rise in concentration which became statistically different ($P<0.05$) at concentrations ranging from 100 μM to 500 μM of GSH-F-Gen0K-MP when compared to low concentrations (25 and 50 μM). However, significant difference in LDH release levels based on incubation period (24 and 48 hours) was not observed (Figure 4.15).

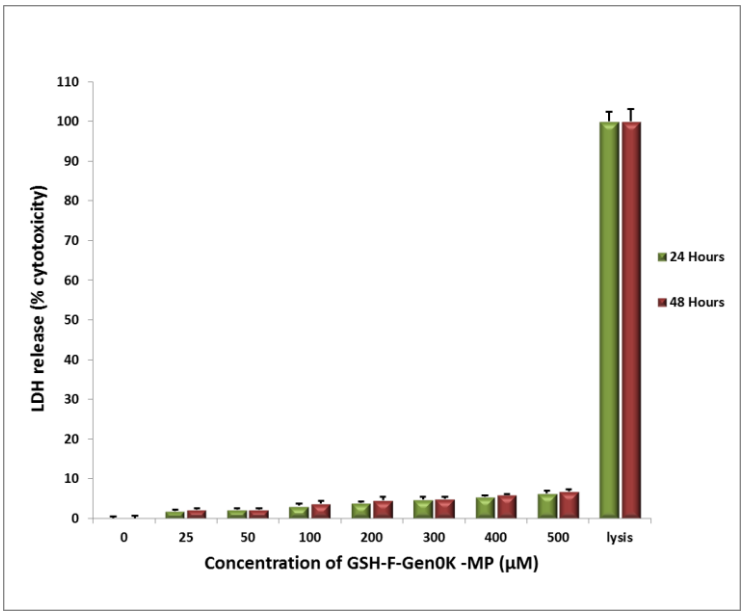

Figure 4.15 LDH release levels from cells treated with different concentration of GSH-F-Gen0K-MP conjugate after 24 and 48 hours. Results are expressed as mean ±SD (*n=4*). Higher doses (400 and 500 μM) caused significantly higher ($P<0.05$) LDH release when compared to lower doses ranging from 25 to 100 μM in each corresponding exposure period. Extending the duration of exposure to 48 hours did not show any significant difference from the corresponding concentration after 24 hours incubation.

Comparison of LDH release levels from GSH-F-Gen0K-MP with free MP based on its total cargo of MP (equimolar concentrations of MP) after 24 and 48 hours incubations are illustrated in Figure 4.16 and Figure 4.17, respectively. The results indicated a significant ($P<0.01$) reduction in LDH release from cells treated with GSH-dendron-MP molecule compared to free drug (MP) in both incubation periods. The maximum reduction was observed in the 100 μM concentration where the percentage of LDH from cells treated with GSH-F-Gen0K-MP dropped to almost 1/3 compared to free MP. However, all the values did not reach the LD_{50} limit.

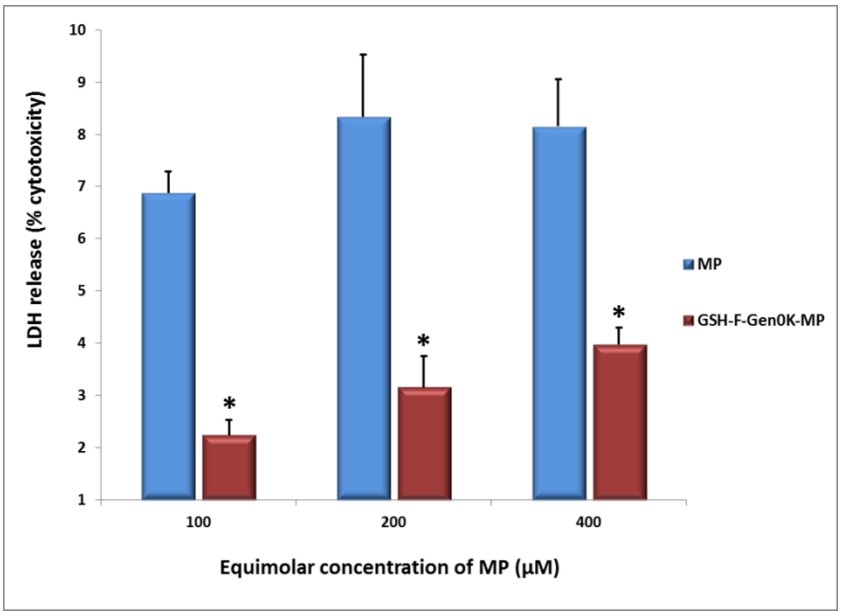

Figure 4.16 LDH release levels of equimolar concentrations of MP and GSH-F-Gen0K-MP after 24 hours exposure. Results are expressed as mean ±SD (*n=4*). The (*) indicates significant difference compared to free MP with P value equal or less than 0.05.

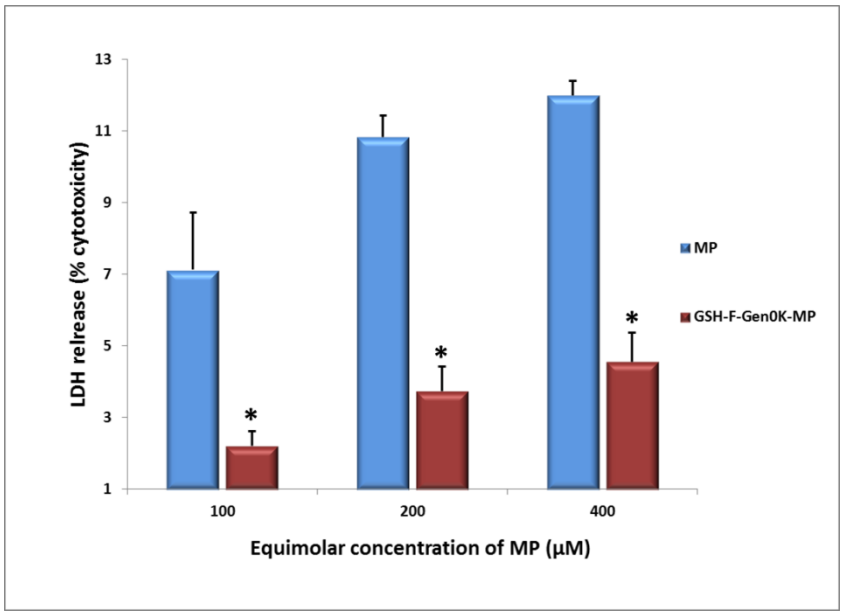

Figure 4.17 LDH release levels of equimolar concentrations of MP and GSH-F-Gen0K-MP after 48 hours exposure. Results are expressed as mean ±SD (*n=6*). Significant drop (P<0.05) in LDH release from cells treated with GSH-F-Gen0K-MP compared to free MP was observed in all tested concentrations (indicated by (*).

4.4.2.2 Toxicity evaluation of GSH-F-Gen0K-MP based on MTT assay

A significant difference (P<0.05) in MTT cell viability results was observed only at higher concentrations of GSH-F-Gen0K-MP (400 and 500 µM) when compared to the control group (untreated). Similar to LDH results, no significant difference was detected after extending the exposure time from 24 hours to 48 hours (Figure 4.18).

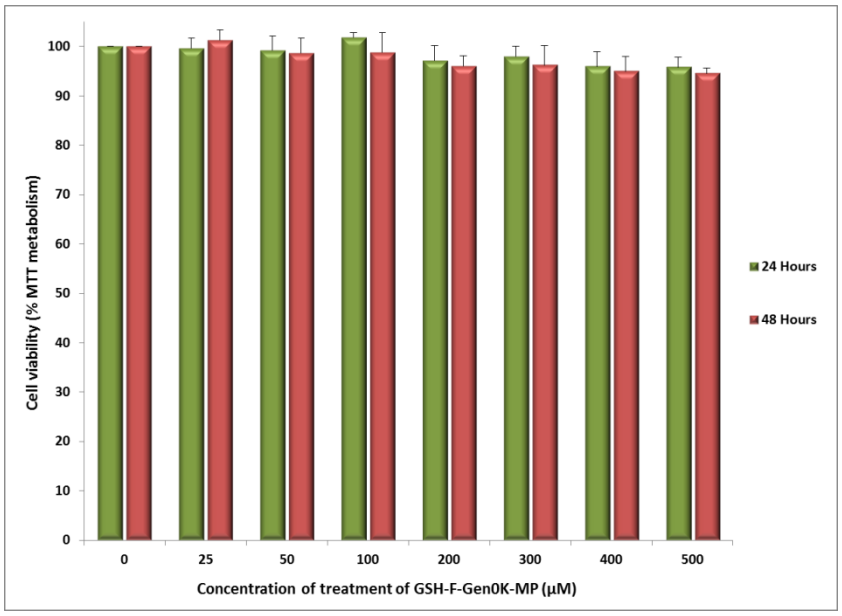

Figure 4.18 MTT cell viability results after 24 and 48 hours exposure to different concentrations of GSH-F-Gen0K dendron. Results are expressed as mean ±SD (*n=4*). The concentration effect on toxicity was only significant (P<0.05) in the 400 and 500 μM concentrations when compared to the control group. Any significant difference in cell viability between 24 and 48 exposure periods was not noticed (P>0.05)

The MTT values of GSH-F-Gen0-MP based on its equimolar contents of MP to free MP after 24 hours exposure are shown in Figure 4.19. The statistical analysis revealed a significant increase (p<0.05) in cell metabolic activity of GSH-F-Gen0-MP compared to free drug only at concentration of 200 μM but no difference was detected at concentration of 100 and 400 μM. However, the cell metabolic activity values for GSH-F-Gen0-MP after 48 hours exposure (Figure 4.20) indicated no significant difference (P>0.05) when compared to free MP at all concentrations tested. The evidence of lack of toxicity of GSH-F-Gen0K-MP within the tested concentration range (25 to 500 μM) obtained from LDH and MTT assays results was backed up by analysing the data obtained from the calcein/ethidium viability-cytotoxicity assay. The test was conducted after 24 hours incubation with 100, 200 and 400 μM of GSH-F-Gen0K-MP (Figure 4.21) using the same procedure detailed in Section 3.3.5. Untreated cells were considered as the positive control. The percentage of viable cells did not drop below 90% in all tested concentrations where it dropped from 97±2.3% for cells treated with 100 μM of GSH-F-Gen0K-MP to 93±3.1% for cell treated with 400 μM (Figure 4.22). These values are much higher than the LD_{50} limit.

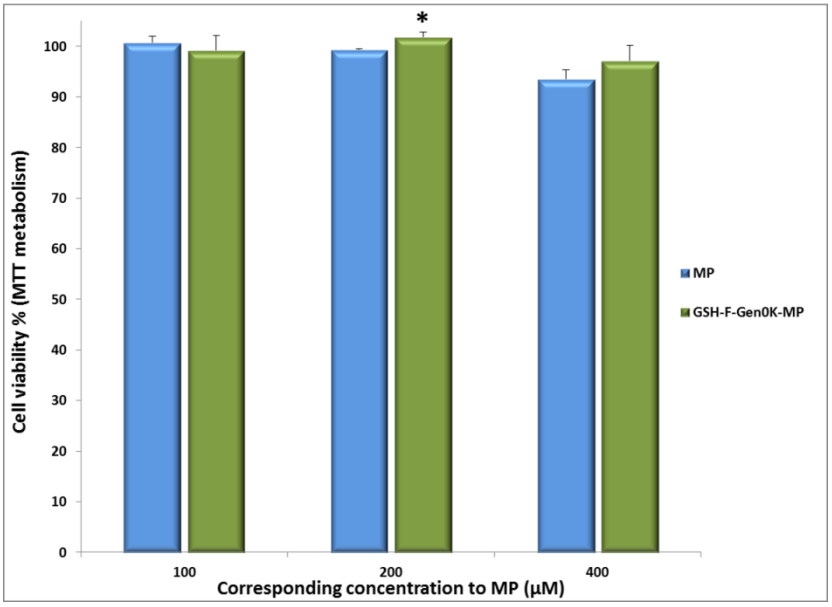

Figure 4.19 MTT cell viability results of equimolar concentrations of free MP and GSH-F-Gen0K-MP after 24 hours. Results are as expressed as mean ±SD (*n=4*). A significant increase (P<0.05) in cell viability was observed in cells treated with 200 μM of GSH-F-Gen0K-MP to its equimolar concentrations of free MP.

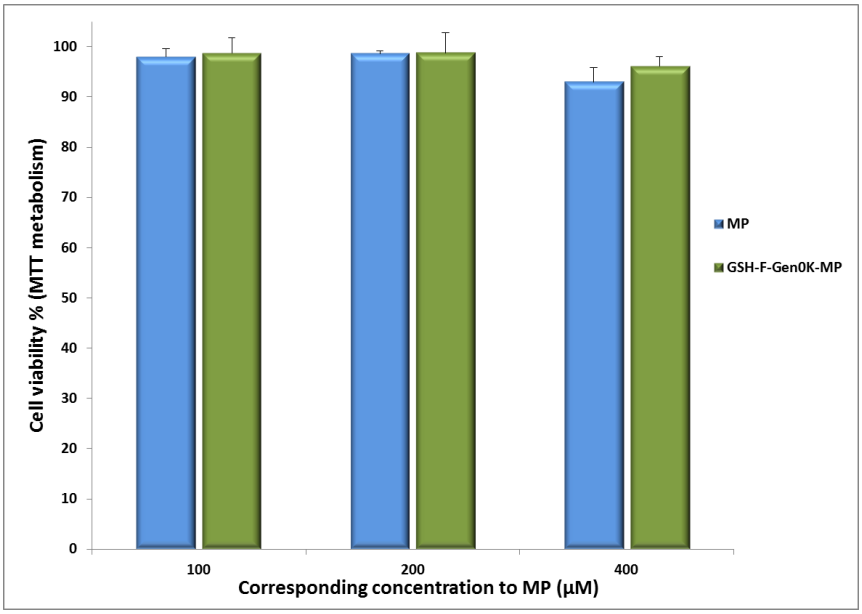

Figure 4.20 MTT cell viability results of equimolar concentrations of free MP and GSH-F-Gen0K-MP after 48 hours. Results are as mean ±SD (*n=4*). No significant change (P>0.05) in cell viability was observed in cells treated with different concentrations of GSH-F-Gen0K-MP with its equimolar concentrations of free MP.

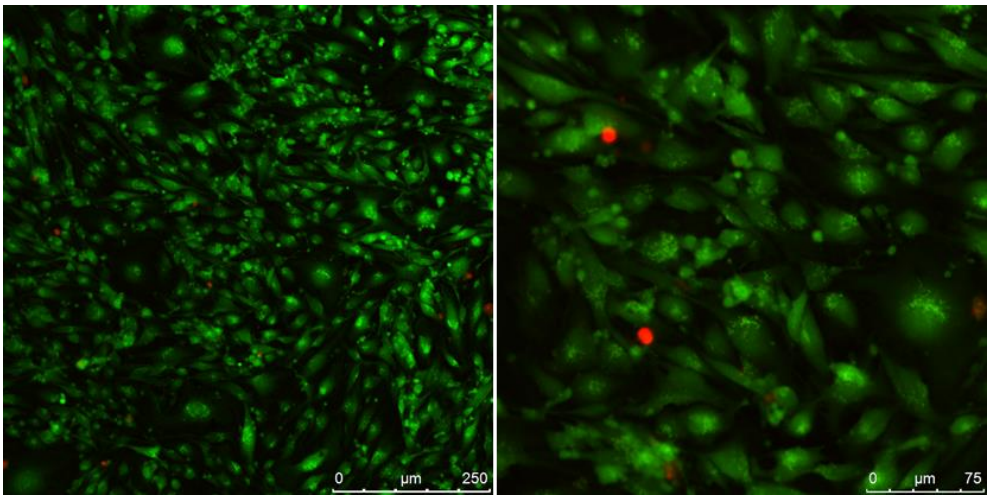

Figure 4.21 Samples of calcein/ethidium viability-cytotoxicity assay flourescent images which reperesnts b.End3 cells treated with 200 µM of GSH-F-Gen0K-MP for 24 hours (left) and its enlarged image (right).

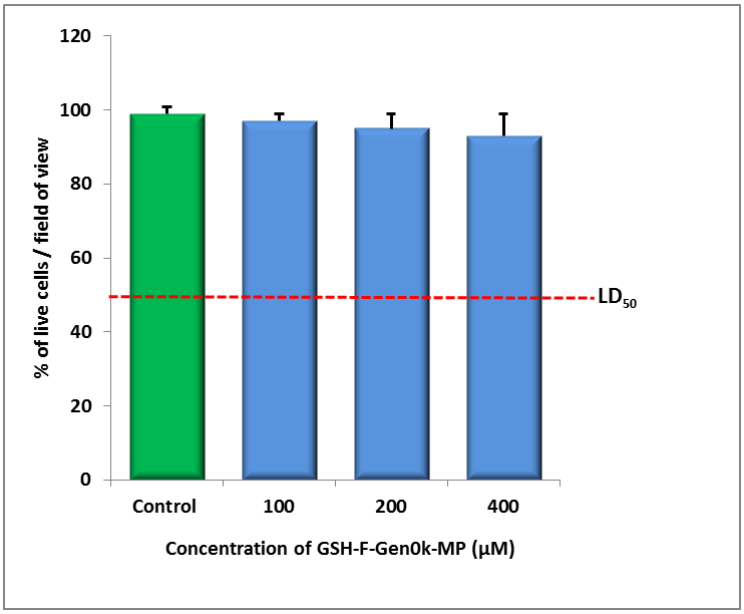

Figure 4.22 Percentage of live b.End3 cells obtained from confocal images of cells treated for 24 hours with different concentrations of GSH-F-Gen0K-MP. Results are expressed as mean ±SD (*n=4*). The green bar represents the negative control (untreated cells). The dotted line represents the LD_{50} limit. No significant difference was observed from the control group with P value equal or less than 0.05.

4.5 Discussion

The concept of using advanced drug delivery technologies to bring both therapeutic advantages and commercial value to health care pharmaceutical products has been widely adopted in the last two decades (Lindqvist *et al.*, 2013).

The discovery and identification of the endogenous BBB-receptor mediated transcytosis systems has led to the development of the molecular "Trojan horse" technology for BBB transport of large MW drugs (Pardridge, 2005a). Transcytosis refers to crossing the BBB *via* certain endogenous endothelial receptors such as insulin, transferrin and GSH (Gaillard, Appeldoorn*, et al.*, 2012). In the transcytosis process, a cell receptor recognises and encloses extracellular material in an invagination of the cell membrane to form a vesicle and that the vesicle carries the enclosed material through the cell and disposes of it outside of its membrane on the other side of brain endothelium.

RMT is rapidly developing as a suitable candidate to synthesise novel drug carrier systems that function in mediating non-invasive blood to brain trafficking by taking advantage of endogenous receptors expressed on the BBB endothelium (Gabathuler, 2010). An endogenous peptide, e.g. GSH or a receptor-specific peptide-mimetic monoclonal antibody that crosses the endothelium *via* a specialised RMT system could theoretically be employed to ferry across the BBB any attached drug (Gaillard, Appeldoorn*, et al.*, 2012).

For drug delivery to the CNS, like delivery to any other tissue, peripheral pharmacokinetics, elimination and biodistribution, including binding to plasma proteins or enzymatic degradation of the drug in blood, are essential factors affecting the overall efficacy of the system (Banks, 2008). Thus, the selection of a suitable drug carrier system, especially of the ligand, can be largely influenced when these requirements are taken into account. Several endogenous ligands that can be recognised by receptors expressed on the surface of BBB endothelial cells have been used to enhance penetration of therapeutic agents to the brain (Georgieva *et al.*, 2014). The most widely studied targeted receptors are insulin receptor, TfR, LDL receptors and more recently GSH receptors. A previous study (Birngruber *et al.*, 2014) indicated the ability of GSH liposomal drug carrier to enhance doxorubicin (anticancer drug) concentration in the brain without affecting the BBB integrity. Another study (Mdzinarishvili *et al.*, 2013) demonstrated that using nanoparticle formulations decorated with GSH can significantly improve the efficacy of neuroprotective drugs (triiodothyronine) in ischemic brain stroke *in vivo*.

In this study, GSH was employed as a ligand to promote the penetration of MP-carrier conjugates through BBB. The choice of GSH offered several advantages: GSH can be found naturally in the CNS and other parts of the body. Therefore, using this endogenous peptide to form conjugates with drugs is deemed to be relatively safe in terms of cytotoxicity (Mytilineou *et al.*, 2002). In addition, GSH is a short peptide consisting of three amino acids (L-glutamine, L-cysteine, and glycine). Hence, it can be easily synthesised using SPPS-based techniques. Moreover, the SPPS technique can be also used to integrate the GSH with the dendrons-drug conjugate as long as these molecules have available carboxyl functional groups. Furthermore, the amide linkage formed between GSH and conjugate can be cleaved easily by glutamates of the brain tissue after the penetration of the BBB thus causing the release of the free active drug (Dringen *et al.*, 2000). Finally, in addition to enhancing penetration to the CNS, GSH by itself can reduce the oxidative stress and inflammation at the BBB and inside the brain, processes associated with many neurodegenerative disorders (Sies, 1999).

The synthesis of GSH-F-Gen0K-MP was performed by SPPS and started by synthesising GSH then continuing the synthesis of the dendron to it and ended by coupling the drug onto the two peripheral amine groups of the lysine amino acid. Separation of the GSH molecule from the conjugate MP by the dendron may help to retain the biological activity of GSH as well as of MP. Thus, dendron not only functioned as a branching unit to load more drug but it may also serve as a spacer (arm) preventing any drug aggregation with consequent loss of their pharmacological actions.

Mass spectrometry gave confirmation of the successful synthesis of the conjugate through comparison of the MW of the synthesised molecule with its theoretical MW value (Figures 4.7-4.9). Comparing the FTIR troughs of GSH-F-Gen0K-MP with free MP and free GSH-F-Gen0K (Figure 4.11) indicated shifting in troughs caused by the increase in amide linkage in GSH-F-Gen0K-MP (7 amide groups) compared to GSH-F-Gen0K (5 amide groups). Moreover, the appearance of the distinctive MP ketone group trough at 1715 cm^{-1} in GSH-F-Gen0K-MP spectrum but not in the GSH-F-Gen0K spectrum (Figure 4.12) provides further evidence of the successful loading of MP to GHS-dendron molecule. The confirmation of the synthesis of GSH-F-Gen0K-MP molecule was supported by the NMR data (Figures 4.13 & 4.14). The spectra of H atoms that are unique in free GSH and free MP were found in the spectra of the final molecule GSH-F-Gen0K-MP. The appearance of a single peak in HPLC spectra of GSH-F-Gen0K-MP (Figure 4.6) after sample purification strongly indicated the purity of the final product.

The successful attachment of MP to the GSH-dendron molecule paves the way for similar therapeutic approaches in addressing several issues. The penetration of MP through the BBB will be governed by the physicochemical properties of the new molecule (GSH-F-Gen0K-MP) rather than MP. Moreover, this DDS (GSH-F-Gen0K) may not only be used for MP, but potentially for other drugs with poor penetration through the BBB as long as they can interact with the peripheral active groups of the dendron to form the amide linkage. Furthermore, the payload of the synthesised molecule will be higher compared to free MP since each GSH-F-Gen0K molecule can carry 2 MP molecules which can potentially be increased if higher generations of dendrons were used.

One of the limitations that appeared in the synthesis process was the relatively low quantity yield of the final molecule (GSH-F-Gen0K-MP) *per* batch which may be caused by incomplete drug incorporation and material loss during the harsh conditions of the cleavage process. Another issue that appeared in the synthesis is the purity of the final molecule after the cleavage process. However, this problem was solved by using HPLC to identify, separate and collect the desired fraction (Figure 4.6) to be used in further experiments.

Combining data from LDH assays, MTT cell viability and calcein/ethidium viability-cytotoxicity tests indicated that the toxicity levels induced by GSH-F-Gen0K-MP at different concentrations ranging from 25 to 500 μM were within the acceptable range and illustrate the safety of GSH-F-Gen0K-MP within the tested concertation range. The toxicity was concentration dependant but not affected by extending the duration of exposure of endothelial cells to GSH-F-Gen0K-MP from 24 to 48 hours. However, the cytotoxicity of F-Gen0K-MP and F-Gen1K-MP was both concentration and time dependant (Chapter 3). Such variation may be attributed to the presence of GSH and internalisation of the GSH-F-Gen0K-MP to the endothelial cells by RMT which was investigated in Chapter 6.

However, the most interesting result was the lowering in the toxicity levels of GSH-F-Gen0K-MP when compared with equimolar concentrations of free MP (Figures 4.16 & 4.17). This reduced toxicity can be attributed to the strong antioxidant activity of GSH against reactive oxygen species which can induce inflammation leading to cellular apoptotic and necrosis. These data are consistent with another study which has showed that using a clinically-approved antioxidant, edaravone, elevated the cell viability and improved TJs of a three dimensional BBB endothelial model (Cho *et al.*, 2015). Another study (Mytilineou *et al.*, 2002) has highlighted that depletion of GSH in the brain causes a cascade of events including

damage to mitochondria, which eventually may result in cell death suggesting that GSH dependent reactions are important for the detoxification of H_2O_2 in the mitochondria.

Finally, following completion of the synthesis and characterisation of dendron-MP conjugates and GSH-dendron-MP molecule as discussed before and proving the safety of these molecules to be used a carriers system for MP within the tested concentration range, quantifying the permeability of these molecules through an *in vitro* BBB compared to free MP can be performed (Chapter 6). However, prior to these penetration studies, the *in vitro* BBB endothelial barrier should be validated to provide a demonstrate that it mimics the *in vivo* barrier permeability properties and is robust enough to be employed in penetration studies of the synthesised molecules (Chapter 5).

4.6 Conclusion

The following conclusions can be high lightened from Chapter 4:

- MP can be successfully integrated into the peripheral groups of the dendron structure functionalised with GSH.
- The toxicity levels of GSH-F-Gen0K-MP were within the range considered acceptable by international standards.
- The toxicity of GSH-F-Gen0K-MP increased at increasing concentration but not with the duration of exposure.
- The toxicity levels of GSH-F-Gen0K-MP were less than its equimolar concentrations of free MP.

Chapter 5. Validation of the *in vitro* BBB model

5.1 Introduction

The BBB is the main obstacle that prevents almost all drugs from entering into the brain to treat CNS disorders. The BBB consists of different types of cells. Among them of particular relevance are the microvascular endothelial cells, an essential part of the neurovascular unit of the brain (Ballabh *et al.*, 2004). These endothelial cells are unique in a number of ways; they possess very low levels of transcellular endocytosis, express specialised ion and peptide transporters on their membranes and form a physical barrier with low permeability between the blood and the brain due to the presence of TJs between adjacent endothelial cells (Fernandes *et al.*, 2010).

Investigations of the BBB's physiological and biological functions have largely fallen into two major types: (i) using *in vivo* perfusion models in animals (Brown *et al.*, 2004) and (ii) *in vitro* BBB cell models using endothelial cells from cerebral microvessels (Abbott *et al.*, 1992). For an *in vitro* BBB cell model to be employed for the transendothelial BBB permeability monitoring of CNS-drug candidates, it must promote reproducible solute permeability and a number of other general criteria (Naik *et al.*, 2012). Such other criteria may include the forming of a restrictive paracellular barrier through TJs; having a physiologically realistic cell architecture; expressing most of the functional key transporter mechanisms present *in vivo*; and allowing easy handling of culture to meet the time and technical requirements of a screening program (Eigenmann *et al.*, 2013).

5.1.1 *In vitro* BBB model

The development of a BBB model that enables a reliable prediction of drug-brain penetration *in vitro* has been a target since the early 1990s (Oller-Salvia *et al.*, 2016). These *in vitro* models offer a number of attractive advantages over other methods (Naik *et al.*, 2012):

- In comparison with animal experimentation, *in vitro* models are relatively inexpensive with a remarkably higher throughput for drug permeability experiments.
- Better control in testing and manipulating the BBB are allowed by the artificial environment of these *in vitro* models without the number of additional variables that must be considered when working with an entire organism.
- They provide highly versatile and manageable physiological environments *in vitro* where cells can be easily manipulated to study the response of a specific tissue/organ to a wide range of physiological and experimental stimuli otherwise hard to reproduce *in vivo*.
- They can be easily developed with any type of cell source (human, animal, or cell line) and to some degree can reproduce *in vitro* pathological abnormalities thus facilitating the study of

BBB dysfunctions in relation to the pathogenesis and progression of neurodegenerative disorders.

However, there are some drawbacks related to the use of any *in vitro* systems including *in vitro* cell-based BBB models. Due to the lack of exposure to physiological factors (whether diffusible from surrounding cells/tissue or dependent upon mechanical and physical stimuli), cells cultured *in vitro* in an artificial environment undergo dedifferentiation (Watanabe *et al.*, 2013). This can affect the deregulation of relevant biological features (e.g., transporters, ligands, enzymes, etc.), which in turn can alter the BBB physiology *in vitro* as well as its response to endogenous and exogenous stimuli. Therefore choosing the most suitable endothelial cell line is a crucial factor to ensure the integrity of the *in vitro* BBB model and to minimise the effect of such drawbacks.

Many immortalised brain endothelial cell lines have been isolated and employed as *in vitro* BBB models (Gumbleton *et al.*, 2001). Among the many immortalised cell lines derived from brain endothelia, b.End3 cells are available from commercial cell banks such as the American Tissue Culture Collection (ATCC) or the European Collection of Cell Cultures (ECACC). This cell line was established using endothelial cells isolated from mouse brain; the BBB characteristics of these cell lines were evaluated by comparing their functions with those of primary brain endothelial cells or the same cell lines grown under different culture conditions (Song *et al.*, 2003)

There are different *in vitro* BBB models that can be used to assess drug penetration. One of the most common and widely used methods involve the culturing of a monolayer of highly specialised brain microvascular endothelial cells on a polymeric membrane system (Naik *et al.*, 2012). These systems (Transwell® inserts) are a specially designed diffusion system composed of a microporous semipermeable membrane that separates the well into a donor compartment and an acceptor compartments (Figure 5.1).

Various sources of brain capillary endothelial cells are grown to reach confluence on the upper (luminal) surface of the membrane immersed in their specific growth media (Eigenmann *et al.*, 2013). The microporous membrane matrix provides a physical surface for the cells to grow which allows nutrient and gas exchange and the passage of different cell-derived materials and exogenous substances but does not permit the movement of cells across the two compartments. This simple BBB model allows high-throughput drug permeability testing and binding affinity measurement (receptor-ligand interaction) (Berezowski *et al.*, 2004).

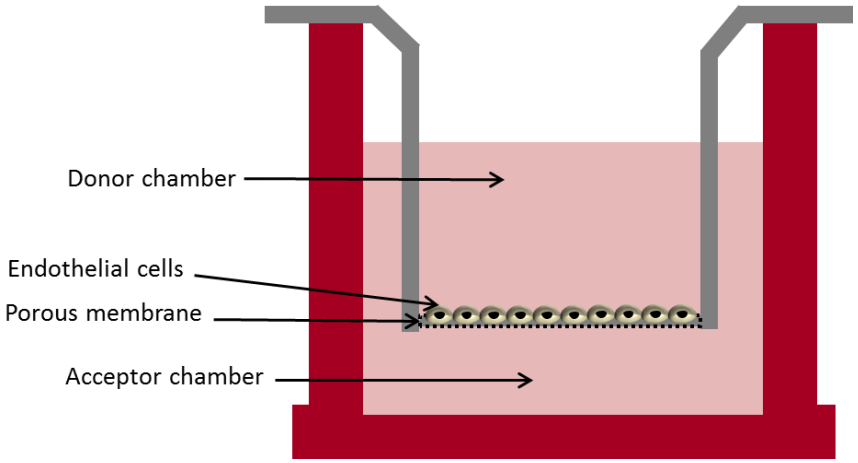

Figure 5.1 A figure representing endothelial cells forming a mono layer on the membrane of a Transwell insert.

Nevertheless, prior to penetration studies of free MP and modified MP through the b.End3 culture model, the paracellular barrier properties formed by this cell line cultured on Transwell inserts must be assessed. Thus, validation tests must be performed to confirm the possibility of employing b.End3 cells as an *in vitro* cell model to proceed with the penetration experiments. These tests may include investigation of the presence of various endogenous carrier-mediated transport systems similar to those expressed within the *in vivo* BBB. In addition, evaluation of the integrity and limitation of the b.End3 cell monolayers with reference to their potential employment in trans-endothelial permeability studies may also be included. Finally, confirming the functional expression of some important select influx and efflux transport systems within the b.End3 cells may be performed (Eigenmann *et al.*, 2013).

In this study, due to its poor penetration through the BBB, MP was integrated into the structure of dendrons (Chapter 2) which were later decorated with GSH (Chapter 4) to form new modified molecules with higher drug load and with a potential to cross the BBB more efficiently. The *in vitro* mono layer was established using b.End3 cells. These cells can express TJs between adjacent cells in *in vitro* models (Ogunshola, 2011). In addition, GSH receptors are expressed on its cell membrane (Gabathuler, 2010). The integrity of the b.End3 cells monolayer grown on Transwell inserts as an *in vitro* BBB model was validated using transepithelial electrical resistance (TEER) measurements in comparison with control cells (HUVEV) which lack this property. Testing the permeability by a predominately penetrating paracellular probe was also performed to assess the *in vitro* model.

A previous study (Omidi *et al.*, 2003) indicated that b.End3 cells monolayers achieved maximal TEER at Day 10 of culturing. The results also confirmed the presence within the b.End3 cells of mRNA transcripts for the different transporters such as GLUT-1, amino acid carriers, nucleoside transporters and the TJ elements such as ZO-1, JAM, occludin, claudin-1 and -5. The study concluded that this cell line can display characteristics that would allow their worthwhile use in studies addressing BBB transport mechanisms. Other study (He *et al.*, 2010) also used TEER measurements plus Western blot technique and fluorescent staining to detect TJs protein expression in these cells. The results indicted high TEER values and elevated expression level of TJ proteins occludin and ZO-1 in these cells. TEER measurements was also used in a later study (Eigenmann *et al.*, 2013) to assess TJs formation in these cells in addition to using two fluorescent marker compounds with low BBB penetration, sodium fluorescein and Lucifer yellow to assess paracellular permeability of these cells.

Aims of the chapter

This chapter aims to:

- Demonstrate that the commercially available cell type, immortalised mouse brain capillary endothelial cell line (b.End3) allows the study of the quantitative aspects of dendron-MP penetration through an *in vitro* BBB model based on these cells.
- Ascertain the culture duration that produces the highest paracellular barrier properties formed by b.End3 cells to be used in further experiments.
- Investigate whether penetration experiments will attenuate the barrier properties formed by b.End3 cells leading to inflated drug penetration values.

5.2 Materials

The materials used in the experimental methods and their supplied companies are detailed in Table 5.1.

Table 5.1 List of materials used in Chapter 5.

Material	Company	Catalogue number
Peroxidase from horseradish lyophilised powder 150U/mg	Sigma-Aldrich UK	7732
3,3',5,5'-Tetramethylbenzidine (TMB) solution	Sigma-Aldrich UK	T-4444
Stop reagent TMB substrate for ELISA	Sigma Aldrich Co. Ltd	S-5814
Support Transwell-Clear 12 well 0.4 μm pore size 12mm membrane diameter	Fisher Scientific	10565482
Ham's F-12K (Kaighn's) Medium	Gibco-UK	21127-022
Endothelial cell growth supplement from bovine neural tissue	Sigma-Aldrich UK	E-2759
Heparin sodium	Fisher BioReagents	10001413
DMEM, high glucose, HEPES, no phenol red	Gibco-UK	21063-029
Formalin solution, neutral buffered, 10%	Sigma-Aldrich UK	HT501128
Phalloidin-tetramethylrhodamine B isothiocyanate	Sigma-Aldrich UK	P1951

5.3 Methods

5.3.1 Human umbilical vein endothelial cells

Human umbilical vein endothelial cells (HUVECs) were used as control for b.End3 cells. Although these primary cells can form TJs when cultured, repeated passages cause these cells to lose this function. These cells were purchased from ATCC® laboratories. HUVECs were routinely cultured in endothelial basal medium (F-12K) containing 0.05 mg/mL of endothelial cell growth supplement, 0.1 mg/mL of heparin adjusted to a final concentration of 10% $^{v}/_{v}$ of FBS according to the manufacturer's recommendations. The cells were incubated at 37°C in a humidified atmosphere (5% CO_2/95% air). The same procedures were used for freezing and storage as b.End3 cell stocks, thawing cells and routine cell culture and passage as described in

Sections 3.3.1.1 to 3.3.1.3 were used for HUVEC cells other than culture media used, which is described in this section.

5.3.2 Preparation of Transwell inserts for TEER measurements

Corning Transwell clear inserts (12 mm diameter and 0.4 μm membrane-pore size) were used to incubate b.End3 cell line (passages 3-6) at a seeding density of 3×10^4 cells/well and HUVEC cells at a seeding density of 3×10^4 cells/well. The quantitative aspects of Transwell inserts were discussed in details in Chapter 6. Cultures were incubated at 37°C in a humidified atmosphere (5% CO_2/95% air) with culturing medium comprising DMEM supplemented with 10% $^{v}/_{v}$ FBS, and antibiotics using 100 units/mL penicillin and 100 μg/mL streptomycin. Culture medium was changed with fresh media every 24 hours. The cells achieved confluency within 2-3 days of seeding. HUVEC and uncultured wells (Transwell inserts plus media) were used as negative control.

5.3.3 Transepithelial electrical resistance

TEER measurements are routinely used as real-time, non-destructive and label-free measurements to characterise monolayer integrity of *in vitro* BBB models in the context of cell monolayer permeability experiments, or to quantify permeability changes, e.g. as a consequence of paracellular permeability enhancers (Jonker-Venter *et al.*, 2006; Masungi *et al.*, 2009). It is a relatively low-cost and suitable method to monitor cell growth on synthetic membranes such as Transwell inserts. TEER measurements were performed by applying a direct current electrical signal across electrodes placed on both sides of b.End3 and HUVEC cellular monolayer and measuring voltage and current to calculate the electrical resistance of the barrier. Higher electrical resistance values indicated stronger barrier functions of the tested cells. The test was performed using an EVOM voltmeter (World Precision Instruments, USA). Prior to each reading the probe was dipped in ethanol then in sterile PBS to ensure sterility. Fresh media was added before each reading (Figure 5.2). The resistance was measured once a day starting from Day 1 to Day 9.

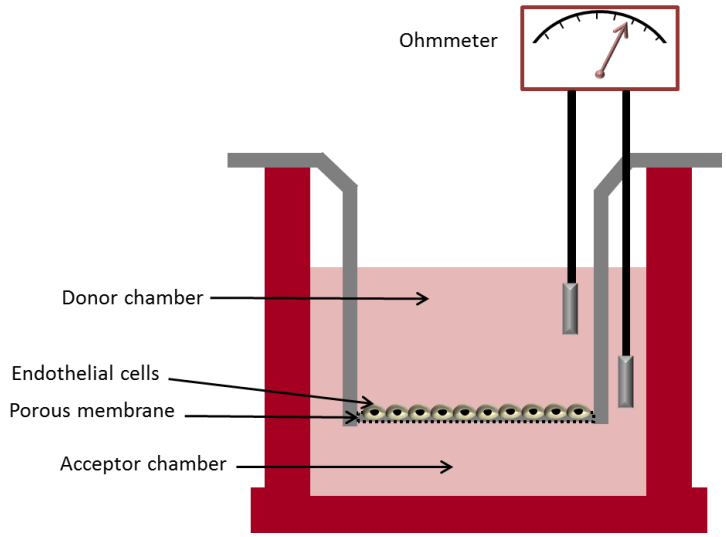

Figure 5.2 Principle of TEER measurements. The probes measure the electrical resistance across the endothelial cells mono layer.

5.3.4 Horseradish peroxidase permeability assay

The permeability of b.End3 monolayers to a paracellular probe was assessed using horseradish peroxidase (HRP). HRP can be isolated from horseradish roots (*Amoracia rusticana*) and belongs to the ferroprotoporphyrin group of peroxidases. HRP is a glycoprotein with 6 lysine residues and it is water soluble and can cross paracellular spaces. However, formation of TJs between monolayer b.End3 cells will dramatically reduce its penetration from the donor to the acceptor chamber of Transwell inserts hence giving an indication of the restrictive barrier features of the b.End3 monolayer barrier. It produces a coloured, fluorimetric or luminescent derivative when incubated with a proper substrate, allowing it to be detected and quantified. One of HRP substrates is 3,3',5,5'-tetramethylbenzidine (TMB) which forms a soluble blue end product that may be read at 370 nm or 655 nm. The TMB reaction may be stopped with 0.5 M H_2SO_4, resulting in a yellow colour, and read at 450 nm (Veitch, 2004).

$$\underset{\text{(colourless)}}{TMB_{reduced}} + H_2O_2 \xrightarrow{Horseradish\ peroxidase} \underset{\text{(blue)}}{TMB_{oxidised}} + 2H_2O$$

To perform this assay, Transwell inserts were cultured with b.End3 cells using the same procedure illustrated in Section 5.3.4. The experiment was undertaken at Day 7 of culturing. Thirty minutes prior to the start of the experiment, HRP was dissolved in phenol red-free DMEM at 50 ng/mL. Transport of the probe (HRP) from the donor to acceptor direction across the b.End3 monolayers was initiated by replacing the culture media in the donor chamber with media containing 50 ng/mL of HRP; the acceptor chamber was filled with phenol red-free DMEM making sure that the level of medium was equal in both chambers of

the inserts. Fifty μL of samples were collected from the acceptor chamber after 1 hour of samples introduction into the donor chamber.

The experiment was also performed with wells cultured with HUVEC cells (positive control) and cell-free Transwell inserts (negative control). The standard curve of HRP was established by taking 100 μL of different concentration standards (4, 8, 16, 32, 64 ng/mL) which were prepared from a 100 ng/mL stock solution of HRP in experimental medium. One hundred μL from each sample was transferred to a 96-well plate and 100 μL of TMB solution was added to each well and incubated at room temperature for 30 minutes yielding a blue solution. The reaction was stopped by adding 100 μL of 0.5 M H_2SO_4 stop solution, resulting in a yellow colour solution, and read at 450 nm using a spectrophotometer (Thermo Multiskan Ascent 354). The assay blank for the test is the value obtained for the 0 μg/mL HRP standard. Correction for the background was made by subtracting the value of this assay blank from all readings.

HRP penetration across b.End3 cells, HUVEC cells, and cell-free Transwell inserts (polyester membrane only) were calculated according to the following equation (He *et al.*, 2010):

$$P_{HRP}\% = (C_{HRP\ acceptor} \times V_{acceptor}) / (C_{HRP\ donor} \times V_{donor}) \times 100\%$$

Where

$P_{HRP}\%$ is the permeability percent of HRP

$C_{HRP\ acceptor}$ is the concentration of HRP in acceptor compartment

$V_{acceptor}$ is the volume of the media in the acceptor compartment

$C_{HRP\ donor}$ is the concentration of HRP in donor compartment

V_{donor} is the volume of the media in the donor compartment

To measure the permeability coefficient of HRP across the b.End3 layer, 50 μL samples were collected from the acceptor chamber after 30 and 60 minutes of samples introduction to the inserts. The permeability coefficient of b.End3 cells to HRP was measured at Day 1, 3, 5, 7, 9 of culturing using the following equation (Omidi *et al.*, 2003):

$$\frac{dm}{dt} = \rho \times A \times C_{\circ}$$

Where:

dm/dt is the rate of change in cumulative mass of HRP transferred to the acceptor chamber

ρ is the permeability coefficient of HRP via the b.End3 cells monolayer

A is the surface area of Transwell membrane (1.03 cm^2)

$C_\circ$ is the initial HRP in the donor chamber assumed to remain essentially constant (i.e. <5% loss) throughout the experiment.

5.3.5 Phalloidin-rhodamine staining of b.End3 cells and HUVEC cells

At Day 7 of culturing, b.End3 and HUVEC cells cultured on 24-well plates was stained with phalloidin-rhodamine. Phalloidin is a fungal toxin isolated from the poisonous mushroom *Amanita phalloides* (Walton *et al.*, 2010). It acts on alpha actin filament leading to muscle paralysis thus identifying cellular spreading and adhesion. Rhodamine is a fluorescent probe with $\lambda_{excitation}$ of 390 nm and $\lambda_{emission}$ of 472 nm that can be attached to phalloidin to be detected by confocal microscopy. The process of staining involved removal of the culture medium from the cells and two washes with PBS. The cells were then fixed by adding 100 μL of 3.7% $^{v}/_{v}$ formalin to each well and left to incubate for 30 minutes. Following fixation, the cells were washed twice with PBS and 100 μL of phalloidin-rhodamine solution was added to each well and incubated further for 1 hour. The cells were washed again with PBS before being imaged using a Leica TCS SP5 confocal laser scanning microscope system using an argon/visible laser (488 nm, 25%).

5.3.6 Effect of MP and dendron-MP conjugates on monolayer integrity

Complementary to TEER measurements, the effect of MP, F-Gen0K-MP, F-Gen1K-MP and GHS-F-Gen0K-MP on the b.End3 monolayer barrier was investigated to eliminate any effects when performing the penetration studies. At the highest time-point peak of TEER values, 100 μM of MP, F-Gen0K-MP, F-Gen1K-MP and GHS-F-Gen0K-MP were introduced in the donor compartment in separated Transwell wells using untreated inserts as positive control. TEER values were measured after 1 hour and 24 hours post sample introduction to assess short and long term exposure to these molecules on the b.End3 barrier.

5.3.7 Transwell insert reuse protocol

The Transwell inserts used to incubate b.End3 cells can be reused again to minimise the cost of the study. However, it is essential to ensure that these previously used inserts will not interfere with the results of subsequent experiments. To achieve this goal, the Transwell inserts were washed as detailed below and then assessed by comparing its barrier functions with new inserts using TEER results. Moreover, the inserts were reused only twice in order to avoid potential reduction in the integrity of the polyester barrier of the inserts. The washing process started after finishing the laboratory experiments on the inserts by removing the culture medium from both chambers. Following washing 3 times with sterilised water, 0.5 mL of trypsin 0.05% $^{w}/_{v}$ EDTA was added to each insert and incubated for 10 minutes to detach all cells from the membrane surface. After incubation, the inserts were shaken by hand for 30

seconds and washed 3 times with sterilised water. To remove any non-detached cells, 100 μL of triton-X surfactant was added to each insert and left for 1 hour to cause cell lysis. The lysis solution was removed, and the inserts were washed 3 times with sterilised water to remove any traces of triton-X or cells debris. Complete removal of cells and its debris from the polyester membrane was confirmed by examining the inserts under light microscope. Finally, the inserts were dipped in 70% ethanol for 1 minute and returned to its plate and allowed to dry in a tissue culture hood overnight under ultraviolet light to sterile the inserts.

5.3.8 Statistical analysis

All experimental data are expressed as mean ±SD (*n=6*). Statistical analysis was performed using one way analysis of variance (ANOVA) with Tukey's *post-hoc* test, using the Minitab®-17 (version 17.2.1) statistical analysis program with a significance level set at $P<0.05$ (two-sided confidence intervals).

5.4 Results

5.4.1 Bioelectric assessments of b.End3 cells cultured on Transwell insert

TEER results of b.End3 cells indicated a steady increase in resistance values which peaked at Day 7 of culturing. The b.End3 cells cultured on Transwell inserts gave the highest reproducible TEER averaging reading of 147 Ω.cm^2 at Day 7, compared to highest reading of 77 Ω.cm^2 for HUVEC cells at Day 8. The control group (inserts without cells) averaged between 28 to 31 Ω.cm^2 throughout the experiment period. Following Day 7, the TEER values of b.End3 cells reached a plateau with slight not significantly different values of 142 and 139 Ω.cm^2 found at Day 8 and 9 (Figure 5.3).

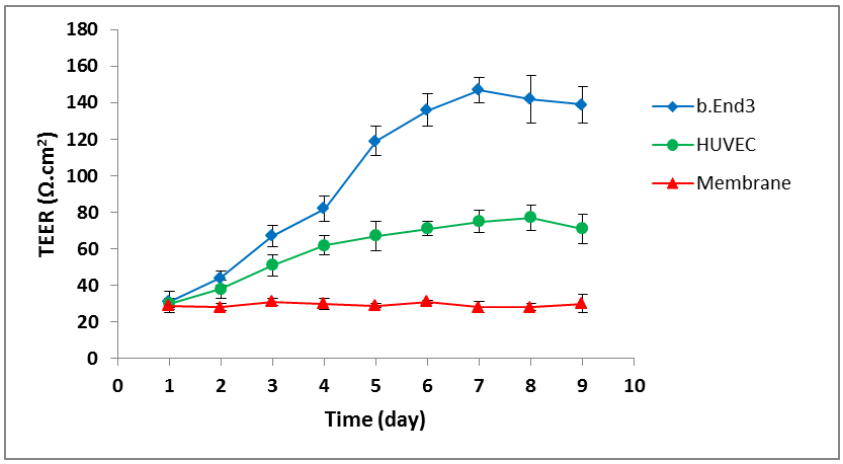

Figure 5.3 Development of TEER of b.End3 cells cultured on Transwell inserts over time. Values are expressed as mean ± SD (*n=6*). TEER values of b.End3 cells at Day 7 of culturing were significantly higher (P<0.01) in comparison with HUVEC cells at Day 8 and the negative controls providing an indication for the formation of TJs between b.End3 cells.

5.4.2 Permeability assessments of HRP across the *in vitro* model

The values obtained from the appropriate HRP standards after background subtraction were used to plot a standard curve of HRP concentration versus the absorbance (Figure 5.4).

Endothelial paracellular barrier function of b.End3 cells was evaluated by measuring the HRP permeability percentage 60 minutes after the introduction of HRP to the donor compartment and comparing it with HUVEC cells and cell free support (membrane only) values at Day 7 of the culturing (Figure 5.5). The b.End3 monolayer model displayed a significant barrier function to solute transport as evidenced by the decreased HRP permeability compared to the permeability of the supporting Transwell membrane alone (P<0.01) and HUVEC cells (P<0.05).

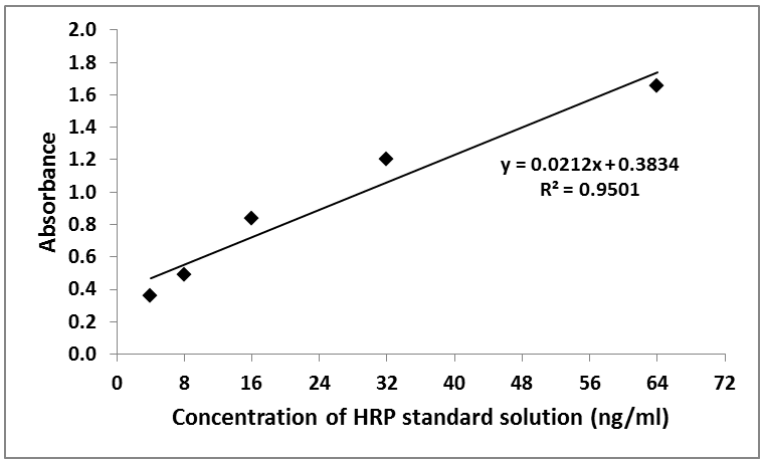

Figure 5.4 Standard curve of HRP (*n=4*). The x axis represents the concentration of standard solutions of HRP used (4, 8, 16, 32, 64 ng/mL) and the y axis represents the corresponding absorbance.

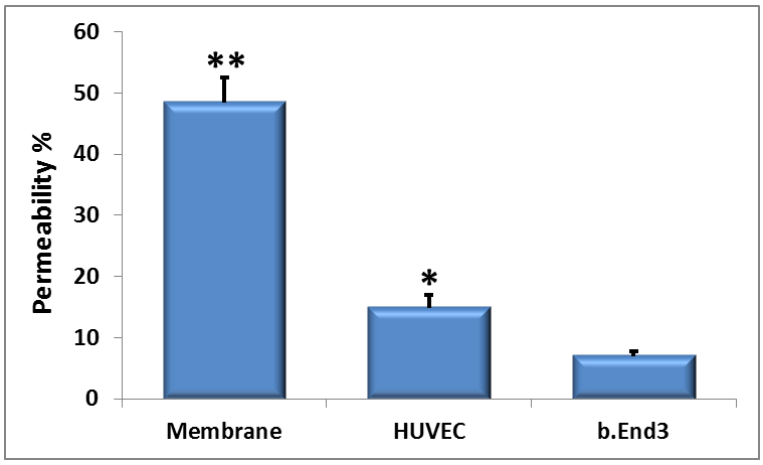

Figure 5.5 Paracellular barrier properties of b.End3 cells, HUVEC cells and cell-free Transwell inserts (membrane only). The permeability was calculated by measuring the amounts of HRP that passed through cell layers to the acceptor chamber after 60 minutes using TMB as a substrate for the enzyme. Values are expressed as mean ± SD (*n=6*). The (*) represents a significant difference from b.End3 cells with $P<0.05$ and $P<0.01$ for the (**).

The permeability coefficient of b.End3 decreased steadily starting from Day 1 of culturing to reach its lowest value of 18.7×10^{-6} cm.s^{-1} at Day 7 indicating the highest paracellular barrier function of the cells to the HRP (Figure 5.6). These results are consistent with the TEER values which indicated the highest resistance at Day 7 (Figure 5.3).

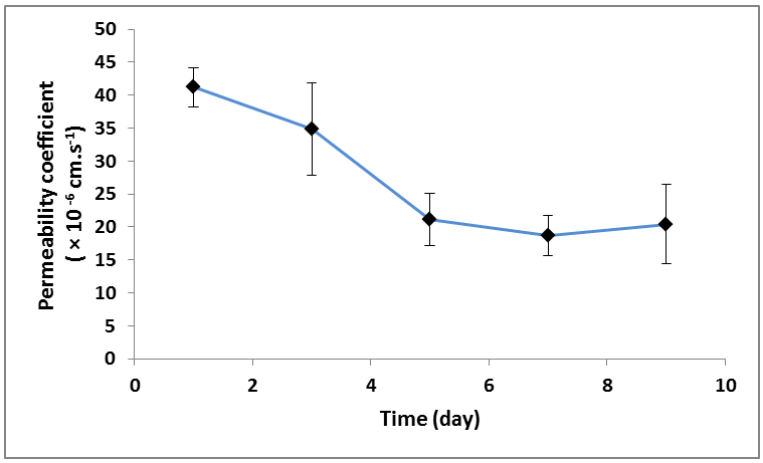

Figure 5.6 Permeability coefficients of b.End3 cells to the paracellular probe, HRP. Values are expressed as mean ± SD (*n=6*). The lowest value was measured at Day 7 of culturing dropping to 18.7×10^{-6} cm.s^{-1}.

TEER experiments were also performed on monolayer b.End3 cells treated with different MP and dendron-drug conjugates (F-Gen0K-MP, F-Gen1K-MP and GHS-F-Gen0K-MP) to eliminate false-positive penetration values caused by a reduction in the cell barrier integrity due to treatment with the tested molecules (Figure 5.7). The data did not indicate any significant difference (P>0.05) in TEER readings of wells treated with MP, F-Gen0K-MP, F-Gen1K-MP and GHS-F-Gen0K-MP molecules when compared to the positive control group (treatment-free b.End3-cultured inserts) in both exposure periods (1 and 24 hours).

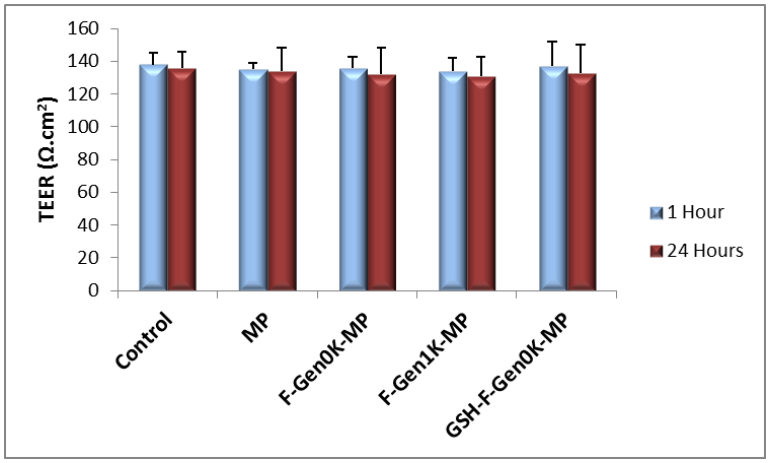

Figure 5.7 TEER readings after treatment with the drug-conjugates. TEER was measured in wells treated with 100 μM of MP, F-Gen0K-MP, F-Gen1K-MP and GHS-F-Gen0K-MP molecules using untreated wells as control. Values are expressed as mean ±SD (*n=6*) of impedance values. The experiment was conducted after 1 and 24 hours of exposure to the MP/dendron-MP molecules in the donor compartment.

5.4.3 Fluorescent staining of b.End3 and HUVEC cells

Confluent b.End3 cells fluorescent imaging (Figure 5.8.a) indicated the formation of a confluent monolayer with no intercellular gaps. However, florescent imaging of HUVEC cells

(Figure 5.7.b) indicated less cellular adhesion with wide paracellular spaces compared to b.End3 cells. These results suggested the ability of b.End3 cells to form a confluent monolayer due to the formation of TJs between the cells.

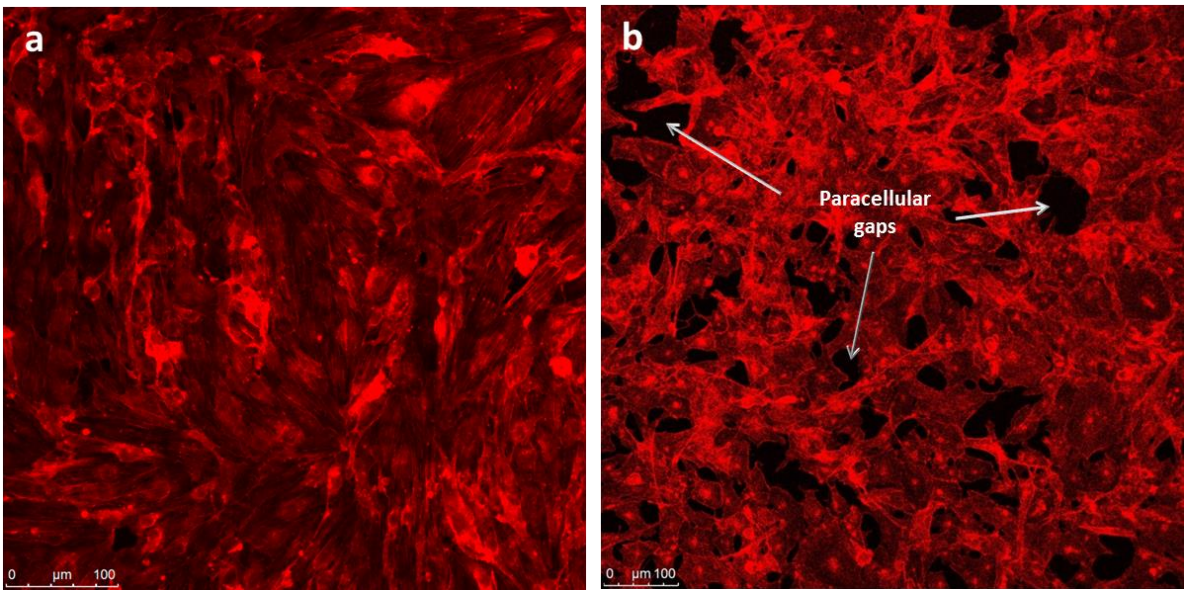

Figure 5.8 Confocal florescent imaging of 100% confluent b.End3 and HUVEC cells stained by phalloidin-rhodamine. (a) B.End3 cells showing minimal gaps between neighbouring cells. (b) HUVEC cells showing large and distinct gaps between adjacent cells.

5.4.4 Comparison of TEER measurements between new and reused inserts

To illustrate any changes in the TEER measurements caused by reusing Transwell inserts, new and reused inserts were seeded with 3×10^4 b.End3 cells/well and allowed to reach confluence. TEER was measured from Day 1 to Day 9 in both plates. No difference in TEER measurements was found between new and pre-used inserts (Figure 5.9).

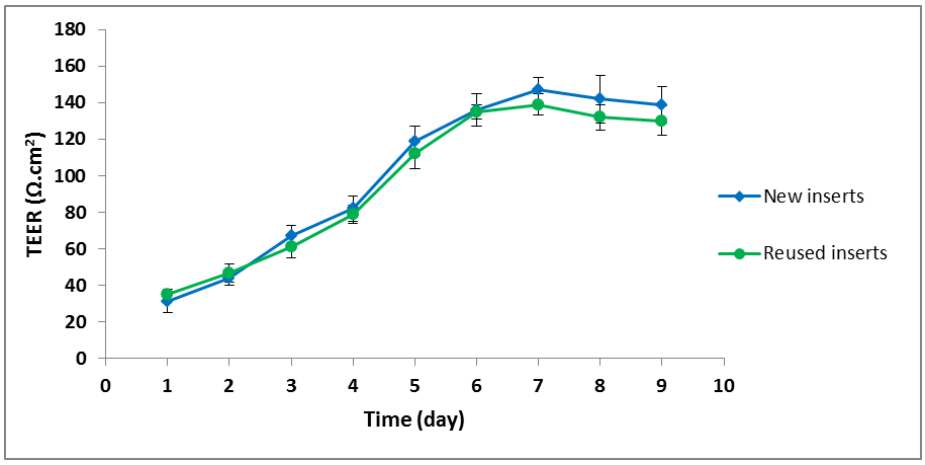

Figure 5.9 Comparison of TEER readings between new and reused inserts. Values represent are expressed as mean ±SD (*n=6*) of the impedance values starting from Day 1 to Day 9 of culturing. The values were insignificant (P>0.05) between time points.

5.5 Discussion

With increasing emphasis on candidate drug molecules for the efficient delivery to the CNS, quantitative experiments of BBB penetration represents an essential part of their therapeutic potential. To meet this purpose, a wide range of *in silico*, *in vitro* and *in vivo* BBB models for prediction of brain permeability of compounds in early stages have been developed and established (Nicolazzo *et al.*, 2006). Although, computational BBB models and non-biological (using artificial barriers) models provide high-throughput screening of drug discovery at early stages, these approaches are only able to predict passive permeation (Bickel, 2005; Di *et al.*, 2009). On the other hand, *in vivo* BBB models such as *in situ* brain perfusion offer high-quality data and the most reliable measurements of BBB drug penetration (Abbott, 2004).

However, such *in vivo* models are expensive in terms of resources and time and, therefore, only suitable for testing of drugs at more advanced stages of development (Cecchelli *et al.*, 2007). Cell-based *in vitro* BBB models using primary cells or immortalised brain capillary endothelial cells of human or animal origin cultured on microporous filter polyester membranes of Transwell systems may fill the gap between *in silico* and *in vivo* methods. They have been employed to assess BBB permeability *in vitro* for a long time, and their simple design enables cost-efficient and high-throughput screening at the same time (Cecchelli *et al.*, 2007; Naik *et al.*, 2012; Ogunshola, 2011). Nevertheless*, in vitro* biological models must possess several features to evaluate the permeability of this barrier to new drugs, xenobiotics and molecules such as those developed in this thesis (Kerns, 2001).

One of the key features of a cell culture system to be employed as an *in vitro* BBB model is the experimental design and whether it is qualitative or quantitative. Another essential tool for the investigation of endogenous solute or drug transport through such a BBB model is the choice of well-characterised cell line which is relevant to that study. Thus, for an *in vitro* model to be useful it must recapitulate a number of *in vivo* BBB characteristics. The chosen cell line should include expression of specific endothelial cell markers and transporter proteins similar to those found in *in vivo* cells and should form monolayers with low paracellular permeability to soluble probes and high TEER values, indicating the presence of TJs (Abbott *et al.*, 1992). TJs between adjacent endothelial cells facilitate the formation of a very efficient and selective barrier (limited paracellular diffusion) (Watanabe *et al.*, 2013). As a functional parameter, TEER measurement of endothelial monolayers is widely used for the functional analysis of TJs (Nagumo *et al.*, 2008). Molecularly, the expression and function of TJ protein, occludin is the most crucial structural factor for TEER changes (Hombach *et al.*, 2008). One of the major

requirements that an *in vitro* BBB model should meet is enabling the expression of inter-endothelial junctions (Eigenmann *et al.*, 2013).

In this study, for the evaluation of b.End3 cell monolayers for transendothelial permeability investigations, TEER was assessed across b.End3 cell monolayers and compared to HUVEC cells. One of the main characteristics of HUVEC cells is that these endothelial cells rapidly lose many of their endothelial characteristics as soon as they are cultured *in vitro*. This de-differentiation is primarily caused by the lack of TJs formation between adjacent HUVEC cells and the absence of the specific microenvironment that is essential for endothelial phenotypic features (Cleaver *et al.*, 2003). Therefore, HUVEC do not hold the specific barrier properties found in highly impermeable endothelial microvascular beds like the BBB endothelial cells. As a result, even when cultured as a tight monolayer culture on Transwell inserts, these cells display intercellular gaps and discontinuous junction strands (Beese *et al.*, 2010) which in this study was confirmed by fluorescent staining images (Figure 5.8.b). However, b.End3 cells exhibited much more uniform monolayer and showed minimal gaps between cells (Figure 5.8.a)

The b.End3 cell monolayer showed a statistically significant increase in TEER values compared to HUVEC cells and cell-free inserts with peak TEER numbers measured at 147 $\Omega.cm^2$ at Day 7 of culturing (Figure 5.3). These data are consistent with other studies. In 2003, using TEER measurements, a study indicated that b.End3 cells display characteristics that would allow their use in quantitative studies addressing BBB transport (Omidi *et al.*, 2003). A later study (He *et al.*, 2010) also indicated a steady increase in TEER values with extending culture time to reach its highest peak at Day 10 rather than Day 7 as in this study. This variation in the day of the highest TEER value might be attributed to differences in the number of passages of the cells (Brown *et al.*, 2007), type of the culture medium used (Brown *et al.*, 2007) and the material type of the Transwell inserts used and its pore size which have a significant impact on barrier tightness (Eigenmann *et al.*, 2013). Optimising the b.End3 *in vitro* model based on these variables (passage number, culture medium and supplier and Transwells type) is a crucial factor for starting the penetration experiments. This optimisation includes determining the exact day of culturing at which the b.End3 cells exhibit the highest paracellular barrier to be used for quantitative-permeability experiments.

Establishing the protocol for Transwell inserts-reuse was an important step and additional finding of this work as it allows reducing the cost of these inserts (UK £ 250-300 per set).

However, prior to applying previously used and washed Transwell inserts, it is crucial to confirm that these pre-used inserts will not give results different from those obtained with new inserts. Reusing Transwell inserts was cost effective and did not impose any significant alteration of cell behaviour as shown by comparison with the TEER results of new inserts (Figure 5.9). Bearing in mind, the inserts were only reused twice to be completely sure of avoiding any bias in the results and were utilised only for TEER measurements rather than penetration studies where only new inserts were used (Chapter 6).

Measurement of TEER alone is not always enough to predict the restrictiveness of the b.End3 paracellular pathway to solute transport. Therefore, determination of the permeability of the *in vitro* b.End3 BBB model to a paracellular soluble probe was also performed. Paracellular solute permeability evaluation was performed using HRP to determine paracellular diffusion across confluent b.End3 monolayer cells. It can only pass through cells monolayers by simple diffusion through extracellular spaces. HRP is a relatively impermeable marker of the BBB due to its size (about 44,000 Da MW) and thus, it will not passively diffuse through TJs between b.End3 cells. Unlike endogenous brain ligands such as GSH, HRP cannot enter the b.End3 cells by specialised endogenous carriers. The permeability percentage of HRP across a b.End3 cell monolayer was almost equal to half of the value obtained from HUVEC cells and about one third of the uncultured Transwell membrane ($P<0.05$ and $P<0.01$, respectively) confirming the suitability of b.End3 for *in vitro* BBB model (Figure 5.5).

These data are in agreement with other studies which indicated low values of permeability coefficient based on paracellular transport of sodium fluorescein with b.End3 cells (Watanabe *et al.*, 2013). Another study investigated the b.End3 monolayer cell model barrier function to a paracellular probe (radio-labelled sucrose) and to a transcellular probe (radio-labelled propranolol) compared to the permeability of the supporting Transwell membrane alone (Omidi *et al.*, 2003). The study was conducted using dual labelled probes (sucrose/propranolol) to reflect permeability across the exact same set of Transwell monolayer cultures. All of the monolayer models displayed in that study, including the b.End3 cell line, exhibited a barrier function to solute transport as confirmed by decreased permeability compared to the permeability of the supporting polyester membrane alone as found in this study.

Previous studies (Brown *et al.*, 2007; Eigenmann *et al.*, 2013; Watanabe *et al.*, 2013) have indicated that the b.End3 cell line expressed a higher level of different types of TJ proteins,

especially claudin-5, occludin and ZOs (ZO-1 and ZO-2) compared to other endothelial cell lines. A further study suggested that the main TJ protein responsible for the paracellular barrier function is claudin-5, and b.End3 cells showed marked distribution and expression of this protein along the intercellular junctions (Honda *et al.*, 2006). These proteins can potentiate the restrictive barrier properties of adjacent b.End3 cells and thereby reduce the penetration of HRP through the endothelial monolayer.

The combination of the data obtained from TEER measurements (Figure 5.4) and paracellular probe (HRP) permeability results (Figures 5.4 & 5.5) indicated that b.End3 cell line can establish a potent paracellular barrier property. These results were supported by previous studies which showed the ability of these cells to exhibit different types of TJs proteins as well as several membrane transport systems (Omidi *et al.*, 2003).

All these data suggest that these cells have the ability to form an *in vitro* barrier that can mimic the *in vivo* BBB to a certain extent. Thus these cells are an attractive candidate to be used an *in vitro* BBB model due to their rapid growth, retaining of BBB characteristics over repeated passages, formation of functional barriers and suitability to several tests including drug molecules uptake and permeability. The highest paracellular barrier function of the b.End3 cells was at Day 7 as indicted by highest peak of TEER measurements for b.End3 cells (Figure 5.3) which was also confirmed by the lowest permeability coefficient value of b.End3 to paracellular HRP probe as shown in Figure 5.6. Finally, these findings can be employed for quantitative determination of the penetration of the synthesised dendron-drug conjugates which will be discussed in Chapter 6. Any enhancement in the permeability of modified MP revealed later by penetration experiments will reflect a physiologically-reflective condition rather than a simple diffusion of the tested material across intercellular spaces.

5.6 Conclusion

Based on the data collected from experimental studies in this chapter it can be concluded that:

- The *in vitro* BBB model of b.End3 cells shows high paracellular barrier function by the formation of TJs between adjacent cells.
- The cells will exert their maximum barrier function at Day 7 of culturing which is the most suitable time to perform penetration experiments (Chapter 6).
- The validated b.End3 model can be used to assess the ability of the candidate molecules synthesised in Chapter 2 and 4 to cross the BBB.

Chapter 6. Permeability of synthesised molecules across the *in vitro* BBB

6.1 Introduction

The treatment of MS acute relapses by MP has so far proven to be challenging since most of the administrated dose of the drug cannot reach the target tissue (the brain) due to the BBB protective role. This necessitates the use of high doses of MP (reaching 1000 mg *per* day) which are usually accompanied by many adverse effects (see Section 1.4.3) (Jongen *et al.*, 2016). For the purpose of improving MP permeability across the BBB, the work of this project led to the incorporation of the drug in a dendron-based DDS with and without decoration with GSH. The assembled DDS toxicity levels were within the acceptable range. The assessment of the potential of such DDS to permeate the BBB is a crucial factor that will ultimately determine the therapeutic efficiency of such carriers. *In vitro* BBB model based on b.End3 cells was deemed useful as screening tools (Chapter 5) which can be used to assess the synthesised molecules (F-Gen0K-MP, F-Gen1K-MP, and GSH-F-Gen0K-MP) permeability.

6.1.1 DDSs targeting the brain

To overcome the BBB obstacle which hurdle the delivery of most therapeutic agents to the CNS, several approaches have been developed. Current divisions of CNS drug delivery approaches are defined in Figure 6.1. Based on the method of drug entry into the CNS, these methods can be divided into two broad categories of non-invasive and invasive drug delivery methods (Kabanov *et al.*, 2004). Unlike invasive treatments which require hospitalisation, risky (as they often require surgery) (Rogawski, 2009) and can be unrealistic in the treatment for chronic CNS disorders requiring long-term intervention, such as neurodegenerative disorders (Craft *et al.*, 2012), non-invasive drug delivery strategies offers a promising solutions to improve drug penetration through the BBB .

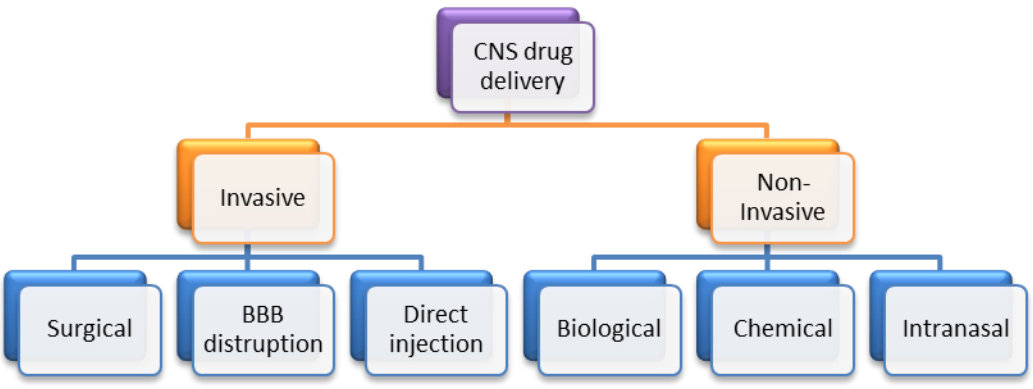

Figure 6.1 Different CNS drug delivery strategies based on the method of penetration.

Three main non-invasive strategies of drug delivery to the brain include chemical modification, which uses structural modification of the drug or prodrug synthesis to enhance

transport through the BBB (Peura *et al.*, 2011), intranasal drug delivery, which bypasses the BBB, taking advantage of the direct pathway to the CNS through the olfactory epithelium (Craft *et al.*, 2012) and biological drug delivery, which uses specialised carriers designs to transport a therapeutic into the CNS (Vlieghe *et al.*, 2013).

One of the promising strategies to deliver drugs to the CNS is by utilising endogenous endothelial receptors via RMT. The presence of insulin in the brain with the absence of insulin mRNA in the brain had led to the discovery of RMT through the BBB (Coker *et al.*, 1990). Therefore, insulin in the brain is of peripheral origin and derived from the blood. Insulin in the blood is transported across the human BBB *via* RMT on the endogenous BBB insulin receptor (Pardridge *et al.*, 1985). RMT utilises the vesicular trafficking machinery of the endothelium to transport substrates between blood and brain. If appropriately targeted, this pathway can also be used to shuttle a wide range of therapeutics into the brain in a non-invasive way (Jones *et al.*, 2007).

Although MP is widely used in neurodegenerative diseases, the knowledge of its pharmacokinetics in the brain and pathways of its penetration across the BBB are still limited. A previous study (Chen *et al.*, 1996) used a vascular brain perfusion technique in Guinea pigs, combined with a capillary depletion method, to determine brain uptake and transport of MP at the BBB. The study concluded that MP first binds to the brain capillaries and then crosses the BBB at a low rate, most likely by using a saturable mechanism that may involve a cytoplasmic endothelial GR. Therefore, it is essential to incorporate MP into specialised carrier systems to improve its permeability across the BBB.

Dendrimers (the carrier system) possess the ability to enhance the permeability of therapeutics across various cell membranes or biological barriers such as the BBB through an endocytosis-mediated cellular internalisation. The modulation of TJ proteins such as occludin and actin is one of the main factors for such enhancement in the intracellular uptake. However, the extent of such an event is dependent on the concentration of the dendrimer used, dendrimer generation and its surface charge (Sadekar *et al.*, 2012). A previous study indicated that the employment of dendrimers carriers suitable for CNS delivery of therapeutics involves 3 steps. First, dendrimers are modified with spacers on the peripheral surface to enhance its biocompatibility, half-life and drug-release kinetics. Second, therapeutic drugs are bioconjugated or complexed with the surfaced-modified dendrimers. Third, specific

endogenous ligands are conjugated to the surface-modified dendrimers to target to the BBB and to facilitate transportation through this barrier (Xu *et al.*, 2014).

A variety of ligands have been developed for CNS-targeted dendrimer DDSs. Among those ligands is GSH which is an endogenous tripeptide that can enter the brain *via* RMT. A previous study (Rip *et al.*, 2010) have shown that free ribavirin (as a model drug) was delivered to the extracellular fluid of the brain when GSH was conjugated to liposomes loaded with the drug. GSH-decorating of PEGylated liposomes resulted in an up to 5 times higher free drug concentration compared to non-decorated liposomes, while their plasma circulation concentrations were comparable.

6.1.2 Drug permeability assessments by *in vitro* BBB models

There are various *in vitro* models that are used to assess the permeability of DDSs across the BBB. Monolayer BBB models is the most widely used and involve culturing of endothelial cells on Transwell inserts (Figure 5.1). Another type of *in vitro* BBB model is static co-culture BBB model which involves the growing of brain endothelial cells on the upper surface of the porous membrane and the culturing of glial cells on the other surface of the membrane (in juxtaposition to the endothelial monolayer) (Figure 6.2).

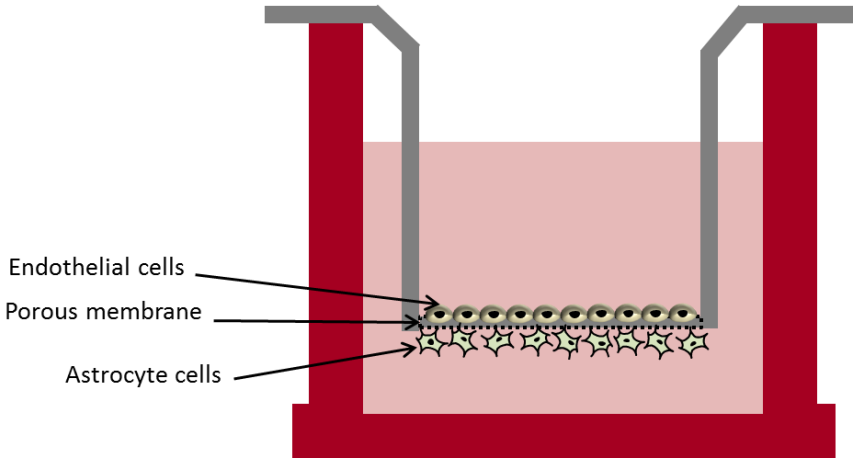

Figure 6.2 Co-culture BBB model with endothelial and astrocyte cells.

More recently, the dynamic *in vitro* BBB culture model utilises artificial capillary-like construction such as hollow fibres (generally made of thermoplastic polymers) to model hollow organ-like structures such as the BBB (Stanness *et al.*, 1996). This model allows brain microvascular endothelial cells to be co-cultured with abluminal astrocytes and under the influence of physiological pulsatile laminar shear stress. This allows for the construction of a BBB model that closely resembles the *in vivo* both functionally and anatomically (Cucullo *et al.*, 2002; Santaguida *et al.*, 2006; Stanness *et al.*, 1997).

Choosing the right type of the *in vitro* BBB model is imperative and it is dependent on the aims of the experiment. Static co-culture BBB models are more suited for cellular uptake and physiological changes in cells triggered in response to different stimuli. However, for penetration studies it is more convenient to use mono culture models.

6.1.3 MP permeability assessment by Transwell inserts

Transwell cell culture inserts are convenient, sterile, easy-to-use permeable support devices for the study of both adherent and suspended cell lines. Initially, the tested drug is introduced in the donor chamber and allowed to diffuse across the membrane (Figure 6.3). The drug diffuses through the microporous semipermeable membrane into the acceptor chamber which is then collected and quantified generally by ultraviolet-visible spectroscopy or HPLC (Nicolazzo *et al.*, 2006).

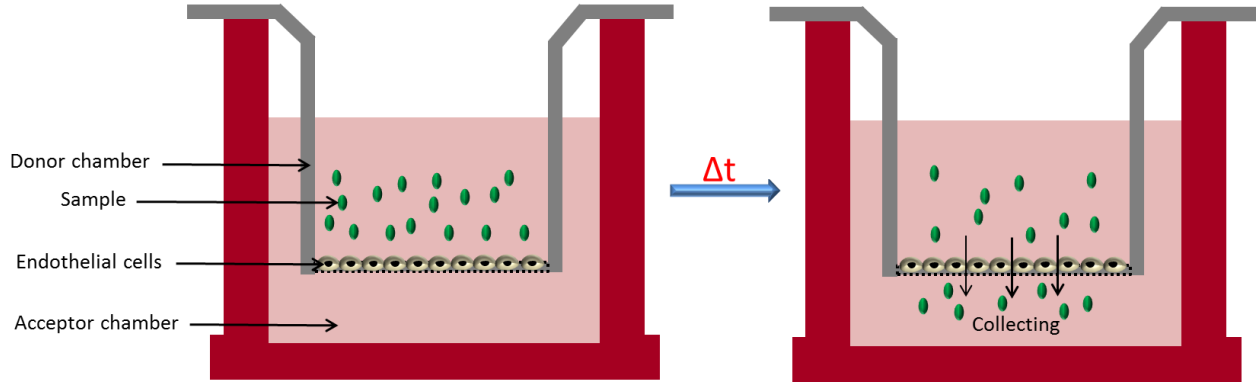

Figure 6.3 Endothelial *in vitro* mono culture model. Sample to be tested is introduced to the donor chamber, after a designated period of time (Δt), samples of the culture medium are collected from the acceptor chamber and analysed to determine the amount which have passed through the b.End3 cells barrier.

Aims of the chapter

The aims of chapter 6 are:

- To confirm the expression of GSH receptors on the membrane of b.End3 cells and investigate the uptake of FITC-labled GSH, GSH-F-Gen0K and free FITC by these cells using laser scanning confocal microscopy.
- Study the permeability of F-Gen0K-MP, F-Gen1K-MP and GSH-F-Gen0K-MP through the previously validated *in vitro* BBB model and compare it with free MP penetration values.

6.2 Materials

The materials used in the experimental methods and their supplied companies are detailed in Table 6.1.

Table 6.1 List of materials used in Chapter 6.

Material	Company	Catalogue number
Acetonitrile, HPLC grade	Fisher Scientific	10660131
Fluorescein isothiocyanate isomer I (FITC)	Sigma-Aldrich UK	F7250-1G
HPLC 2 ml vials, amber, PTEF/silicone	Sigma-Aldrich UK	29654-U
Transwell-12 insert, 12 mm, 0.4 μm, 12-well plate, sterile	Fisher Scientific	10619141
Trifluoroacetic acid	Fisher Scientific	13464279
Water, HPLC grade	Fisher Scientific	10449380

In addition to above, the same materials used for cell culturing as detailed in Chapter 3.

6.3 Methods

6.3.1 Culturing b.End3 cells on Transwell inserts for penetration studies

In this project 12-well plate (clear polyester tissue culture treated) were used. Each well had a 12 mm diameter, 1.12 cm^2 culture area with 0.4 μm pore size and 10 μm membrane thickness. Culturing of b.End3 cells on the permeable supports of Transwell inserts *in vitro* allows cells to be studied in a polarised state under more natural conditions. It also results in better morphological and functional representation of b.End3 cells. To construct the BBB *in vitro* model using b.End3 cells and Transwell inserts, the same procedures detailed in Section 5.3.2 were used.

6.3.2 Detection of GSH receptors on b.End3 cells

Providing evidence for the expression of GSH receptors on the membrane of b.End3 cells is an imperative factor that must be addressed in order to use GSH as an endogenous "Trojan horse" (ligand) for improving MP permeability through the *in vitro* BBB model (Gaillard, Appeldoorn*, et al.*, 2012). To achieve this aim, GSH was labelled with a fluorescent probe and incubated with b.End3 cells to detect any interactions with GSH receptors on the endothelial membrane as well as any uptake of these fluorescent molecules by the cells as detected by confocal microscopy.

6.3.2.1 Attachment of fluorescein isothiocyanate to GSH

Fluorescein isothiocyanate (FITC) is a derivative of fluorescein used widely in dye-labelling of biomaterials, especially peptides and proteins. FITC consists of the original fluorescein molecule functionalised with an isothiocyanate reactive moiety (-N=C=S), replacing a hydrogen atom on the bottom ring of the fluorescein molecule (Figure 6.4). The isothiocyanate group of FITC molecule is reactive towards nucleophilic compounds including amine and sulfhydryl groups on proteins.

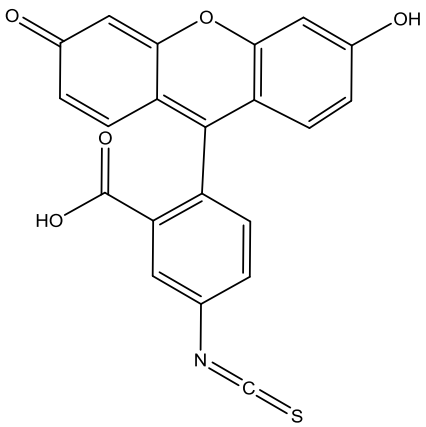

Figure 6.4 Chemical structure of FITC. The chemical formula is $C_{21}H_{11}NO_5S$ and the MW is 389.38 Da.

GSH was synthesised using the same procedures detailed in Section 4.3.2 with the only exception of prolonging the final deprotection step by 20% piperidine to 20 minutes rather than 2 minutes to ensure complete removal of the sidechain protecting group. Excess FITC (0.8 mmole) was dissolved in 3 mL DMF with 140 μL DIPEA and added to GSH and allowed to couple for 9 hours. The attachment occurs between the isothiocyanate group and the peripheral amine group of GSH (Figure 6.5). The resin was washed with dichloromethane, methanol and diethylether using the same procedures detailed in Section 2.3.1 and left overnight to dry. The synthesised GSH-FITC was cleaved from the solid support and precipitated in ice cold diethyl ether using the same protocol detailed in Section 2.4.2.

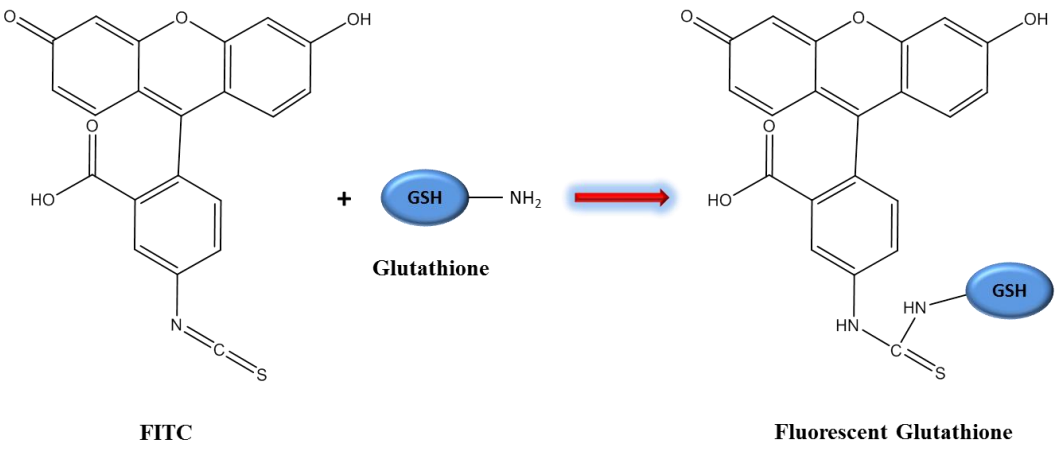

Figure 6.5 Labelling of GSH by FITC.

6.3.2.2 Fluorescent labeling of GSH-F-Gen0K by FITC

In order to detect the possibility of penetration of GSH-F-Gen0K through b.End3 cells by RMT, GSH-F-Gen0K was synthesised and FITC was attached to it using the protocols detailed in Sections 4.3.3 & 6.3.2.1 to produce the final fluorescent molecule, GSH-F-Gen0K-FITC.

6.3.2.3 Treatment of b.End3 with GSH-FITC and GSH-F-Gen0K-FITC

The synthesised fluorescent-labelled GSH and GSH-F-Gen0K were dissolved in the culture medium of b.End3 cells at 100 μM concentration and sterilised by filtration through a 0.42 μm pore size filter. B.End3 cells, cultured to 80% confluent on 24-well plates, were washed with PBS 2 times and 1 mL of GSH-FITC or GSH-F-Gen0K-FITC were added to each well and incubated at 37°C for 1 hour. After incubation the cells were washed twice with PBS and fixed by adding 100 μL of 3.7% $^{v}/_{v}$ formalin to each well and left to incubate for 30 minutes followed by washing with PBS to remove any unattached GSH-FITC or GSH-F-Gen0K-FITC. The cells were imaged using laser scanning confocal microscopy (Leica TCS SP5 / UK) to detect any interactions of GSH with its receptors on b.End3 cells and to examine the uptake of GSH-F-Gen0K by these cells. The images were compared with cells treated with FITC alone without GSH.

6.3.3 Penetration studies through the endothelial cells monolayer

Prior to penetration studies, the wavelength of maximum absorbance (λ_{max}) for MP, F-Gen0K-MP, F-Gen1K-MP and GSH-F-Gen0K-MP were determined by Lambda 25 UV-VIS spectrophotometer/PerkinElmer to be used in governing the HPLC method. The experiment was performed by dissolving each of the synthesised molecules in methanol to from 10 μM solutions. The samples were analysed using the spectrophotometer to determine λ_{max} for each individual molecule.

The b.End3 cells cultured on Transwell clear inserts (at a seeding density of 3×10^4 cells/well). At Day 7 of culturing, the point at which the cells exhibited maximum barrier function properties (based on data collected from TEER and permeability experiments discussed in Chapter 5), the cells were treated with each of the drug formulations under investigation for their penetration properties. To achieve this objective, the culture medium was removed from both Transwell insert chambers, and both chambers were washed 3 times with PBS to remove any traces of coloured medium that might interfere with HPLC experiments. Phenol red free DMEM medium (without FBS and antibiotics) containing 100 μM of MP, F-Gen0K-MP, F-Gen1K-MP and GSH-F-Gen0K-MP were added to specific wells of the inserts (in the donor side); the acceptor chamber of the inserts were filled with phenol red free DMEM ensuring that the level of liquids in both chambers are equal. The inserts were cultured at 37°C and 1 mL samples were withdrawn from the acceptor chamber at 1 and 3 hours after sample spiking with the candidate drug molecules.

HPLC was used for the quantitative determination of the penetration of MP, F-Gen0K-MP, F-Gen1K-MP and GSH-F-Gen0K-MP through the *in vitro* BBB model. The HPLC (Agilent 1260 infinity, G7117 Diod array detector and G7167 auto sampler) conditions were set using a reverse phase C18 Fortis® column (150 mm, 4.6 mm and 5 μm pore size). The mobile phase consisted of a gradient of 0.1% $^{v}/_{v}$ TFA in acetonitrile and 0.1% $^{v}/_{v}$ TFA in water using 0.6 mL/min flow rate and run time of 20-21 minutes with a maximum pressure of 400 pounds per square inch using the determined λ_{max} for each material.

To demonstrate that the polyester membrane of the Transwell inserts does not by itself represent an obstacle, cell free Transwell inserts were treated with 100 μM of free MP, F-Gen0K-MP, F-Gen1K-MP and GSH-F-Gen0K-MP. Samples were collected from the acceptor chambers after 1 hour and run through HPLC to detect permeability percentages.

The collected samples from the accepter chamber after treatment were analysed by HPLC and the corresponding concentrations to each area under the curve (AUC) were calculated from the standard curves obtained from relative HPLC of the tested drugs in a concentration range from 6.25 to 100 μM. The penetration percentages were calculated using the following equation (He *et al.*, 2010):

$$P_{Material}\% = (C_{Material\ acceptor} \times V_{Acceptor}) / (C_{Material\ donor} \times V_{Donor}) \times 100\ \%$$

Where

$P_{Material}\%$ is the permeability percentage of tested material.

$C_{Material\ acceptor}$ is the concentration of tested material in acceptor compartment (calculated by HPLC and standard curves).

$V_{Acceptor}$ is the volume of the culture media in the acceptor compartment (which is equal to 1.8 mL).

$C_{Material\ donor}$ is the initial concentration of tested material introduced in the donor compartment (which is equal to 100 μM).

V_{Donor} is the volume of the culture media in the donor compartment (which is equal to 0.9 mL).

6.3.4 Statistical analysis

All experimental data are expressed as mean ±SD (*n=6*). Statistical analysis was performed using one way analysis of variance (ANOVA) with Tukey's *post-hoc* test, using the Minitab®-17 (version 17.2.1) statistical analysis program with a significance level set at $P<0.05$ (two-sided confidence intervals).

6.4 Results

6.4.1 Culturing of b.End3 cells on Transwell inserts

Light microscopy showed successful culturing of b.End3 cells on Transwell inserts (Figure 6.6). The cells reached confluence within 2-3 days forming a monolayer (distinctive characteristic of endothelial cells) (Eigenmann *et al.*, 2013).

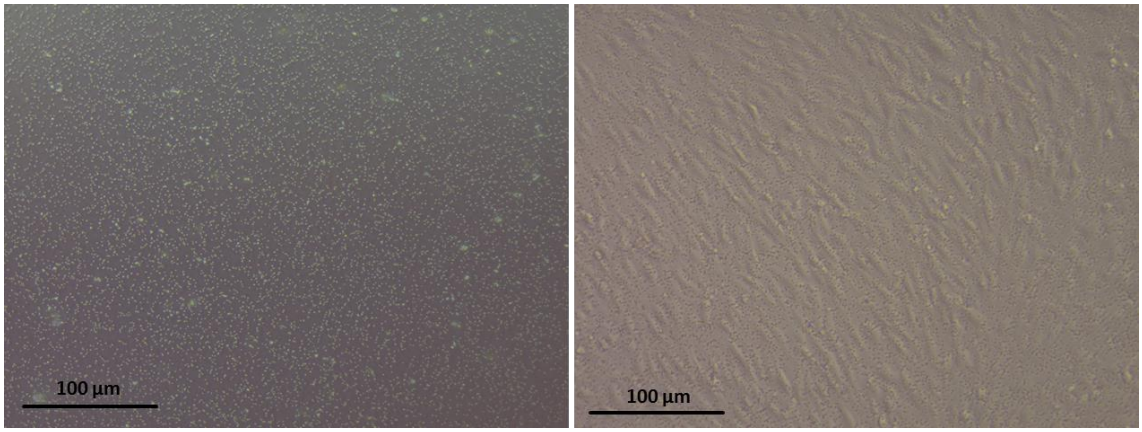

Figure 6.6 Phase-contrast light microscopic images of Transwell inserts. The porous polyester membrane without cells (left) and 80% confluent b.End3 cells cultured on the membrane (right).

6.4.2 Detection of GSH receptors on b.End3 cells and uptake of fluorescent GSH-F-Gen0K

GSH was labelled with the fluorescent probe, FITC, to detect its uptake by b.End3 cells through receptor mediated transport. After 1 hour of exposure to the florescent GSH, the cells were demonstrated to successfully uptake of GSH into the cells as shown by confocal microscopy (Figure 6.7). Moreover, confocal images illustrated the ability of GSH-F-Gen0K to penetrate into the b.End3 cells (Figure 6.8). However, confocal images of cells treated with FITC alone did not reveal any uptake of the fluorescent probe by the endothelial cells (Figure 6.9).

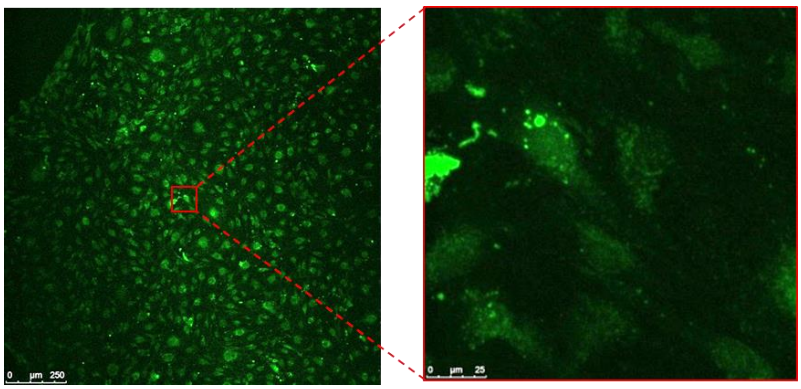

Figure 6.7 Florescent confocal image of b.End3 cells treated for 1 hour with GSH labelled with FITC. Enlarged image showed vacuoles of fluorescent-labelled GSH on the cell membrane of the endothelial cells.

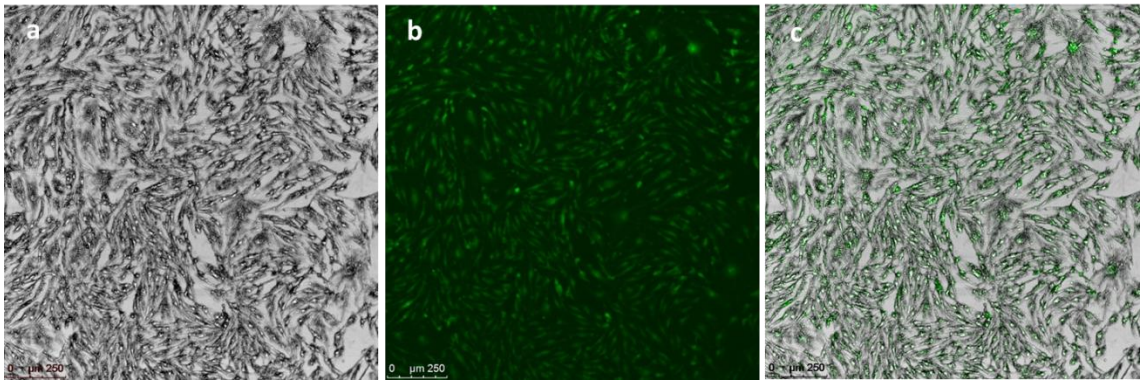

Figure 6.8 Confocal images of b.End3 cells treated with 100 μM of GSH-F-Gen0K labelled with FITC for 1 hour. (a) Light microscopic image, while (b) Fluorescent image and the combined 2 images are represented in (c).

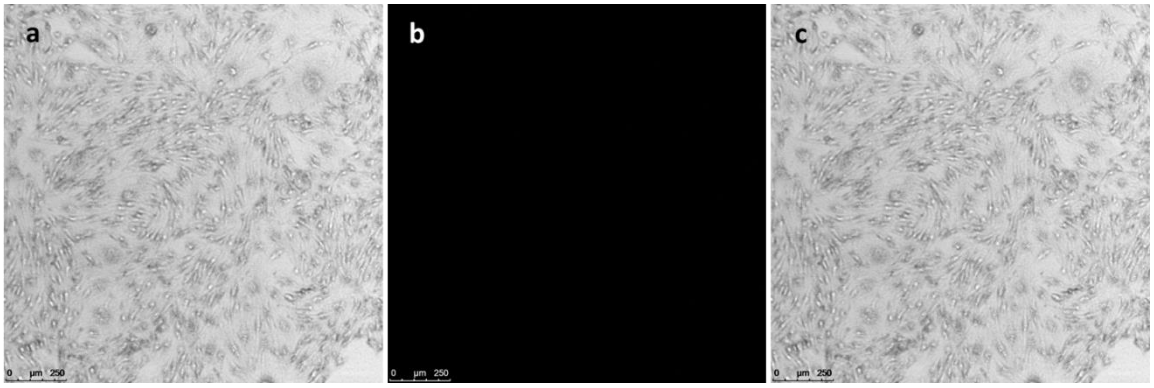

Figure 6.9 Confocal images of b.End3 cells treated with 100 μM of FITC. (a) Light microscopic image, while (b) Fluorescent image and the combined 2 images are represented in (c).

6.4.3 Penetration results of the synthesised molecules across the BBB model

Determination of the specific maximum wave length of absorbance (λ_{max}) of free MP and synthesised molecules was essential to govern the HPLC method. The λ_{max} of free and modified MP was determined by analysing the UV spectra and identifying the maximum wavelength for the peak point of absorbance (Table 6.2). The result showed slight increase in λ_{max} values of modified MP compared to the free drug.

Table 6.2 Maximum wavelengths of absorbance (λ_{max}) of free and conjugated MP molecules.

Material	λ_{max}
MP	254 nm
F-Gen0K-MP	274 nm
F-Gen1K-MP	280 nm
GSH-F-Gen0K-MP	272 nm

HPLC analysis of samples collected from the acceptor chamber of cell-free Transwell inserts revealed that the membrane of the inserts did not represent a significant barrier for the

transport of free MP, F-Gen0K-MP, F-Gen1K-MP and GSH-F-Gen0K-MP. The permeability percentages of these molecules (Table 6.3) reached approximately 50% within 1 hour of the samples introduction i.e. the concentration was equal in both sides of the membrane with no statistical difference to be detected (P>0.05).

Table 6.3 Permeability percentages of free and attached MP across cell-free Transwell inserts. The results represents the mean ±SD (*n=6*).

Material	% Permeability
MP	50.3±0.52
F-Gen0K-MP	49.4±0.30
F-Gen1K-MP	51.1±0.66
GSH-F-Gen0K-MP	50.6±0.02

HPLC analysis of MP resulted in a distinctive single peak which appeared after 10.9 minutes of sample injection (Figure 6.10.a). The DMEM gave several peaks which appeared between 2.5 and 6.5 minutes. To provide confirmation that these peaks related to the media and not the sample, another HPLC was run injecting only DMEM medium without any sample which resulted in similar peaks from 2.5 to 6.5 minutes but without the MP peak at 10.9 minute (Figure 6.10.b).

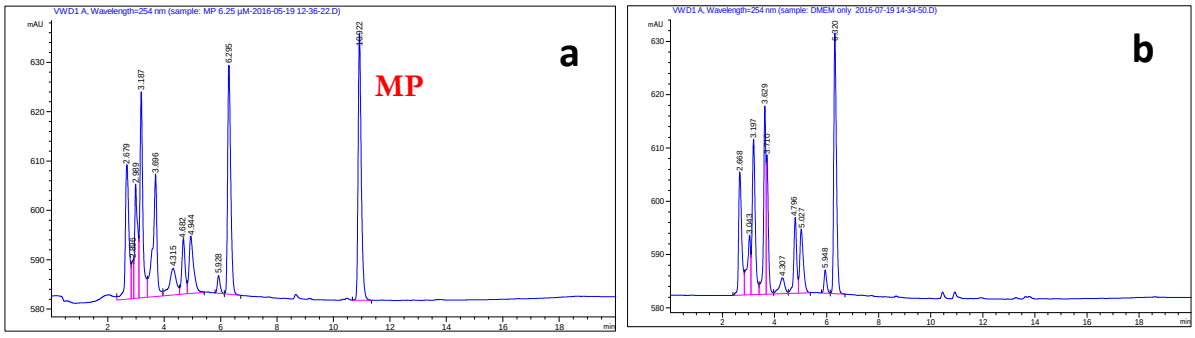

Figure 6.10 HPLC spectra of phenol red free DMEM with and without MP dissolved in it. (a) MP appeared as a distinctive peak at minute 10.9 while DMEM peaks appeared between 2.5 to 6.5 minutes. (b) The same peaks of DMEM with the same retention time observed in the drug free media.

The HPLC spectra of the standard dilutions of MP, F-Gen0K-MP, F-Gen1K-MP and GSH-F-Gen0K-MP plus the standard curves generated by plotting the concentration versus the AUC are represented in Figure 6.11 to 6.14 respectively using the corresponding wavelength for each tested material (Table 6.1). The retention time of F-Gen0K-MP was longer than free MP giving a distinctive peak at minute 16 (Figure 6.12). The same delay in the retention time

was also observed in GSH-F-Gen0K-MP at minute 15 (Figure 6.14). However, the relatively larger MW, F-Gen1K-MP peak appeared at minute 11 (Figure 6.13).

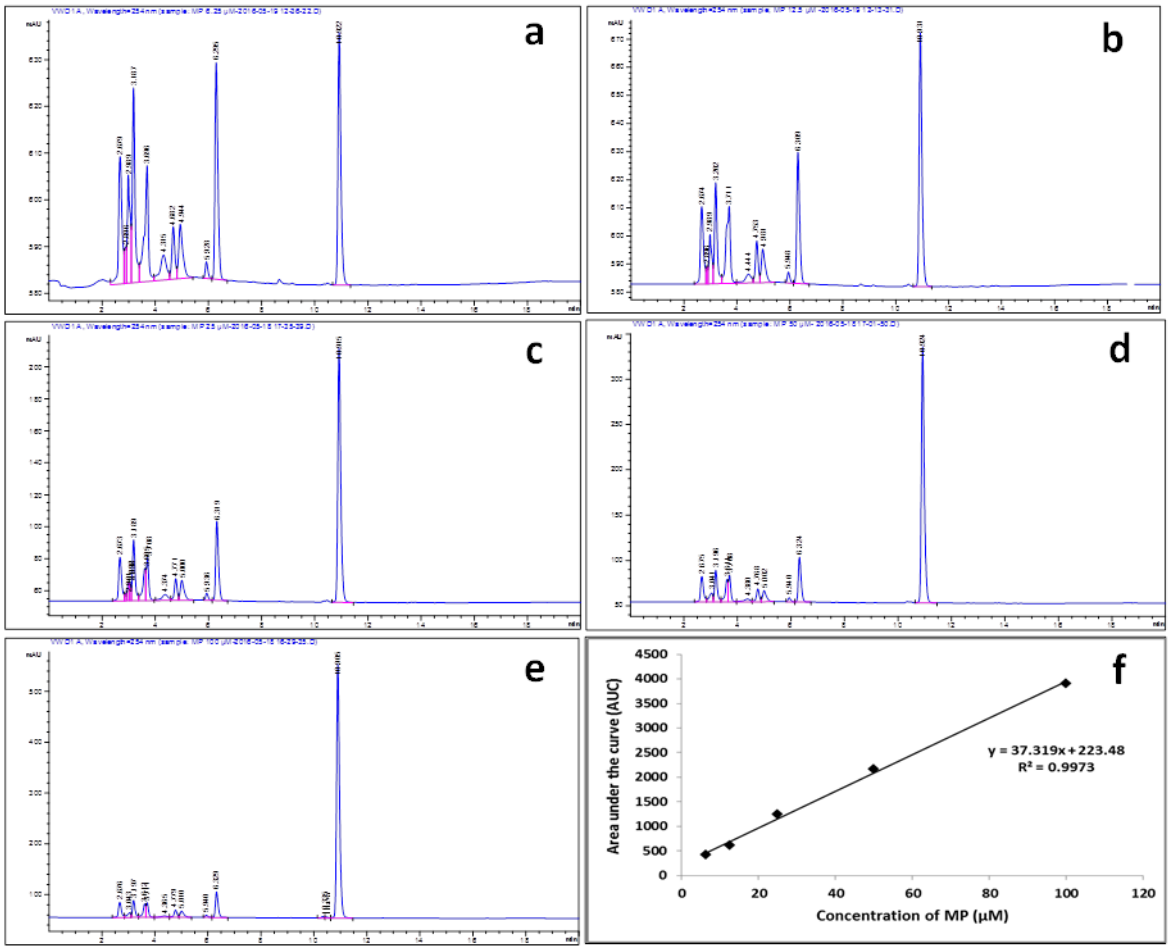

Figure 6.11 HPLC spectra of standard dilutions of MP in phenol red free DME and the standard curve.
(a) HPLC spectra of 6.25 µM concentration. (b) HPLC spectra of 12.5 µM concentration. (c) HPLC spectra of 25 µM concentration. (d) HPLC spectra of 50 µM concentration. (d) HPLC spectra of 100 µM concentration. (f) The standard curve established by intersecting the concentration versus the AUC.

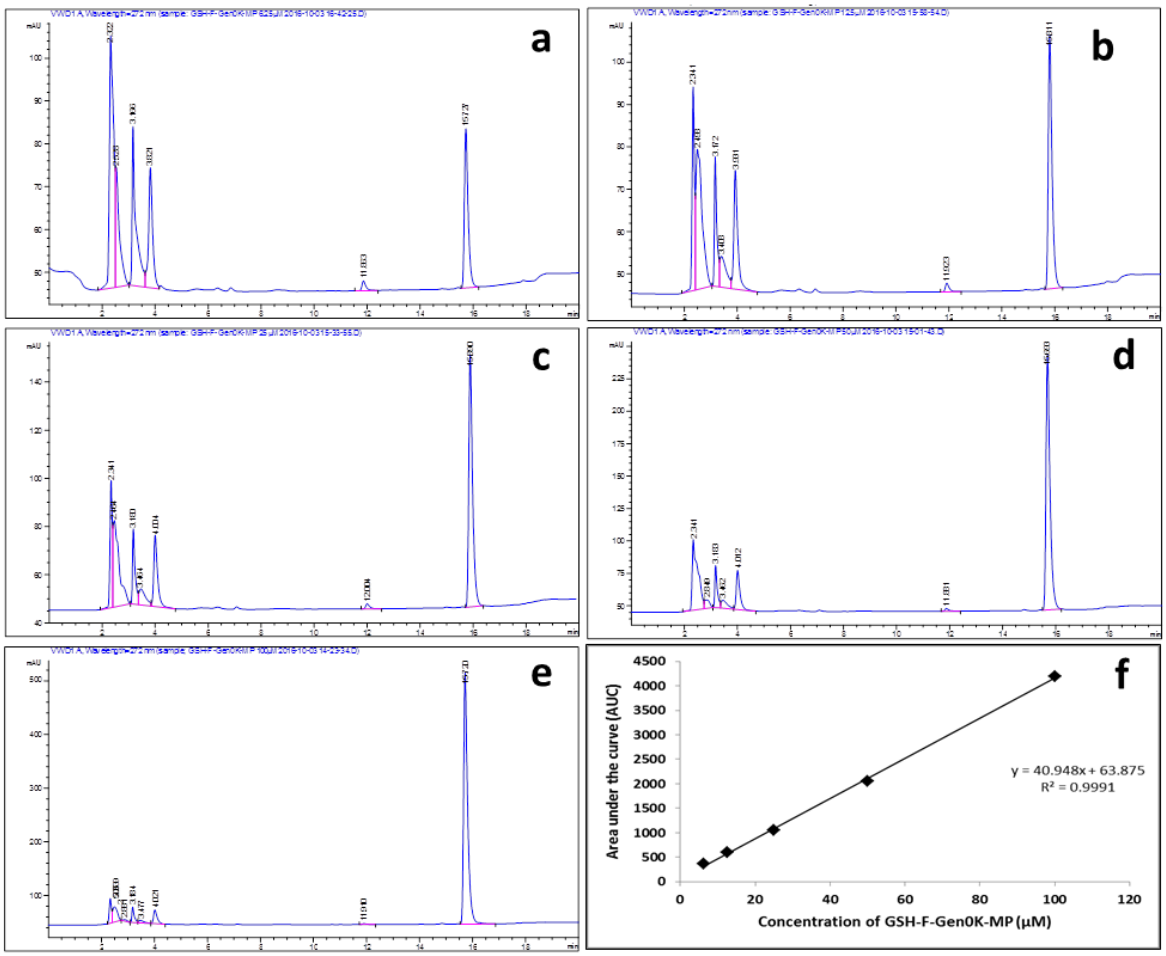

Figure 6.12 HPLC spectra of standard dilutions of F-Gen0K-MP in phenol red free DME and the standard curve. (a) HPLC spectra of 6.25 μM concentration. (b) HPLC spectra of 12.5 μM concentration. (c) HPLC spectra of 25 μM concentration. (d) HPLC spectra of 50 μM concentration. (d) HPLC spectra of 100 μM concentration. (f) The standard curve established by intersecting the concentration versus the AUC.

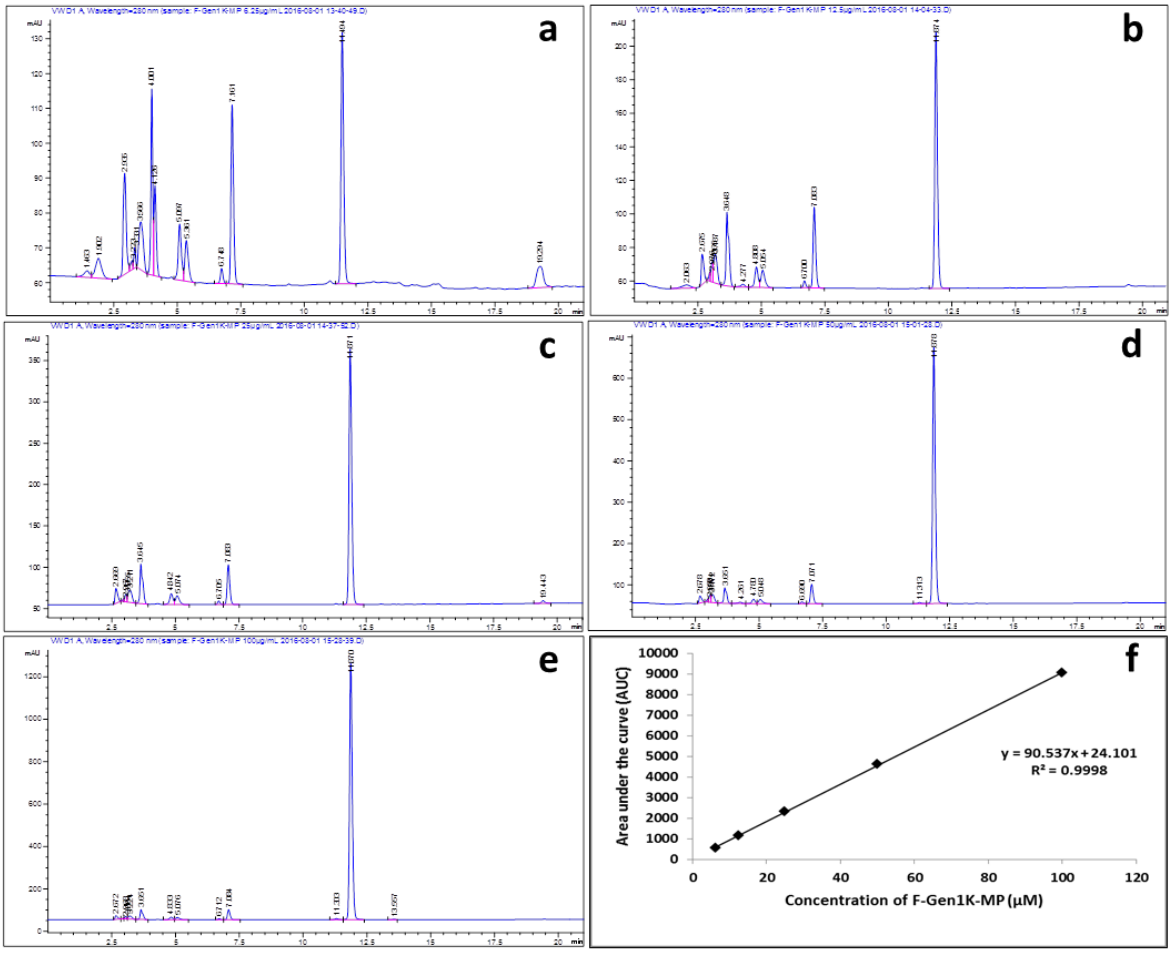

Figure 6.13 HPLC spectra of standard dilutions of F-Gen1K-MP in phenol red free DME and the standard curve. (a) HPLC spectra of 6.25 μM concentration. (b) HPLC spectra of 12.5 μM concentration. (c) HPLC spectra of 25 μM concentration. (d) HPLC spectra of 50 μM concentration. (d) HPLC spectra of 100 μM concentration. (f) The standard curve established by intersecting the concentration versus the AUC.

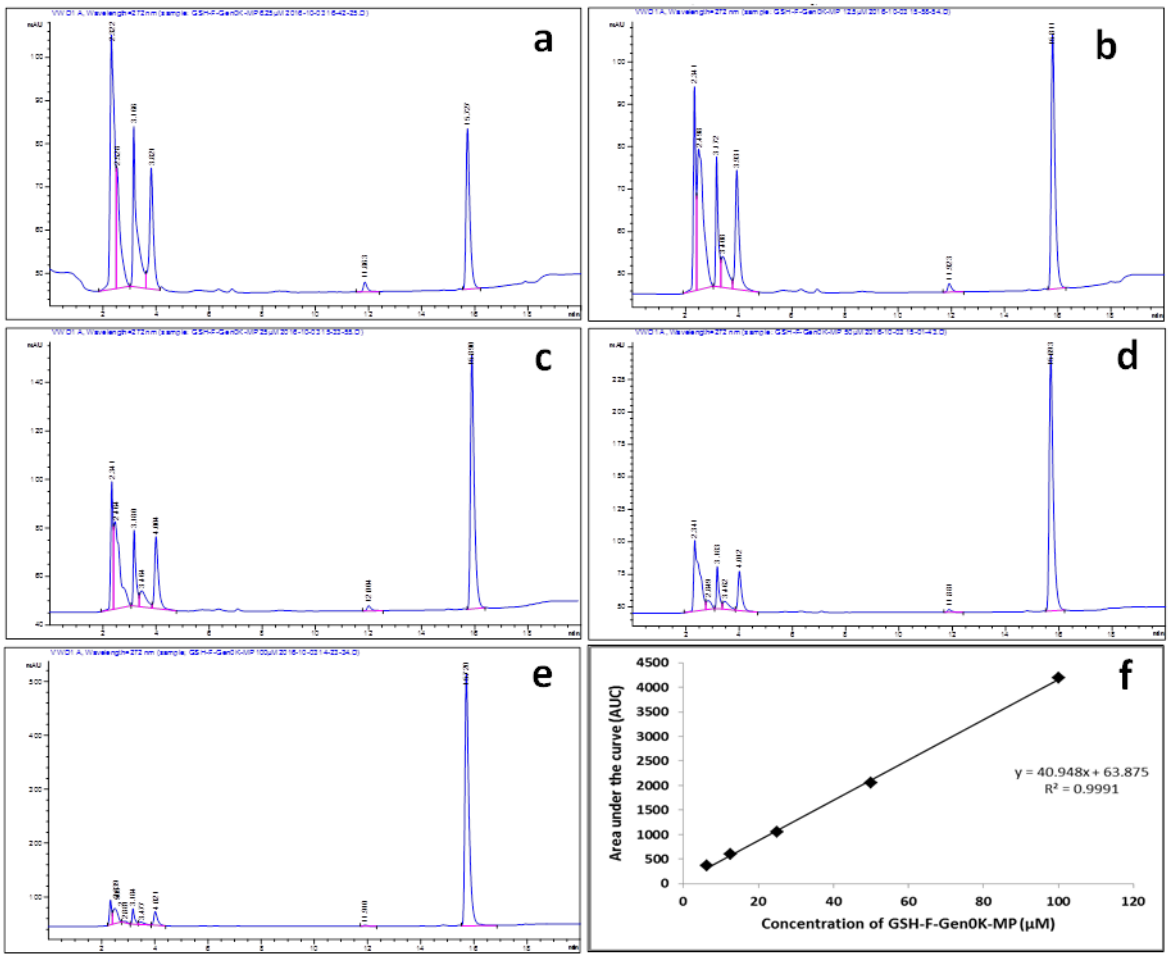

Figure 6.14 HPLC spectra of standard dilutions of GSH-F-Gen0K-MP in phenol red free DME and the standard curve. (a) HPLC spectra of 6.25 μM concentration. (b) HPLC spectra of 12.5 μM concentration. (c) HPLC spectra of 25 μM concentration. (d) HPLC spectra of 50 μM concentration. (d) HPLC spectra of 100 μM concentration. (f) The standard curve established by intersecting the concentration versus the AUC.

After treatment of b.End3 cells cultured on Transwell inserts with 100 μM of MP, F-Gen0K-MP, F-Gen1K-MP and GSH-F-Gen0K-MP, samples were collected after 1 and 3 hours from the acceptor chamber. The collected samples were analysed by HPLC to obtain the relative AUC. The corresponding concentrations were calculated from the standard curves to enable calculating percentage penetration for each martial.

The average percentage penetration for free MP, F-Gen0K-MP, F-Gen1K-MP and GSH-F-Gen0K-MP through the *in vitro* BBB after 1 and 3 hours of introduction of samples is represented in Table 6.4. The permeability of MP conjugated to dendrons and GSH was compared with free MP. The average penetration of free MP through the *in vitro* BBB barrier did not exceed 4.4% and 10.3% of the used dose after 1 and 3 hours of exposure respectively. The mean penetration values of F-Gen0K-MP were slightly higher than free MP reaching 6.6% after 1 hour exposure and 11.1% after 3 hours. However, statistical analysis did not reveal any significant difference ($P>0.05$). F-Gen1K-MP showed lower permeability compared to free MP not peaking higher than 2.7% at the 3 hours point. The F-Gen1K-MP permeability values were significantly lower ($P<0.05$) than those of free MP and F-Gen0K-MP in both exposure periods. However, the average permeability percentages of GSH-F-Gen0K-MP were almost 3.5 fold higher than free MP at both exposure periods (1 and 3 hours) reaching 16.8% and 40.9%, respectively. These numbers were significantly higher ($P<0.001$) when compared to all other molecules (free MP, F-Gen0K-MP and F-Gen1K-MP) after 1 and 3 hours of samples introduction.

Table 6.4 The average penetration percentages of free MP, F-Gen0K-MP, F-Gen1K-MP and GSH-F-Gen0K-MP based on HPLC tests after 1 and 3 hours of sample introduction into the donor chamber. Results represent the mean ±SD (*n=6*).

Material	% Penetration ±SD	
	1 Hour	3 Hours
MP	4.3 ±1.3	10.2 ±3.4
F-Gen0K-MP	6.6 ±1.3	11.1 ±0.6
F-Gen1K-MP	1.4 ±0.3	2.6 ±0.7
GSH-F-Gen0K-MP	16.8 ±3.0	40.9 ±5.0

6.5 Discussion

Due to the high brain perfusion rate and the small distance separating capillaries, nearly all neurons in the brain are perfused by their own capillary (Pardridge, 2007). Consequently, the most beneficial way of delivering neuroactive therapeutics is by utilising endogenous transporters or internalising receptors on these capillaries to act as "Trojan horses" to overcome the BBB obstacle (Chen *et al.*, 2012). The development of these molecular Trojan horses is a promising drug targeting technology which allows for efficient and non-invasive delivery of medications into the brain (Jones *et al.*, 2007). This concept relies on the application of endogenous molecules or small peptides, capable of specifically ferrying a drug-payload that is either directly coupled or encapsulated in an appropriate carrier, across the BBB via RMT. Specifically, in this process the specialised drug carrier system is transported transcellularly across the brain endothelium, from the blood to the brain interface, essentially trailed by a native receptor (Oller-Salvia *et al.*, 2016).

Mimicking the physiological features and reactions of the brain microcapillaries *in vitro* represents a significant step forward towards the *in vitro* clinically-reflective testing of novel drugs. Such *in vitro* models may provide valuable data about the mechanisms involved in the cerebrovascular reaction to different physiological and pathological stimuli. This, in turn, will pave the way to accelerate the development of novel CNS drug therapies and lower the burden of major neurological diseases especially neurodegenerative disorders (Pardridge, 2005a).

The most common and widely utilised BBB model is based on culturing of highly specialised endothelial cells on semi-permeable supports. In this study, b.End3 cells were cultured on Transwell inserts to form a monolayer. Such design of the *in vitro* BBB model offered several advantages. Cellular functions such as transport, absorption and secretion can be efficiently studied since cells grown on permeable supports provide convenient, independent access to apical and basolateral plasma membrane domains. Furthermore, these inserts allow incubated b.End3 cells to feed baso-laterally and hence carry out metabolic activities in a more natural way hence producing a close approximation to the *in vivo* situation (Naik *et al.*, 2012).

In this study, the monolayer *in vitro* model was chosen for the permeability experiments rather than the co-culture type because the former is more suitable for permeability studies while the latter is more convenient for drug-cellular uptake studies (Naik *et al.*, 2012). The presence of glial cells in the acceptor chamber might result in some uptake of the drug from the donor chamber to the acceptor by the cells. Such uptake will result in reduction of real concentration

of the drug in the acceptor chamber causing underestimated detection of concentrations when samples were analysed using HPLC.

Labelling by fluorochromes such as FITC is a commonly used method for detecting the interaction of peptides and small proteins with the cells and in many cases is an alternative to the use of radioactive materials (Jullian *et al.*, 2009). FITC has been extensively used to react with amino groups in peptides or proteins (Boturyn *et al.*, 2004). In this study, it was more convenient to introduce FITC during the chemical synthesis of GSH and GSH-F-Gen0K by SPPS, to chemically react with the primary amino groups at the N-terminal side which is in agreement with other studies (Carrigan *et al.*, 2005; Song *et al.*, 2004).

The successful fluorescent staining of b.End3 cells by FITC-labelled GSH and GSH-F-Gen0K molecules as demonstrated by confocal microscopy (Figures 6.7 & 6.8 respectively) confirmed the ability of GSH and GSH-F-Gen0K to penetrate these endothelial cells. However, the lack of staining of b.End3 cells by free FITC (Figure 6.9), despite its lower MW compared FITC-labelled GSH and GSH-F-Gen0K molecules, suggests that the uptake of these GSH-based molecules by the endothelial cells occurred through a specialised transport or receptor mediated pathway rather than the simple transcellular-lipophilic pathway. Consequently, this uptake of stained molecules by endothelial cells can be attributed to the presence of the GSH which can interact with its receptors on these cells (Rotman *et al.*, 2015). This assumption was confirmed by the appearance of fluorescent vacuoles on the cell membrane of b.End3 cells treated with fluorescent-labelled GSH (Figure 6.7). Moreover, the effective staining of cells treated with fluorescent-labelled GSH-F-Gen0K rather than those treated with free FITC provides proof that the GSH moieties enables its cargo (dendron and FITC) to penetrate the cells. These data are in agreement with other studies (Gabathuler, 2010; Kannan *et al.*, 1990) which confirmed the expression of GHS receptors on the membranes of BBB endothelial cells and the possibility of its application in enhancing delivery of poorly penetrating molecules to the brain through RMT. Unfortunately, labelling of GSH-F-Gen0k-MP by FITC was not possible since the peripheral amino groups of GSH-F-Gen0K needed to attach FITC were already used to attach the drug.

It is crucially important to determine the BBB permeability of CNS novel DDSs in the early stages of development, so that poor BBB permeability candidates can be excluded or structurally modified, and promising BBB candidates can be expedited through the development process (Nicolazzo *et al.*, 2006). There are various methods that can be used to

evaluate the permeability of drugs across the BBB. The most commonly used methods depend on colorimetric assays and HPLC. However, colorimetric assays are inconvenient if the tested candidate lacks fluorescent moieties and interference from the culture medium. DMEM media is rich in contents like amino acids, salts and vitamins (such as folic acid, nicotinamide, riboflavin and cyanocobalamin) which can potentially affect colorimetric assay of the tested molecules.

The drawback of quantitative detection of MP, F-Gen0K-MP, F-Gen1K-MP, and GSH-F-Gen0K-MP penetration across the *in vitro* BBB model by colorimetric assays prompted the use of another technique. HPLC was chosen to perform this task since the presence of culture medium did not interfere with the peaks of the tested-molecules. After governing of its method, HPLC techniques provided a very sensitive approach to quantify each of the tested molecules in the acceptor chambers even at lower concentrations (1-3 μM) making it very convenient for the penetration studies.

As expected, free MP exhibited limited penetration through the *in vitro* BBB barrier. After 1 hour of sample introduction, MP permeability did not exceed 4.4% of the applied dose (100 μM) which rose to almost 10% after 3 hours (Table 6.4). This low permeability, compared to about 50% permeability after only one hour of free MP in cell free Transwell inserts (polyester membrane only) (Table 6.2), gives an indication of the efficiency of the b.End3 cells mono layer as a barrier. This finding of MP's limited permeability is in agreement with the study of Benjamin (2011) which indicated that only 5-8 % of the injected dose of MP can reach the brain under clinical conditions forcing the administration of 10 to 20 fold the stated dose of MP (up to 1000 mg/day) (Benjamin *et al.*, 2011).

The permeability results of F-Gen0K-MP were not significantly different from free MP. However, it should be taken in consideration that each molecule of F-Gen0K-MP contains two moieties of MP so these numbers are doubled based on its MP content making the values significantly higher than free MP in this case. This emphasise the advantage provided by the use of the dendron carrier in terms of drug penetration. These data are in agreement with another study (Diwan *et al.*, 2007) which highlighted the ability of dendrons to promote the penetration of specific drugs through biological barriers. The study synthesised folate-dendrimer conjugates as suitable carriers for the site specific delivery of indomethacin (anti-arthritis drug) to inflammatory sites. Folic acid was coupled to the surface amino groups of

Gen4 PAMAM dendrimer and loaded with indomethacin. The conjugated indomethacin showed better tissue distribution than free drug at equivalent doses.

F-Gen1K-MP showed the lowest permeability numbers of all tested molecules. Its permeability did not exceed 1.9% after 1 hour and 2.7% after 3 hours of sample introduction. One of the crucial factors of molecules ability to cross the BBB is its MW. To cross the BBB in pharmacologically sufficient amounts, a drug molecule must have a molecular mass less than 400 Da (Pardridge, 2007). Increasing the MW will dramatically decrease the permeability. The MW of F-Gen1K-MP is 2419 Da, which exceeds the MW limit (400 Da) of penetrable molecules and can explain these low permeability numbers (Boado *et al.*, 2014). Despite the fact that four moieties of MP are contained in each F-Gen1K-MP molecule, the permeability remains low compared to free MP and F-Gen0K-MP. In addition, the presence of multiple drug attachment in F-Gen1K-MP (4 MP moieties) can result in a relatively compact and dense molecule that eventually limits its penetration. MW, lipophilicity (the more lipophilic, the better the permeability) and charge (low hydrogen bonding capabilities) are essential characteristics for molecules to diffuse from the blood into the CNS (Gabathuler, 2010). Moreover, any preferable penetration property by the dendron (the positive charge on peripheral amine groups which can interact with the negatively-charged cell membranes) is likely to be masked by these multiple drug attachments.

Perhaps, the most promising result revealed by the permeability experiments was the data of GSH-F-Gen0K-MP. The permeability of this ligand-enhanced drug carrier system was almost four folds higher than free MP reaching approximately 17% after 1 hour and 41% after 3 hours. It is apparent that the presence of the ligand (GSH) in the molecule is the dominant factor for such increment and enhanced permeability figures. These data are in agreement with several other studies which indicated that using GSH as ligand enhanced brain delivery of various materials including drugs such as doxorubicin (Birngruber *et al.*, 2014), triiodothyronine (Mdzinarishvili *et al.*, 2013), MP (Gaillard, Appeldoorn*, et al.*, 2012; Lee *et al.*, 2014); peptides such as anti-amyloid domain (Rotman *et al.*, 2015), opioid peptide (Lindqvist *et al.*, 2013); proteins such as siRNA (Kim *et al.*, 2010); and others (Oller-Salvia *et al.*, 2016).

Another factor in analysing the permeability results that must be considered is that the GSH-F-Gen0K-MP molecule is loaded with two MP drug molecules. Hence, the dendron not only increased the permeability of MP through the BBB model, it improved the payload of MP to

the other side of the *in vitro* barrier by two-fold compared to free MP and it is likely to increase the retention time in the target brain tissue allowing the reduction of the dosage.

Despite the potential increase in the permeability of poorly penetrating drugs across the *in vitro* BBB model by RMT approach, the method exhibits some limitations. A previous study (Moos *et al.*, 2000) indicated the accumulation of the carried drug in the brain capillary endothelial cells and not in the targeted parenchymal compartment. Such a drawback may be attributed to the lower dissociation from specific receptors due to the high affinity of the ligands. Additionally, widespread expression of the targeted receptors including GSH on peripheral organs limits its capabilities for targeted brain delivery. However, this issue was not an obstacle in this study since MP is used for the treatment of MS both centrally and peripherally.

Improving MP permeability across the BBB model by the GSH-F-Gen0K carrier system (as confirmed by the data shown in this chapter) can result in lowering of MP dose administrated to MS patients to almost 12% the current dose. Such dose reduction can result in a consequent decrease in the adverse effects of MP since such adverse effects are concentration dependant (Schacke *et al.*, 2002). Moreover, the carrier system (GSH-F-Gen0K) may be utilised for other poor penetrating drugs.

The modification of MP *via* its attachment to the carrier system developed in this study has clearly been shown to improve its transport across a model of the BBB. However, it is necessary to confirm that, following its passage across the endothelial cell monolayer, the drug maintains its anti-inflammatory action on the target neuroglial cells of the brain. To this end, the following chapter (Chapter 7) will investigate the ability of the transported MP to reduce inflammation, when compared to free drug, using an *in vitro* model of C6 glial cells (target cells for MP).

6.6 Conclusion

The following points can be concluded from this chapter:

- The GSH-decorated dendron can increase the permeability of MP conjugated to it across an *in vitro* BBB model by four fold compared to free MP. Two moieties of MP can be efficiently delivered through the endothelial cell barrier per GSH-F-Gen0K molecule.
- Using F-Gen0K (without GSH) as a carrier system for MP also delivered a higher amount of the drug across the barrier than free MP but to a less extent than the GSH decorated carrier system.

- Employing F-Gen1K as MP drug carrier did not improve delivery of MP despite its high payload (1F-Gen1K : 4MP) highlighting the effect of the molecule size in the permeability process.

Chapter 7. Biochemical investigation of anti-inflammatory activity of conjugated MP molecules

7.1 Introduction

MP is a very effective anti-inflammatory drug in the treatment of many acute and chronic inflammatory conditions and neurodegenerative diseases such as MS (Gaillard, Appeldoorn*, et al.*, 2012). Its effects may be broadly classified into two major categories which are immunological effects (or the anti-inflammatory action) and metabolic effects (profound alterations in carbohydrate, protein and lipid metabolism such as increasing gluconeogenesis and reducing protein uptake and the adjustment of body homeostasis by modulation of electrolyte and water balance) (Pelt, 2011). The drug imposes these effects by binding to GRs which are highly expressed in numerous brain regions (Lu *et al.*, 2006). In the absence of a ligand, these receptors reside predominantly in the cytoplasm of different glial cells of the brain tissue (Jauregui-Huerta *et al.*, 2010). Upon binding with its ligand (such as MP), they are translocated into the cell nucleus where they work as gene transcription regulators through binding to specific DNA response elements causing up- or down-regulation of the expression of numerous genes implicated in the inflammation process (Buckingham, 2006).

TNF-α is among the cytokines that could be inhibited by this anti-inflammatory action of MP. TNF-α levels are highly related to neurodegenerative conditions and it was previously detected in patients with neurological disorder at ~1 ng/mL (Larrick *et al.*, 1990; Liu *et al.*, 1994; Mark *et al.*, 1999). In a recent study (Cho *et al.*, 2015), an *in vitro* BBB model has been constructed by arranging endothelial monolayers in 3 dimensional tube-like structures on a single-layered platform. The tightness of the constructed model was validated by visualising the TJ proteins and by observing the blockage of neutrophil migration across the barrier membrane. The study has confirmed the induction of neuroinflammation condition by TNF-α treatment in the BBB model.

Moreover, TNF-α can initiate a series of inflammatory cascade events in *in vitro* neuroglial models that will eventually result in cell apoptosis and death. The inflammatory response involves the formation of arachidonic acid from the phospholipids of the cell membrane which is mediated by the activity of the phospholipase A2 enzyme. Arachidonic acid is the precursor of several inflammatory cytokines, such as vascular endothelial growth factor, tissue inhibitors of metalloproteinases and cytokine-induced neutrophil chemoattractant-1 (CINC-1). The anti-inflammatory effects of MP are thought to involve phospholipase A2 inhibitory proteins (Figure 7.1), which control the biosynthesis of these potent mediators of inflammation (Gaillard, Appeldoorn*, et al.*, 2012).

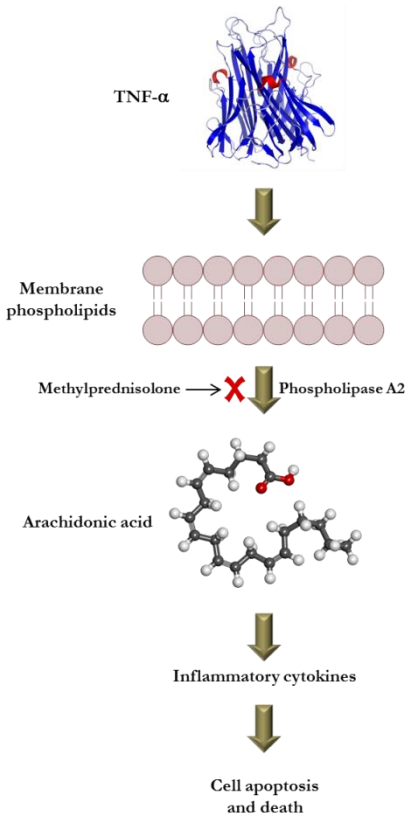

Figure 7.1 Inhibition of cytokines synthesis by MP. TNF-α induces inflammatory response in glial cells which can be blocked by MP through inhibition of phospholipase A2 enzyme.

MP's poor penetration through the BBB hinders its anti-inflammatory action in MS patients and forces the use of alternative methods to improve its targeting of the brain (Rotman *et al.*, 2015). The successful conjugation of MP to a GSH-decorated dendron enhanced its permeability as well as its payload through the *in vitro* BBB model. The ligand (GSH) improved the penetration of MP by almost 3.5 fold compared to free MP through the validated BBB model (Chapter 6). Nevertheless, despite this significant improvement in the drug permeability through the *in vitro* barrier, attaching MP to dendrons and GSH will result in molecular modification of its chemical structure that may lead to alteration of its pharmacological activity. It is possible that changes in activity may result from the loss of affinity between the modified MP and its target receptors on the target cells. Based on these facts, it is imperative to study the pharmacodynamics of MP after attachment to dendrons and GSH to identify whether the drug retains its anti-inflammatory activity or not.

To demonstrate the ability (or lack of it) of the synthesised MP molecules (F-Gen0K-MP, F-Gen1K-MP and GSH-F-Gen0K-MP) to relieve neuroinflammation situations, TNF-α was added to cultured C6 glial cells to mimic the inflammatory state. Glial cells were chosen to perform this experiment based on the fact that it is the target cells for MP after it crosses the

BBB. TNF-α has previously been reported to mediate inflammation in C6 glial cells *in vitro* models (Mark *et al.*, 1999). Thus, the constructed *in vitro* C6 glial cells model can be treated with TNF-α to spike neuroinflammation. Such TNF-α treatment raises the release of several inflammatory cytokines (including CINC-1). These inflammatory cytokines are recognised to mediate a neuroinflammatory response and trigger inflammatory effect on constructed neuroglial models. CINC-1 belongs to the chemokines family which consists of a number of structurally related proteins that play a pivotal role in inflammation and are able to induce migration and activation of specific leukocytes (Pease *et al.*, 2006).

CINC-1 and other chemokines exert their effects by binding to its seven-transmembrane G-protein-coupled receptors. These receptors are located not only on the membrane of neutrophils but also in a wide-range of cell types including brain microglia (Denker *et al.*, 2007), neurons of the brain and spinal cord (Horuk *et al.*, 1997), and oligodendroglial cells of rats (Nguyen *et al.*, 2001). CINC-1 is recognised as an acute-phase protein (Campbell *et al.*, 2003). Such proteins are always released in infections or severe inflammation. Moreover, its synthesis is induced by a number of endogenous and exogenous pyrogens, including TNF-α (Watanabe *et al.*, 1989). Within the CNS, CINC-1 is involved in vascular, immune and behavioural changes occurring during neuroinflammation (Pan *et al.*, 2001).

Glucocorticoids including MP exert their anti-inflammatory activity by interfering with phospholipase A2 enzymes involved in the synthesis of CINC-1. Glucocorticoids can inhibit phospholipase A2 activity by directly controlling its synthesis and extra-cellular release. Glucocorticoids functional mode is believed to be due to their suppressive actions on the gene transcription and protein synthesis of inflammatory mediators including CINC-1 (Jantz *et al.*, 1999). A previous study showed that TNF-induced phospholipase A2 release response from smooth muscle cells was almost completely blocked by using 10 and 100 nM of the glucocorticoid drug, dexamethasone (Nakano *et al.*, 1990). Another study indicated the ability of MP to reduce cytokine release (including CINC-1) from glial cells treated with TNF-α and thereby reduces the apoptotic cell death initiated by the inflammation process (Gaillard, Appeldoorn*, et al.*, 2012). Glucocorticoids are the most potent and widely used anti-inflammatory agents in inflammatory conditions (Jantz *et al.*, 1999; Schwiebert *et al.*, 1996). The occurrence or not of reductions in these 2 parameters (CINC-1 release and cell death) as well as its extent will provide evidence for whether MP in its attached form retains its activity or not when compared to its free MP form.

Aims of the chapter

This chapter focuses on the efficacy of MP in its bound form on target neuroglial cells. A neuroinflammation state was produced in C6 glial cells using TNF-α to mimic the inflammatory condition associated with MS. The level of reduction in the release of inflammatory marker (CINC-1) and cell death caused by treating the cells by MP in its attached form was compared to the reduction in levels imposed by free MP. Thus, this chapter aims to understand whether the conjugated MP maintains its efficacy by:

- Assessing the cytotoxicity of neuro inflamed C6 cells induced using conjugated MP forms and compare it with free MP using the LDH assay.
- Illustrating the anti-inflammatory activity of conjugated MP molecules (F-Gen0K-MP, F-Gen1K-MP and GSH-F-Gen0K-MP) compared to free MP using CINC-1 release levels as a marker.

7.2 Materials

The materials used in the experimental methods and their supplied companies are detailed in Table 7.1.

Table 7.1 List of materials used in Chapter 7.

Material	Company	Catalogue number
C6 glial cells, *Rattus norvegicus*, brain, rat	ATCC laboratories, UK	CCL-107
CINC-1 ELISA Kit, Rat	Thermo-Fisher Scientific	ERCXCL1
CryoTube™ Vials from Nunc®	Fisher Scientific UK	CRY960-070B
CytoTox 96® Non-Radioactive Cytotoxicity (LDH) Assay	Promega, Southamption, UK	G1780
Dimethylsulfoxide (DMSO) Hybri-Max®	Sigma-Aldrich UK	D2650
F-12K (Kaighn's) Medium	Thermo-Fisher Scientific	21127022
Fetal Bovine Serum (FBS), heat inactivated, EU approved	PAA Laboratories Ltd., UK.	A15-104
Horse serum 100 mL	Thermo-Fisher Scientific	16050130
T-75 Thermo Scientific Nunc® tissue culture flask	Fisher Scientific UK	TKT-130-370U
Triton X-100 lysis solution (1% solution in PBS)	MatTek Corporation	TC- TRI
Trypsin 0.05% $^{w}/_{v}$ EDTA (1X), from Invitrogen	Fisher Scientific	VX25300054
Tumor Necrosis Factor-α from rat	Sigma-Aldrich UK	T5944-10UG

7.3 Methods

7.3.1 Glial cells strain C6

C6 glial cells are cloned from rat glial tumor induced by N-nitrosomethylurea. This cell line has a fibroblast-like morphology and is equipped with receptors for neurotransmitters, neuropeptides, hormones, nutrients and other molecules including glucocorticoids (Napoli *et al.*, 2009). C6 glial cells possess extensive chemical and functional analogy to *in vivo* astrocytes and can recapitulate numerous features and expressions of *in vivo* brain astrocytes (Syapin *et al.*, 2001). Moreover, these cells include gene induction by proinflammatory cytokines (Murphy *et al.*, 1993) which is essential for the CINC-1 detection experiment.

7.3.1.1 Routine cell culture and passage of C6 cells

C6 glioma cell line (passage 6) was purchased from ATCC® laboratories. The culture media of C6 cells comprised F-12 medium, supplemented with fetal bovine serum to a final concentration of 2.5% $^{v}/_{v}$ and horse serum to a final concentration of 15% $^{v}/_{v}$. The C6 cells were incubated at 37°C in a humidified, 5% CO_2, 95% air atmosphere (Sanyo-MCO715). Cell stocks were maintained by routinely culturing as monolayers at a seeding density of 2×10^4 cells/cm^2 in T-75, surface treated polystyrene flasks for cell culture. The medium was changed every 2 days after washing with PBS to remove cell debris. The cells were allowed to grow to approximately 80-90% confluence prior to routine passage. Passage was carried out by trypsinisation (0.05% $^{w}/_{v}$ trypsin/EDTA for 5 minutes at 37°C, 5% CO_2 and 95% air). Cell suspensions were removed from the flask and centrifuged at 500 ×g for 5 minutes. Cell pellets were re-suspended in fresh medium and cells counted using a haemocytometer.

7.3.1.2 Freezing and storage of C6 cell stocks

Cells at passages between 7 to 10 at 90% confluence were used to obtain a stock of cells. The freezing media comprised of 10% $^{v}/_{v}$ DMSO solution in C6 cells culture medium. The cell pellet was resuspended in this freezing solution at 0.5×10^6 cells/mL then 1 mL was transferred into sterile cryovials. Cells were frozen slowly (approximately -1°C *per* minute, to -70°C) and then transferred to liquid nitrogen for long term-storage.

7.3.1.3 Thawing of C6 glial cells from freezing

The C6 glial cells vial was thawed by gentle agitation in a 37°C water bath for approximately 2 minutes. Once thawed, the vial was removed from the water bath and sprayed with 70% $^{v}/_{v}$ ethanol. The vial contents were transferred to a centrifuge tube containing 9 mL complete culture medium and centrifuged at 500 ×g for 5 minutes (Sigma/Phillips-Harris 2K15). The supernatant was decanted and the cell pellet was resuspended in 1 mL of complete culture medium before seeding into a T-25 surface treated polystyrene flask containing 9 mL of complete culture medium.

7.3.1.4 Preparation of 24-well plate for experiments

The cells were seeded in 24-well plates at a seeding density of 2×10^4 cells/cm^2 and left to grow to 80% confluence (2-3 days). Prior to treatment, the cells were washed with PBS and the medium in the wells was replaced by 1 mL of fresh complete culture medium for each well. Prior to the LDH assay, the cells were treated with different concentrations of TNF-α (10, 25, 50 and 100 ng/mL) to determine the highest concentration of TNF-α that will produce a maximum inflammatory response in the C6 glial cells without causing excessive cell death at the same time. The cells were treated with the chosen concentration of TNF-α plus 100 μM

of each substance under investigation (free MP, F-Gen0K-MP, F-Gen1K-MP and GSH-F-Gen0K-MP). Cells treated with TNF-α only were considered as positive control, while treatment-free cells were used as negative control. The culture supernatant was collected after 6 and 24 hours and stored at -20°C and tested to measure the LDH release levels and the inflammatory marker, CINC-1 levels.

7.3.2 Measurements of LDH release levels

Samples from C6 cells treated with TNF-α and free MP, F-Gen0K-MP, F-Gen1K-MP and GSH-F-Gen0K-MP as well as untreated cells were subjected to the LDH release experiment using the same procedure and equipment detailed in Section 3.2.2. The samples were collected after 6 and 24 hours (to detect early cytotoxicity after 6 hours of treatment and delayed effects after 24 hours of treatment).

7.3.3 Measurements of CINC-1 levels

A rat CINC-1 ELISA kit was used to measure the levels of CINC-1 release from glial cells. This assay is based on the sandwich enzyme-linked immunosorbent assay (ELISA) principle (Figure 7.2). The wells of the supplied microtiter plate were pre-coated with a CINC-1 capture antibody. CINC-1 antigen in the added standards or samples will bind to this capture antibody and any unbound standard or sample was washed away. A biotin-conjugated detection antibody was then added which binds to the captured antigen (CINC-1) and the unbound form of it was washed away. An avidin-HRP conjugate was then added to the wells to bind to the biotin with removal of any unbound avidin-HRP conjugate by washing. A colour development was produced by adding TMB substrate which reacts with the HRP enzyme. The reaction was stopped by adding sulfuric acid to terminate colour development reaction. Finally, the optical density of each well was measured at a wavelength of 450 nm. The concentration of CINC-1 in the unknown samples was measured using an optical density standard curve generated by a series of standard concentrations in order to determine its CINC-1 concentration.

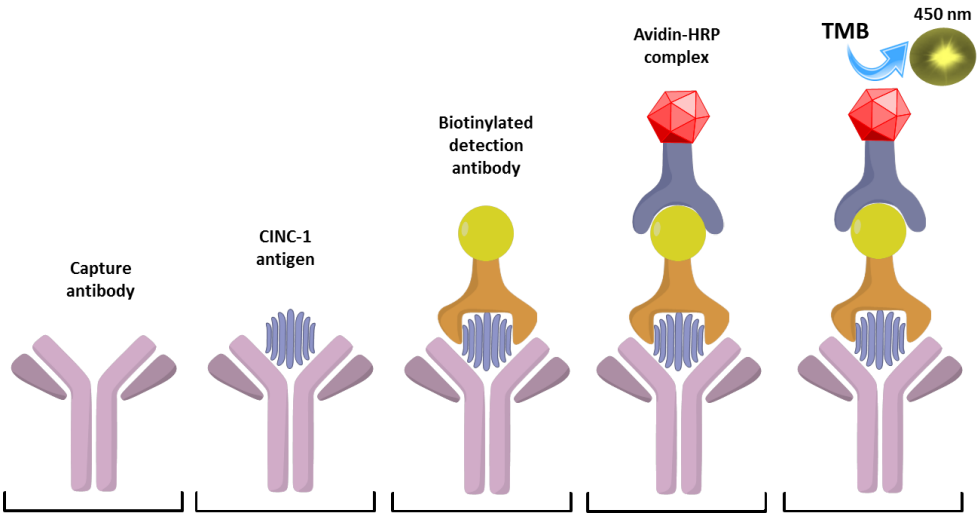

Figure 7.2 The principle of sandwich ELISA kit for quantitative determination of CINC-1 levels released from inflamed neuroglial cells.

The standard solutions of CINC-1 were prepared by adding 500 µL of assay diluent B solution to CINC-1 lyophilised standard vial (both supplied with the kit) with gentle mixing to dissolve the powder to prepare a 50 ng/mL standard-stock solution. Using assay diluent B as a diluent, the stock-standard solution was employed to produce a dilution series ranging from 0.1875 to 12 ng/mL of CINC-1 protein. Assay diluent B serves as the zero-standard (0 ng/mL).

The biotinylated antibody reagent solution was prepared by adding 100 µL of assay diluent B into the biotinylated antibody vial (supplied with the kit) to prepare a concentrated solution then diluted 80-fold with assay diluent B to prepare the final solution. The streptavidin-HRP reagent solution was prepared by diluting its vial (supplied with the kit) 200-fold with assay diluent B. The wash buffer (supplied with the kit) was prepared by mixing with deionised or distilled water in a 1:20 ratio.

Eighty percent confluent C6 glial cells were treated with 25 ng/mL of TNF-α alone or a mixture of TNF-α plus 100 µM of the tested materials (free MP, F-Gen0K-MP, F-Gen1K-MP and GSH-F-Gen0K-MP). Samples (culture media) were collected after 6 and 24 hours to detect the early and delayed release of CINC-1 based on the half-life of the drug (16 hours for MP).

The analysis was performed by adding 100 µL of each standard and sample into the pre-coated 96-wells plate supplied with the kit. The wells were covered and incubated for 2.5 hours at room temperature with gentle shaking. Following incubation, the solution was

discarded from the wells and washed 4 times with 300 μL wash buffer each time with complete removal of liquid at each step to ensure better performance. After the last wash, any remaining wash buffer was removed by aspirating or decanting and inverting the plate with blotting it against clean paper towels. To each well, 100 μL of prepared biotinylated antibody solution was added and incubated for 1 hour at room temperature with gentle shaking. The solutions in the wells were discarded and washed again 4 times with 300 μL wash Buffer. After removing all solutions, 100 μL of prepared streptavidin-HRP solution (supplied with the kit) was added to each well and further incubate for 45 minutes at room temperature with gentle shaking. Following discarding of the solutions and the washing, 100 μL of TMB substrate (supplied with the kit) was added to each well and incubated for the last time for 30 minutes at room temperature in the dark with gentle shaking. The reaction was stopped by adding 50 μL of stop solution (supplied with the kit) and the plate was evaluated within 30 minutes of stopping the reaction by measuring absorbance on ELISA microplate reader (ELx800/BIO-TEK/USA) at 450 nm wavelength. CINC-1 levels were calculated with reference to a standard curve.

7.3.4 Statistical analysis

Any significant difference in mean between groups was reported after verifying normality of data, and carrying out a one-way ANOVA with Tukey's *post-hoc* test, using the Minitab® 17 (version 17.2.1) statistical analysis program. The means ($n=6$) were compared and differences were considered significant at $P<0.05$ (two-sided confidence intervals).

7.4 Results

C6 glial cells were fast growing cells and reached 80% confluence within 2-3 days of culturing. These cells provide structural and metabolic support for neuronal networks by their numerous projections which surround the neurons (Figure 7.3).

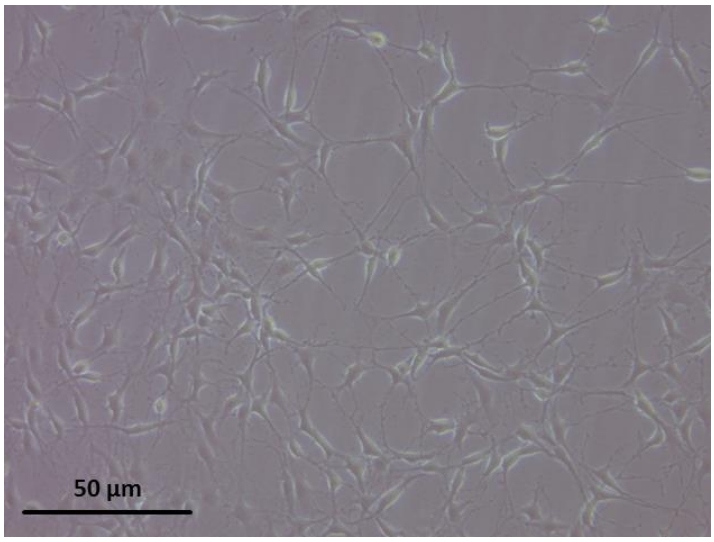

Figure 7.3 Phase-contrast light microscopy image of C6 glial cells after 24 hours of culturing. The cells connected to each other to form networks by their numerous projections.

7.4.1 LDH release assay

Cells treated with 50 and 100 ng/mL TNF-α for 24 hours showed excessive LDH release levels reaching 70% and 71.4% respectively (exceeding the LD_{50} limit). While cells treated with 10 and 25 ng/mL TNF-α for the same exposure period showed 34.2% and 35.5% LDH release respectively (below the LD_{50} limit) with no significant difference between the two values ($P>0.05$) and significantly different ($P<0.05$) from the 50 and 100 ng/mL concentrations (Figure 7.4).

Light microscopy images of C6 glial cells (Figure 7.5) treated with different concentrations of TNF-α revealed severe aggregation and contraction of cells treated with high concentrations (50 and 100 ng/mL). These morphological changes were also observed in cells treated with the low concentrations (10 and 25 ng/mL), but to a much lower severity and extent.

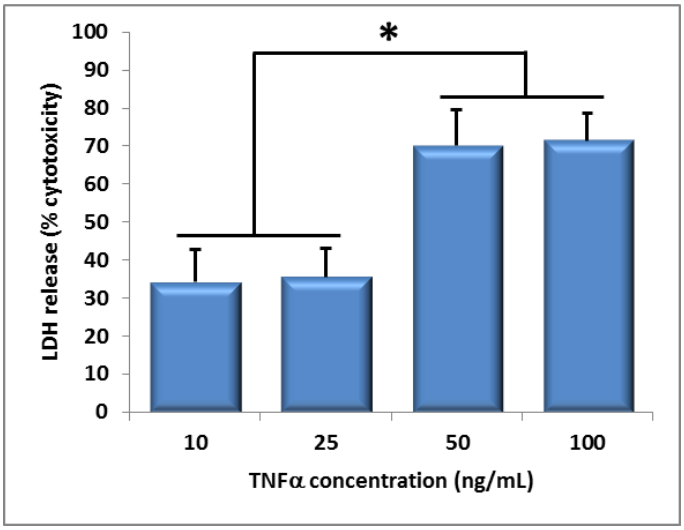

Figure 7.4 LDH release levels from C6 glial cells treated with different concentration of TNF-α for 24 hours. Results are expressed as mean ±SD (*n=6*). Higher doses (50 and 100 ng/mL) caused significantly higher ($p<0.05$) LDH release when compared to lower doses (10 and 25 ng/mL). The (*) indicates significant difference with P value equal or less than 0.05.

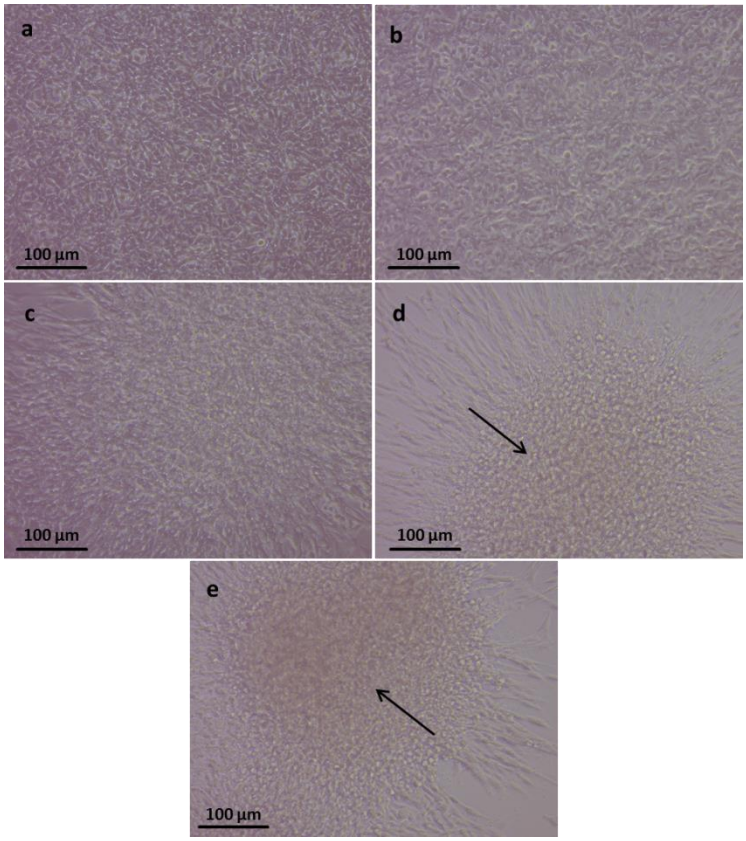

Figure 7.5 Light microscopic images of C6 glial cells treated with different concentrations of TNF-α for 24 hours. (a) Control cells (untreated). (b) Cells treated with 10 ng/mL concentration of TNF-α. (c) Cells treated with 25 ng/mL concentration of TNF-α. (d) Cells treated with 50 ng/mL concentration of TNF-α. (e) Cells treated with 100 ng/mL concentration of TNF-α. High concentrations caused severe cell deformation and aggregation into large clumps as indicated by the arrows.

Thus, the 25 ng/mL concentration of TNF-α was chosen for CINC-1 and LDH experiments to avoid causing cell death higher than the LD_{50} and attempt to achieve the maximum level of CINC-1 release.

The LDH release levels of the C6 glial cells treated with 100 μM of free MP, F-Gen0K-MP, F-Gen1K-MP and GSH-F-Gen0K-MP together with 25 ng/mL of TNF-α after 6 and 24 hours exposure periods are illustrated in Figure 7.6. The values were compared with cells treated with TNF-α only (positive control). The results indicated a significant decrease ($P<0.05$) in LDH release after 6 hours from cells treated with free MP, F-Gen0K-MP, F-Gen1K-MP and GSH-F-Gen0K-MP plus 25 ng/mL concentration of TNF-α when compared with cells treated with TNF-α only. However, such a difference was not observed after the 24 hours exposure period. Moreover, no significant difference was detected when comparing LDH release levels of cells treated with free MP, F-Gen0K-MP, F-Gen1K-MP and GSH-F-Gen0K-MP plus 25 ng/mL of TNF-α at either 6 or 24 hours exposure. Finally, the levels from all tested materials were significantly higher ($P<0.05$) than the negative control group (untreated cells) after both exposure periods.

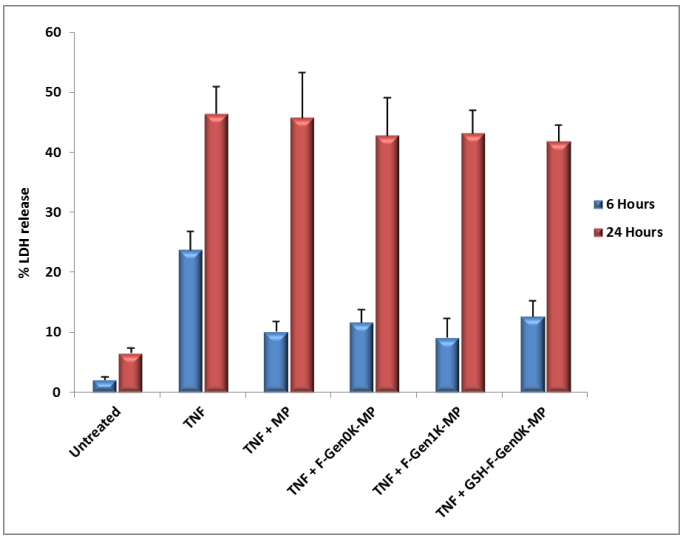

Figure 7.6 LDH release levels from C6 glial cells treated with 100 μM of free MP, F-Gen0K-MP, F-Gen1K-MP and GSH-F-Gen0K-MP together with 25 ng/mL of TNF-α after 6 and 24 hours exposure periods. Results are expressed as mean ±SD (*n=6*). Cells treated with 25 ng/mL of TNF-α were considered as positive control while untreated cells were considered as negative control. All tested material showed significant decrease ($P<0.05$) in the levels of LDH release compared to positive control after 6 hours of exposure period but not the extended duration (24 hours). No significant difference ($P>0.05$) was detected when comparing the levels of tested materials (free MP, F-Gen0K-MP, F-Gen1K-MP and GSH-F-Gen0K-MP) against each other in both exposure periods.

7.4.2 CINC-1 release modification by free and attached MP from C6 glial cells

The values obtained from the CINC-1 standards were used to plot a standard curve of CINC-1 concentration versus the absorbance (Figure 7.7).

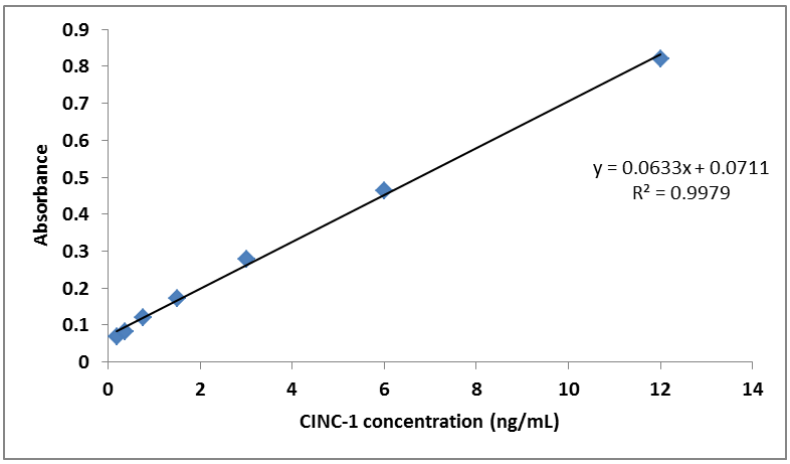

Figure 7.7 Standard curve of CINC-1. The x axis represents the concentration of standard solutions of CINC-1 used (ng/mL) and the y axis represents the corresponding absorbance.

CINC-1 concentrations detected in the media from C6 cells treated with TNF-α and each material under investigation are shown in Figure 7.8. All tested materials (including untreated cells) exhibited significantly lower CINC-1 release levels ($P<0.05$) after 6 hours of exposure when it was compared with its corresponding values after 24 hours.

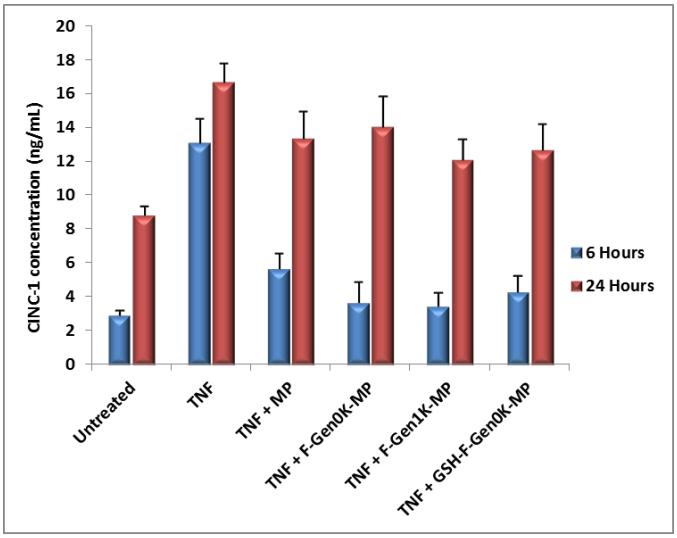

Figure 7.8 CINC-1 release levels from C6 glial cells treated with 100 μM of free MP, F-Gen0K-MP, F-Gen1K-MP and GSH-F-Gen0K-MP together with 25 ng/mL of TNF-α after 6 and 24 hours exposure periods. Results are expressed as mean ±SD (*n=6*). Cells treated with 25 ng/mL of TNF-α were considered as positive control while untreated cells were considered as a negative control. All tested materials showed a significant decrease ($P<0.05$) in the levels of CINC-1 release when compared to the positive control after 6 and 24 hours of exposure periods.

The results were further analysed statistically to detect any significant differences between different groups (Tables 7.2 & 7.3). The C6 glial cells treated with TNF-α only exhibited significantly higher ($P<0.001$) CINC-1 levels than untreated cells after both 6 and 24 hours exposure periods. These data provided the evidence that spiking C6 glial cells with TNF-α was successful causing elevated cell death indicated by raised LDH levels and triggers neuroinflammation confirmed by elevated inflammatory cytokines release levels. Adding free MP, F-Gen0K-MP, F-Gen1K-MP and GSH-F-Gen0K-MP to cells subjected to TNF-α treatment resulted in a significant reduction ($P<0.005$) of CINC-1 levels after 6 and 24 hours of exposure compared with cells treated with TNF-α only for the corresponding periods. These data suggest the ability of both forms of MP (free and conjugated) to lower the inflammatory status in the glial cells. A significantly higher CINC-1 concentration was observed from cells treated with free MP ($P=0.006$) when compared to untreated cells after 6 hours of exposure. However, such a difference was not detected when comparing the values of cells treated with F-Gen0K-MP, F-Gen1K-MP and GSH-F-Gen0K-MP with untreated cells for the same duration of exposure. No significant difference ($P>0.05$) was noticed when comparing CINC-1 release levels from cells treated with F-Gen0K-MP, F-Gen1K-MP and GSH-F-Gen0K-MP against each other after 6 hours of exposure. However, all three materials showed significantly lower values of CINC-1 compared to free MP. Such variation can be related to the higher payload of MP in the attached molecules compared to free drug (Table 7.2).

The P values generated statistically through comparing CINC-1 levels after 24 hours of exposure are shown in Table 7.3. Although, CINC-1 values of all tested materials were significantly higher ($P<0.001$) when compared to untreated cells, it was significantly lower than cells treated with TNF-α only. Moreover, for the same duration of treatment, all tested materials (free MP, F-Gen0K-MP, F-Gen1K-MP and GSH-F-Gen0K-MP) showed no significant difference ($P>0.05$) when compared against each other except when comparing F-Gen0K-MP versus F-Gen1K-MP and GSH-F-Gen0K-MP with P values equal to 0.006 and 0.014 respectively (Table 7.3).

Table 7.2 P values generated by ANOVA test comparing CINC-1 release levels from C6 glial cells treated with different tested materials plus TNF-α to the positive control (only TNF-α) and negative control (untreated cells) after 6 hours of exposure. The values were considered significantly different when the P value was lower than 0.05 (green shading).

P value (6 Hours)	Untreated	TNF-α	MP + TNF-α	F-Gen0K-MP + TNF-α	F-Gen1K-MP + TNF-α	GSH-F-Gen0K-MP + TNF-α
Untreated	-	<0.001	0.006	0.283	0.482	0.078
TNF-α	<0.001	-	<0.001	<0.001	<0.001	<0.001
MP + TNF-α	0.006	<0.001		0.001	0.003	0.017
F-Gen0K-MP + TNF-α	0.283	<0.001	0.001	-	0.621	0.081
F-Gen1K-MP + TNF-α	0.482	<0.001	0.003	0.621	-	0.104
GSH-F-Gen0K-MP + TNF-α	0.078	<0.001	0.017	0.081	0.104	-

Table 7.3 P values generated by ANOVA test comparing CINC-1 release levels from C6 glial cells treated with different tested materials plus TNF-α to the positive control (only TNF-α) and negative control (untreated cells) after 24 hours of exposure. The values were considered significantly different when the P value was lower than 0.05 (green shading).

P value (24 Hours)	Untreated	TNF-α	MP + TNF-α	F-Gen0K-MP + TNF-α	F-Gen1K-MP + TNF-α	GSH-F-Gen0K-MP + TNF-α
Untreated	-	<0.001	<0.001	<0.001	<0.001	<0.001
TNF-α	<0.001	-	0.002	0.005	<0.001	0.001
MP + TNF-α	<0.001	0.002	-	0.118	0.056	0.209
F-Gen0K-MP + TNF-α	<0.001	0.005	0.118	-	0.006	0.014
F-Gen1K-MP + TNF-α	<0.001	<0.001	0.056	0.006	-	0.345
GSH-F-Gen0K-MP + TNF-α	<0.001	0.001	0.209	0.014	0.345	-

7.5 Discussion

It is well known that glial cells are involved in neurodegenerative diseases and inflammatory processes (Pekny *et al.*, 2005). The neuroinflammation can be initiated in *in vitro* glial cells by using several types of stress factors. Stress factor refers to "any threatening situation that induces behavioural or physiological readjustments aimed to preserve homeostasis" (McEwen *et al.*, 1995). These stress factors such as bacterial endotoxin, peroxide and inflammatory cytokines will lead to an elevation in inflammatory mediators (such as CINC-1) expression in glial cells and promote cellular death (Uehara *et al.*, 1998). To mimic the neuroinflammation conditions *in vitro*, C6 glial cells were incubated in a culturing medium including TNF-α at 25 ng/mL for 6 and 24 hours. TNF-α can mediate neuroinflammation in *in vitro* models and its levels are elevated in patients with neurological disorders (Larrick *et al.*, 1990; Liu *et al.*, 1994).

After incubation, levels of CINC-1 released by the glial cells were measured and cell death was assessed by measuring LDH release levels. Choosing the right concentration of TNF-α for treatment was based on a delicate balance between promoting the highest neuroinflammatory response in the cells for better detection of CINC-1 and avoiding excessive cellular death at the same time. Treatment with the 50 and 100 ng/mL concentrations of TNF-α for 24 hours caused the death of almost 70% of the cultured C6 glial cells based on LDH release levels, and thus these concentrations were excluded. However, treatment with 25 ng/mL of TNF-α did not show such high levels of cell death and it was not significantly higher than the LDH release levels of cells treated with the 10 ng/mL concentration which favoured its choice as the optimum concentration for the treatment of the cells. Although it is reported that TNF-α was found to increase in patients with neurodegenerative diseases reaching 1 ng/mL (Mark *et al.*, 1999), using such high concentration of TNF-α (25 ng/mL) was preferred to produce the maximum induction of inflammatory response (without causing excessive cell death) rather than mimicking the exact neuroinflammation situation.

Glucocorticoids (including MP) possess powerful anti-inflammatory effects and have a varied array of effects upon the brain (Buckingham, 2006). These steroid hormones affect all brain cells, including glial cells. The actions of glucocorticoids on brain cells are mediated by the expression of corticosteroid receptors which are either mineralocorticoid receptors or GRs (Buckingham, 2006). Binding of GRs, which are highly expressed on glial cells (De Kloet *et al.*, 1998), with its ligand (MP) results in receptor translocation into the nucleus and triggers an anti-inflammatory cascade through gene transcription. Activation of GRs will enhance energy metabolism control, facilitate retrieval of cellular homeostasis, restrain stress-induced cellular

responses, encourage behavioural adaptation and promote information storage (Buckingham, 2006; de Kloet, 2003; Roozendaal *et al.*, 2001; Roozendaal *et al.*, 1996).

A previous study (Gaillard, Appeldoorn*, et al.*, 2012) has indicated the ability of conjugated MP to improve neuroinflammation in a brain model. MP was conjugated to a brain-targeting GSH-PEG liposome. When the treatment was initiated in rats with induced acute neuro inflammation, free MP showed no effect, while GSH-PEG liposomal MP remarkably reduced the clinical signs. Moreover, MP-GSH-PEG liposomes were notably more effective compared to MP-PEG liposomes (without GSH). Another study (Lee *et al.*, 2014) has indicated that a conjugated MP in a liposomal drug carrier was clinically as effective as free MP at 1/10 of the dosage as well as at a lower application frequency and significantly more effective than the same dosage of the free drug.

The extent of MP's effects on glial cells was detected by measuring the degree of change in the CINC-1 release from inflammed cells and the variation in cell death as a result of administration of the drug. Thus, the more active drug formulation results in less cell death and therefore less LDH release and lower CINC-1 levels from cells following activation with TNF-α.

The free form of MP as well as all 3 conjugated forms of the drug (F-Gen0K-MP, F-Gen1K-MP and GSH-F-Gen0K-MP) caused a reduction in LDH release after 6 hours compared to cells treated with TNF-α only (Figure 7.6) for the same period. This gave an indication that MP retained its anti-inflammatory activity even after attaching to the dendrons and GSH. However, such variation was not noticed after 24 hours of exposure (Figure 7.6). This may be attributed to drug duration of action (the half-life of MP is 16 hours) or drug stability issues caused by extending the duration from 6 to 24 hours. Studying the release profile of MP from the carrier system and its stability patterns in different conditions would provide better understanding of this issue. Such studies were not performed in this project.

All forms of MP (free and conjugated) did not cause the reduction in LDH release to reach the level of the negative control (untreated cells) even in the short duration of exposure. This may be assigned to the fact that, even with the presence of MP (free or conjugated), TNF-α will continue to exert its inflammatory effects on C6 glial cells to a certain extent. TNF-α is a cell signalling cytokine involved in inflammation and although it is released mainly by activated macrophages, it can be produced by many other cell types including neurons (Mark *et al.*,

1999). TNF-α is able to induce apoptotic cell death and its dysregulation of production has been implicated in a variety of diseases including neurodegenerative diseases (Swardfager *et al.*, 2010). Studies (Lethaby *et al.*, 2013; Moreland, 2004) have indicated that using anti TNF-α can supress its apoptotic effects and can prevent cell death. Thus, the anti-inflammatory effects of MP can explain the reduction in LDH release levels from cells treated with MP after 6 hours of exposure. Since this reduction of LDH was noticed in cells treated with free MP as well as conjugated MP, it can be assumed that the attached forms of MP retain their anti-inflammatory activities.

The observation that MP in its conjugated forms kept its anti-inflammatory activity was further supported by measuring the cytokine; CINC-1 release levels (Figure 7.8). Statistical analysis of CINC-1 levels based on P values after 6 hours of exposure to TNF-α with tested materials revealed the ability of conjugated MP to lower CINC-1 release levels compared to cells treated with TNF-α alone. Moreover, all 3 forms of conjugated MP (F-Gen0K-MP, F-Gen1K-MP and GSH-F-Gen0K-MP) caused significant lowering in CINC-1 release levels compared to cells treated with free MP (Table 7.2). This difference when compared with free MP may be attributed to the higher MP cargo in the conjugated forms when compared to equimolar concentrations of free MP. Although, equimolar concentrations of free MP and attached MP forms were used in the experiment (100 μM), the total content of MP in the attached molecules is higher than free MP. Each Gen0K-MP or GSH-F-Gen0K-MP molecule is loaded with 2 MP molecules which increase to 4 in case of F-Gen1K-MP molecule.

The same reduction of CINC-1 release levels by conjugated forms of MP, when compared to cells treated by TNF-α only, were also observed after 24 hours of exposure (Table 7.3) but with higher P values observations compared to the 6 hours experiment. These higher numbers may be related to the fact that the pro-inflammatory effect of TNF-α on the cells is dominant over MP's anti-inflammatory effect protracted exposure. Furthermore, C6 glial cells possess a very rapid population doubling time and during the 24 hours exposure periods; the starting 80% confluent cells at the onset of treatment might have reached 100% confluence leading to cellular overcrowding resulting in the triggering of inflammatory processes (Eisenhoffer *et al.*, 2012). This assumption may explain the increase in CINC-1 release levels in untreated cells after 24 hours of exposure reaching almost 3-fold the 6 hours exposure value (Figure 7.8). However, the reduction in the levels of CINC-1 release from the cells caused by these 3 conjugated forms of MP did not reach the levels of the untreated cells (which were noticed in

the short exposure period) (Table 7.3). Furthermore, unlike the observation after 6 hours of exposure, no significant difference was identified when comparing CINC-1 levels associated with the 3 conjugated forms of MP with free MP despite carrying higher contents of the drug. This lack of difference may be related once more to the predominant inflammatory effect of TNF-α after extended duration of exposure which can restrain MP effects even if the latter is used in larger doses.

Finally, the synthesised molecules, especially GSH-F-Gen0K-MP, proved the concept that the permeability of MP across the BBB model can be improved while retaining the drug pharmacological activity. Such a concept paves the way for new strategies for an efficient delivery of MP to the CNS in MS patients. Such improvement in drug delivery will result in reduction of the administrated dose to the patients thereby reducing the adverse effects associated with the drug use.

7.6 Conclusion

This chapter aimed to detect the anti-inflammatory activity of the synthesised molecules compared to free MP in neuro-inflammed cells. Examining the data generated from this chapter, the following conclusions can be drawn:

- An inflammatory response can be achieved using an *in vitro* C6 glial model by spiking the cells with TNF-α which is accompanied by an increase in cytokine release levels.
- All 3 molecules of conjugated MP (F-Gen0K-MP, F-Gen1K-MP and GSH-F-Gen0K-MP) caused a significant reduction in cell death based on LDH release levels when compared to cells treated with TNF-α only in the short duration of exposure (6 hours).
- MP in its conjugated form retained its anti-inflammatory activity based on the reductions in CINC-1 release levels from spiked C6 cells and even showed higher action compared to free MP especially after short duration of exposure (6 hours).

Chapter 8. General discussion, study conclusions and future study

8.1 General discussion

In recent decades, increases in life expectancy, plus changing population demographics have caused an elevation in the incidence of CNS disorders and their further increase is predicted to be significant in the 21st century (Chen *et al.*, 2012). Among CNS diseases, neurodegenerative conditions are the most challenging to treat and are characterised by age-linked gradual decline in neurological function, usually accompanied by neuronal death (Rotman *et al.*, 2015). Alzheimer's disease, Parkinson's disease, Huntington's disease and MS are some examples of neurodegenerative diseases and each one of them has been characterised in terms of disease mechanisms (Barchet *et al.*, 2009).

Lack of efficient delivery of drugs through the BBB is a prime limiting factor in the successful treatment of such neurodegenerative diseases. The specialised endothelium of the brain microvessels, which constitute most of the BBB, preserves brain homeostasis by restricting the influx of molecules and cells and controlling the efflux of a variety of molecules, including therapeutic drugs. Yet, the BBB enables the supply of nutrients and other essential compounds as well as the extrusion of waste materials out of the brain. Anatomically, the organisation of the BBB is composed of endothelial cells, basal lamina, astrocytes end-feet and pericytes (Bernacki *et al.*, 2008). Unlike the systemic endothelium, endothelial cells of the BBB are firmly connected to each other *via* TJs and adherence junctions, and consequently lack fenestrations between adjacent cells (Ballabh *et al.*, 2004). These special anatomical features of TJs strands "zip" adjacent endothelial cells and close the paracellular space for access of blood-borne molecules. The unique structural arrangement is further stabilised by ZO-1, -2 and -3 proteins that act as a linker between the TJ and the actin cytoskeleton (Fernandes *et al.*, 2010).

Despite its role in preventing random penetration of molecular compounds into the brain, the BBB does permit selective entry of nutrients and regulatory factors such as enzymes and hormones into the brain (Pardridge, 2007). Thus, the BBB endothelial cells enable transport of molecules both in a passive, gradient-driven mode and by an active, energy-dependent mechanism. Some small molecules with suitable lipophilicity, MW and charge may diffuse from the blood through the BBB into the CNS (Pardridge, 2005a). Polar molecules such as glucose, amino acids and several peptides have specific carriers expressed on the endothelium cell membranes. These carriers are highly selective transporters and can mediate transport into the endothelium cytosol. Yet, the vast majority of small molecules (MW<400 Da) and large molecules such as proteins and peptides do not cross the BBB (Pardridge, 2007).

Potential treatments for brain-related diseases are severely hampered based on the fact that numerous possible drug candidates are recognised as "brain-hostile", thus, precluding their permeability through the BBB into the brain (Chen *et al.*, 2012).

One of the most well-known neurodegenerative diseases is MS. MS is a leading cause of chronic disability that predominantly affects young adults (between 30-40 years old) (Vosoughi *et al.*, 2010). The disease is characterised by the infiltration of the CNS by leukocytes causing overt inflammation and demyelination of the neurons, resulting in neuronal dysfunction. This chronic disease manifests itself by attacks (relapses) and phases of relative quiescence (Reichardt *et al.*, 2006). The disease is not currently curable and treatments aim to delay neuronal damage and relieve symptoms, especially those caused by the acute-relapse episodes. Glucocorticoids are the drugs of choice for the treatment of MS acute-relapse phases (Berkovich, 2013). These drugs can act systemically as well as locally inside the brain since its receptors (GRs) are widely expressed in most cell types (Buckingham, 2006). The current therapeutic approach for acute MS relapses is mainly dependant on MP (Brusaferri *et al.*, 2000), applying doses ranging from 500 mg to 1000 mg of the drug *per* day with some dose-response effect (Oliveri *et al.*, 1998). Although using such high doses (almost 20-fold the stated dose of MP) is necessary, the risk-benefit ratio is very high (Lee *et al.*, 2014).

Poor penetration of MP through the BBB to reach the brain obligates the use of such high doses. Despite its beneficial therapeutic effects, MP in such raised doses will result in many adverse effects in the treated patients. MP, like other corticosteroid drugs, is associated with several adverse effects especially in prolonged use and high daily doses. The main adverse effect are thin skin, fatigue, elevated blood pressure, metabolism and electrolyte balance disturbance, immune suppression, and gastrointestinal system disturbance (Schacke *et al.*, 2002). Although most serious adverse effects occur in the long-term oral administration, short-term corticosteroid-induced symptoms are common, especially with high-dose treatment needed to treat MS relapses (Jongen *et al.*, 2016) causing a disturbance to patients and affect their quality of life (Guidry *et al.*, 2009).

To overcome this problem, research efforts are currently focused on developing and applying safe and efficient delivery carriers, capable of promoting MP transport across the BBB to improve the efficacy of treatment and reduce MP side-effects. Such novel drug delivery approaches for MP and other poorly penetrating drugs to the CNS represent a wide and important field of drug research and development (Georgieva *et al.*, 2014). Ideally, DDSs

should not cause toxicity or trigger an immune response, should be biocompatible, biodegradable and stable in the blood-stream with prolonged circulation time. Furthermore, they should bear a specific site-targeted moiety (such as a ligand), maintain parent drug stability and release cargo at the desired site (Ulbrich *et al.*, 2011).

Usually, a DDS includes a carrier having functional surface groups, a cargo (drug or other molecule) that is either covalently attached or encapsulated into the carrier and a suitable ligand (based on the targeted site) grafted on the surface of the carrier (Pardridge, 2006). Several carriers can be used in DDSs each with its own specific advantages and drawbacks. Among these carriers is the emerging polymeric architectures, dendrimers.

Currently, dendrimers are widely used in a variety of industrial, cosmetic, diagnostic and biomedical applications (Ebelegi *et al.*, 2017; Madaan *et al.*, 2014; Pedro *et al.*, 2017). Dendrimers are well recognised for their defined and highly controllable structures, versatility in drug delivery field and high functionality by offering a wide potential for multiple interactions (Svenson *et al.*, 2005). These well-defined macromolecules have shown their potential abilities to entrap and/or conjugate the high MW hydrophilic/hydrophobic molecules by host-guest interactions and chemical covalent bonding, respectively. Owing to these properties, plus the high ratio of surface groups to molecular volume, has led to the development of new DDSs using dendrimers as carriers (Tanis *et al.*, 2009). Using the amino acid, lysine, as a branching unit offers the ability to attach more drug moieties to its peripheral amine groups with increasing generations of the dendron. Different therapeutic moieties were incorporated in DDSs using dendrimers as a platform carrier (Madaan *et al.*, 2014; Prashant *et al.*, 2014). However, utilising dendrimers to improve MP penetration to the brain has not yet been investigated.

Attachment of MP to Gen0 and Gen1 dendrons by SPPS was successfully achieved by covalently conjugating the carboxyl group of MP to the functional amine groups of the dendrons to form an amide linkage. Governing the coupling and deprotection protocols, plus the tight control on the cleavage process (removal of the synthesised molecule from the solid support) were crucial factors for the drug attachment. One of the limitations of using SPPS is based on the fact that using a different MP salt that lacks the carboxyl groups makes it very difficult to attach MP covalently to the dendrons. An alternative method to conjugate these MP salts to the dendron carriers is to entrap the drug molecules by the molecular architecture of the dendrons rather than chemical binding. However, to construct such "drug-cage"

structures, higher generations of dendrons must be used (Gen3 and above) causing an increase in the MW of the final molecule with the potential of lower permeability. Another limitation is the difficulty to synthesise the dendrimer-MP in large quantities, due to repeated reaction occurring during the coupling process that necessitates the protection of active site. However, such a drawback had a limited impact in this project since the synthesis was conducted on a laboratory scale. Using Gen0 dendron assured the coupling of 2 moieties of MP by its 2 peripheral amine groups with double that number (4) by using Gen1 dendron, resulting in an increase in the total cargo of MP which is a crucial factor to improve MP delivery to the desired site of action. MP in its conjugated form showed better BBB model penetration by almost 8 fold compared to free MP (when considering its total cargo of MP) which in turn may potentially lower the administered dose of MP to MS patients to 12% of the current used dose (from 1000 to 120 mg *per* day). Such a reduction in MP has the potential to result in a marked reduction in its adverse effects in MS patients.

The covalent binding of MP to the dendrons *via* chemical bonding (amide linkage) rather than its complexation or entrapment offered an additional advantage. The amide bonds are very stable in aqueous solutions and at physiological pH and it has been proposed that among all lysosomal proteases, cathepsin B enzyme is primarily responsible for the cleavage of the amide linkage (D'Souza *et al.*, 2004). Further studies on the peptide linkage have found it to be stable in plasma, but cleavable by cellular cathepsin (D'Souza *et al.*, 2004; Madaan *et al.*, 2014).

Results from other studies have also shown that polyamide dendrimers, in comparison to other types of linkages have higher stability due to their lower rate of hydrolysis in systemic circulation (Khandare *et al.*, 2011). Direct amide linking of naproxen (non-steroidal anti-inflammatory drug) with PAMAM dendrimer showed a higher chemical stability in plasma and liver homogenate and in different pH buffers including 7.4 and 1.2, than that of ester linking (Najlah *et al.*, 2006). Moreover, using biodegradable units (dendrons) as carrier system will not only be beneficial for the final dissociation of the molecule but also may result in reduction in toxicity as the linking bonds can be proteolysed by cellular enzymes (Prashant *et al.*, 2014; Xu *et al.*, 2014).

Although using dendrimers as a carrier for MP can improve the cargo load of the drug, it may not necessarily ensure improvement in its penetration across the BBB (Madaan *et al.*, 2014). Thus, one of the current approaches to efficiently allow active compounds such as MP to cross into the brain is to decorate their carriers by endogenous substances that can act as a

"Trojan horse" to be recognised and transported across the brain endothelium *via* RMT. One of the most recent utilised substances is the endogenous antioxidant, GSH. Receptors for this molecule are widely expressed on BBB endothelial cells (Gabathuler, 2010) and it can exist in brain, astrocyte and endothelial cells in mM concentrations (Zlokovic, 1995).

Synthesising GSH and attaching it to the dendron-MP was achieved by SPPS owing to the fact that GSH is formed of 3 amino acids and can be easily synthesised by the convergent method especially for low-scale synthesis. Synthesising GSH-F-Gen0K-MP represented a huge step forward in this project. This step indicated the ability to conjugate MP in a dendron-based carrier with a higher cargo plus the potential enhancement in its penetration across the BBB by grafting it with GSH.

One of the main limitations of using dendrons for drug delivery is its potential for cellular toxicity. The positive charge of the functional amine groups of the dendrons can easily interact with the negatively-charged cell membranes causing its lysis and eventual cell death (Prashant *et al.*, 2014). Although the positive charges of dendrons were hidden by grafting MP to them, the synthesised dendron-MP molecules with and without GSH are still novel molecules and their toxicity patterns may be quite different from the parent molecules (free MP and dendrons) and needed to be studied. Using different toxicity assays to test the modified MP and compare them with free MP can provide a complete picture of the toxicity patterns of these molecules. Such overall patterns can reveal not only the toxicity levels and whether they are within the acceptable range or not, but it can also highlight other issues such as the causes or mechanisms behind this toxicity and the possible rise in late toxicity (initiation of apoptotic response prior to cell death).

One of the most interesting results revealed from analysing toxicity assay data was the toxicity profile of the final DDS, GHS-F-Gen0K-MP. The data indicated a reduction in the toxicity levels induced in b.End3 cells treated with GHS-F-Gen0K-MP when compared to equimolar concentrations of free MP. Powerful GSH anti-oxidant activity could be the key factor and may explain such variation in toxicity levels. GSH is capable of preventing damage to essential cellular elements induced by reactive oxygen species like free radicals, peroxides, lipid peroxides and heavy metals (Pompella *et al.*, 2003). However, it should be kept in mind that GSH can only exert this action in its free form after dimerisation with other GSH molecule (Figure 4.3) to form reduced GSH. This suggests partial dissolution of GSH from the DDS in the culture medium with time. Shedding more light on this issue by studying the dissociation

of the DDS to release its cargo of free drug (MP) and the ligand (GSH) was not performed during this project.

A major challenge for the discovery and development of novel drugs intended to treat neurodegenerative diseases is the establishment of an *in vitro* model that can mimic the BBB. Different *in vitro* BBB models, applying primary brain capillary endothelial cells from different sources have been developed which exhibit a broad and uneven spectrum of features (Mária *et al.*, 2005). In most BBB models, a monolayer of brain endothelium forming TJs is grown on a synthetic microporous membrane filter culture insert. Choosing the most suitable BBB *in vitro* model such as the type of endothelial cells, type of inserts, and type of model (single or co-culture models) was part of the aims of this study. Moreover, the constructed *in vitro* model must be validated prior to any quantitative-penetration experiments (Omidi *et al.*, 2003).

In order to elucidate the ability of b.End3 cells cultured on Transwell insert to form TJs between adjacent cells, the *in vitro* model was validated by measuring TEER readings and paracellular permeability to a soluble probe and comparing it to data obtained from negative control cells (HUVEC). The b.End3 cells used to construct the model cannot only form TJs between adjacent cells, but also GSH receptors are highly expressed on its membrane which was confirmed by confocal microscopy imaging. This validation was not only performed to assure formation of a confluent monolayer with high TJ expression, but also to ascertain the exact day in culturing to display the highest barrier functions to be used in the penetration experiments. Several studies using different types of endothelial cells and different paracellular probes have been carried out for basic TJs characterisations and barrier functions and therefore such investigation was not considered in this study (Boveri *et al.*, 2005; Eigenmann *et al.*, 2013; Hayashi *et al.*, 2004; Omidi *et al.*, 2003).

The quantitative determination of the amount of the drug passing through these *in vitro* BBB model is another challenge. Traditional quantitative techniques such as fluorescent assays and radiometric detection-based assays are not applicable in many cases (due to lack of fluorescent moieties or inapplicable attaching radio-labelled probes). Despite all the efforts to optimise the protocol for quantitative determination of conjugated MP (F-Gen0K-MP, F-Gen1K-MP, GSH-F-Gen0K-MP), fluorescent assays were not applicable in this project. The problem emerged as a result of using culture medium which can interfere with the colorimetric determination of the synthesised molecules. Using PBS as a solvent would solve the issue but

it can support cells viability only for short periods of time (30-60 minutes) and cannot be used for relatively long-duration studies (hours and days) of drug penetration.

As an alternative to colorimetric assays, HPLC was employed for the quantitative determination of the synthesised molecules-penetration across the BBB model. HPLC was used to quantify free and attached drug levels by collecting samples from the acceptor chamber of Transwell inserts. The tests were performed only after extensive study to govern the exact method of HPLC protocols especially the type of mobile and stationary phases, the exact maximum wavelength for detection, mass of drug injected and the flow rate. HPLC was also used to purify the samples from any remaining contaminants acquired during the synthesis and cleavage process. No report has been found where MP detection by HPLC has been applied to Transwell cultures of b.End3 cells.

Decorating the carrier system with the ligand (GSH) dramatically increased the penetration of conjugated MP across the *in vitro* BBB compared to free MP. This increment in MP penetration was doubled when considering the total cargo of MP since 2 moieties of the drug are conjugated in each single drug-carrier molecule. These data confirmed the uptake of the carrier system by the b.End3 cells by recognising GSH as a biospecific molecule. Indeed, applying dendrons alone (without GSH) also resulted in an increase in MP permeability but to a lesser extent than GSH-grafted dendrons and it was limited by the MW of the final molecule. The enhanced permeability of GSH-dendron-MP over free MP and non-targeted dendron-MP proves the concept that enhanced delivery of MP across the BBB model has the potential to be beneficial for the future treatment of neuroinflammation associated MS relapses. It may also be used for further research into the treatment of neuroinflammation associated with other CNS disorders such as Alzheimer disease and Parkinson disease.

MP exerts its biological activity (anti-inflammatory effect) by binding to its receptors (GRs) in the nuclear membrane and initiating a cascade of anti-inflammatory response. Such "key and lock" binding is totally dependent on the exact molecular structure of MP (Pelt, 2011). Despite the vast improvement in conjugated MP permeability across the BBB model, it should be kept in mind that modifying MP by grafting it to the carrier system may result in partial or total loss of the drug pharmacological activity due to loss of affinity between the modified MP and its target receptors. Retaining the anti-inflammatory activity in conjugated MP (see Chapter 7) suggests that the attachment did not affect the chemical moieties of MP that interact with its receptor-domains on target cells (glial cells). The effect of MP modification

(by attaching to the dendron carrier) on its activity is novel information that has not been reported in previous studies.

Finally, in 2008, it was reported that the worldwide economic burden caused by neurodegenerative diseases has reached over UK £1.7 trillion *per* year, and it is likely that this cost will continue to grow with the increasingly ageing population (NeuroInsights, 2008). Treatments for many neurodegenerative diseases are not yet widely available due to the presence of the BBB. Despite the various routes for drug delivery to the brain, the most suitable approach for the treatment of CNS diseases will be best achieved by safely promoting the non-invasive blood-to-brain delivery of drugs using DDS that utilise endogenous endothelial transporters. Using dendrons as the carrier systems for such DDSs can protect carried drugs against systemic circulation. This carrier-drug stability in the systemic circulation in turn may reduce undesired interactions with health tissues during the delivery process and thereby lower their systemic toxicity (Popova *et al.*, 2016). This could allow the formulation of MP in this conjugated form to be administrated to the patients as parenteral injection to circulate in blood for enough time without losing the drug activity or affecting healthy tissues.

8.2 Study conclusions

Findings from this study have led to the following conclusions:

i. MP hemisuccinate salt can be covalently grafted efficiently to GSH-dendrons DDS by SPPS. The drug is attached to the dendrons covalently by the formation of amide linkages between the carboxyl groups of the drug the peripheral amine groups of the dendrons during the synthesis of the carrier thus ensuring a controlled grafting. The carried cargo of the drug by dendrons will increase with the dendron generation (Gen0 can host 2 MP moieties compared to 4 moieties of MP carried by Gen1 dendrons).

ii. The synthesised molecules are non-cytotoxic according to current cytotoxicity testing protocols. Moreover, using GSH (strong anti-oxidant molecule) as the ligand in the DDS results in lowering the cytotoxicity of modified MP compared to free MP.

iii. Consistent with the literatures, using an *in vitro* BBB model composed of endothelial cells (b.End3) cultured on Transwell inserts can be applied for quantitative determination of the permeability of the novel synthesised molecules.

iv. As predicted, the presence of GSH in the DDS improved the permeability of MP across the BBB model with enhanced bioavailability at the targeted site of action achieved by using dendrons as carriers.

v. Despite the molecular structure modification of MP after its grafting to the DDS, the drug retained its anti-inflammatory activity.

These conclusions are reached from analysing the outcomes of the *in vitro* experimental work carried out within this investigation. The study can be described as having been successful in answering the main research questions of the project. It demonstrated that the ability of MP to cross BBB model can be critically improved by using RMT approach to deliver the drug to the other side of the barrier. The data generated from this study, especially the permeability experiments, provides a suitable base for other poorly penetrating medications intended for the treatment of neurodegenerative diseases. Through attempts to answer the key research questions, the initial aims of the study were achieved with regards to fully characterising and purifying the synthesised molecules. This enabled the successful cytotoxicity screening and the identification of permeability differences between biospecific and non-specific dendron carriers. The cytotoxicity testing was carried out successfully without the use of animals. Through the optimisation of an *in vitro* BBB model for the permeability studies reliable data were achieved to demonstrate that conjugated MP can retain its anti-inflammatory activity by mimicking the inflammatory situation in an *in vitro* BBB model.

8.3 Future study

Outstanding questions about the performance of the synthesis of the candidate DDS and their BBB permeability require further research. These can be formulated as new research questions to guide future investigations leading to their clinical validation:

1) What are the effects of using different core moiety on the cytotoxicity, permeability and pharmacological patterns of the final synthesised molecule?

Changing the core amino acid of the carrier dendron will result in variation in the MW of the final synthesised DDS plus alteration in its molecular structure. Such changes may in turn cause alteration in the behaviour of the final molecule that might be different from the tested molecule (GSH-F-Gen0K-MP). Using different amino acid-cores like arginine or tryptophan rather than phenylalanine may be worth studying especially regarding the effect on MP permeability across the *in vitro* BBB model. The core amino acid can greatly influence the characteristic and permeability properties of the final molecule caused by changing in MW and method of interaction with cells membrane.

2) Can higher generations of carrier dendrons improve the payload of MP through drug entrapment in the dendron architecture rather than chemical binding?

Employing higher generation dendrons (Gen3 and above) can be used to entrap more MP molecules, thus, increasing its bioavailability in the targeted tissue. The permeability studies of such relatively large MW DDS and the threshold for the ligand (GSH) to ferry them through the *in vitro* BBB models requires further investigation to shed light on these issues, but the data of this project seem to show a reduction in BBB penetration for larger dendrimers.

3) What is the effect of using *in vivo* models on the permeability studies of MP using the same novel carrier system?

Despite the advancements achieved in the past two decades in the *in vitro* BBB modelling field, mimicking the ability to reproduce all the complex functions of the BBB *in vivo* remains extremely challenging. In spite of the process of optimisation of the *in vitro* BBB model of this study, the GSH-F-Gen0K-MP, penetration efficiency cannot be achieved totally *in vitro*. Thus, measuring the enhancement in the bioavailability of the drug conjugates in the brain of live animals is a crucial factor to promote their further validation..

4) Is it possible to use this novel DDS for other poorly penetrating CNS drugs intended for neurodegenerative diseases?

After proving the enhancement in MP permeability through the *in vitro* BBB loaded by the specialised carrier system (GSH-F-Gen0K), the concept can be applied to the design of other drugs conjugates where the free molecule is limited in its penetration across the BBB. Anti-cancer drugs (such as doxorubicin), non-steroidal anti-inflammatory drugs (such as indomethacin and flurbiprofen) and gene therapy may utilise the same carrier system for better permeability results across the BBB. However, such utilisation requires further molecular design about the methods of drug grafting to the carrier system, the cytotoxicity of the final new molecules and any required drug dissociation from the carrier system.

5) What is the extent of drug accumulation in the endothelial cells monolayer?

Due to the high affinity of GSH to its receptors on the endothelial cells, some of the GSH-F-Gen0K-MP might remain entrapped in the endothelial cells rather than being transported to the other side of the barrier. Future transcytosis investigations are needed to measure the level of entrapment and its effect on elevating the neuroinflammation of the BBB itself caused by the neurodegenerative diseases.

6) What are the dissociation patterns of MP from the carrier system both *in vivo* and *in vitro*? What are the stability figures of the synthesised molecule in different storage conditions?

Measuring the extent of drug release from the carrier system in different pH buffers and biological environments (such as plasma) requires additional studies. The stability of the final molecule in different physical conditions, the effect of storage time, temperature and humidity also worth further investigations.

7) What are the pharmacokinetics of the conjugated drug and their efficacy *in vivo*?

Studying the *in vivo* properties of the synthesised molecules (such as plasma protein binding, bioavailability in the target tissue, general toxicity and the molecule fate) is an imperative necessity to take the clinical validation of these drug conjugates to the next step.

Chapter 9. References

Abbasi, E., Aval, S., Akbarzadeh, A., Milani, M.*, et al.* (2014). Dendrimers: synthesis, applications, and properties. *Nanoscale Research Letters, 9*(1), 247-247.

Abbott, N. (2000). Inflammatory mediators and modulation of blood-brain barrier permeability. *Cellular and Molecular Neurobiology, 20*, 131-147.

Abbott, N. (2004). Prediction of blood-brain barrier permeation in drug discovery from in vivo, in vitro and in silico models. *Drug Discov Today Technol, 1*(4), 407-416.

Abbott, N. (2005). Dynamics of the CNS barriers: evolution, differentiation, and modulation. *Cellular and Molecular Neurobiology, 25*, 5-23.

Abbott, N., Hughes, C., Revest, P., & Greenwood, J. (1992). Development and characterisation of a rat brain capillary endothelial culture: towards an *in vitro* blood-brain barrier. *Journal of Cell Science, 103*, 23-37.

Abbott, N., & Romero, I. (1996). Transporting therapeutics across the blood-brain barrier. *Molecular Medicine Today, 2*, 106-113.

Abbott, N., Rönnbäck, L., & Hansson, E. (2006). Astrocyte-endothelial interactions at the blood-brain barrier. *Nature Reviews Neuroscience, 7*, 41-53.

Abdullahi, W., Davis, T., & Ronaldson, P. (2017). Functional Expression of P-glycoprotein and Organic Anion Transporting Polypeptides at the Blood-Brain Barrier: Understanding Transport Mechanisms for Improved CNS Drug Delivery? *AAPS J, 19*(4), 931-939.

Abu-Rmaileh, R., Attwood D, & A, D. E. (2003). Dendrimers in cancer therapy. *Drug Deliv. Syst. Sci, 3*, 65- 70.

Adenot, M., Merida P, & R, L. (2007). Applications of a blood-brain barrier technology platform to predict CNS penetration of various chemotherapeutic agents. 2. Cationic peptide vectors for brain delivery. *Chemotherapy, 53*, 73-76.

Agashe, H., Dutta T., Garg M., & Jain N. (2006). Investigations on the toxicological profile of functionalized fifth-generation poly (propylene imine) dendrimer. *J. Pharm. Pharmacol, 58*(11), 1491-1498.

Al-Warhi, T., Al-Hazimi HM, & A, E.-F. (2012). Recent development in peptide coupling reagents. *J Saudi Chem Soc, 16*, 97-116.

Albert, E., & Kerns J. (1981). Reversible microwave effects on the blood-brain barrier. *Brain Research Review, 230*, 153-164.

Albrecht, M., Gossage R., Lutz M., Spek A., & van Koten G. (2000). Diagnostic organometallic and metallodendritic materials for SO_2 gas detection: reversible binding of sulfur dioxide to arylplatinum(II) complexes. *Chem Eur J, 6*, 1431-1445.

Andersson, P., & Goodkin, D. (1998). Glucocorticosteroid therapy for multiple sclerosis: A critical review. *Journal of the Neurological Sciences, 160*(1), 16-25.

Andrews, K., & Husmann D. (1997). Bladder dysfunction and management in multiple sclerosis. *Mayo Clin Proc, 72*, 1176-1183.

Ascherio, A., & Munger, K. (2007). Environmental risk factors for multiple sclerosis. Part II: Noninfectious factors. *Ann Neurol, 61*(6), 504-513.

Aulenta, F., Hayesa W., & Rannard S. (2003). Dendrimers: a new class of nanoscopic containers and delivery devices. *European Polymer Journal, 39*, 1741-1771.

Balda, M., Flores-Maldonado C., Cereijido M., & Matter K. (2000). Multiple domains of occludin are involved in the regulation of paracellular permeability. *J Cell Biochem, 78*, 85-96.

Balkovetz, D., Tiruppatchi C., Leibach F., Mahesh V., & Ganapathy V. (1989). Evidence for an impiramine-sensitive serotonin transporter in human placental brush-border membranes. *J Biol Chem, 264*, 2195-2198.

Ballabh, P., Braun, A., & Nedergaard, M. (2004). The blood-brain barrier: an overview. Structure, regulation, and clinical implications. *Neurobiology of Disease, 16*, 1-13.

Bandopadhyay, R., Orte C, Lawrenson J., Reid A.*, et al.* (2001). Contractile proteins in pericytes at the blood-brain and blood-retinal barriers. *J Neurocytol, 30*, 35-44.

Banks, W. (2004). The source of cerebral insulin. *European Journal of Pharmacology, 490*, 5-12.

Banks, W. (2008). Delivery of peptides to the brain: emphasis on therapeutic development. *Biopolymers, 90*, 589-594.

Barchet, T., & Amiji M. (2009). Challenges and opportunities in CNS delivery of therapeutics for neurodegenerative diseases. *Expert Opin. Drug Deliv., 6(3)*, 211-225.

Barnes, P. (1998). Anti-inflammatory actions of glucocorticoids: molecular mechanisms. *Clin. Sci. (Lond), 94*, 557-572.

Barnes, P. (2004). Mediators of chronic obstructive pulmonary disease. *Pharm. Rev, 55*, 515-548.

Barnes, P. (2006a). Corticosteroid effects on cell signalling. *J. Eur. Respir, 27*, 413–426.

Barnes, P. (2006b). How corticosteroids control inflammation. *Br. J. Pharmacol, 148*, 245–254.

Barnes, P., & Adcock I. (2009). Glucocorticoid resistance in inflammatory diseases. *Lancet, 342*, 1905–1917.

Barnes, P., Adcock I, & Ito K. (2005). Histone acetylation and deacetylation: importance in inflammatory lung diseases. *Eur. Respir. J, 25*, 552-563.

Baron-Van Evercooren, A., & Blakemore W. (2004). *Remyelination through engraftment*. San Diego: Elsevier.

Batrawi, N., Wahdan, S., & Al-Rimawi, F. (2017). A Validated Stability-Indicating HPLC Method for Simultaneous Determination of Amoxicillin and Enrofloxacin Combination in an Injectable Suspension. *Sci Pharm, 85*(1).

Beatty, W. (1999). Assessment of cognitive and psychological functions in patients with multiple sclerosis: considerations for databasing. *Multiple Sclerosis, 5*, 239-243.

Beese, M., Wyss k., Haubitz M., & Kirsch T. (2010). Effect of cAMP derivates on assembly and maintenance of tight junctions in human umbilical vein endothelial cells. *BMC Cell Biol, 11*, 68. doi: 10.1186/1471-2121-11-68

Begley, D. (2004). ABC transporters and the blood–brain barrier. *Curr. Pharm, 10*, 1295-1312.

Benjamin, K., & Tsang T. (2011). Multiple sclerosis: Diagnosis, management and prognosis. *Australian Family Physician, 40*, 948-955.

Benoiton, N. (2005). *Chemistry of peptide synthesis*. Boca Raton: Taylor and Francis.

Berezowski, V., Landry, C., Lundquist, S., Dehouck, L.*, et al.* (2004). Transport screening of drug cocktails through an *in vitro* blood-brain barrier: is it a good strategy for increasing the throughput of the discovery pipeline? *Pharm Res, 21*(5), 756-760.

Bergmann, M., Staples K., Smith S., Barnes P., & Newton R. (2004). Glucocorticoid inhibition of GM-CSF from T cells is independent of control by NF-B and CLE0. *Am. J. Respir. Cell. Mol. Biol, 30*, 555-563.

Berkovich, R. (2013). Treatment of acute relapses in multiple sclerosis. *Neurotherapeutics, 10*, 97-105.

Bernacki, J., Dobrowolska A., Nierwinska K., & Malecki A. (2008). Physiology and pharmacological role of the blood-brain barrier. *Pharmacol. Rep, 60*, 600-622.

Bickel, U. (2005). How to measure drug transport across the blood-brain barrier. *NeuroRx, 2*, 15-26.

Bidanset, D., Placidi L., Rybak R., Palmer J.*, et al.* (2001). Intravenous infusion of cereport increases uptake and efficacy of acyclovir in herpes simplex virus-infected rat brains. *Antimicrob. Agents Chemother, 45*, 2316-2323.

Birngruber, T., Raml, R., Gladdines, W., Gatschelhofer, C.*, et al.* (2014). Enhanced doxorubicin delivery to the brain administered through glutathione PEGylated liposomal doxorubicin (2B3-101) as compared with generic Caelyx,(®)/Doxil(®)--a cerebral open flow microperfusion pilot study. *J Pharm Sci, 103(7)*, 1945-1948.

Blasberg, R., Patlak C., & Fenstermacher J. (1975). Intrathecal chemotherapy: brain tissue profiles after ventriculocisternal perfusion. *J Pharmacol Exp Ther, 195*, 73-83.

Boado, J., Hui K., Lu Z., & Pardridge M. (2014). Re-engineering iduronate 2-sulfatase for penetration of the blood-brain barrier via transport on the insulin receptor. *Molecular Genetics and Metabolism, 111*(2), S27.

Boado, R., Zhang Y., & Pardridge M. (2007). Humanization of anti-human insulin receptor antibody for drug targeting across the human blood-brain barrier. *Biotechnol. Bioeng, 96*, 381-391.

Boas, U., Sontjens S., Jensen K., Christensen J., & Meijer E. (2002). New dendrimer-peptide host-guest complexes: towards dendrimers as peptide carriers. *ChemBioChem, 3*, 433-439.

Bolten, B., & Degregorio T. (2002). Trends in development cycles. *Nature Rev Drug Discov, 1*, 335-336.

Borlongan, C., & Emerich D. (2003). Facilitation of drug entry into the CNS via transient permeation of blood brain barrier: laboratory and preliminary clinical evidence from bradykinin receptor agonist. *Cereport. Brain Res. Bull, 60*, 297-306.

Bosman, A., Janssen H., & Meijer E. (1999). About Dendrimers: Structure, Physical Properties, and Applications. *Chem Rev, 99*(7), 1665-1688.

Boturyn, D., Coll J., Garanger E., Favrot M., & Dumy P. (2004). Template assembled cyclopeptides as multimeric system for integrin targeting and endocytosis. *J Am Chem Soc, 126*(18), 5730-5739.

Bourne, N., Stanberry L., Kern E., Holam G.*, et al.* (2000). Dendrimers, a newclass of candidate topical microbiocides with activity against herpes simplex virus infection. *Antimicrob Agents Chemother, 44*, 2471-2474.

Boveri, M., Berezowski V., Price A., Slupek S.*, et al.* (2005). Induction of blood-brain barrier properties in cultured brain capillary endothelial cells: Comparison between primary glial cells and C6 cell line. *Glia, 51*, 187-198.

Brana, M., Dominguez G., & Saez B. (2002). Synthesis and anti-tumor activity of new dendritic polyamines- (imide-DNA-intercalator) conjugates: potent Lck inhibitors. *European Journal of Medicinal Chemistry, 37*(7), 541-551.

Brightman, M., & Reese T. (1969). Junctions between intimately apposed cell membranes in the vertebrate brain. *Cell Biol, 40*, 648-677.

Brown, R., Egleton R., & Davis T. (2004). Mannitol opening of the blood-brain barrier: regional variation in the permeability of sucrose, but not 86Rb+ or albumin. *Brain Research Review, 1014*, 221-227.

Brown, R., Morris A., & O'Neil R. (2007). Tight junction protein expression and barrier properties of immortalized mouse brain microvessel endothelial cells. *Brain Res, 1130*(1), 17-30.

Brusaferri, F., & Candelise, L. (2000). Steriods for multiple sclerosis and optic neuritis: a meta-analysis of randomized controlled clinical trials. *Journal of Neurology, 247*(6), 435-442.

Buckingham, J. (2006). Glucocorticoids: exemplars of multi-tasking. *Br J Pharmacol, 147 Suppl 1*, S258-268.

Caminade, A., Laurent, R., & Majoral, J. (2005). Characterization of dendrimers. *Advanced Drug Delivery Reviews, 57*(15), 2130-2146.

Campbell, S., Hughes, P., Iredale, J., Wilcockson, D.*, et al.* (2003). CINC-1 is an acute-phase protein induced by focal brain injury causing leukocyte mobilization and liver injury. *FASEB J, 17*(9), 1168-1170.

Cao, G., Pei W., Ge H., Liang Q.*, et al.* (2002). *In vivo* delivery of a Bcl xL fusion protein containing the TAT protein transduction domain protects against ischemic brain injury and neuronal apoptosis. *J. Neurosci, 22*, 5423-5431.

Carrigan, C., & Imperiali, B. (2005). The engineering of membrane-permeable peptides. *Anal Biochem, 341*(2), 290-298. doi: 10.1016/j.ab.2005.03.026

Cecchelli, R., Berezowski, V., Lundquist, S., Culot, M.*, et al.* (2007). Modelling of the blood-brain barrier in drug discovery and development. *Nat Rev Drug Discov, 6*(8), 650-661.

Chan, W., & White P. (2009). *Fmoc solid phase peptide synthesis. A practical approach*. New York: Oxford university Press Inc.

Charcot, J. (1877). *Lectures on the diseases of the nervous system*. The New Sydenham Society. London, United Kingdom.

Chat, M., Bayol-Denizot C., Suleman G., Roux F., & Minn A. (1998). Drug metabolizing enzyme activities and superoxide formation in primary and immortalized rat brain endothelial cells. *Life Sci, 62*, 151-163.

Chaudhuri, J. (2000). Blood-brain barrier and infection. *Med Sci Monit, 6*, 1213-1222.

Chen, C., & Duan, Z. (2017). Peptide-22 and Cyclic RGD Functionalized Liposomes for Glioma Targeting Drug Delivery Overcoming BBB and BBTB. *9*(7), 5864-5873.

Chen, H. (2004). Cytotoxicity, hemolysis, and acute in vivo toxicity of dendrimers based on melamine, candidate vehicles for drug delivery. *J Am Chem Soc, 126*(32), 10044-10048.

Chen, T., Mackic, J., McComb, J., Giannotta, S., *et al.* (1996). Cellular uptake and transport of methylprednisolone at the blood-brain barrier. *Neurosurgery, 38*(2), 348-354.

Chen, Y., Dalwadi G., & Benson H. (2004). Drug delivery across the blood–brain barrier. *Curr. Drug Deliv., 1*, 361-376.

Chen, Y., & Liu, L. (2012). Modern methods for delivery of drugs across the blood–brain barrier. *Advanced Drug Delivery Reviews, 64*(7), 640-665.

Cho, H., Seo, J., Wong, K., Terasaki, Y., *et al.* (2015). Three-Dimensional Blood-Brain Barrier Model for *in vitro* Studies of Neurovascular Pathology. *Scientific Reports, 5*, 15222.

Choi, J., Lee, S., Na , A., Hyeon T, & Seo, T. (2010). *In vitro* cytotoxicity screening of water-dispersible metal oxide nanoparticles in human cell lines. *Bioprocess and Biosystems Engineering, 33*, 21-30.

Choi, S., Lee S., & Park T. (2006). Temperature-sensitive pluronic/poly(ethylenimine) nanocapsules for thermally triggered disruption of intracellular endosomal compartment. *Biomacromolecules, 7*(6), 1864-1870.

Clark, A. (2003). MAP kinase phosphatase 1: a novel mediator of biological effects of glucocorticoids? *J. Endocrinol., 178*, 5-12.

Cleaver, O., & Melton, D. (2003). Endothelial signaling during development. *Nat Med, 9*(6), 661-668.

Coker, G., Studelska, D., Harmon, S., Burke, W., & O'Malley, K. (1990). Analysis of tyrosine hydroxylase and insulin transcripts in human neuroendocrine tissues. *Brain Res Mol Brain Res, 8*(2), 93-98.

Compston, A., & Coles, A. (2008). Multiple sclerosis. *The Lancet, 372*(9648), 1502-1517.

Cook, J., & Mitchell J. (1989). Viability measurements in mammalian cell systems. *Anal. Biochem, 179*, 1-7.

Cordenonsi, M., D'Atri F., Hammar E., Parry DA., *et al.* (1999). Cingulin contains globular and coiled-coil domains and interacts with ZO-1, ZO-2, ZO-3 and myosin. *J Cell Biol, 147*, 1569-1582.

Couto, N., Malys, N., Gaskell, S., & Barber, J. (2013). Partition and Turnover of Glutathione Reductase from Saccharomyces cerevisiae: a Proteomic Approach. *Journal of Proteome Research, 12(6)*, 2885-2894.

Craft, S., Baker, L., Montine, T., Minoshima, S., *et al.* (2012). Intranasal insulin therapy for Alzheimer disease and amnestic mild cognitive impairment: a pilot clinical trial. *Arch Neurol, 69*(1), 29-38.

Cucullo, L., McAllister, M., Kight, K., Krizanac-Bengez, L., *et al.* (2002). A new dynamic *in vitro* model for the multidimensional study of astrocyte-endothelial cell interactions at the blood-brain barrier. *Brain Res, 951*(2), 243-254.

Cuevas, P., Gutierrez-Diaz J., Reimers D., Dujovny M., *et al.* (1984). Pericyte-endothelial gap junctions in human cerebral capillaries. *Anat Embryol, 170*, 155-159.

D'Souza, A., & Topp, E. (2004). Release from polymeric prodrugs: linkages and their degradation. *J Pharm Sci, 93*(8), 1962-1979.

Dahlslett, S., Goektas O., Schmidt F., Harms L., *et al.* (2012). Psychophysiological and electrophysiological testing of olfactory and gustatory function in patients with multiple sclerosis. *Eur Arch Otorhinolaryngol, 269*(4), 1163-1169.

Daleke, D., Hong K., & Papahadjopoulos D. (1990). Endocytosis of liposomes by macrophages: binding, acidification and leakage of liposomes monitored by a new fluorescence assay. *Biochim. Biophys. Acta, 1024*, 352-366.

Dallasta, L., Pisarov L., Esplen J., Werley J., *et al.* (1999). Blood-brain barrier tight junction disruption in human immunodeficiency virus-1 encephalitis. *Am. J. Pathol, 155*, 1915-1927.

de Boer, A., & Gaillard P. (2007). Drug targeting to the brain, Annu. Rev. Pharmacol. *Toxicology, 47*, 323-355.

De Jong, W., & Borm P. (2008). Drug delivery and nanoparticles: Applications and hazards. *International Journal of Nanomedicine, 3(2)*, 133-149.

de Kloet, E. (2003). Hormones, brain and stress. *Endocr Regul, 37*(2), 51-68.

De Kloet, E., Vreugdenhil, E., Oitzl, M., & Joels, M. (1998). Brain corticosteroid receptor balance in health and disease. *Endocr Rev, 19*(3), 269-301.

de Lange, E. (2004). Potential role of ABC transporters as a detoxification system at the blood-CSF barrier. *Drug Delivery, 56*, 1793–1809.

Dean, G., & Kurtzke JF. (1971). On the risk of multiple sclerosis according to age at immigration to South Africa. *Br Med J, 3*, 725-729.

Deli, M. (2009). Potential use of tight junction modulators to reversibly open membranous barriers and improve drug delivery. *Biochim. Biophys, 1788*, 892–910

Denker, S., Ji, S., Dingman, A., Lee, S., *et al.* (2007). Macrophages are comprised of resident brain microglia not infiltrating peripheral monocytes acutely after neonatal stroke. *J Neurochem, 100*(4), 893-904.

Dennig, J., & Duncan E. (2002). Gene transfer into eukaryotic cells using activated polyamidoamine dendrimers. *J Biotechnol, 90*, 339-347.

Deshayes, S., Morris M., Divita G., & Heitz F. (2005). Cell-penetrating peptides: tools for intracellular delivery of therapeutics. *Cell. Mol. Life Sci, 62*, 1839-1849.

Di, L., Kerns, E., Bezar, I., Petusky, S., & Huang, Y. (2009). Comparison of blood-brain barrier permeability assays: in situ brain perfusion, MDR1-MDCKII and PAMPA-BBB. *J Pharm Sci, 98*(6), 1980-1991.

Di Stefano, A., & Caramori G. (2002). Increased expression of NF-*κ*B in bronchial biopsies from smokers and patients with COPD. *Eur. Resp. J, 20*, 556-563.

Dichtel, W., Serin J., Edder C., J., F*., et al.* (2004). Singlet oxygen generation via two-photon excited FRET. *J Am Chem Soc, 126*, 5380-5381.

Diwan, P., Chandrasekar D., Sistlaa R., Ahmad F., & Khar R. (2007). The development of folate-PAMAM dendrimer conjugates for targeted delivery of anti-arthritic drugs and their pharmacokinetics and biodistribution in arthritic rats. *T Biomaterials, 28*, 504-512.

Doolittle, N., Miner M., Hall W., Siegal T*., et al.* (2000). Safety and efficacy of a multicenter study using intraarterial chemotherapy in conjunction with osmotic opening of the blood-brain barrier for the treatment of patients with malignant brain tumors. *Cancer Treat. Res, 88*, 637-647.

Dostert, A., & Heinzel T. (2004). Negative glucocorticoid receptor response elements and their role in glucocorticoid action. *Curr. Pharm. Des, 10*, 2807-2816.

Drbohlavova, J., Chomoucka J., Adam V., Ryvolova M*., et al.* (2013). Nanocarriers for Anticancer Drugs-New Trends in Nanomedicine. *Current Drug Metabolism, 14(5)*, 547-564.

Dringen, R., Gutterer, J., & Hirrlinger, J. (2000). Glutathione metabolism in brain metabolic interaction between astrocytes and neurons in the defense against reactive oxygen species. *Eur J Biochem, 267*(16), 4912-4916.

Duncan, R., & Izzo, L. (2005). Dendrimer biocompatibility and toxicity. *Advanced Drug Delivery Reviews, 57*(15), 2215-2237.

Ebelegi, A., Tobin, E., Ayawei, N., ., & Donbebe, W. (2017). *A Review of Synthesis, Characterization and Applications of Functionalized Dendrimers* (Vol. 2017).

Ebnet, K., Schulz C., Meyer Zu Brickwedde M., Pendl G., & Vestweber D. (2000). Junctional adhesion molecule interacts with the PDZ domain-containing proteins AF-6 and ZO-1. *J Biol Chem, 275*, 27979-27988.

Edmondson, J., Armstrong L., & Martinez A. (1988). A rapid and simple MTT-based spectrophotometric assay for determination drug sensitivity in monolayer cultures. *J Tissue Cult Methods, 11*, 15-17.

Eigenmann, D., Xue, G., Kim, K., Moses, A., *et al.* (2013). Comparative study of four immortalized human brain capillary endothelial cell lines, hCMEC/D3, hBMEC, TY10, and BB19, and optimization of culture conditions, for an in vitro blood-brain barrier model for drug permeability studies. *Fluids Barriers CNS, 10*(1), 33-49.

Eisenhoffer, G., Loftus, P., Yoshigi, M., Otsuna, H., *et al.* (2012). Crowding induces live cell extrusion to maintain homeostatic cell numbers in epithelia. *Nature, 484*(7395), 546-549.

Elovaara, I., Kuusisto, H., Paalavuo, R., Sarkijarvi, S., *et al.* (2006). Effect of high-dose methylprednisolone treatment on CCR5 expression on blood cells in MS exacerbation. *Acta Neurol Scand, 113*(3), 163-166.

Emerich, D., Dean R., Marsh J., Pink M., *et al.* (2000). Intravenous cereport (RMP-7) enhances delivery of hydrophilic chemotherapeutics and increases survival in rats with metastatic tumors in the brain. *Pharm. Research, 17*, 1212-1219.

Emerich, D., Snodgrass P., Dean R., Agostino M., *et al.* (1999). Enhanced delivery of carboplatin into brain tumours with intravenous Cereport (RMP-7): dramatic differences and insight gained from dosing parameters. *Br. J. Cancer, 80*, 964-970.

Emerich, D., Snodgrass P., Pink M., Bloom F., & Bartus R. (1998). Central analgesic actions of loperamide following transient permeation of the blood brain barrier with Cereport (RMP-7). *Brain Research, 801*, 259-266.

Esfand, R., & Tomalia D. (2001). Poly(amidoamine) (PAMAM) dendrimers: from biomimicry to drug delivery and biomedical applications. *Drug Dis Today, 6*, 427-436.

Feinstein, A., Roy P., Lobaugh N., Feinstein K., *et al.* (2004). Structural brain abnormalities in multiple sclerosis patients with major depression. *Neurology, 62*, 586-590.

Fernandes, C., Soni, U., & Patravale, V. (2010). Nano-interventions for neurodegenerative disorders. *Pharmacological Research, 62*(2), 166-178.

Fields, G., & Noble R. (1990). Solid-phase peptide synthesis utilizing 9-fluorenylmethoxycarbonyl amino acids. *International journal of peptide and protein research, 35*(3), 161-214.

Fischer, D., Li, Y., Ahlemeyer, B., Krieglstein, J., & Kissel, T. (2003). *In vitro* cytotoxicity testing of polycations: influence of polymer structure on cell viability and hemolysis. *Biomaterials, 24*(7), 1121-1131.

Fischer, H., Gottschlich R., & Seelig A. (1998). Blood–brain barrier permeation: molecular parameters governing passive diffusion. *J Membr Biol, 165*, 201-211.

Frohman, E., Racke M., & Raine C. (2006). Multiple sclerosis -the plaque and its pathogenesis. *N. Engl. J. Med, 354*, 942-955.

Fu, Y., Nitecki D., Maltby D., Simon G.*, et al.* (2006). Dendritic iodinated contrast agents with PEG-cores for CT imaging: synthesis and preliminary characterization. *Bioconjug Chem, 17*, 1043-1056.

Gabathuler, R. (2010). Approaches to transport therapeutic drugs across the blood-brain barrier to treat brain diseases. *Neurobiol Dis, 37*(1), 48-57.

Gabriel, C., Gabriel S., Grant E., Halstead B., & Mingos M. (1998). Dielectric parameters relevant to microwave dielectric heating. *Chem. Soc. Rev, 27*, 213-224.

Gagliardi, M. (2017). Recent Advances in Preclinical Studies and Potential Applications of Dendrimers as Drug Carriers in the Central Nervous System. *Curr Pharm Des, 23*, 1-15.

Gaillard, P., Appeldoorn, C., Rip, J., Dorland, R.*, et al.* (2012). Enhanced brain delivery of liposomal methylprednisolone improved therapeutic efficacy in a model of neuroinflammation. *J Control Release, 164*(3), 364-369.

Gaillard, P., Visser, C., Appeldoorn, C., & Rip, J. (2012). Enhanced brain drug delivery: safely crossing the blood-brain barrier. *Drug Discov Today Technol, 9*(2), e71-e174.

Gan, N., Yin F, Peng J., & Wang W. (2008). Effect of lysophosphatidic acid increase the permeability of blood-brain barrier model. *Zhonghua Yi Xue Za Zhi, 88*, 416-418.

Georgieva, J., Hoekstra, D., & Zuhorn, I. (2014). Smuggling Drugs into the Brain: An Overview of Ligands Targeting Transcytosis for Drug Delivery across the Blood-Brain Barrier. *Pharmaceutics, 6*(4), 557-583.

Gerets, H., Hanon, E., Cornet, M., Dhalluin, S.*, et al.* (2009). Selection of cytotoxicity markers for the screening of new chemical entities in a pharmaceutical context: a preliminary study using a multiplexing approach. *Toxicol In Vitro, 23*(2), 319-332.

Ghose, A., Viswanadhan V., & Wendoloski J. (1999). A knowledge-based approach in designing combinatorial or medicinal chemistry libraries for drug discovery. 1. A qualitative and quantitative characterization of known drug databases. *J Comb Chem, 1*, 55-68.

Giordano, G., Afsharinejad, Z., Guizzetti, M., Vitalone, A.*, et al.* (2007). Organophosphorus insecticides chlorpyrifos and diazinon and oxidative stress in neuronal cells in a genetic model of glutathione deficiency. *Toxicology and Applied Pharmacology, 219 (2-3)*, 181-189.

Goldfarb, D., Corbett A., Mason D., & Harreman M. (2004). Adam S.A. Importin alpha: a multipurpose nuclear-transport receptor. *Trends Cell Biol, 14*, 505–514.

Gong, L., Hu Q., & Pu L. (2001). Optically active dendrimers with a binaphthyl core and phenylene dendrons: light harvesting and enantioselective fluorescent sensing. *J Org Chem, 66*, 2358-2367.

Grayson, S., & Frechet, J. (2001). Convergent dendrons and dendrimers: from synthesis to applications. *Chem Rev, 101*(12), 3819-3868.

Grieb, P., Forster R., Strome D., Goodwin C., & Pape P. (1985). O_2 exchange between blood and brain tissues studied with 18O2 indicator dilution technique. *J Appl Physiol, 58*, 1929-1941.

Griffiths, P., & De Haseth, J. (2007). *Fourier Transform Infrared Spectrometry* (2nd ed.): John Wiley & Sons.

Guidry, J., George, J., Vesely, S., Kennison, S., & Terrell, D. (2009). Corticosteroid side-effects and risk for bleeding in immune thrombocytopenic purpura: patient and hematologist perspectives. *Eur J Haematol, 83*(3), 175-182.

Gumbleton, M., & Audus, K. (2001). Progress and limitations in the use of in vitro cell cultures to serve as a permeability screen for the blood-brain barrier. *J Pharm Sci, 90*(11), 1681-1698.

Gupta, U., & Perumal, O. (2014). Dendrimers and Its Biomedical Applications / Chapter 15 In C. T. Laurencin & M. Deng (Eds.), *Natural and Synthetic Biomedical Polymers* (pp. 243-257). Oxford: Elsevier.

Haensler, J., & Szoka F. (1993). Polyamidoamine cascade polymers mediate efficient transfection of cells in culture. *Bioconjugate Chem, 4*, 372-379.

Hafler, D. (2004). Multiple sclerosis. *J. Clin Invest, 113*(6), 788-794.

Hart, L., Krishnan V., Adcock I., & Barnes P. (1998). Activation and localization of transcription factor, nuclear factor-κB, in asthma. *Am. J. Respir. Crit. Care Med, 158*, 1585-1592.

Hawaker, C., Wooley K., & Frechet J. (1993). Unimolecular micelles and globular amphiphiles: dendritic macromolecules as novel recyclable solubilization agents. *J. Chemical Society. Perkin Transactions,, 1*(12), 1287-1289.

Hawker, C., & Fréchet J. (1990). Preparation of polymers with controlled molecular architecture. A new convergent approach to dendritic macromolecules. *J Am Chem Soc, 112*, 7638–7647.

Hawkins, R., O'Kane R., Simpson I., & Viña J. (2006). Structure of the blood-brain barrier and its role in the transport of amino acids. *J Nutr, 136*, 218-226.

Hayashi, K., Nakao, S., Nakaoke, R., Nakagawa, S., *et al.* (2004). Effects of hypoxia on endothelial/pericytic co-culture model of the blood–brain barrier. *Regulatory Peptides, 123*(1–3), 77-83.

Hayes, A. W. (1995). Principles and Methods of Toxicology. *Toxicity letters, 78(1)*, 31-33.

He, F., Yin, F., Peng, J., Li, K. Z., *et al.* (2010). Immortalised mouse brain endothelial cell line b.End3 displays the comparative barrier characteristics as the primary brain microvascular endothelial cells. *Zhongguo Dang Dai Er Ke Za Zhi, 12*(6), 474-478.

Herrmann, A., Mihov G., Vandermeulen G., Klok H., & Mullen K. (2003). Peptide-functionalized polyphenylene dendrimers. *Tetrahedron, 59*, 3925-3935.

Herve, F., Ghinea N., & Scherrmann J. (2008). CNS delivery via adsorptive transcytosis. *AAPS J, 10*, 455-472.

Herz, J., & Marschang, P. (2003). Coaxing the LDL receptor family into the fold. *Cell Biol, 112*, 289-292.

Hirase, T., Staddon J., & Saitou M. (1997). Occludin as a possible determinant of tight junction permeability in endothelial cells. *J. Cell Sci, 110*, 1603-1613.

Holman, D., Klein R., & Ransohoff R. (2011). The blood–brain barrier, chemokines and multiple sclerosis. *Biochim. Biophys. Acta, 1812*, 220-230.

Holtman, L., van Vliet, A., Appeldoorn, C., Gaillard, J., *et al.* (2014). Glutathione pegylated liposomal methylprednisolone administration after the early phase of status epilepticus did not modify epileptogenesis in the rat. *Epilepsy Research, 108*(3), 396-404.

Hombach, J., Hoyer, H., & Bernkop-Schnurch, A. (2008). Thiolated chitosans: development and *in vitro* evaluation of an oral tobramycin sulphate delivery system. *Eur J Pharm Sci, 33*(1), 1-8.

Honda, M., Nakagawa, S., Hayashi, K., Kitagawa, N., *et al.* (2006). Adrenomedullin Improves the Blood–Brain Barrier Function Through the Expression of Claudin-5. *Cellular and Molecular Neurobiology, 26*(2), 109-118.

Hong, S., Hessler, J., Holl, M., Leroueil, P., *et al.* (2006). Physical interaction of nanoparticles with biological membranes: the observation of nanoscale hole formation. *J. Chem. Health Saf, 13*(3), 16-20.

Horuk, R., Martin, A., Wang, Z., Schweitzer, L., *et al.* (1997). Expression of chemokine receptors by subsets of neurons in the central nervous system. *J Immunol, 158*(6), 2882-2890.

Howl, J. (2005). Peptide synthesis and applications [Press release]

Huber, J., Egleton R., & Davis T. (2001). Molecular physiology and pathophysiology of tight junctions in the blood–brain barrier. *Trends Neuroscience, 24*, 719-725.

Hudson, D. (1988). Methodological implications of simultaneous solidphase peptide synthesis-comparison of different coupling procedures. *J Org Chem, 53*, 617-624.

Huisinga, J., Filipi M., & Stergiou N. (2011). Elliptical exercise improves fatigue ratings and quality of life in patients with multiple sclerosis. *J. Rehabil Res Dev, 48*(7), 881-890.

Hynynen, K. (2008). Ultrasound for drug and gene delivery to the brain. *Adv. Drug Deliv. Rev., 60*, 1209-1217.

Ihre, H., Hult A, Fréchet J, Gitsov I. (1998). Double-stage convergent approach for the synthesis of functionalized dendritic aliphatic polyesters based on 2,2-bis(hydroxymethyl) propionic acid. *Macromolecules, 31*, 4061-4068.

Inamura, T., Nomura T., Ikezaki K., Fukui M.*, et al.* (1994). Intracarotid histamine infusion increases blood tumour permeability in RG2 glioma. *Neurol. Res., 16*, 125-128.

Issa, R., Meikle S., ames S., & Cooper I. (2015). Poly(ε-lysine) dendrons as modulators of quorum sensing in Pseudomonas aeruginosa. *Journal of Materials Science: Materials in Medicine, 26*(5), 1-7.

Ito, K., Barnes P., & Adcock I. (2000). Glucocorticoid receptor recruitment of histone deacetylase 2 inhibits IL-1 -induced histone H4 acetylation on lysines 8 and 12. *Mol. Cell. Biol, 20*, 6891–6903.

Itoh, M., Furuse M., Morita K., Kubota K.*, et al.* (1999). Direct binding of three tight junctionassociated MAGUKs, ZO-1, ZO-2, and ZO-3, with the COOH termini of claudins. *J Cell Biol, 147*, 1351-1363.

Jansen, J., de Brabander van den Berg E., & Meijer E. (1994). Encapsulation of guest molecules into a dendritic box. *Science, 266*, 1226-1229.

Jantz, M., & Sahn, S. (1999). Corticosteroids in acute respiratory failure. *Am. J. Respir. Crit. Care Med., 160(4)*, 1079-1100.

Jauregui-Huerta, F., Ruvalcaba-Delgadillo, Y., Gonzalez-Castaneda, R., Garcia-Estrada, J.*, et al.* (2010). Responses of glial cells to stress and glucocorticoids. *Curr Immunol Rev, 6*(3), 195-204.

Jones, A., & Shusta, E. (2007). Blood-brain barrier transport of therapeutics via receptor-mediation. *Pharm Res, 24*(9), 1759-1771.

Jongen, P., Stavrakaki, I., Voet, B., Hoogervorst, E.*, et al.* (2016). Patient-reported adverse effects of high-dose intravenous methylprednisolone treatment: a prospective web-

based multi-center study in multiple sclerosis patients with a relapse. *Journal of Neurology, 263*, 1641-1651.

Jonker-Venter, C., Snyman, D., Janse van Rensburg, C., Jordaan, E.*, et al.* (2006). Low molecular weight quaternised chitosan (11): in vitro assessment of absorption enhancing properties. *Pharmazie, 61*(4), 301-305.

Jullian, M., Hernandez, A., Maurras, A., Puget, K.*, et al.* (2009). N-terminus FITC labeling of peptides on solid support: the truth behind the spacer. *Tetrahedron Letters, 50*(3), 260-263.

Kabanov, A., & Batrakova, E. (2004). New Technologies for Drug Delivery across the Blood Brain Barrier. *Curr Pharm Des, 10*(12), 1355-1363.

Kabanov, A., Batrakova E., & Miller D. (2003). Pluronic block copolymers as modulators of drug efflux transporter activity in the blood-brain barrier. *Adv. Drug Deliv. Rev., 55*, 151-164.

Kabat, E., & Freedman, D. (1950). A study of the crystalline albumin, gamma globulin and total protein in the cerebrospinal fluid of 100 cases of multiple sclerosis and in other diseases. *Am J Med Sci, 219*(1), 55-64.

Kannan, R., Kuhlenkamp, J., Jeandidier, E., Trinh, H.*, et al.* (1990). Evidence for carrier-mediated transport of glutathione across the blood-brain barrier in the rat. *Journal of Clinical Investigation, 85(6)*, 2009-2013.

Karyekar, C., Fasano A., Raje S., Lu R.*, et al.* (2003). Zonula occludens toxin increases the permeability of molecular weight markers and chemotherapeutic agents across the bovine brain microvessel endothelial cells. *J. Pharm. Sci, 92*, 414-423.

Kato, K., Kokeguchi S., Ishihara H., Murayama Y.*, et al.* (1987). Chemical composition and immunobiological activities of sodiumdodecyl sulphate extracts from the cell envelopes of Actinobacillus actinomycetemcomitans, Bacteroides gingivalis and Fusobacterium nucleatum. *J. Gen. Microbiol, 133*, 1033-1043.

Kawaguchi, T., Walker K., Wilkins C., & Moore J. (1995). Double exponential dendrimer growth. *J Am Chem Soc, 117*, 2159-2165.

Kerns, E. (2001). High throughput physicochemical profiling for drug discovery. *J Pharm Sci, 90*(11), 1838-1858.

Khandare, J., & Kumar, S. (2011). Biodegradable Dendrimers and Dendritic Polymers *Handbook of Biodegradable Polymers* (pp. 237-262): Wiley-VCH Verlag GmbH & Co. KGaA.

Kim, S., Ye, C., Kumar, P., Chiu, I.*, et al.* (2010). Targeted delivery of siRNA to macrophages for anti-inflammatory treatment. *Mol Ther, 18*(5), 993-1001.

King, D., Fields C., & Fields G. (1990). A cleavage method which minimizes side reactions following Fmoc solid phase peptide synthesis. *Int J Pept Prot Res, 36*, 255-266.

Kinnunen, E., Koskenvuo M., Kaprio J., & Aho K. (1987). Multiple sclerosis in a nationwide series of twins. *Neurology, 37*, 1627-1629.

Kobayashi, H., Kawamoto S, Jo S-K, Bryant Jr HL, Brechbiel MW, Star RA. (2003). Macromolecular MRI contrast agents with small dendrimers: pharmacokinetic differences between sizes and cores. *Bioconjug Chem, 14*, 388-394.

Kobayashi, H., Kawamoto S., Saga T., Sato N.*, et al.* (2001). Novel liver macromolecular MR contrast agent with a polypropylenimine diaminobutyl dendrimer core: comparison to the vascular MRcontrast agent with the polyamidoamine dendrimer core. *Magn Reson Med, 46*, 795-802.

Kolhatkar, R., Kitchens K., Swaan P., & Ghandehari H. (2007). Surface acetylation of polyamidoamine (PAMAM) dendrimers decreases cytotoxicity while maintaining membrane permeability. *Bioconj. Chem, 18*(6), 2054-2060.

Kolhe, P., Misra E., Kannan R., Kannan S., & Lieh-Lai M. (2003). Drug complexation, *in vitro* release and cellular entry of dendrimers and hyperbranched polymers. *Int J Pharm, 259*, 143-160.

Krewson, C., Klarman M., & Saltzman W. (1995). Distribution of nerve growth factor following direct delivery to brain interstitium. *Brain Res, 680*, 196-206.

Kuang, Y., Lackay S., Zhao L., & Fu Z. (2009). Role of chemokines in the enhancement of BBB permeability and inflammatory infiltration after rabies virus infection. *Virus Research, 144*, 18-26.

Kumar, P., Shen Q., Pivetti C., Lee E.*, et al.* (2009). Molecular mechanisms of endothelial hyperpermeability: implications in inflammation. *Expert Rev. Mol. Med, 11*, 19.

Kusuhara, H., & Sugiyama Y. (2001). Efflux transport systems for drugs at the blood-brain barrier and blood cerebrospinal fluid barrier (Part 1). *Drug Discov. Today, 6*, 150-156.

Labbe, G., Forier B., & Dehaen W. (1996). A fast double-stage convergent synthesis of dendritic polyethers. *Chem Commun, 18*, 2143-2144.

Lai, C., & Kuo K. (2005). The critical component to establish *in vitro* BBB model: pericyte. *Brain Res. Rev, 50*, 258-265.

Larrick, J., & Wright, S. (1990). Cytotoxic mechanism of tumor necrosis factor-alpha. *FASEB J, 4*(14), 3215-3223.

Lee, D., Rotger, C., Appeldoorn, C., Reijerkerk, A., *et al.* (2014). Glutathione PEGylated liposomal methylprednisolone (2B3-201) attenuates CNS inflammation and degeneration in murine myelin oligodendrocyte glycoprotein induced experimental autoimmune encephalomyelitis. *J Neuroimmunol, 274*(1-2), 96-101.

Lee, H., Lim Y. , Choi J., Lee Y., *et al.* (2003). Polyplexes assembled with internally quaternized PAMAM-OH dendrimer and plasmid DNA have a neutral surface and gene delivery potency. *Bioconjug. Chem, 14*, 1214-1221.

Lee, J., & Nan, A. (2012). Combination Drug Delivery Approaches in Metastatic Breast Cancer. *Journal of Drug Delivery, 2012*, 17.

Lee, S., Choi S., Kim S., & Park T. (2008). Thermally sensitive cationic polymer nanocapsules for specific cytosolic delivery and efficient gene silencing of siRNA: swelling induced physical disruption of endosome by cold shock. *J. Control Release, 125*, 25-32.

Lethaby, A., Lopez-Olivo, M., Maxwell, L., Burls, A., *et al.* (2013). Etanercept for the treatment of rheumatoid arthritis. *Cochrane Database Syst Rev*(5), Cd004525.

Lindqvist, A., Rip, J., Gaillard, P. J., Bjorkman, S., & Hammarlund-Udenaes, M. (2013). Enhanced brain delivery of the opioid peptide DAMGO in glutathione pegylated liposomes: a microdialysis study. *Mol Pharm, 10*(5), 1533-1541.

Liu, D., Ahmet, A., Ward, L., Krishnamoorthy, P., *et al.* (2013). A practical guide to the monitoring and management of the complications of systemic corticosteroid therapy. *Allergy, Asthma, and Clinical Immunology : Official Journal of the Canadian Society of Allergy and Clinical Immunology, 9*(1), 30-30.

Liu, M., & Fréchet J. (1999). Designing dendrimers for drug delivery. *Pharmaceutical science & technology today, 2*(10), 393-401.

Liu, T., Clark, R., McDonnell, P., Young, P., *et al.* (1994). Tumor necrosis factor-alpha expression in ischemic neurons. *Stroke, 25*(7), 1481-1488.

Longmire, M., Ogawa, M., Choyke, P., & Kobayashi, H. (2011). Biologically Optimized Nanosized Molecules and Particles: More than Just Size. *Bioconjugate Chemistry, 22*(6), 993-1000.

Löscher, W., & Potschka H. (2005). Blood–brain barrier active efflux transporters: ATP binding cassette gene family. *NeuroRx, 2*, 86-98.

Lossinsky, A., Vorbrodt A., & Wisniewski H. (1995). Scanning and transmission electron microscopic studies of microvascular pathology in the osmotically impaired blood-brain barrier. *J. Neurocytol., 24*, 795-806.

Lu, N., Wardell, S., Burnstein, K., Defranco, D., *et al.* (2006). International Union of Pharmacology. LXV. The pharmacology and classification of the nuclear receptor superfamily: glucocorticoid, mineralocorticoid, progesterone, and androgen receptors. *Pharmacol Rev, 58*(4), 782-797.

Lublin, F., Reingold, S., Cohen, J., Cutter, G., *et al.* (2014). Defining the clinical course of multiple sclerosis: The 2013 revisions. *Neurology, 83(3)*, 278-286

Mackic, J., Stins M., Jovanovic S., Kim K., *et al.* (1999). Cereport (RMP-7) increases the permeability of human brain microvascular endothelial cell monolayers. *Pharm. Research, 16*, 1360-1365.

Madaan, K., Kumar, S., Poonia, N., Lather, V., & Pandita, D. (2014). Dendrimers in drug delivery and targeting: Drug-dendrimer interactions and toxicity issues. *Journal of Pharmacy & Bioallied Sciences, 6*(3), 139-150.

Maimone, D., & Reder A. (1991). Soluble CD8 levels in the cerebrospinal fluid and serum of patients with multiple sclerosis. *Neurology, 41*, 851-854.

Malik, N., Wiwattanapatapee R., Klopsch R., Lorenz K., *et al.* (2000). Dendrimers: Relationship between structure and biocompatibility in vitro, and preliminary studies on the biodistribution of 125I-labelled polyamidoamine dendrimers *in vivo*. *J. Controlled Release, 65*, 133−148.

Mária, D., Csongor, Á., Yasufumi, K., & Masami, N. (2005). Permeability Studies on In Vitro Blood–Brain Barrier Models:Physiology, Pathology, and Pharmacology. *Cellular and Molecular Neurobiology, 25*(1), 59-127.

Mark, K., & Miller, D. (1999). Increased permeability of primary cultured brain microvessel endothelial cell monolayers following TNF-alpha exposure. *Life Sci, 64*(21), 1941-1953.

Martyn, C., Cruddas M., & Compston D. (1993). Symptomatic Epstein-Barr virus infection and multiple sclerosis. *J Neurol Neurosurg Psychiatry, 56*, 167-168.

Masungi, C., Mensch, J., Willems, B., Van Dijck, A., *et al.* (2009). Usefulness of a novel Caco-2 cell perfusion system II. Characterization of monolayer properties and peptidase activity. *Pharmazie, 64*(1), 36-42.

Matter, K., & Balda M. (2003). Signalling to and from tight junctions. *Mol Cell Biol, 4*, 225-236.

McDonald, W., Compston A., & Edan G. (2001). Recommended diagnostic criteria for multiple sclerosis: guidelines from the International panel on the diagnosis of multiple sclerosis. *Ann Neurol, 50*, 121-127.

McEwen, B., & Sapolsky, R. (1995). Stress and cognitive function. *Curr Opin Neurobiol, 5*(2), 205-216.

Mdzinarishvili, A., Sutariya, V., Talasila, P., Geldenhuys, W., & Sadana, P. (2013). Engineering triiodothyronine (T3) nanoparticle for use in ischemic brain stroke. *Drug Deliv Transl Res, 3*(4), 309-317.

Meikle, S., Bianchi G., Olivier G., & Santin M. (2013). Osteoconductive phosphoserine-modified poly(ε-lysine) dendrons: synthesis, titanium oxide surface functionalization and response of osteoblast-like cell lines. *Journal of the Royal Society Interface, 10*(79), 20120765.

Menjoge, A., Kannan, R., & Tomalia, D. (2010). Dendrimer-based drug and imaging conjugates: design considerations for nanomedical applications. *Drug Discov Today, 15*(5-6), 171-185.

Menjoge, A., Kannan R., & Tomalia D. (2010). Dendrimer-based drug and imaging conjugates: design considerations for nanomedical applications. *Drug Discov Today, 15*(5), 171-185.

Merrifield, B. (1985). Automated solid-phase peptide synthesis to obtain therapeutic peptides Chem. *Int. Ed. Engl, 24*, 799-810.

Merrifield, B. (1986). Solid phase synthesis. *Science, 232*, 341-347.

Miller, D., Batrakova E., Waltner T., Alakhov V., & Kabanov A. (1997). Interactions of pluronic block copolymers with brain microvessel endothelial cells: evidence of two potential pathways for drug absorption. *Bioconjug. Chem, 8*, 649-657.

Milligan, N., Newcombe R., & Compston D. (1987). A double-blind controlled trial of high dose methylprednisolone in patients with multiple sclerosis. *Neural Neurosurg Psychiatry, 50*, 511-516.

Minagar, A., & Alexander J. (2003). Blood–brain barrier disruption in multiple sclerosis. *Multiple Sclerosis, 9*, 540-549.

Miranda, L., & Alewood P. (1999). Accelerated chemical synthesis of peptides and small proteins. *Proc Natl Acad Sci, 96*, 1181-1186.

Mitic, L., & Anderson J. (1998). Molecular architecture of tight junctions. *Annu Rev Physiol, 60*, 121-142.

Mitic, L., Van Itallie C., & Anderson j. (2000). Molecular physiology and pathophysiology of tight junctions I. Tight junction structure and function: lessons from mutant animals and proteins. *Am J Physiol: Gastrointest Liver Physiol, 279*, 250-254.

Mohamadi, A., Chan, J., Claessen, F., Ring, D., & Chen, N. (2017). Corticosteroid Injections Give Small and Transient Pain Relief in Rotator Cuff Tendinosis: A Meta-analysis. *Clin Orthop Relat Res, 475*(1), 232-243.

Monaco, C., & Paleolog E. (2004). Nuclear factor kappaB: a potential therapeutic target in atherosclerosis and thrombosis. *Cardiovasc. Res, 61*, 671-682.

Montalbetti, C., & Falque V. (2005). Amide bond formation and peptide coupling. *Tetrahedron, 740*, 10827-10851.

Moore, A., Donahue, C., Bauer, K., & Mather, J. (1998). Chapter 15 Simultaneous Measurement of Cell Cycle and Apoptotic Cell Death. In P. M. Jennie & B. David (Eds.), *Methods in Cell Biology* (Vol. Volume 57, pp. 265-278): Academic Press.

Moos, T., & Morgan, E. (2000). Transferrin and transferrin receptor function in brain barrier systems. *Cell Mol Neurobiol, 20*(1), 77-95.

Moreland, L. (2004). Drugs that block tumour necrosis factor: experience in patients with rheumatoid arthritis. *Pharmacoeconomics, 22*(2 Suppl 1), 39-53.

Moriyama, E., Salcman M., & Broadwell R. (1991). Blood-brain barrier alteration after microwave-induced hyperthermia is purely a thermal effect: I, temperature and power measurements. *Surg. Neurol, 35*, 177-182.

Mosmann, T. (1983). Rapid colorimetric assay for cellular growth and survival: application to prolifration and cytotoxicity assays. *J immunol methods, 65*, 55-63.

Muller, L., Guy R., & Guy S. (2002). Role of nuclear factor kB in synovial inflammation. *Curr. Rheumatol. Rep, 4*, 201-207.

Mumford, C. (1992). The UK study of MS in twins. *J. Neurol, 239*, 62.

Murphy, S., Simmons, M., Agullo, L., Garcia, A.*, et al.* (1993). Synthesis of nitric oxide in CNS glial cells. *Trends Neurosci, 16*(8), 323-328.

Myriam, W., Valery F., Wim P., Barry M.*, et al.* (2000). Polyanionic (i.e., polysulfonate) dendrimers can inhibit the replication of human immunodeficiency virus by interfering with both virus adsorption and later steps (reverse transcriptase/integrase) in the virus replicative cycle. *Mol Pharmacol, 58*, 1100-1108.

Mytilineou, C., Kramer, B., & Yabut, J. (2002). Glutathione depletion and oxidative stress. *Parkinsonism Relat Disord, 8*(6), 385-387.

Nachlas, M., Stanley I., Jerome D., & Arnold M. (1960). The determination of lactic dehydrogenase with a tetrazolium salt. *Anal. Biochem, 1*, 317-326.

Nadal, A., Fuentes E., Pastor J., & McNaughton P. (1995). Plasma albumin is a potent trigger of calcium signals and DNA synthesis in astrocytes. *Proc. Natl. Acad. Sci. U.S.A, 92*, 1426–1430.

Nag, S. (2003). *Morphology and molecular properties of cellular components of normal cerebral vessels. In: The Blood- Brain Barrier: Biology and Research Protocols*. New Jersey: Humana Presss.

Nagahori, N., Lee R., Nishimura S., Page D.*, et al.* (2002). Inhibition of adhesion of type 1 fimbriated Escherichia coli to highly mannosylated ligands. *ChemBioChem, 3*, 836-844.

Nagumo, Y., Han, J., Bellila, A., Isoda, H., & Tanaka, T. (2008). Cofilin mediates tight-junction opening by redistributing actin and tight-junction proteins. *Biochem Biophys Res Commun, 377*(3), 921-925.

Naik, P., & Cucullo, L. (2012). *In vitro* blood-brain barrier models: current and perspective technologies. *J Pharm Sci, 101*(4), 1337-1354.

Najlah, M., & D'Emanuele, A. (2006). Crossing cellular barriers using dendrimer nanotechnologies. *Current Opinion in Pharmacology, 6*(5), 522-527.

Nakano, T., Ohara, O., Teraoka, H., & Arita, H. (1990). Glucocorticoids suppress group II phospholipase A2 production by blocking mRNA synthesis and post-transcriptional expression. *J Biol Chem, 265*(21), 12745-12748.

Napoli, I., & Neumann, H. (2009). Microglial clearance function in health and disease. *Neuroscience, 158*(3), 1030-1038.

NeuroInsights. (2008). The Neurotechnology Industry 2008 Report.

Newkome, G., Yao Z., Baker G., & Gupta V. (1985). Micelles. Part 1. Cascade molecules: a new approach to micelles. *J Org Chem, 50*, 2003-2004.

Nguyen, D., & Stangel, M. (2001). Expression of the chemokine receptors CXCR1 and CXCR2 in rat oligodendroglial cells. *Brain Res Dev Brain Res, 128*(1), 77-81.

NHS. (2017). Multiple sclerosis [Online]. NHS Choices: UK government. Available: http://www.nhs.uk/Conditions/Multiple-sclerosis/Pages/Introduction.aspx. Retrieved 10/07, 2017

Nicolazzo, J., Charman, S., & Charman, W. (2006). Methods to assess drug permeability across the blood-brain barrier. *J Pharm Pharmacol, 58*(3), 281-293.

Nomura, T., Ikezaki K., Matsukado K., & Fukui M. (1994). Effect of histamine on the bloodtumor barrier in transplanted rat brain tumors. *Neurochir. Suppl (Wien)*, 400-402.

Noriega, B., Luis A., & Francisco J. (2014). Applications of Dendrimers in Drug Delivery Agents, Diagnosis, Therapy, and Detection. *Journal of Nanomaterials, 2014*, 19-38.

Noseworthy, J., Lucchinetti C., Rodriguez M., & Weinshenker B. (2000). Multiple sclerosis. *N Engl J Med, 343*, 938-952.

Ogunshola, O. (2011). *In vitro* modeling of the blood-brain barrier: simplicity versus complexity. *Curr Pharm Des, 17*(26), 2755-2761.

Ohsaki, M., Okuda T., Wada A. , HirayamaT.*, et al.* (2002). *In vitro* gene transfection using dendritic poly(l-lysine). *Bioconjug Chem, 13*, 510-517.

Oliveri, R., Valentino, P., Russo, C., Sibilia, G.*, et al.* (1998). Randomized trial comparing two different high doses of methylprednisolone in MS: a clinical and MRI study. *Neurology, 50*(6), 1833-1836.

Oller-Salvia, B., Sanchez-Navarro, M., Giralt, E., & Teixido, M. (2016). Blood-brain barrier shuttle peptides: an emerging paradigm for brain delivery. *Chem Soc Rev, 45*(17), 4690-4707.

Omidi, Y., Campbell, L., Barar, J., Connell, D.*, et al.* (2003). Evaluation of the immortalised mouse brain capillary endothelial cell line, b.End3, as an *in vitro* blood-brain barrier model for drug uptake and transport studies. *Brain Res, 990*(1-2), 95-112.

Padilla, O., Ihre H R., Gagne L., Fréchet J., & Szoka J. (2002). Polyester dendritic systems for drug delivery applications: *in vitro* and *in vivo* evaluation. *Bioconjug Chem, 13*, 453-461.

Page, N., & Spiteri M. (1982). Lhermitte's sign in Behçet's disease. *British medical journal, 284*(6317), 704-705.

Palmeri, D., van Zante A., Huang CC., Hemmerich S., & Rosen SD. (2000). Vascular endothelial junction-associated molecule, a novel member of the immunoglobulin superfamily, is localized to intercellular boundaries of endothelial cells. *J Biol Chem, 275*, 19139-19145.

Pan, W., & Kastin, A. (2001). Changing the chemokine gradient: CINC1 crosses the blood-brain barrier. *J Neuroimmunol, 115*(1-2), 64-70.

Panyam, J., & Labhasetwar V. (2003). Dynamics of endocytosis and exocytosis of poly (D, Llactide- co-glycolide) nanoparticles in vascular smooth muscle cells. *Pharm. Research, 20*, 212-220.

Papadopoulos, N. G., Dedoussis, G. V., Spanakos, G., Gritzapis, A. D.*, et al.* (1994). An improved fluorescence assay for the determination of lymphocyte-mediated cytotoxicity using flow cytometry. *J immunol methods, 177*(1-2), 101-111.

Pardridge, W. M. (1997). Drug delivery to the brain. *J. Cereb. Blood Flow Metab., 17*, 713–731.

Pardridge, W. M. (2002a). Drug and gene delivery to the brain: the vascular route. *Neuron, 36*, 555-558.

Pardridge, W. M. (2002b). Why is the global CNS pharmaceutical market so under-penetrated? *Drug Discov. Today, 7*, 7-5.

Pardridge, W. M. (2003). Blood–brain barrier drug targeting: the future of brain drug development. *Mol. Interv, 90*, 150-151.

Pardridge, W. M. (2005a). The blood-brain barrier: bottleneck in brain drug development. *NeuroRx, 2*, 3-14.

Pardridge, W. M. (2005b). Molecular biology of the blood-brain barrier. *Mol. Biotechnol, 30*, 57-70.

Pardridge, W. M. (2006). Molecular Trojan horses for blood-brain barrier drug delivery. *Discovery Medicine, 6(34)*, 139-143.

Pardridge, W. M. (2007). Blood-brain barrier delivery. *Drug Discovery Today, 12*, 54-61.

Pardridge, W. M., Eisenberg, J., & Yang, J. (1985). Human blood-brain barrier insulin receptor. *J Neurochem, 44*(6), 1771-1778.

Park, K. (2008). Trojan monocytes for improved drug delivery to the brain. *J Control Release, 132*, 75.

Patel, H. (2013). Dendrimer applications - a review. *Int J Pharm Bio Sc, 4(2)*, 454 - 463.

Patri, A., & Simanek, E. (2012). Biological applications of dendrimers. *Mol Pharm, 9*(3), 341.

Patton, D., Cosgrove Sweeney, Y., McCarthy, T., & Hillier, S. (2006). Preclinical Safety and Efficacy Assessments of Dendrimer-Based (SPL7013) Microbicide Gel Formulations in a Nonhuman Primate Model. *Antimicrobial Agents and Chemotherapy, 50*(5), 1696-1700.

Pease, J., & Williams, T. (2006). The attraction of chemokines as a target for specific anti-inflammatory therapy. *Br J Pharmacol, 147*(Suppl 1), S212-S221.

Pedro, L., Martínez, E., Cortez, S., Mendoza, S.*, et al.* (2017). Synthesis, Characterization, and Nanomedical Applications of Conjugates between Resorcinarene-Dendrimers and Ibuprofen. *Nanomaterials, 7*(7), 163-172.

Pekny, M., & Nilsson, M. (2005). Astrocyte activation and reactive gliosis. *Glia, 50*(4), 427-434.

Pelt, A. (2011). *Glucocorticoids: effects, action mechanisms, and therapeutic uses*. New York: Hauppauge, Nova Science.

Peppiatt, C., Howarth C., Mobbs P., & Attwell D. (2006). Bidirectional controls of CNS capillary diameter by pericytes. *Nature, 443*, 700-704.

Persidsky, Y., Ramirez S., Haorah J., & Kanmogne G. (2006). Blood–brain barrier: structural components and function under physiologic and pathologic conditions. *J. Neuroimmune Pharmacol., 1*, 223-236.

Petty, M., & Lo E. (2002). Junctional complexes of the bloodbrain barrier: permeability changes in neuroinflammation. *Prog Neurobiol, 68*, 311-323.

Peura, L., Malmioja, K., Laine, K., Leppanen, J.*, et al.* (2011). Large amino acid transporter 1 (LAT1) prodrugs of valproic acid: new prodrug design ideas for central nervous system delivery. *Mol Pharm, 8*(5), 1857-1866.

Pires, D., Bemquerer M., & Nascimento C. (2014). Some Mechanistic Aspects on Fmoc Solid Phase Peptide Synthesis. *Int J Pept Res Ther, 20*, 53-69.

Polman, C., Reingold S., Banwell B., Clanet M., *et al.* (2011). Diagnostic criteria for multiple sclerosis: 2010 Revisions to the McDonald criteria. *Ann Neurol, 69*(2), 292-302.

Pompella, A., Visvikis, A., Paolicchi, A., Tata, V., & Casini, A. (2003). The changing faces of glutathione, a cellular protagonist. *Biochem Pharmacol, 66(8)*, 1499-1503.

Popova, E., Okrugin B., & Neelov I. (2016). Molecular dynamics simulation of interaction of short lysine brush and oppositely charged semax peptides. *Natural Science, 8*, 8499-8510.

Prashant, K., Keerti, J., & J., N. K. (2014). Dendrimer as nanocarrier for drug delivery. *Progress in Polymer Science, 39*(2), 268-307.

Pushkar, S., Philip A., Pathak K, & Pathak D. (2006). Dendrimers: Nanotechnology Derived field, Polymers in Drug Delivery. *Indian Journal of Pharmaceutical Education and Research, 40*(3), 153-158.

Qiu, L., Ding G., Li K., Wang X., *et al.* (2010). The role of protein kinase C in the opening of blood-brain barrier induced by electromagnetic pulse. *Toxicology, 273*, 29-34.

Quintana, A., Raczka E., Piehler L., Lee I., *et al.* (2002). Design and function of a dendrimer-based therapeutic nanodevice targeted to tumor cells through the folate receptor. *Pharm Res, 19*, 1310-1316.

Quock, R., Kouchich F., Ishii T., & Lange D. (1987). Microwave facilitation of domperidone antagonism of apomorphine-induced stereotypic climbing in mice. *Bioelectromagnetics, 8*, 45-55.

Rabolli, V., Thomassen L., Princen C., Napierska D., *et al.* (2010). Influence of size, surface area and microporosity on the *in vitro* cytotoxic activity of amorphous silica nanoparticles in different cell types. *Nanotoxicology, 4*, 307-318.

Ramagopalan, S., Dobson R., Meier U., & Giovannoni G. (2010). Multiple sclerosis: risk factors, prodromes, and potential causal pathways. *Lancet Neurol, 9*, 727.

Ramsauer, M., Krause D., & Dermietzel R. (2002). Angiogenesis of the blood-brain barrier in vitro and the function of cerebral pericytes. *FASEB J, 16*, 1274-1278.

Reder, A., & Antel J. (1983). Clinical spectrum of multiple sclerosis. *Neurol Clin, 1*, 573-599.

Reese, T., & Karnovsky M. (1967). Fine structural localization of a blood-brain barrier to exogenous peroxidase. *Cell Biol, 34*, 201-217.

Reichardt, H., Gold R., & Luhder F. (2006). Glucocorticoids in multiple sclerosis and experimental autoimmune encephalomyelitis. *Expert Rev. Neurother, 6(11)*, 1657-1670.

Reichenbach, A., & Wolburg H. (2004). Morphology and ultrastructure of glial cells, astrocytes and ependymal glia In: Neurologia [Press release]

Remuzgo, C., Andrade G., Temperini M., & Miranda M. (2009). Acanthoscurrin fragment 101-132: total synthesis at 60 C of a novel difficult sequence. *Biopolym Pept Sci, 92*, 65-75.

Reuter, J., et al., Myc A., Hayes W., Gan Z.*, et al.* (1999). Inhibition of viral adhesion and infection by sialic acid conjugated dendritic polymers. *Bioconjugate Chem, 10*, 271-278.

Rhen, T., & Cidlowski J. (2005). Antiinflammatory action of glucocorticoids-new mechanisms for old drugs. *N. Engl. J. Med, 353*, 1711–1723.

Rip, J., C., A., Manca F., Dorland R.*, et al.* (2010). *Receptor-mediated delivery of drugs across the blood-brain barrier*. Paper presented at the Pharmacology and Toxicology of the Blood-Brain Barrier: State of the Art, Needs for Future Research and Expected Benefits for the EU.

Rip, J., Schenk G., & de Boer A. (2009). Differential receptor-mediated drug targeting to the diseased brain. *Drug Deliv., 6*, 227-237.

Rivers, T., Sprunt D., & Berry G. (1933). Observations on attempts to produce acute disseminated encephalomyelitis in monkeys. *J Exp. Med., 58*, 39-53.

Roberts, J. (1990). Poly peptide: dendrimer complexes. *Bioconjugate Chem, 1*, 305-308.

Rodriguez, M. (2003). A function of myelin is to protect axons from subsequent injury: implications for deficits in multiple sclerosis. *Brain, 126*, 751-752.

Rogawski, M. (2009). Convection-enhanced delivery in the treatment of epilepsy. *Neurotherapeutics, 6*(2), 344-351.

Rogers, W., & Basu P. (2005). Factors regulating macrophage endocytosis of nanoparticles: implications for targeted magnetic resonance plaque imaging. *Atherosclerosis, 178*, 67-73.

Roozendaal, B., Phillips, R., Power, A., Brooke, S.*, et al.* (2001). Memory retrieval impairment induced by hippocampal CA3 lesions is blocked by adrenocortical suppression. *Nat Neurosci, 4*(12), 1169-1171.

Roozendaal, B., Portillo-Marquez, G., & McGaugh, J. (1996). Basolateral amygdala lesions block glucocorticoid-induced modulation of memory for spatial learning. *Behav Neurosci, 110*(5), 1074-1083.

Roseita, E., & Tomalia D. (2001). Poly (amidoamine) (PAMAM) dendrimers: from. biomimicry to drug delivery and biomedical applications. *Drug Delivery Today, 6*(8), 427-436.

Rotman, M., Welling, M., Bunschoten, A., de Backer, M.*, et al.* (2015). Enhanced glutathione PEGylated liposomal brain delivery of an anti-amyloid single domain antibody fragment in a mouse model for Alzheimer's disease. *J Control Release, 203*, 40-50.

Rousselle, C., Clair P., Lefauconnier J., Kaczorek M.*, et al.* (2000). New advances in the transport of doxorubicin through the blood-brain barrier by a peptide vector-mediated strategy. *Mol. Pharmacol, 57*, 679-686.

Sadekar, S., & Ghandehari, H. (2012). Transepithelial transport and toxicity of PAMAM dendrimers: implications for oral drug delivery. *Adv Drug Deliv Rev, 64*(6), 571-588.

Sahoo, S., Parveen, S., & Panda, J. (2007). The present and future of nanotechnology in human health care. *Nanomedicine: Nanotechnology, Biology and Medicine, 3*(1), 20-31.

Saija, A., Princi P., Trombetta D., Lanza M., & De Pasquale A. (1997). Changes in the permeability of the blood-brain barrier following sodium dodecyl sulphate administration in the rat. *Exp. Brain Research, 115*, 546-551.

Salahuddin, T., Johansson B., Kalimo H., & Olsson Y. (1988). Structural changes in the rat brain after carotid infusions of hyperosmolar solutions. An electron microscopic study. *Acta Neuropathol. (Berl.), 77*, 5-13.

Sanovich, E., Bartus R., Friden P., Dean R.*, et al.* (1995). Pathway across blood-brain barrier opened by the bradykinin agonist, RMP-7. *Brain Research, 705*, 125-135.

Santaguida, S., Janigro, D., Hossain, M., Oby, E.*, et al.* (2006). Side by side comparison between dynamic versus static models of blood-brain barrier in vitro: a permeability study. *Brain Res, 1109*(1), 1-13.

Satoh, H., Zhong Y., Isomura H., Saitoh M.*, et al.* (1996). Localization of 7H6 tight junction associated antigen along the cell border of vascular endothelial cells correlates with paracellular barrier function against ions, large molecules, and cancer cells. *Exp Cell Res, 222*, 269-274.

Sawcer, S., Hellenthal, G., Pirinen, M., Spencer, C. C.*, et al.* (2011). Genetic risk and a primary role for cell-mediated immune mechanisms in multiple sclerosis. *Nature, 476*(7359), 214-219.

Schacke, H., Docke, W., & Asadullah, K. (2002). Mechanisms involved in the side effects of glucocorticoids. *Pharmacol Ther, 96*(1), 23-43.

Schaeffer, W. (1984). Usage of vertebrate, invertebrate and plant cell, tissue and organ culture terminology. *In vitro, 20*, 19-24.

Scheers, M., Ekwall B., & Dierickx, J. (2001). *In vitro* long-term cytotoxicity testing of 27 MEIC chemicals on HepG2 cells and comparison with acute human toxicity data. *Toxicol. In Vitro, 15*, 153-161.

Schiavon, O., Pasut G., & Moro S. (2004). PEG-Ara-C conjugates for controlled release. *European Journal of Medicinal Chemistry, 39*(2), 123-133.

Schinkel, A., & Jonker J. (2003). Mammalian drug efflux transporters of the ATP binding cassette (ABC) family: an overview. *Adv. Drug Deliv. Rev., 55*, 3-29.

Schnolzer, M., Alewood P., Jones A., Alewood D., & Kent S. (2007). *In situ* neutralization in Boc-chemistry solid phase peptide synthesis. *Int J Pept Res Ther, 13*, 31-44.

Schoenberg, H. (1983). Bladder and sexual dysfunction in multiple sclerosis. In: Antel JP, editor. Multiple sclerosis. *Neurol Clin, 1*, 601-613.

Schulze, C., Smales C., Rubin L., & Staddon J. (1997). Lysophosphatidic acid increases tight junction permeability in cultured brain endothelial cells. *J Neurochem, 68*, 991-1000.

Schwarze, S., Ho A., Vocero-Akbani A., & Dowdy S. (1999). *In vivo* protein transduction: delivery of a biologically active protein into the mouse. *Science, 285*, 1569-1572.

Schwid, S., Thornton C., & Pandya S. (1999). Quantitative assessment of motor fatigue and strength in Multiple Sclerosis. *Neurology, 53*, 743-750.

Schwiebert, L., Beck, L., Stellato, C., Bickel, C.*, et al.* (1996). Glucocorticosteroid inhibition of cytokine production: relevance to antiallergic actions. *J Allergy Clin Immunol, 97*(1 Pt 2), 143-152.

Sellebjerg, F., Barnes, D., Filippini, G., Midgard, R.*, et al.* (2005). EFNS guideline on treatment of multiple sclerosis relapses: report of an EFNS task force on treatment of multiple sclerosis relapses. *Eur J. Neurol, 12*(12), 939-946.

Shah, N., Sattar, A., Benanti, M., Hollander, S., & Cheuck, L. (2006). Magnetic resonance spectroscopy as an imaging tool for cancer: a review of the literature. *The Journal of the American Osteopathic Association, 106*(1), 23-27.

Shukla, S., Wu G., Chatterjee M., Yang W.*, et al.* (2003). Synthesis and biological evaluation of folate receptor-targeted boronated PAMAM dendrimers as potential agents for neutron capture therapy. *Bioconjug Chem, 14*, 158-167.

Siddiqui, M., AlOthman, Z., & Rahman, N. (2017). Analytical techniques in pharmaceutical analysis: A review. *Arabian Journal of Chemistry, 10*, S1409-S1421.

Sies, H. (1999). Glutathione and its role in cellular functions. *Free Radic Biol Med, 27*(9-10), 916-921.

Sirotkin, H., Morrow B., Saint-Jore B., Puech A.*, et al.* (1997). Identification, characterization, and precise mapping of a human gene encoding a novel membrane-spanning protein from the 22q11 region deleted in velo-cardio-facial syndrome. *Genomics, 42*, 245-251.

Smith, K., Kapoor R., Hall S., & Davies M. (2001). Electrically active axons degenerate when exposed to nitric oxide. *Ann Neurol, 49*, 470-476.

Smith, R., & Warren, D. (1983). Effects of high-dose intravenous methylprednisolone on circulation in humans. *Transplantation, 35*(4), 349-351.

Smoak, K., & Cidlowski J. (2006). Glucocorticoids regulate tristetraprolin synthesis and posttranscriptionally regulate tumor necrosis factor alpha inflammatory signaling. *Mol. Cell. Biol, 26*, 9126-9135.

Song, A., Wang, X., Zhang, J., Marik, J.*, et al.* (2004). Synthesis of hydrophilic and flexible linkers for peptide derivatization in solid phase. *Bioorg Med Chem Lett, 14*(1), 161-165.

Song, L., & Pachter, S. (2003). Culture of murine brain microvascular endothelial cells that maintain expression and cytoskeletal association of tight junction-associated proteins. *In Vitro Cellular & Developmental Biology - Animal, 39*(7), 313-320.

Søren, L., Pedersen A., Pernille T., Leila M., & Knud J. (2012). Microwave heating in solid-phase peptide synthesis. *Chem. Soc. Rev, 41*, 1826-1844.

Soto-Castro, D., Cruz-Morales, J., Apan, M., & Guadarrama, P. (2012). Solubilization and anticancer-activity enhancement of Methotrexate by novel dendrimeric nanodevices synthesized in one-step reaction. *Bioorganic Chemistry, 41–42*, 13-21.

Sparkman, O. (2000). *Mass spectrometry desk reference.* Pittsburgh: Global View Pub.

Spies, C., Strehl, C., van der Goes, M., Bijlsma, J., & Buttgereit, F. (2011). Glucocorticoids. *Best Practice & Research Clinical Rheumatology, 25*(6), 891-900.

Srinivas, N., Anusha, G., Malath, K., & Preetika, A. (2014). Dendrimer - for novel drug delivery system- a review article. *Indo American Journal Of Pharmaceutical Sciences, 1(5)*, 295-304.

Stam, R. (2010). Electromagnetic fields and the blood-brain barrier. *Brain Res. Rev, 65*, 80-97.

Stamatovic, S., Keep R., & Andjelkovic A. (2008). Brain endothelial cell-cell junctions: how to "open" the blood brain barrier. *Curr Neuropharmacol, 6*(3), 179-192.

Stanness, K., Guatteo, E., & Janigro, D. (1996). A dynamic model of the blood-brain barrier "in vitro". *Neurotoxicology, 17*(2), 481-496.

Stanness, K., Westrum, L., Fornaciari, E., Mascagni, P.*, et al.* (1997). Morphological and functional characterization of an in vitro blood-brain barrier model. *Brain Res, 771*(2), 329-342.

Stears, R., Getts R., & Gullans S. (2000). A novel, sensitive detection system for high-density microarrays using dendrimer technology. *Physiol Genomics, 3*, 93-99.

Stern, D., Yan, S., Yan, S., & Schmidt, A. (2002). Receptor for advanced glycation endproducts: a multiligand receptor magnifying cell stress in diverse pathologic settings. *Advanced Drug Delivery Reviews, 54*, 1615-1625.

Svenson, S., & Tomalia D. (2005). Dendrimers in biomedical applications-reflections on the field. *Advanced Drug Delivery Reviews, 57*, 2106- 2129.

Swardfager, W., Lanctôt, K., Rothenburg, L., Wong, A.*, et al.* (2010). A Meta-Analysis of Cytokines in Alzheimer's Disease. *Biological Psychiatry, 68*(10), 930-941.

Syapin, P., Militante, J., Garrett, D., & Ren, L. (2001). Cytokine-induced iNOS expression in C6 glial cells: transcriptional inhibition by ethanol. *J Pharmacol Exp Ther, 298*(2), 744-752.

Sztriha, L., & Betz A. (1991). Oleic acid reversibly opens the blood-brain barrier. *Brain Research Rev, 550*, 257-262.

Takahashi, D., & Yamamoto T. (2012). Development of an efficient liquidphase peptide synthesis protocol using a novel fluorene-derived anchor support compound with Fmoc chemistry. *Tetrahed Lett, 53*(15), 1936-1939.

Takeichi, M. (1995). Morphogenetic roles of classic cadherins. *Curr Opin Cell Biol, 7*, 619-927.

Talukder, M., Takeuchi T., & Harada E. (2003). Receptor-mediated transport of lactoferrin into the cerebrospinal fluid via plasma in young calves. *J Vet. Med. Sci., 65*, 957-964.

Tamai, I., & Tsuji A. (2000). Transporter-mediated permeation of drugs across the blood-brain barrier. *J Pharm. Sci., 89*, 1371–1388.

Tanis, I., & Karatasos K. (2009). Association of a Weakly Acidic Anti-Inflammatory Drug (Ibuprofen) with a Poly(Amidoamine) Dendrimer as Studied by Molecular Dynamics Simulations. *J Phys. Chem, 113*, 10984-10993.

Tansey, W., Ke S., Cao X., Pasuelo M.*, et al.* (2004). Synthesis and characterization of branched poly(l-glutamic acid) as a biodegradable drug carrier. *J Control Release, 94*, 39-51.

Tao, T., Lan J., Lukacs G., Hache R., & Kaplan F. (2006). Importin 13 regulates nuclear import of the glucocorticoid receptor in airway epithelial cells. *Am. J. Respir. Cell. Mol. Biol, 35*, 668–680.

Tariq, B., Jyoti N., Vandana D., Akanksha S.*, et al.* (2015). A Review about Dendrimers: Synthesis, Types, Characterization and Applications. *IJAPBC, 4*(1), 44-59.

Thrower, B. (2009). Relapse management in multiple sclerosis. *Neurologist, 15*, 1-5.

Tomalia, D. (2005). Birth of a new macromolecular architecture: dendrimers as quantized building blocks for nanoscale synthetic polymer chemistry. *Progress in Polymer Science, 30*(3–4), 294-324.

Tomalia, D., Baker H., Dewald J., Hall M.*, et al.* (1985). A new class of polymers: starburst-dendritic macromolecules. *Polym J, 17*, 117-132.

Tomalia, D., Naylor A., & Goddard W. (1990). Starburst Dendrimers: Molecular- Level Control of Size, Shape, Suface Chemistry, Topology and Flexibility from Atoms to Macroscopic Matter. *Angewandte International Edition England, 29*(2), 138-175.

Tripathy, S., & Das M. (2013). Dendrimers and their Applications as Novel Drug Delivery Carriers. *Journal of Applied Pharmaceutical Science, 3*(9), 142-114.

Troiano, R., Cook, S., & Dowling, P. (1987). Steroid therapy in multiple sclerosis. Point of view. *Arch Neurol, 44*(8), 803-807.

Tsukita, S., Furuse M., & Itoh M. (2001). Multifunctional strands in tight junctions. *Nat Rev Mol Cell Biol, 2*, 285-293.

Uehara, T., Baba, I., & Nomura, Y. (1998). Induction of cytokine-induced neutrophil chemoattractant in response to various stresses in rat C6 glioma cells. *Brain Res, 790*(1-2), 284-292.

Ulbrich, K., Hekmatara T., Herbert E., & Kreuter J. (2009). Transferrin- and transferrin-receptor-antibody-modified nanoparticles enable drug delivery across the blood–brain barrier. *European Journal of Pharmaceutics and Biopharmaceutics, 71*(2), 251-256.

Ulbrich, K., Knobloch T., & Kreuter J. (2011). Targeting the insulin receptor: nanoparticles for drug delivery across the blood-brain barrier. *J Drug Targeting, 19*(2), 125-132.

Utz, U., Biddison, W., McFarland, H., McFarlin, D.*, et al.* (1993). Skewed T-cell receptor repertoire in genetically identical twins correlates with multiple sclerosis. *Nature, 364*(6434), 243-247.

Vajkoczy, P., & Menger M. (2004). Vascular microenvironment in gliomas. *Cancer Treat. Res, 117*, 249-262.

van den Berg, B., Nieuwdorp M., Stroes E., & Vink H. (2006). Glycocalyx and endothelial (dys) function: from mice to men. *Pharmacol Rep, 58*, 75-80.

Veitch, N. (2004). Horseradish peroxidase: a modern view of a classic enzyme. *Phytochemistry, 65*(3), 249-259.

Verkman, A. (2002). Aquaporin water channels and endothelial cell function. *J Anatomy, 200*, 617-627.

Visser, C., Voorwinden, L., Crommelin, D., Danhof, M., & de Boer, A. (2004). Characterisation of the transferrin receptor on brain capillary endothelial cells. *Pharmacy Research, 21*, 761-769.

Vlieghe, P., & Khrestchatisky, M. (2013). Medicinal chemistry based approaches and nanotechnology-based systems to improve CNS drug targeting and delivery. *Med Res Rev, 33*(3), 457-516.

Voges, J., Reszka R., Gossmann A., Dittmar C., *et al.* (2003). Imaging-guided convection-enhanced delivery and gene therapy of glioblastoma. *Ann Neurol, 54*, 479-487.

Vorbordt, A., & Dobrogowska D. (2004). Molecular anatomy of interendothelial junctions in human blood-brain barrier microvessels. *Folia Histochem Cytobiol, 42*, 67-75.

Vosoughi, R., & Freedman, M. (2010). Therapy of multiple sclerosis. *Clin. Neurol. Neurosurg., 112*(5), 365-385.

Wade, L., & Katzman R. (1975). 3-O-methyldopa uptake and inhibition of L-dopa at the blood-brain barrier. *Life Sci, 17*, 131-136.

Wakerley, B., Nicholas R., & Malik O. (2008). Multiple sclerosis. *Medicine, 36*(12), 625-629.

Walton, J., Hallen-Adams, H., & Luo, H. (2010). Ribosomal Biosynthesis of the Cyclic Peptide Toxins of Amanita Mushrooms. *Biopolymers, 94*(5), 659-664.

Wang, H., Matsui, M., Araya, S., Onai, N., *et al.* (2003). Immune parameters associated with early treatment effects of high-dose intravenous methylprednisolone in multiple sclerosis. *Journal of the Neurological Sciences, 216*(1), 61-66.

Watanabe, K., Kinoshita, S., & Nakagawa, H. (1989). Purification and characterization of cytokine-induced neutrophil chemoattractant produced by epithelioid cell line of normal rat kidney (NRK-52E cell). *Biochem Biophys Res Commun, 161*(3), 1093-1099.

Watanabe, T., Dohgu, S., Takata, F., Nishioku, T., *et al.* (2013). Paracellular barrier and tight junction protein expression in the immortalized brain endothelial cell lines bEND.3, bEND.5 and mouse brain endothelial cell 4. *Biol Pharm Bull, 36*(3), 492-495.

Waubant, E., du Montcel S., Jedynak C., Obadia M., *et al.* (2003). Multiple sclerosis tremor and the Stewart-Holmes manoeuvre. *Mov Disord, 18*, 948-952.

Wilhelm, I., & Krizbai, I. (2014). *In vitro* models of the blood-brain barrier for the study of drug delivery to the brain. *Mol Pharm, 11*(7), 1949-1963.

Williams, R., Risau W., Zerwes H, Drexler H., *et al.* (1989). Endothelioma cells expressing the polyoma middle T oncogene induce hemangiomas by host cell recruitment. *Cell Biology, 57*, 1053- 1063.

Wolburg, H. (2006). *The endothelial frontier. In: Blood-Brain Interfaces – from Ontology to Artificial Barriers*: Weinheim.

Wolburg, H., & Lippoldt A. (2002). Tight junctions of the blood-brain barrier: development, composition and regulation. *Pharmacol. Rep, 38*, 323-337.

Wolswijk, G. (1998). Oligodendrocyte regeneration in the adult rodent CNS and the failure of this process in multiple sclerosis. *Prog. Brain res, 117*, 233-247.

Wyles, C., Houdek, M., Wyles, S., Wagner, E.*, et al.* (2015). Differential Cytotoxicity of Corticosteroids on Human Mesenchymal Stem Cells. *Clin Orthop Relat Res, 473*(3), 1155-1164.

Xu, L., Zhang, H., & Wu, Y. (2014). Dendrimer advances for the central nervous system delivery of therapeutics. *ACS Chem Neurosci, 5*(1), 2-13.

Yang, H., Liu C, Yang D, Zhang H, Xi Z. (2009). Comparative study of cytotoxicity, oxidative stress and genotoxicity induced by four typical nanomaterials: the role of particle size, shape and composition. *Journal of Applied Toxicology, 29*, 69-78.

Yang, H., & Lopina S. (2003). Penicillin V-conjugated PEG-PAMAM star polymers. *J Biomater. Sci., Polym. Ed, 14*, 1043- 1056.

Yasukawa, T., Ogura Y., Tabata Y., Kimura H.*, et al.* (2004). Drug delivery systems for vitreo retinal diseases. *Progress in Retinal and Eye Research, 23*(3), 253-281.

Yates, C., & Hayes, W. (2004). Synthesis and applications of hyperbranched polymers. *European Polymer Journal, 40*(7), 1257-1281.

Yoon, H., Hong M., & Kim H. (2000). Affinity biosensor for avidin using a double functionalized dendrimer monolayer on a gold electrode. *Anal Biochem, 282*, 121-128.

Yordanov, A., Lodder L., Woller K., Cloninger J.*, et al.* (2002). Novel iodinated dendritic nanoparticles for computed tomography (CT) imaging. *Nano Lett, 2*, 595-599.

Zbinden, G., & Flury-Roversi M. (1981). Significance of the LD_{50}-test for the toxicological evaluation of chemical substances. *Archives of Toxicology, 47*, 77-99.

Zeng, F., & Zimmerman S. (1996). Rapid synthesis of dendrimers by an orthogonal coupling strategy. *J Am Chem Soc, 118*, 5326–5327.

Zhuo, R., Du B., & Lu Z. (1999). *In vitro* release of 5-fluorouracil with cyclic core dendritic polymer. *J Control. Release, 57*, 249- 257.

Zimmerman, S., Zharov I., Wendland M., Rakow N., & Suslik K. (2003). Molecular Imprinting Inside Dendrimers. *J Am. Chem. Soc, 125*, 13504-13518.

Zlokovic, B. (1995). Cerebrovascular permeability to peptides: Manipulations of transport systems at the blood-brain barrier. *J Pharm. Res., 12*(10), 1395-1406.

Zorko, M., & Langel U. (2005). Cell-penetrating peptides: mechanism and kinetics of cargo delivery. *Adv. Drug Deliv. Rev, 57*, 529-545.

Dissemination

1. Improving blood-brain barrier penetration of drugs used for the treatment of multiple sclerosis using a dendrimer-ligand based carrier system.
Poster presentation / Brighton doctoral college research student conference, 22-23th July 2014.

2. Dendrimer based drug delivery system used for delivery of methylprednisolone for the treatment of multiple sclerosis.
Poster presentation / UK society for biomaterials 14th annual conference and postgraduate day, 25-26th June 2015 / Belfast - Ireland.

3. Functionalisation of dendronised-drug carrier system with glutathione to enhance brain penetration and targeting of drug used in multiple sclerosis.
Poster presentation / International conference on medicinal chemistry / interfacing chemical biology and drug delivery / RICT, 6-8th July 2016 / Caen - France.

4. Synthesis and characterisation of a glutathione decorated dendrimer for improved drug loading and penetration of methylprednisolone across the blood-brain barrier.
Poster presentation / The 7th APS International PharmSci / Pharmaceutical Sciences: Improving World Health, 5-7th September 2016 / Glasgow - Scotland.

5. Evaluation of a novel glutathione-dendron carrier system for methylprednisolone
Rapid fire and poster presentation / 28th annual conference of the European Society for Biomaterials (ESB), 4-8th September 2017 Athens - Greece.